

**Thiazine Derivatives: Synthesis, Anti Tubercular Activities and Basic
Pharmacokinetic Evaluation**

THESIS

Submitted in partial fulfillment
of the requirements for the degree of

DOCTOR OF PHILOSOPHY

by

A.V.Ramani

Under the Supervision of

Dr. D. SRIRAM



BIRLA INSTITUTE OF TECHNOLOGY AND SCIENCE

PILANI (RAJASTHAN) INDIA

2012

**BIRLA INSTITUTE OF TECHNOLOGY AND SCIENCE
PILANI (RAJASTHAN)**

CERTIFICATE

This is to certify that the thesis entitled, “**Thiazine Derivatives: Synthesis, Anti Tubercular Activities and Basic Pharmacokinetic Evaluation**” and submitted by **A.V.Ramani** ID.No. **2009PHXF446P** for the award of Ph.D. degree of the Institute, embodies the original work done by her under my supervision.

Signature in full of
The Supervisor : _____

Name in capital block
letters : **D. SRIRAM**

Designation : **Associate Professor**

Date:

Dedicated
to my
dearest father

ACKNOWLEDGEMENTS

I would like to offer my gratitude and reverence to the Almighty for having showered his blessings on me and for granting me this blessed opportunity.

I am grateful to **Prof. B. N. Jain**, Vice-Chancellor (BITS Pilani), for allowing me to carry out my research work in this esteemed institute.

I am also thankful to **Prof. V. S. Rao**, Director (BITS Pilani, Hyderabad Campus) for his benevolence in allowing me to continue my research in the Hyderabad campus of this institute.

I am thankful to Dean, Research & Consultancy Division, BITS, Pilani, for his encouragement at every stage of this research work. I sincerely acknowledge Research & Consultancy Division of BITS Pilani, Hyderabad Campus for the timely help.

It gives me immense pleasure to express my heart-felt gratitude towards my supervisor, **Dr. D. Sriram**, Associate professor, BITS Pilani, Hyderabad Campus, who guided and motivated me every day of my research tenure. His zeal for perfection has disciplined me to plan my research work and produce excellent results within short time. I consider myself blessed to have got this opportunity to work under a versatile person like him. Had it not been for his supportive guidance, inspiration and critical suggestions, this thesis would never have come to its present form.

I am grateful to **Dr. P. Yogeewari**, Head of the Pharmacy department (previous), BITS Pilani, Hyderabad campus, and Doctoral Advisory Committee (DAC) member, who was kind enough in guiding me in all the possible ways when in need. She is also instrumental in bringing me to BITS Hyderabad campus or else I would not have even got an opportunity to do my PhD. I would like to thank **Dr. Vamsi Krishna Venuganti** (present) Head of the Pharmacy department in all possible ways.

I am grateful to **Dr. Punna Rao Ravi**, my Doctoral Advisory Committee (DAC) member for his valuable suggestions.

I express my heartfelt thanks to **Mr. Jean Kumar** for his active participation, unstinting assistance, which are undoubtedly a fillip to this work.

I also express my sincere thanks to my students Lakshmi Indira, Monika A, Sripriya and Karyavardhi, for all the valuable support given to me during research work. I extend my thanks to my fellow researchers Mallika Alvala, Reshma C Alokam and Madhu Babu Bhattu who assisted in computational studies and experimental work. I am grateful to Elena Salina of Institution of the Russian Academy of Sciences A.N. Bach Institute of Biochemistry RAS, Moscow, Russia for assisting me in screening in-vitro dormant antimycobacterial activity of my compounds.

I express my thanks to our laboratory technicians and attendants for all their help in one way or the other. Thanks are also due to other staff members of Pharmacy department.

A special love and thanks to all of my friends especially to Dhanya and Nirmala for the unconditional support, constant source of encouragement and inspiration given to me during my work.

Special thanks to my life partner, friend my husband, Srinivas, and my son, Abhishek for their enthusiastic support and love, all through this long process. I wish to extend my sincere thanks and gratitude to my mother and sister Nagini for their selfless love and support throughout the years. Last but not least, I lovingly remember and thank my father who persuaded me towards my research and my in-laws, whose spirit stays with us in our hearts forever. At the end, I would like to dedicate this thesis to my family as a gesture of gratitude for all that they have done for me in a selfless way.

Date:

A.V.Ramani

Abstract

In the present series, two series of compounds (84 compounds), 1,3 thiazines and 1,4 thiazine were designed and synthesized by simple and commercially feasible methods. Purity of the synthesized compounds were ascertained by TLC and their structures were elucidated by spectral (IR and NMR) and elemental analysis. The synthesized compounds were evaluated for *in vitro* antimicrobial activity against MTB and cytotoxicity. One of the compound [N-(2-(4-(benzyloxy) phenyl)-4-oxo- 1, 3-thiazinan-3-yl) isonicotinamide – “Compound 17”] from the 1,3 thiazine series was found to be very active so evaluated for pharmacokinetic, tissue distribution, excretion and interaction with other marketed drugs. One compound from 1,4 thiazine series possessed in-vitro dormant antimycobacterial activity and structure activity relation of this series correlated well with the 3D- QSAR studies.

Table of Contents

	Page No
<i>Certificate</i>	i
<i>Acknowledgements</i>	ii
<i>List of figures</i>	iv
<i>List of tables</i>	vii
<i>List of abbreviations</i>	ix
<i>Abstract</i>	xi
Chapter 1. Introduction	
1.1 Tuberculosis	4
1.2 Latent Tuberculosis	6
1.3 Current TB Drugs	8
1.4 Drug Resistance	11
Chapter 2. Literature Review	
2.1 Drug targets	16
2.2 Rational drug design	25
2.3 Drugs in clinical trials	54
Chapter 3. Objective and plan of work	
3.1 Objective and Rationale for the design of proposed compounds	66
3.2 Plan of work	66
3.2.1 [1,3]-Thiazine derivatives	66
3.2.2 [1,4]-Thiazine derivatives	67
Chapter 4. 1,3-Thiazine derivatives as anti-tubercular agents	
4.1. Synthesis and biological screening	
4.1.1 Chemistry	71
4.1.2 Biological Screening and results	78

4.1.2.1 In vitro antimycobacterial Screening	78
4.1.2.2 Cytotoxicity evaluation	80
4.1.3 Discussion	82
4.2. Pharmacokinetics, tissue distribution and excretion of compound N-(2-(4-(benzyloxy) phenyl)-4-oxo-1,3-thiazinan-3-yl) isonicotinamide – “Compound 17”	
4.2.1 Method Validation in plasma and tissue homogenates	86
4.2.2 Pharmacokinetic Study	97
4.2.3 Tissue Distribution Study	101
4.2.4 Excretion	106
4.3. Interaction of compound N-(2-(4-(benzyloxy) phenyl)-4-oxo-1,3-thiazinan-3-yl) isonicotinamide – “Compound 17” with other drugs	
4.3.1 Distribution of cyp enzymes	112
4.3.2 Mechanism of pharmacokinetic drug-drug interaction	113
4.3.3 Role of in vivo animal studies	114
4.3.4 General methodology adopted for experimentation	115
4.3.5 CYP1A	118
4.3.6 CYP2C	127
4.3.7 CYP3A	136
4.3.8 Discussion:	146
4.3.9 Conclusion	147
Chapter 5. 1,4-Thiazine derivatives as antitubercular agents	
5.1 Chemistry	149
5.2 In-vitro biological activity	171
5.3 Atom based 3D QSAR methods	179
5.4 Discussion	186
5.5 Conclusion	192

Chapter 6. Summary and conclusion	195
Future perspectives	198
References	199
Appendix	222
List of Publications	223
Biography of Supervisor and Candidate	225

LIST OF TABLES

Table no.	Description	Page No.
Table 1.1	Current TB Drugs and their Targets	10
Table 1.2	Current regimens for treatment of drug susceptible tuberculosis	12
Table 1.3	Desired target product profile for a new TB drug	13
Table 2.1	Remodelling the existing antibacterial drug classes	59
Table 2.2	Some compounds under clinical trials along with the funding agencies	62
Table.4.1.1	Physical constants, anti-tubercular activity & cytotoxicity of the compounds	81
Table.4.2.1	Linear regression of peak areas and concentration for compound 17 in biological sample	92
Table.4.2.2	Intra day and inter day precision and accuracy of compound 17 from Biological samples	93
Table.4.2.3	Stability data of compound 17 quality controls in Plasma	94
Table.4.2.4	Stability data of compound 17 quality controls in Liver, lungs, heart and brain	95
Table.4.2.5	Stability data of compound 17 quality controls in stomach, blood, large intestine, small intestine	96
Table.4.2.6	Pharmacokinetic parameters of compound 17 following oral and intravenous administration	99
Table.4.2.7	Biological sample concentrations ($\mu\text{g/ml}$) of compound 17 at various time points along with ratios (tissue to plasma)	104
Table.4.2.8	Cumulative Individual and Mean Recovery in Excreta of Male Wistar Rats Following Oral Administration of compound 17 at 50 mg/kg	109
Table.4.3.1	Sparsing for pharmacokinetic study of Test Drug + compound 17	116
Table.4.3.2	Mini Validation of Ondansetron	119
Table.4.3.3	Pharmacokinetic parameters of compound 17 administered with ondansetron	120
Table.4.3.4	Pharmacokinetic parameters of ondansetron administered with compound 17	121
Table.4.3.5	Mini Validation of Ciprofloxacin	123
Table.4.3.6	Pharmacokinetic parameters of compound 17 with Ciprofloxacin	124
Table.4.3.7	Pharmacokinetic parameters of Ciprofloxacin with compound 17	125
Table.4.3.8	Mini Validation of Glipizide	128
Table.4.3.9	Pharmacokinetic parameters of compound 17 with Glipizide	129
Table.4.3.10	Pharmacokinetic parameters of Glipizide with compound 17	130

Table.4.3.11	Mini Validation of Ranitidine	132
Table.4.3.12	Pharmacokinetic parameters of compound 17 with Ranitidine	133
Table.4.3.13	Pharmacokinetic parameters of Ranitidine with compound 17	134
Table.4.3.14	Mini Validation of Atorvastatin	138
Table.4.3.15	Pharmacokinetic parameters of compound 17 with Atorvastatin	139
Table.4.3.16	Pharmacokinetic parameters of Atorvastatin with compound 17	139
Table.4.3.17	Linearity and precision of Ketoconazole	142
Table.4.3.18	Pharmacokinetic parameters of Compound 17 with Ketoconazole	144
Table.4.3.19	Pharmacokinetic parameters of Ketoconazole with Compound 17	144
Table 5.1	Structure and Physical constants, of [1,4]-thiazines	159
Table 5.2	In-vitro antimycobacterial activity	173
Table 5.3	In-vitro enzyme assay	176
Table 5.4	Aligned compounds for 3D QSAR study and their experimental and predicted biological activity	183

LIST OF FIGURES

Figure No.	Description	Page No.
Figure 1.1	TB incidence per 100,000 inhabitants	2
Figure 1.2	(a) Mycobacterium tuberculosis scanning electron micrograph and prokaryotic cell structure. (b) Cell wall structure.	5
Figure 1.3	Stages of M. tuberculosis infection.	6
Figure 1.4	Spread of TB at the molecular level	7
Figure 1.5	Structures of a list of first-line and second-line TB drugs	9
Figure 1.6	An outline of Patent Protected drug targets of Mycobacterium tuberculosis	11
Figure 1.7	Incidence of tuberculosis, 1990–2004, also includes the targets for 2015	14
Figure 2.1	(a) Structure of peptidoglycan (b) Peptidoglycan biosynthetic pathway	17 & 18
Figure 2.2	AG structure of an AGP molecule	19
Figure 2.3	A typical arabinogalactan molecule from M. Tuberculosis	21
Figure 2.4	Tuberculosis drugs-and their mechanism of action	26
Figure 2.5	Structure of compounds derivatives of anti-TB first line drugs.	28
Figure 2.6	Structure of SQ109 and analogs	29
Figure 2.7	Ethambutol analogs as anti-TB agents	30
Figure 2.8	General structure of salicylanilides derivatives with anti-TB activity	32
Figure 2.9	General structure of 1,3-benzoxazine derivatives	33
Figure 2.10	Quinoline as scaffold for designing new anti-TB agents	36
Figure 2.11	Quinoline and oxazole derivatives as anti-TB agents.	37
Figure 2.12	General structure of phenazine-1-carboxamides, quinoline and quinoxaline derivatives	38
Figure 2.13	Triazole and benzimidazole scaffold for designing new anti-TB agents	40
Figure 2.14	Triazole derivatives as anti-TB agents	41
Figure 2.15	Dibenzofurane, triazole, methylphenyl and acetamide moiety in compounds with anti-TB activity	42
Figure 2.16	General structure of pyrazoles and thiazoles derivatives as anti-TB agents	43
Figure 2.17	Spiro-pyrrolothiazoles derivative with anti-TB activity	44
Figure 2.18	Hydrazone derivatives as anti-TB agents	45
Figure 2.19	Purine derivatives as anti-TB agents	46
Figure 2.20	General structure of pyrimidine derivatives as anti-TB	47

	agents	
Figure 2.21	Pyridine derivatives with potential activity anti-TB	48
Figure 2.22	N-substituted-pyridazinones derivatives	48
Figure 2.23	N-substituted- thiazines derivatives	49
Figure 2.24	General structure of 1H-indole-2,3-dione 3-thiosemicarbazone with anti-TB activity	51
Figure 2.25	Benzothiadiazine derivatives as anti-TB agents	51
Figure 2.26	Structure of benzofurobenzopyrane as anti-TB agents	52
Figure 2.27	Phthalimide derivatives as anti-TB agent	53
Figure 2.28	Cinnamic derivatives	54
Figure 2.29	In vitro anti-TB structure activity relationships (SAR) of the nitroimidazo[2,1-b]oxazine series	55
Figure 2.30	Summary of the SAR in the nitroimidazo[2,1-b]oxazole series	56
Figure 2.31	Diagram showing the interactions between TMC207 and the binding site of M.tb ATP synthase	57
Figure 2.32	Structures of few promising anti-TB	58
Figure 2.33	Existing and NCE's at various stages of development	60
Figure 2.34	A bull's-eye representation of the current clinical pipeline for TB.	61
Figure 2.35	Representative underexplored and new chemical scaffolds	63
Figure 4.2.1	Structure of compound 17	85
Figure 4.2.2	Standard chromatogram	90
Figure 4.2.3	Specificity chromatogram in plasma	90
Figure 4.2.4	Quality control standards in plasma	90
Figure 4.2.5	Blank tissue (A); Blank tissue spiked with compound 17 and IS (B); Rat liver tissue sample obtained after 2 h after 50 mg/kg oral dose of compound 17(C); Rat lung tissue sample obtained after 2 h after 50 mg/kg oral dose of compound 17(D)	91
Figure 4.2.6	Concentration time profile of compound 17 after oral and intravenous administration	100
Figure 4.2.7	Pie chart representation of drug distribution at different time points after oral administration of compound 17 (50mg/kg)	103
Figure 4.2.8	Bar graph representation of drug distribution after oral administration of compound 17 (50mg/kg)	105
Figure 4.2.9	Metabolic cage	108
Figure 4.2.10	Mean Cumulative Recovery in Excreta Following a Single dose administration of compound 17 to Male Wistar Rats at a Target Dose of 50 mg/kg	110
Figure.4.3.1	Relative abundance of CYP450 enzymes in liver	112
Figure.4.3.2	Mechanisms of enzyme Inhibition	113
Figure.4.3.3	Mechanism of enzyme induction	114
Figure.4.3.4	Chromatogram of compound 17 and IS	117

Figure.4.3.5	Ondansetron	118
Figure.4.3.6	A typical chromatogram of Ondansetron, IS and compound 17	120
Figure.4.3.7	Log linear Concentration time profile of Ondansetron and in combination with compound 17	121
Figure.4.3.8	Ciprofloxacin	122
Figure.4.3.9	A typical chromatogram of Ciprofloxacin, IS and compound 17	124
Figure.4.3.10	Log linear Concentration time profile of ciprofloxacin and compound 17	125
Figure.4.3.11	Glipizide	127
Figure.4.3.12	A typical chromatogram of Glipizide, IS and compound 17	129
Figure.4.3.13	Log linear Concentration time profiles of glipizide and compound 17	130
Figure.4.3.14	Ranitidine	131
Figure.4.3.15	A typical chromatogram of Ranitidine, IS and compound 17	133
Figure.4.3.16	Log linear concentration time profile of ranitidine and compound 17	134
Figure.4.3.17	Atorvastatin	136
Figure.4.3.18	A typical chromatogram of Atorvastatin, IS and compound 17	138
Figure.4.3.19	Log linear Concentration time profiles of atorvastatin and compound 17	140
Figure.4.3.20	Ketoconazole	141
Figure.4.3.21	Atypical chromatograms of Ketoconazole, IS and Compound 17	143
Figure.4.3.22	Log linear Concentration time profiles of ketoconazole and Compound 17	145
Figure.5.1	In-vitro cytotoxicity studies on HEK293T cell lines	178
Figure.5.2	The effectiveness of the compound 7 for killing M. tuberculosis 'non-culturable' cells.	180
Figure.5.3	Scatter plots plotted between Predicted vs. Observed activity of MTB inhibition by the best model obtained using 41 compounds	185
Figure.5.4	Illustration of the Phase QSAR map visualization on most active / inactive molecules	186

List of Abbreviations

% F	Bioavailability of the drug orally administered.
¹ H NMR	Proton Nuclear Magnetic Resonance
ACN	Acetonitrile
ACP	arabinogalactan
ADC	albumin-dextrose-catalase
ADME	Absorption, Distribution, Metabolism, and Excretion
ADP	Adenosine-5'-diphosphate
AFB	Acid-Fast Bacillus
AIDS	Acquired Immunodeficiency Syndrome
ATP	Adenosine-5'-triphosphate
AUC _(0-t)	Area under the curve till 't' hours
C ₀	Initial plasma concentration (at 0 hrs)
CC ₅₀	50% - Cytotoxic Concentration
CDCl ₃	Deuterated Chloroform
CFU	Colony Forming Unit
Cl	Clearance
C _{max}	Peak plasma concentration
CMC	Sodium Carboxymethylcellulose
CYP	Cytochrome P
DCC	Dicyclohexylcarbodiimide
DCM	Dichloromethane
DIPEA	N-diisopropylethylamine

DMA	N, N' - Dimethylacetamide
DMEM	Dulbecco's Modification of Eagle's Medium
DMF	Dimethylformamide
DMSO	Dimethyl sulphoxide
DNA	Deoxyribonucleic acid
d-TDP	Thymidine diphosphate
DTT	dithiothreitol
EA	Ethylacetate
EDC	ethyl(dimethylaminopropyl) carbodiimide
EDTA	Ethylene Diamine Tetra acetic acid
equiv.	Equivalent
FAS	Fatty acid synthase
FBS	fetal bovine serum
FMO	flavin-containing monooxygenase
HEK293	human embryonic kidney cells
HIV	Human immunodeficiency virus
HMG COA	3-hydroxy-3-methyl-glutaryl-CoA reductase
HQC	High QC
IC ₅₀	50% - Inhibitory Concentration
INH	Isoniazid
INHR-MTB	INH-resistant <i>M.tuberculosis</i>
IPTG	isopropyl-β-D-thiogalactopyranoside
IR	Infra Red
IS	Internal Standard
K _{el}	Elimination rate constant

LCMS	Liquid chromatography–mass spectrometry
LLOQ	Lower Limit of Quantification
LQC	Low QC
M.p	Melting Point
m-AGP	Arabinogalactan-peptidoglycan
MC ²	Mycobacterium smegmatis
MDR	Multi-Drug Resistance
MIC	Minimum Inhibitory Concentration
MPN	Most Probable Numbers
MQC	Middle QC
MTB	<i>Mycobacterium tuberculosis</i>
MTCYP51	Cytochrome P450
MTT	(3-[4, 5-dimethylthiazol-2-yl]-2, 5-diphenyltetrazolium bromide)
NAD	Nicotinamide adenine dinucleotide
NCE	new chemical entity
NDA	New Drug Application
PAS	p-aminosalicylic acid
PDA	Photodiode Array Detectors
PG	Peptidoglycan
QC	Quality Control
QSAR	Quantitative Structure-Activity Relationship
RIF	Rifampicin
RMSE	root mean square error
RNA	ribonucleic acid
RSD	relative standard deviation

SAR	Structure-Activity Relationship
SD	Standard Deviation
SLS	Sodium dodecyl sulfate
$t_{1/2}$	Half life
TB	Tuberculosis
TEA	Triethyl amine
TFA	Trifluoro acetic acid
THF	tetrahydrofuran
TLC	Thin Layer Chromatography
T_{max}	Time taken to attain peak plasma concentration
UDP	Uridine diphosphate
UV	ultraviolet spectrometer
V_d	Volume of distribution
WHO	World Health Organization
XDR-TB	Extensive Drug - Resistant Tuberculosis

Chapter 1- Introduction

Tuberculosis is a common, lethal, infectious disease caused by various strains of mycobacteria, usually *Mycobacterium tuberculosis*. Tuberculosis attacks the lungs but can also affect other parts of the body. It is spread through the air when people who have an active TB infection cough, sneeze, or otherwise transmit their saliva through the air. Most infections are asymptomatic and latent, but about one in ten latent infections eventually progresses to active disease which, if left untreated, kills more than 50% of those so infected [1].

In 1882, Robert Koch identified *Mycobacterium tuberculosis* as the causative agent of TB, but since his discovery the global TB epidemic seems unabated. Tuberculosis is estimated about 1.7 million deaths each year. Worldwide numbers of new cases (more than 9.8 million) are quite high (Figure 1.1) [2]. Low-income and middle-income countries account for more than 80% of the active cases in the world. Due to the devastating effect of HIV on susceptibility to tuberculosis, sub-Saharan Africa has been disproportionately affected and accounts for four of every five cases of HIV-associated tuberculosis.

Tuberculosis notification rates, 2011

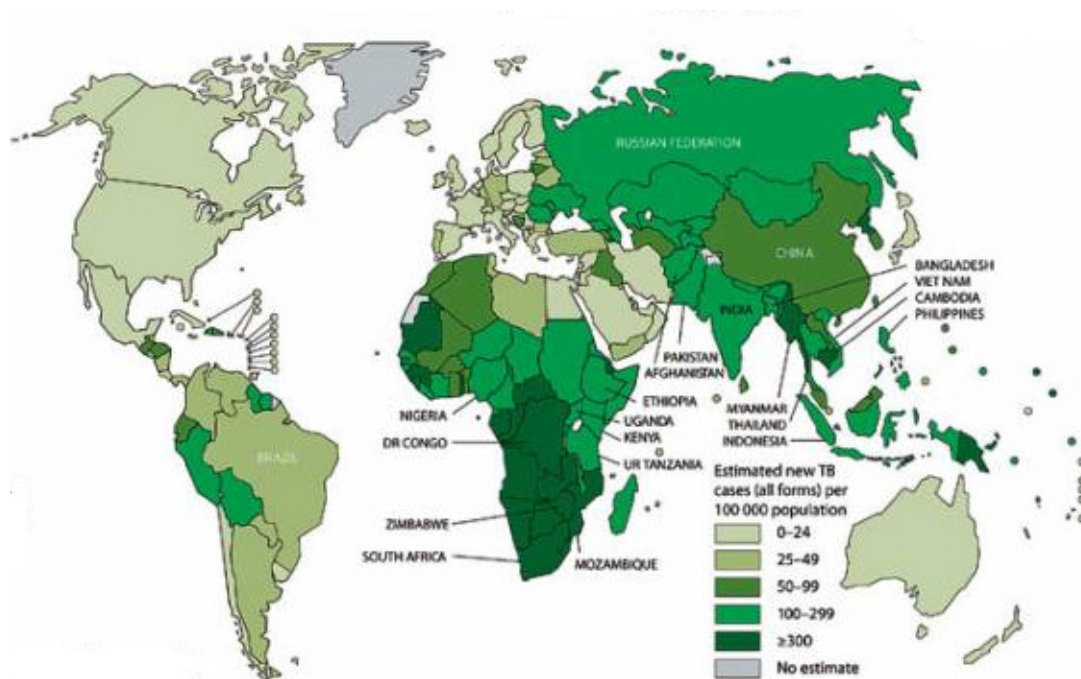


Figure 1.1: TB incidence per 100,000 inhabitants [2]

Diagnosis continues to rely on century-old sputum microscopy; there is no vaccine with adequate effectiveness and tuberculosis treatment regimens are protracted and have a risk of toxic effects.

Increasing rates of drug-resistant tuberculosis in Eastern Europe, Asia, and sub-Saharan Africa now threaten to undermine the gains made by worldwide tuberculosis control programs [3]. Moreover, our fundamental understanding of the pathogenesis of this disease is inadequate. However, increased investment has allowed basic, translational and applied research to produce new data, leading to promising progress in the development of improved tuberculosis diagnostics, biomarkers of disease activity, drugs, and vaccines. The growing scientific momentum must be accompanied by much greater investment and political commitment to meet this huge persisting challenge to public.

Equally important, especially in the highest-burden countries of India, China, and Russia, will be a commitment to tuberculosis control including improvements in national policies and health systems that remove financial barriers to treatment, encourage rational drug use, and create the infrastructure necessary to manage multi drug resistant (MDR-TB) tuberculosis. The world's two most populous countries, India and China, account for more than 50% of the world's MDR-TB cases and as such these countries are encountering a high and increasing TB disease burden. However, due to the size of the population and the number of TB cases reported annually, India ranks second among the 27 MDR-TB high-burden countries worldwide after China [4, 6].

The WHO figures that put the number of Multi-Drug Resistant Tuberculosis (MDR-TB) cases in India at 63,000, saying there were only 10,267. As many as 38,287 suspected cases were examined till the end of 2011 and of them, 10,267 have been diagnosed with MDR-TB and 6,994 put on treatment, according to TB India - 2012 - the annual status report of the Revised National TB Control Programme (RNCTP) brought out by the Health Ministry [4].

But the RNCTP report points out that most studies on drug resistant TB in India were undertaken using non-standardised methodologies with bias and small samples usually from tertiary level care facilities. To obtain a more precise estimate of MDR-TB burden, the RNTCP carried out drug resistance surveillance (DRS) in accordance with global guidelines in selected States — Gujarat, Maharashtra, Andhra Pradesh — which indicated that the prevalence of MDR-TB was low, less than 3 per cent among new cases and 12-17 per cent in re-treatment cases. To substantiate the findings, two more DRS surveys are being carried out in western Uttar Pradesh and Tamil Nadu and two more are planned in Rajasthan and Madhya Pradesh. The surveys will be undertaken to periodically monitor and study the trend of MDR prevalence.

On Extensive Drug Resistant TB (XDR-TB), a subset of MDR-TB with resistance to second line drugs and injectable drugs, the report says the extent and magnitude of this problem is yet to be determined. No separate DRS surveys have been undertaken to estimate the burden of XDR-TB in the country. However, DRS surveys in Gujarat and Andhra Pradesh reported 14 XDR-TB cases and 112 XDR-TB patients were diagnosed at the National Reference Laboratories as reported by the States from 2008 to September 2011.

1.1. Tuberculosis

In 1898, Harvard pathologist Theobald Smith demonstrated that tubercle bacilli isolated from humans differed significantly from bacilli isolated from cattle in their capacity to cause disease in different animal species. Eventually, the two bacilli were granted separate species status, with *M. tuberculosis* designating the typical human pathogen, and *Mycobacterium bovis* referring to the bovine form. Because *M. bovis* has the capacity to cause disease in a variety of animal species, including humans, it was originally thought to exhibit a much broader host range than *M. tuberculosis* [7-8].

The genus of *Mycobacterium tuberculosis* consists of aerobic acid-fast bacillus, rod shaped organism (Figure 1.2a) [9]. The cell wall complex contains peptidoglycan, but

otherwise it is composed of complex lipids. Over 60% of the mycobacterial cell wall is lipid. The lipid fraction of *M. tuberculosis*'s cell wall consists of three major components, mycolic acids, cord factor, and wax-D. Mycolic acids, the major lipid of the *Mycobacterium tuberculosis* cell wall (Figure 1.2b).

M. tuberculosis produces three main types of mycolic acids: alpha-, methoxy-, and keto-. Alpha-mycolic acids comprise at least 70% of the mycolic acids present in the organism and contain several cyclopropane rings. Methoxy-mycolic acids, which contain several methoxy groups, comprise between 10% and 15% of the mycolic acids in the organism. The remaining 10% to 15% of the mycolic acids are keto-mycolic acids, which contain several ketone groups [10-11]. Mycolic acids are modified by cyclopropane rings, methyl branches, and oxygenation through the action of eight S-adenosyl methionine (SAM) - dependent mycolic acid methyltransferases (MAMTs), encoded at four genetic loci. Mycolic acid modification has been shown to be important for *M. tuberculosis* pathogenesis, in part through effects on the inflammatory activity of trehalose dimycolate (cord factor).

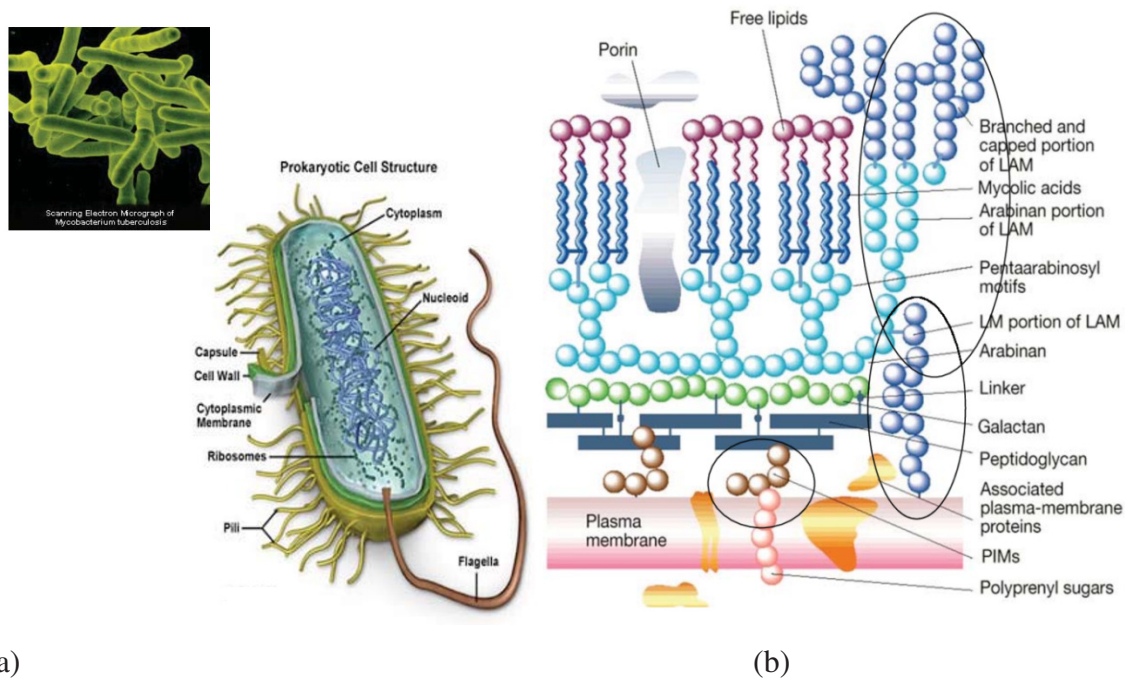


Figure 1.2 :(a) *Mycobacterium tuberculosis* scanning electron micrograph and prokaryotic cell structure. (b) Cell wall structure. [9]

1.2. Latent Tuberculosis

The pathogen responsible for TB uses diverse strategies to survive in a variety of host lesions and to evade immune surveillance. This situation highlights the relative shortcomings of the current treatment strategies for TB and the limited effectiveness of public health systems, particularly in resource-poor countries where the main TB burden lies. The ease with which TB infection spreads (for example, by inhalation of a few droplet nuclei 2–5 mm in diameter containing as few as 1–3 bacilli), has helped to sustain this scourge. In spite of half a century of anti-TB chemotherapy, one-third of the world's population asymptotically still harbor a dormant or latent form of *M. tuberculosis* with a life long risk of disease reactivation (Figure 1.3) [12].

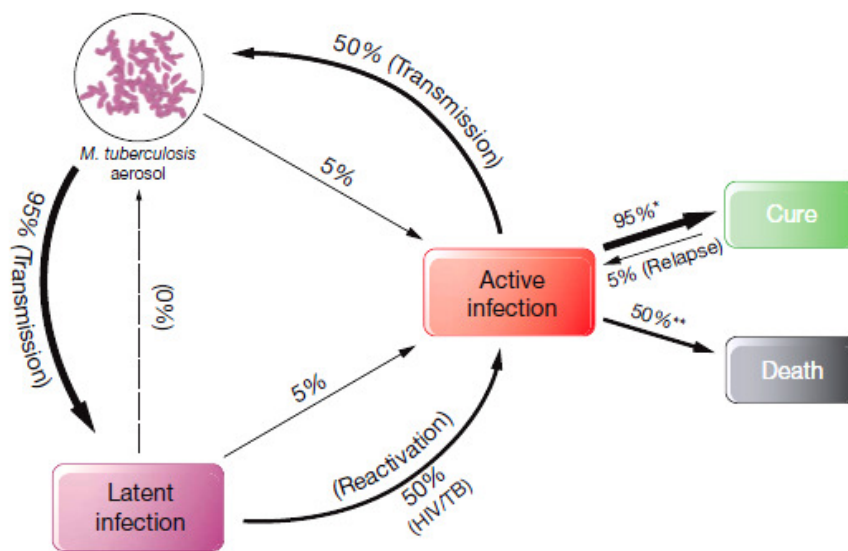


Figure 1.3: Stages of *M. tuberculosis* infection [12].

M. tuberculosis is an aerosol transmission and progression to infectious TB or non-infectious (latent) disease [13-17]. A sizeable pool of latently infected people may relapse into active TB, years after their first exposure to the bacterium. Latent TB is commonly activated by immune suppression, as in the case of HIV. In cases of drug-susceptible

(DS)-TB, 95% of patients recover upon treatment, whereas 5% relapse. If untreated high mortality results.

Reactivation of latent TB, even after decades of subclinical persistence, is a high risk factor for disease development particularly in immune compromised individuals such as those co-infected with HIV, an anti-tumors necrosis factor therapy or with diabetes. Figure 1.4 illustrates the spread of TB at the cellular level [17].

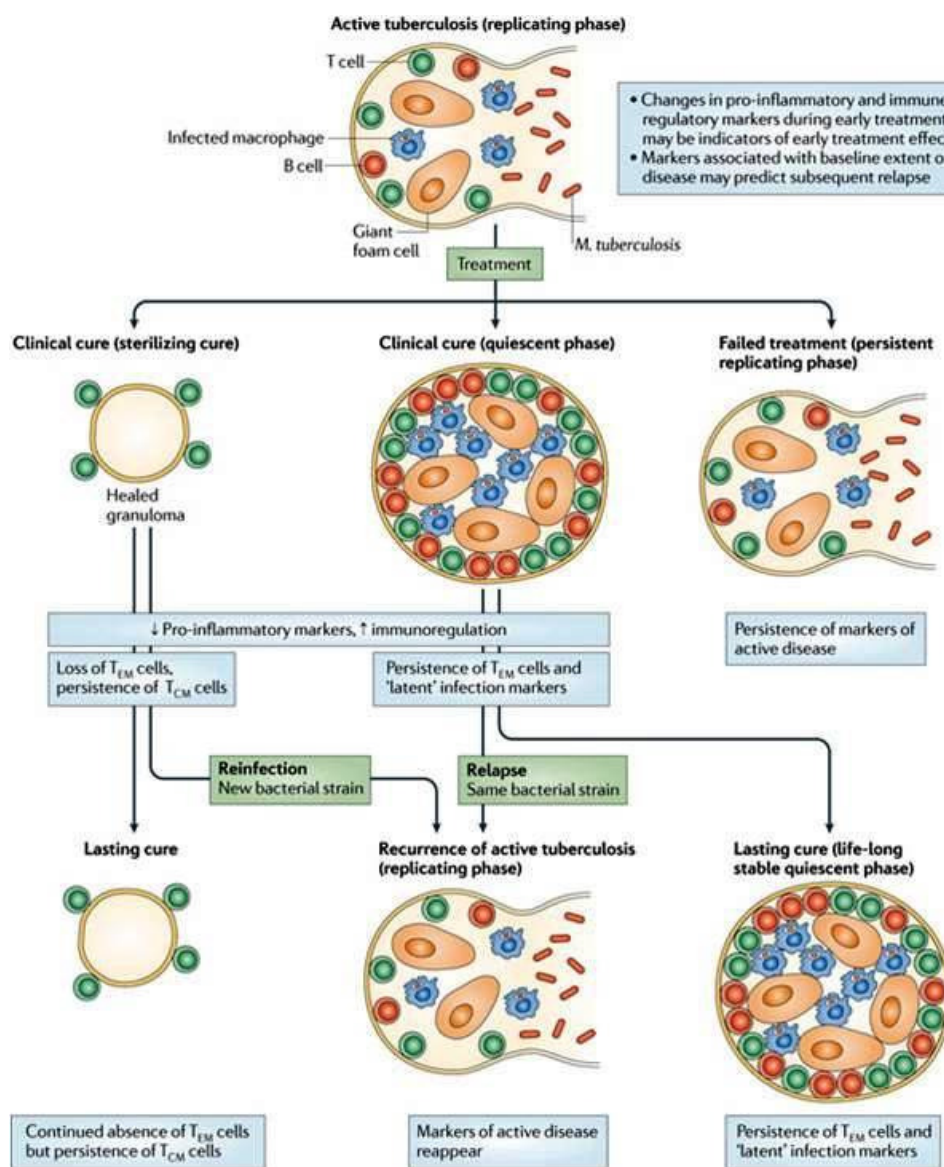


Figure 1.4: Spread of TB at the molecular level. [17]

1.3. Current TB Drugs

Modern TB chemotherapy started with the discovery of streptomycin (SM) in 1944 by Schatz, Bugie and Waksman. Two years later, para-amino-salicylate (PAS) was discovered by Lehmann based on a previous observation by Bernheim that salicylate uniquely stimulated oxygen consumption in tubercle bacillus [18-19]. In 1952, two important front-line TB drugs, isoniazid (INH) Zhang et al. and pyrazinamide (PZA), both of which were discovered based on the weak activity of nicotinamide against tubercle bacilli, were introduced in the clinical treatment of TB. Despite their structural similarity (Figure 1.5) and their nicotinamide origin, INH and PZA have very different mechanisms of action (Table 1.1). Ethambutol (EMB), a synthetic antitubercular, was discovered in 1961, followed by the introduction of rifampin (RIF) in 1967; both compounds are effective TB drugs. Various other drugs such as kanamycin, amikacin, capreomycin, cycloserine, ethionamide, thiacetazone, were mainly used as second-line drugs in the treatment of relapsed or drug-resistant cases. An important observation in the early days of TB chemotherapy was that use of single drugs invariably led to selection of drug-resistant bacilli but a combination of two or more drugs greatly reduced emergence of drug resistance [20-22]. The course of treatment between the 1950s and 70s was typically 12-24 months, but through the efforts of the British Medical Research Council in the 1970s and early 1980s, it was found that inclusion of RIF and PZA greatly reduced the treatment duration from 12-24 months to 6 months. This was the beginning of short course chemotherapy and is the basis for the current TB therapy (Table 1.2).

Current TB drugs can be divided into first-line drugs isoniazid (INH), rifampin (RIF), pyrazinamide (PZA), Ethambutol, Streptomycin, and second-line drugs para-amino-salicylate (PAS), kanamycin, cycloserine (CS), ethionamide (ETA), amikacin, capreomycin, thiacetazone, and fluoroquinolones. TB drugs can also be classified according to their specificity into TB specific drugs (INH, PZA, EMB, PAS, CS, ETA, thiacetazone etc.) and broad-spectrum drugs (RIF, SM, kanamycin, amikacin, capreomycin, fluoroquinolones). While mechanisms of resistance to TB specific drugs are specific to *M. tuberculosis*, mechanisms of resistance to the broad-spectrum drugs are the

same as in other bacterial species such as *E. coli*. First-line and second-line TB drugs, their structures and targets of inhibition are shown in Table 1.1, Figure 1.5 and 1.6 [23-27].

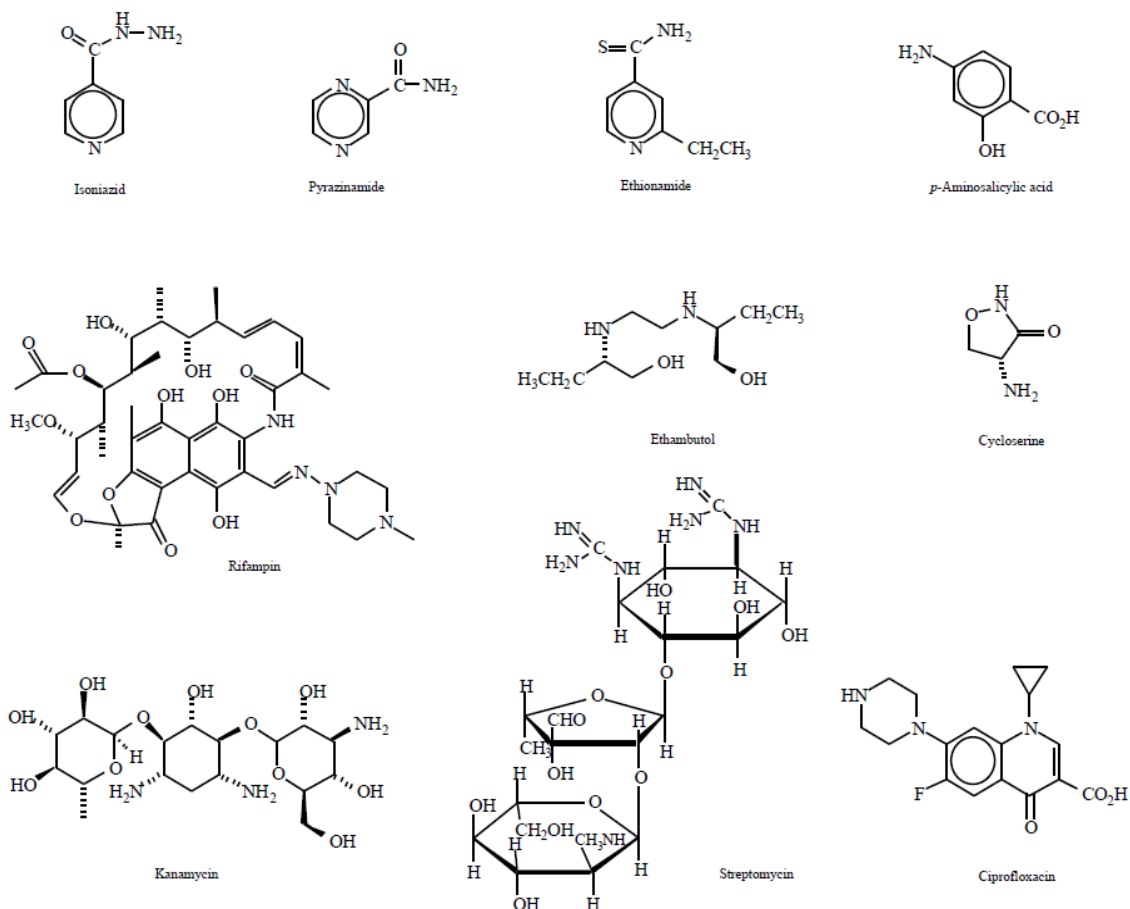


Figure 1.5. Structures of a list of first-line and second-line TB drugs [23]

Table 1.1: Current TB Drugs and their Targets

Drugs	Mechanisms of action	Genes involved in resistance	Targets
Isoniazid	Inhibition of cell wall mycolic acid synthesis, and other potential multiple effects on DNA, lipids, carbohydrates, and NAD metabolism	<i>katG</i> * <i>inhA</i> <i>kasA</i> <i>ndh</i>	Multiple targets including acyl carrier protein reductase (InhA), β -ketoacyl synthase (KasA)
Rifampin	Inhibition of RNA synthesis	<i>rpoB</i>	RNA polymerase β subunit
Pyrazinamide	Disruption of membrane function and energy metabolism, Inhibition of fatty acid synthesis?	<i>pncA</i> * <i>fasI</i> ?	Membrane function and energy metabolism, FasI?
Ethambutol	Inhibition of cell wall arabinogalactan synthesis	<i>embCAB</i>	Arabinosyl transferase
Streptomycin	Inhibition of protein synthesis	<i>RpsL</i> <i>rrs</i>	Ribosomal S12 protein and 16S rRNA
Amikacin/Kanamycin /Capreomycin	Inhibition of protein synthesis	<i>rrs</i>	16S rRNA
Fluoroquinolones	Inhibition of DNA gyrase	<i>GyrA</i> <i>gyrB</i>	DNA gyrase
Ethionamide	Inhibition of mycolic acid synthesis	<i>InhA</i> <i>etaA</i> *	Acyl carrier protein reductase (InhA)
Cycloserine	Inhibition of peptidoglycan synthesis	<i>alrA/dadB</i>	D-alanine racemase/synthase
PAS	Inhibition of folic acid synthesis and iron uptake?	unknown	unknown

*KatG, PncA and EtaA are not targets of inhibition but enzymes involved in the activation of prodrugs INH, PZA and ETA, respectively

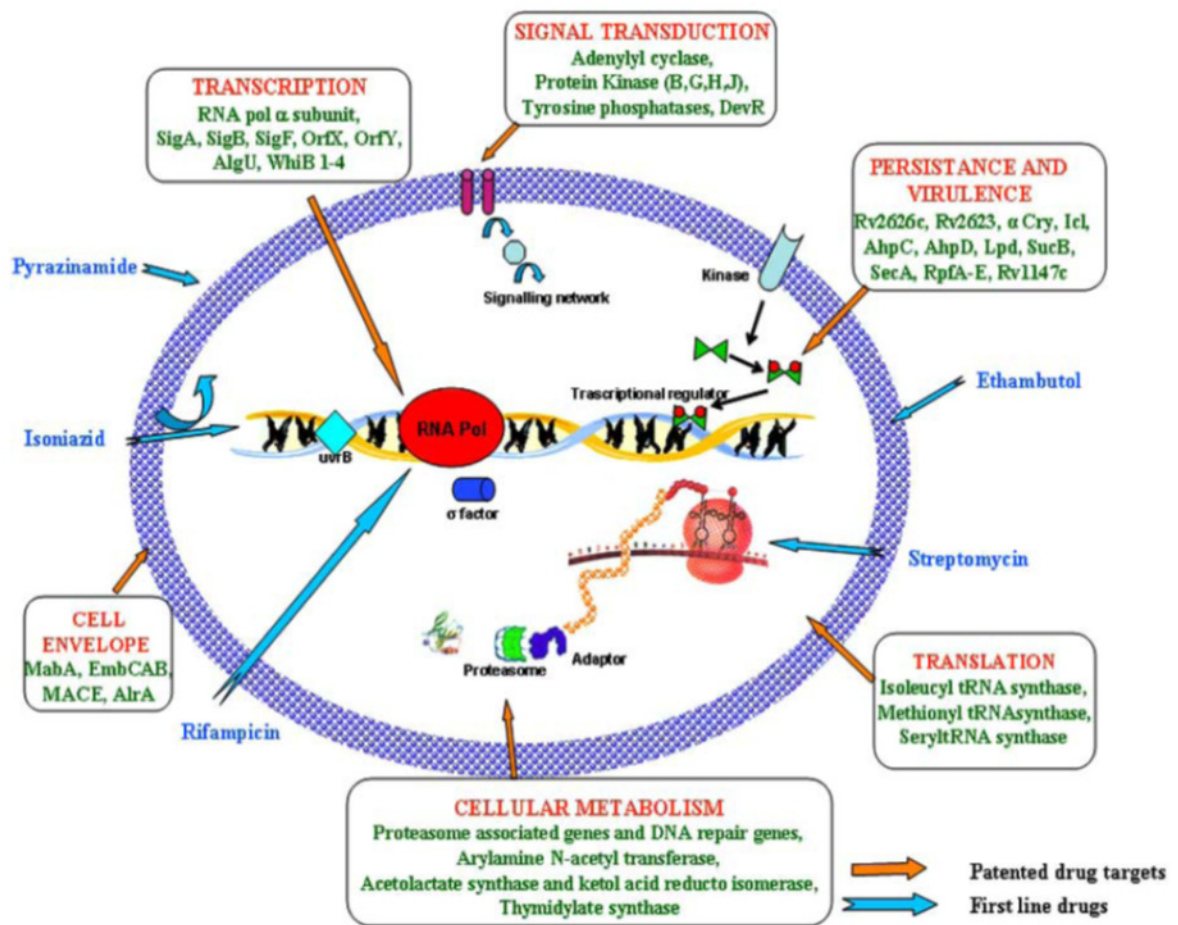


Figure 1.6: An outline of Patent Protected drug targets of *M. tuberculosis* [26]

1.4. Drug Resistance

Drug resistance in tuberculosis (TB) is a matter of great concern for TB control programs since there is no cure for some multidrug-resistant TB (MDR-TB) strains of *M. tuberculosis*. There is concern that these strains could spread around the world, stressing the need for additional control measures, such as new diagnostic methods, better drugs for treatment, and a more effective vaccine. MDR-TB, defined as resistance to at least

rifampicin (RIF) and isoniazid (INH), is a compounding factor for the control of the disease, since patients harboring MDR strains of *M. tuberculosis* need to be entered into alternative treatment regimens involving second-line drugs that are more costly, more toxic, and less effective.

Moreover, the problem of extensively drug resistant (XDR) strains has recently been introduced. These strains, in addition to being MDR, were initially defined as having resistance to at least three of the six main classes of second-line drugs (aminoglycosides, polypeptides, fluoroquinolones, thioamides, cycloserine, and paraaminosalicylic acid). More recently, at a consultation meeting of the World Health Organization (WHO) Global Task Force on XDR-TB, held in Geneva, a revised laboratory case definition was agreed: “XDR-TB is TB showing resistance to at least rifampicin and isoniazid, which is the definition of MDR-TB, in addition to any fluoroquinolone, and to at least 1 of the 3 following injectable drugs used in anti-TB treatment: capreomycin, kanamycin and amikacin.” XDR-TB now constitutes an emerging threat for the control of the disease and the further spread of drug resistance, especially in HIV-infected patients, as was recently reported. For this reason, rapid detection of drug resistance to both first- and second line anti-tuberculosis drugs has become a key component of TB control programs. Current regimen for treatment of drug susceptible tuberculosis is illustrated in Table 1.2 and the illustration of resistance at cellular level is seen in figure 1.4 [28].

Table 1.2: Current regimens for treatment of drug susceptible tuberculosis

Regimen	Initial phase	Continuation phase
Daily*	2 months of isoniazid, rifampicin, and pyrazinamide, with or without ethambutol	4 months of isoniazid and rifampicin
Intermittent†	2 weeks of daily isoniazid, rifampicin, pyrazinamide and streptomycin or ethambutol	24 weeks of twice weekly isoniazid and rifampicin
	8 weeks of thrice weekly isoniazid, rifampicin, pyrazinamide and streptomycin or ethambutol	18 weeks of thrice weekly isoniazid and rifampicin

*The daily regimen is used when patients self-administer their drugs. There is enough redundancy that, if patients miss some of their doses, the outcome will remain acceptable

†The intermittent regimens are intended for directly observed therapy

The last drug with a new mechanism of action approved for TB was rifampicin (discovered in 1963). Further complicating the situation are drug–drug interactions that preclude the co-administration of some available TB drugs with certain anti-HIV treatments or other chronic disease medications, such as those used in diabetics. To achieve global control of this epidemic, and there is an urgent need for new TB drugs with the features described in Table 1.3.

Table 1.3 Desired target product profile for a new TB drug

Desired target product profile	Biological characteristics
Treat MDR-TB and XDR-TB	New chemical class with a new mechanism of action Existing chemical class covering resistant isolates Drugs with low toxicity issues, like hepatotoxicity
Shorten treatment duration	Strongly bactericidal activity Good activity on latent or dormant or heterogeneous populations More potent and safer regimens of a novel drug and its combinations
Lower dosing frequency	Good pharmacokinetics including longer half-life and target tissue levels Retain potency when administered intermittently (for example, 1–3 times a week) Novel fixed-dose formulations and delivery technologies
Reducing pill burden	Combinations of more efficacious drugs to reduce number of pills taken Child-friendly formulation of newer drugs
Drug–drug interactions	No cytochrome P450 induction liabilities Minimal drug–drug induction particularly with antiretrovirals or oral diabetics

Each target product profile feature is accompanied by the biological characteristics needed to accomplish that respective feature

The challenge of meeting the expectations of this desired target product profile complicates drug discovery efforts. Considering how few drugs from the discovery stage successfully enter the TB clinical pipeline, an increased understanding of the drug discovery hurdles should facilitate development of novel intervention strategies. The situation is further hampered by the unfavourable economics of TB drug development and the lack of proper policy incentives.

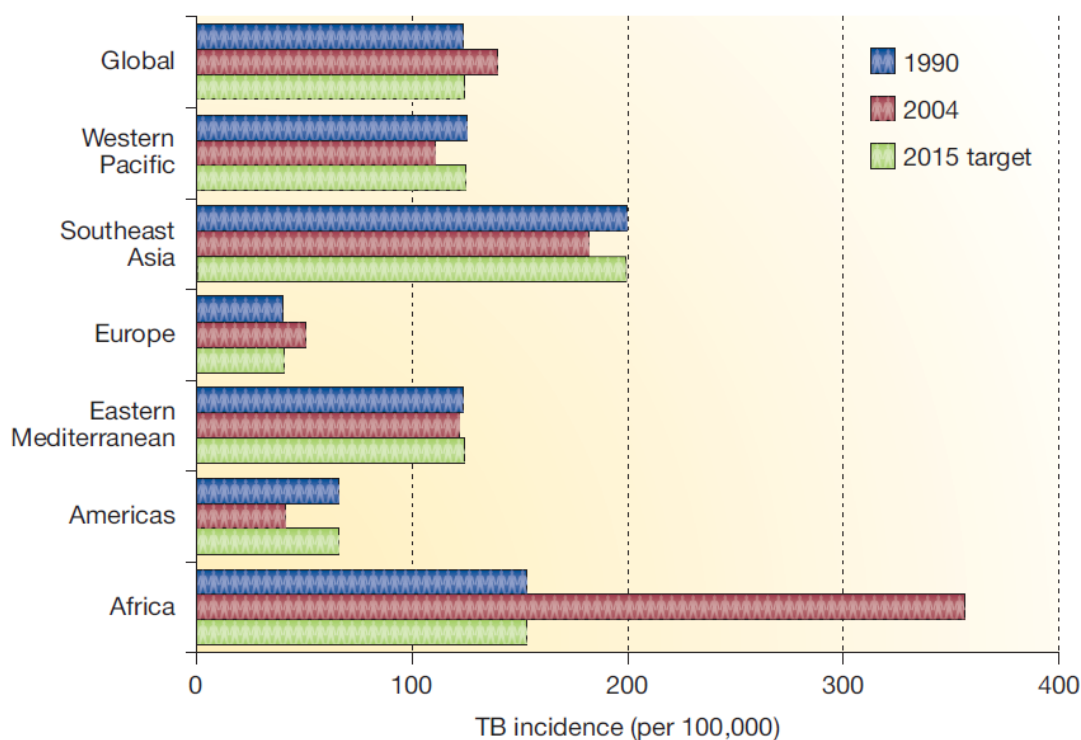


Figure 1.7: Incidence of tuberculosis, 1990–2004, also includes the targets for 2015[29].

WHO-led global control programs aim to reverse the rise in TB incidence by 2015 and to halve the 1990 prevalence and morbidity rates globally. The costs of reaching these targets will be substantial: the WHO estimates a total cost of \$56 billion over 10 years to implement its global plan to stop TB, but anticipates that funding of only around 45% of this total will be available.

Chapter 2- Literature Review

Despite the relative efficacy of current treatment, the various antibiotics that constitute first and second-line drugs for TB therapy target only a small number of core metabolic processes such as DNA and RNA synthesis, cell wall synthesis, and energy metabolism pathways [30]. New classes of drugs with additional drug targets that are difficult to overcome by mutation are urgently needed [31]. Desirable new targets should be involved in vital aspects of bacterial growth, metabolism and viability whose inactivation would lead to bacterial death or inability to persist, thus therapy could be shortened and drug resistant strains could be eliminated or drastically reduced [32,33]. Moreover, targets involved in the pathogenesis of the disease process should also be considered for drug development [34, 35].

The discovery of the complete genome sequence of TB bacteria helped to identify several important drug targets [36]. Various groups have used this genomic information to identify and validate targets as the basis for development of new Anti-TB agents. Besides, mycobacterial genetic tools, such as transposon mutagenesis, gene knockout, and gene transfer, greatly facilitate target identification.

2.1. Drug targets

2.1.1. Cell wall biosynthesis related targets

Cell wall biosynthesis is a particularly good source of molecular targets because the biosynthetic enzymes do not have homologues in the mammalian system [32]. The cell wall of *M. tuberculosis* is very important for its survival within constrained conditions such as those inside of human macrophages. The biosynthesis of the cell wall components involves many important stages and different enzymes that are absent in mammals and could be attractive drug targets [37-39]. Few such targets are as follows:

Isoprenoid precursors, which are a large group of natural products and play key roles in many biological pathways, can only be biosynthesized by the 2-C-methyl-D-erythritol 4-phosphate pathway in *M. tuberculosis* [40-42]. The 4-diphosphocytidyl-2-C-methyl D-

erythritol kinase (IspE), which is an essential enzyme in the isoprenoid precursor biosynthesis pathway, catalyzes ATP-dependent phosphorylation of 4-diphosphocytidyl-2-C-methyl-D-erythritol (CDP-ME) to 4-diphosphocytidyl-2-C-methyl-D-erythritol-2-phosphate and plays a crucial role in *M. tuberculosis* survival. Therefore, IspE is characterized as an attractive and potential target for antimicrobial drug discovery. However, no experimental structure of *M. tuberculosis* IspE has been reported, which has hindered our understanding of its structural details and mechanism of action. Here, the expression and purification of fully active full-length *M. tuberculosis* IspE and solve the high-resolution crystal structures of IspE alone and in complex with either the substrate CDP-ME or non hydrolyzable ATP analog or ADP. The structures present a characteristic galactose /homoserine /mevalonate /phosphor mevalonate kinase superfamily α/β -fold with a catalytic center located in a cleft between 2 domains and display clear substrate and ATP binding pockets. Distinct differences in ligand binding of *M. tuberculosis* IspE with other reported IspEs. Combined with the results of mutagenesis and enzymatic studies, our results provide useful information on the structural basis of IspE for future anti-tubercular drug discovery targeting this kinase.

Peptidoglycan biosynthesis (Figure 2.1) [44] is another source of potential drug targets. For instance, alanine racemase and D-Ala-D-Ala-ligase catalyze the first and second committed steps in bacteria and are good drug targets.

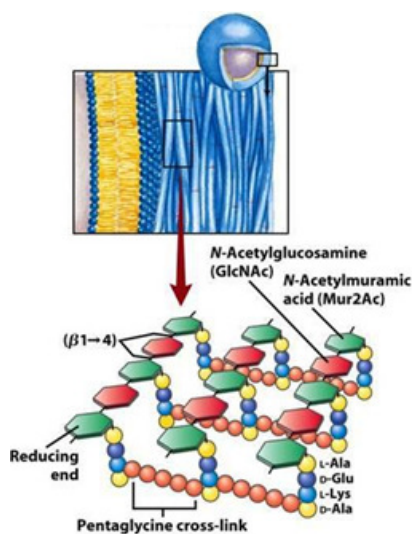


Figure. 2.1(a) Structure of peptidoglycan [44]

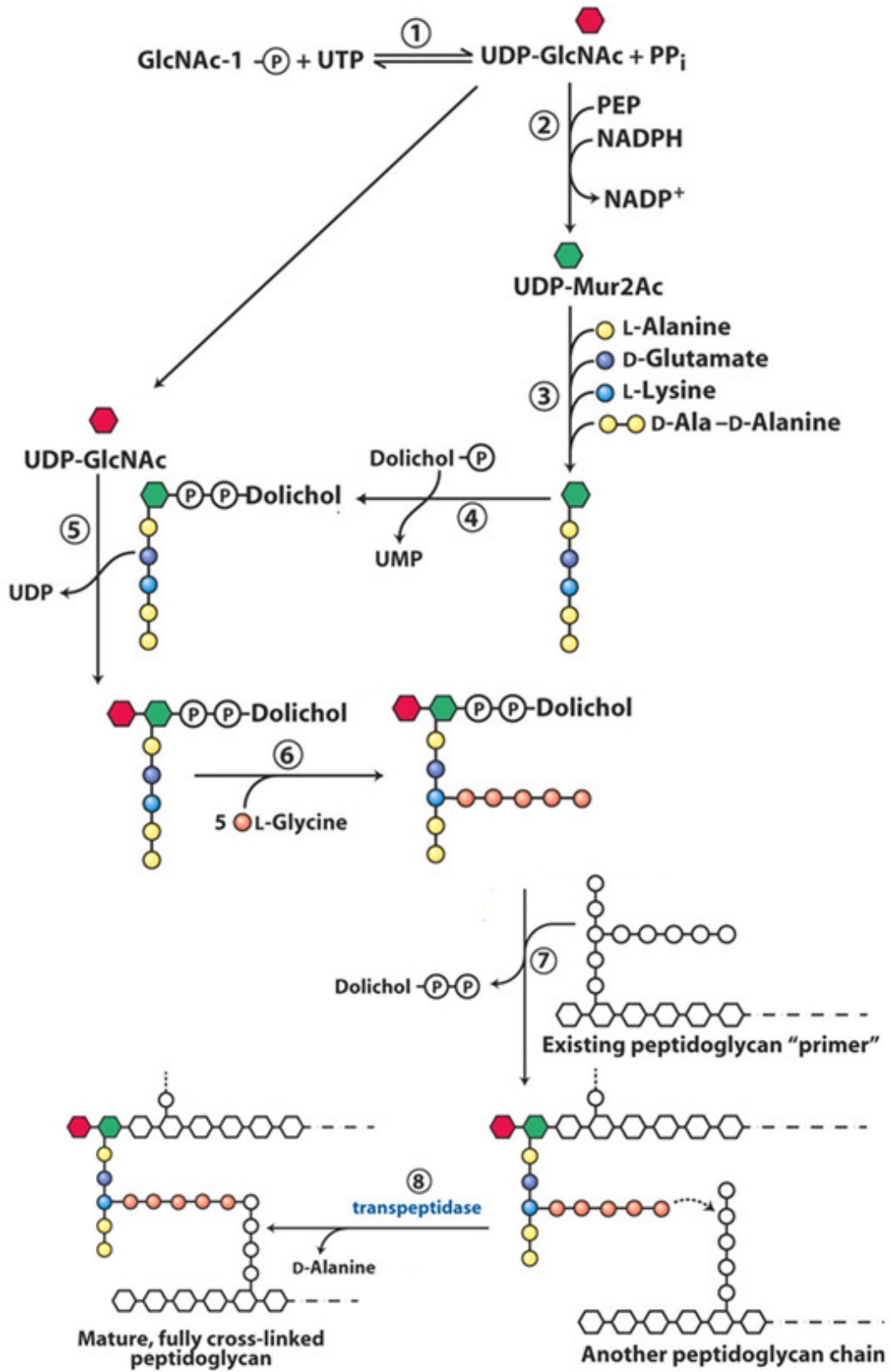


Figure. 2.1: (b) Peptidoglycan biosynthetic pathway

Both alanine racemase and D-Ala-D-Ala ligase are inhibited by D-cycloserine, a second line anti-TB drug [45-46].

Another good drug target is the **pyridoxal 5'-phosphate** containing enzyme Alr that catalyzes the racemization of L-Alanine into D-Alanine, a major component in the biosynthesis of peptidoglycan [47].

Arabinogalactan biosynthesis, (Figure. 2.2) a novel arabinofuranosyltransferase that catalyzes the addition of the first key arabino furanosyl residue of the galactan core, is not sensitive to EMB, but is essential for viability [48]. The first committed step in the synthesis of decaprenyl phosphoryl-D-arabinose, the lipid donor of mycobacterial D-arabino furanosyl residues during arabinogalactan biosynthesis, is the transfer of a 5-phosphoribosyl residue from phosphoribose diphosphate to decaprenyl phosphate to form decaprenylphosphoryl-5-phosphoribose. The ribosyltransferase that catalyzes the first committed step in the synthesis of decaprenyl-phosphoryl-D-arabinose, the lipid donor of mycobacterial d-arabinofuranosyl residues, has also recently been characterized and shown essential for growth [50].

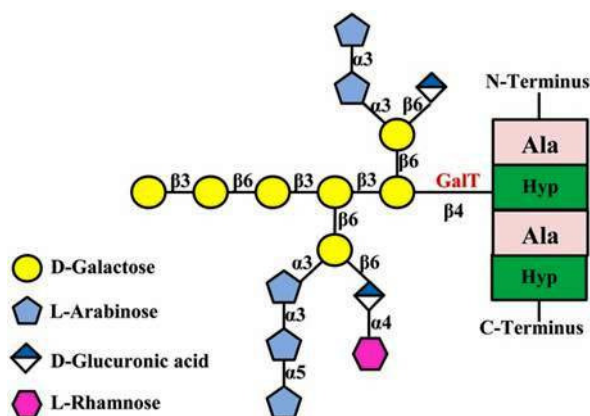


Figure. 2.2: AG structure of an AGP molecule [50].

Studies into the mechanism of action of ethambutol in *M. avium* identified a gene cluster that conferred resistance to this antibiotic when overexpressed [51]. Further studies

showed that the products of this gene cluster - EmbA, EmbB and EmbC - are involved in the formation of the terminal hexaarabino furanoside portion of arabinogalactan, where mycolic acids are attached [52].

Other enzymes essential for arabinogalactan biosynthesis have been identified, including UDP-galactopyranosemutase (encoded by the *M. tuberculosis* *glf* gene) [53], galactofuranosyltransferase [54] and dTDP-6-deoxy-Llyxo-4-hexulose reductase, the enzyme that catalyzes the final step in the formation of dTDP-rhamnose. dTDP-rhamnose is a product of four enzymes, RmlA–D, and a recent report has demonstrated that both RmlB and RmlC are essential for mycobacterial growth [55].

2.1.2. Mycolic acid biosynthesis related targets

Within the mycobacteria lipid metabolism, mycolic acids are essential structural components of the mycobacterial cell wall [56]. The early stage of fatty acid biosynthesis, which generates the precursors of mycolic acids, is a rich source of antibacterial targets [57]. Mycolic acids (Figure 2.3), which are key components of the mycobacterial cell wall, are alpha-alkyl, beta-hydroxy fatty acids, with a species-dependent saturated "short" arm of 20-26 carbon atoms and a "long" mero mycolic acid arm of 50-60 carbon atoms. The latter arm is functionalized at regular intervals by cyclopropyl, alpha-methyl ketone, or alpha-methyl methyl ethers groups. The mycolic acid biosynthetic pathway has been proposed to involve five distinct stages: (i) synthesis of C20 to C26 straight-chain saturated fatty acids to provide the alpha-alkyl branch; (ii) synthesis of the mero mycolic acid chain to provide the main carbon backbone, (iii) modification of this backbone to introduce other functional groups; (iv) the final Claisen-type condensation step followed by reduction; and (v) various mycolyl transferase processes to cellular lipids [58].

It is also the site of action of INH and ethionamide. *M. tuberculosis* has both types of fatty acids synthase (FAS) systems found in nature, FAS-I and FAS-II. FAS-I is the system responsible for de novo synthesis of C16-C26 fatty acids and the FAS-II system

extends these fatty acids up to C56 chains to make precursors of mycolic acids, which are essential for growth. Since enoil-ACP reductase (InhA) is the target of INH, it is reasonable to assume that all steps in the FAS-II pathway will be essential for the viability of *M. tuberculosis*. Many of the individual enzymes of the FAS-II system have been expressed, purified and characterized this is proven target for new antibacterial drugs.

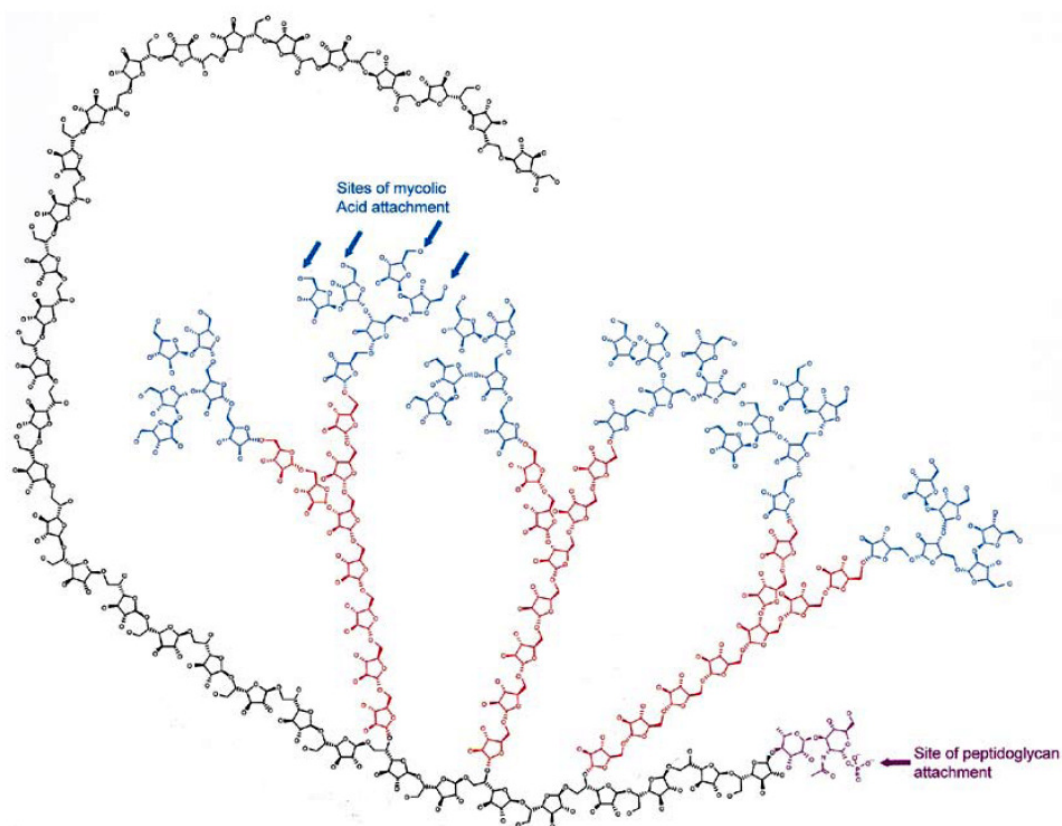


Figure 2.3: A typical arabinogalactan molecule from *M. Tuberculosis* [53]

2.1.3. Energy production related targets

All bacteria require energy to remain viable. Although the energy production pathways in *M. tuberculosis* are not well characterized, their importance as drug targets is demonstrated by the recent finding that PZA (a frontline TB drug that is more active against non-growing persistent bacilli than growing bacilli and shortens TB therapy) acts

by disrupting membrane potential and depleting energy in *M. tuberculosis*. This study implies that energy production or maintenance is important for the viability of persistent non-growing tubercle bacilli in vivo. The recent discovery of the highly effective TB drug diaryl quinoline also highlights the importance of energy production pathways for mycobacteria. It is likely that energy production pathways, such as the electron transport chain, glycolytic pathways (like the Embden–Meyerhof pathway) and fermentation pathways, could be good targets for TB drug development.

Isocitrate lyase (ICL) is an important enzyme in this category and also an important drug target. ICL is involved in energy production via the metabolism of acetyl-CoA and propionial CoA of the glyoxylate pathway. The enzyme isocitrate lyase (ICL) is jointly required for fatty acid catabolism and virulence in *Mycobacterium tuberculosis* [59, 60]. Although deletion of *icl1* or *icl2*, the genes that encode ICL1 and ICL2, respectively, had little effect on bacterial growth in macrophages and mice, deletion of both genes resulted in complete impairment of intracellular replication and rapid elimination from the lungs. The feasibility of targeting ICL1 and ICL2 for chemical inhibition was shown using a dual-specific ICL inhibitor, which blocked growth of *M. tuberculosis* on fatty acids and in macrophages. The absence of ICL orthologs in mammals should facilitate the development of glyoxylate cycle inhibitors as new drugs for the treatment of tuberculosis.

2.1.4. Amino acid biosynthesis related drug targets

Amino acid biosynthesis is another important target for developing anti-TB drugs. The shikimate pathway is very important and is involved in the synthesis of aromatic amino acids in algae, fungi, bacteria, and higher plants; however, it is absent in the mammalian system. The final product of the shikimate pathway, chorismate, is a key biosynthetic intermediate involved in generating aromatic amino acids and other metabolites. The entire pathway is essential in *M. tuberculosis* [39, 61]. This feature makes the pathway an attractive target for developing anti-TB drugs with minimum cross reactivity [62]. Other enzymes of this pathway are also likely to be essential and shikimate dehydrogenase [63] and 5-enol pyruvyl shikimate 3-phosphate synthase [64] have been characterized in

detail. The biosynthesis of non-aromatic amino acids is also emerging as a potential drug target. The impact of amino acids such as lysine [65], proline, tryptophan and leucine [66] is evident from the fact that knocked out *M.tuberculosis* strains of the genes required for amino acid biosynthesis showed less virulence [65,67]. Another attractive target of the lysine biosynthesis pathway is the enzyme dihydro dipicolinate reductase, for which potent inhibitors have been identified [68].

2.1.5. Cofactor-related drug targets

Several cofactor biosynthetic pathways and pathways requiring some cofactors are good candidates for identification of new drug targets. Folate derivatives are cofactors utilized in the biosynthesis of essential molecules including purines, pyrimidines, and amino acids. While bacteria synthesize folate de novo, mammals must assimilate preformed folate derivatives through an active transport system [32]. Dihydrofolate reductase, which catalyses the reduction of dihydrofolate to tetrahydrofolate, a key enzyme in folate utilization whose inhibition may affect the growth of *M. tuberculosis* [69] and dehydropteroate synthase are validated targets of the widely used antibacterial sulfonamide, trimethoprim [70].

Two enzymes involved in the de novo biosynthesis of NAD that affects the NADH/NAD⁺ ratio upon which *M. tuberculosis* is dependent, have been studied as possible drug targets [71]. Maintaining redox balance and shuttling reducing equivalents with NAD/NADH is important to all cells, but especially for hypoxic MTB, where alternative electron acceptors must be used. Boshoff et al performed a careful analysis of the salvage versus de novo synthesis pathway for these nicotinamide cofactors [72]. The salvage pathway was upregulated and functionally active under in vitro hypoxia, and in vivo. The conclusion for therapeutic intervention is that an inhibitor must target NAD synthesis after the two pathways have converged, since either pathway alone is capable of maintaining homeostasis. Genomic analysis studies have suggested that the riboflavin biosynthesis pathway is essential in *M. tuberculosis* [73] and the lumazine synthase pathway has been validated as a target for anti-TB drug discovery.

2.1.6. DNA metabolism

Differences in mammalian and mycobacterial thymidin monophosphate kinase have been studied and exploited in an attempt to find selective inhibitors for this drug target [74, 75]. Other targets are ribonucleotide reductases that catalyze the first committed step in DNA synthesis and have differences with corresponding mammalian enzymes [76, 77]; DNA ligases, that play an important role in the replication and repair of DNA, are classified as NAD⁺ or ATP dependent. NAD⁺ dependent ligases are only found in some viruses and eubacteria. LigA is essential for growth of *M. tuberculosis* [78] and inhibitors that distinguish between the two types of ligases and have anti-TB activity have been identified [79]. DNA gyrase has also been validated as a target for *M. tuberculosis*, since this is the only type II topoisomerase [36] that it possesses. Its inhibition by fluoroquinolones results in highly mycobactericidal activity.

2.1.7. Menaquinone biosynthesis

It appears that menaquinone is the only quinone in mycobacterial electron transport chain and, since the pathway leading to the biosynthesis of menaquinone is absent in humans, the bacterial enzymes catalyzing the synthesis of menaquinone from chorismate are potential novel targets for drug discovery [80]. The bacterial homologues of MenA-E and MenH have been described in *M. tuberculosis*. Since latent MTB must presumably respire at some low rate in order to remain viable; compounds that target respiration have the potential to be active against non-replicating MTB.

2.1.8. Other potential drug targets in *M. tuberculosis*

The tubercle bacillus produces no less than 20 cytochrome p450 enzymes, some of which appear to play essential roles [81]. Antifungal azole drugs target these enzymes and the cytochrome p450 homologues in the bacteria. Drugs like miconazole and clotrimazole are active against *M. tuberculosis* [82]. Subsequent crystallization studies of

the *M. tuberculosis* cytochrome p450 enzyme system evoked studies to evaluate new drugs [83].

Peptide deformylase inhibitors may be effective against *M. tuberculosis* since peptide deformylase catalyzes the hydrolytic removal of the B-terminal formyl group from nascent proteins. It is a metallo protease essential for maturation of nascent polypeptides in bacteria but not essential for humans, making it an attractive target for antibacterial drug development; however, it has little effect on slow growing TB bacteria [84, 85].

Another important set of emerging drug targets are the components of the siderophore biosynthesis of *M. tuberculosis* [86]. Upon infection, as a part of the defense mechanism, the host has several mechanisms to withdraw or control the free extracellular, as well as intracellular, iron concentration [87, 88]. Mycobacteria have an unusual reliance on serine/threonine protein kinases as the main component of signal transduction pathways [89], and there is considerable activity around this transduction system since some of these enzymes are essential for growth [90]. *M. tuberculosis* synthesizes mycothiol in a multistep process involving four enzymatic reactions for protection against the damaging effects of reactive oxygen species. This pathway is absent in humans, and it has been shown to be essential to *M. Tuberculosis* [91].

2.2. Rational drug design

One of the design strategies for new anti-TB compounds (Figure 2.4) is based on the development of analogs of first-line and/or second line drugs. In this section we review the strategies employed and analyze structure-activity relationships (SAR), which have led to the development of new anti-TB agents. In addition, we review new pharmacophore groups. One problem that must be considered in the design of anti-TB compounds is that there is a subpopulation of bacteria in a persistent non-replicating state. This is considered a major contributing factor to long drug treatments for TB. For this reason, it is important to determine if compounds have potential activity against these bacteria at the onset of design. We should also consider the physicochemical properties

that directly affect the pharmacokinetics and pharmacodynamics of drugs. An example of this is the influence of stereoisomers on biological activity, because individual enantiomers have significant differences in activity, although sometimes the activity of some enantiomers cannot be explained.

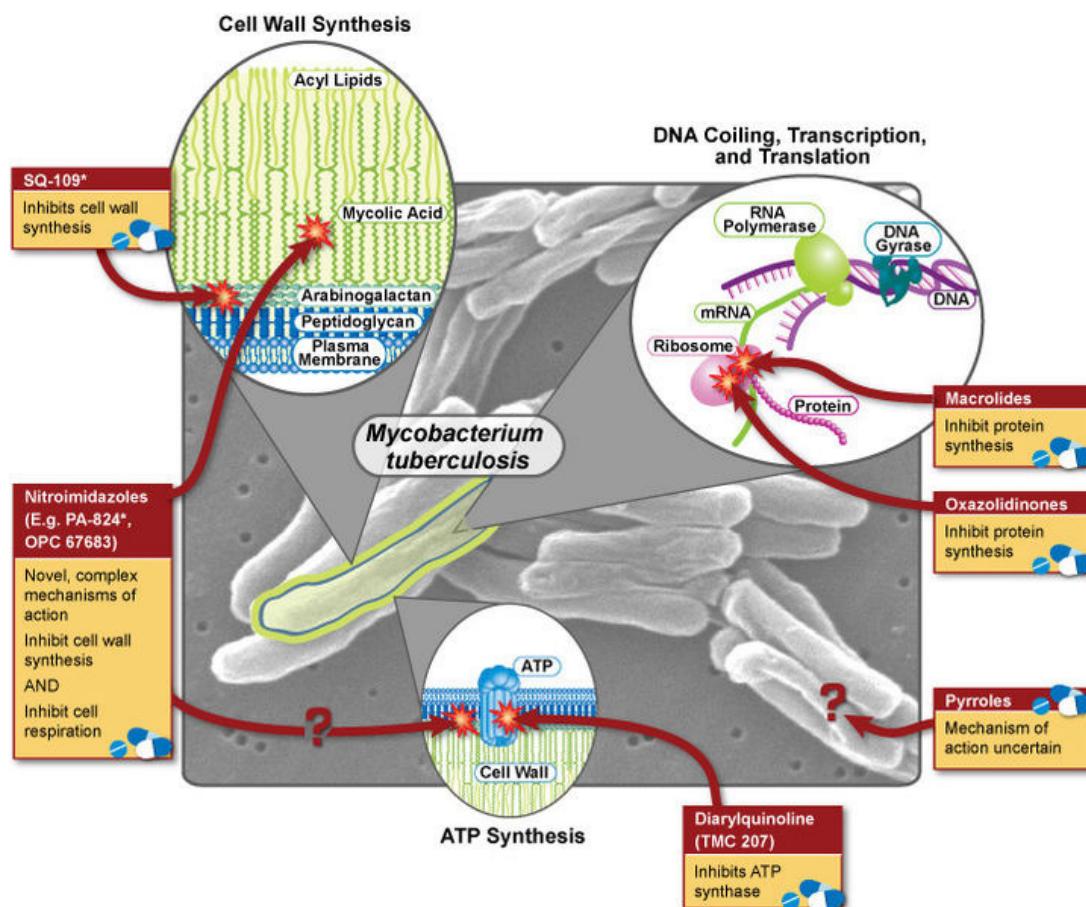


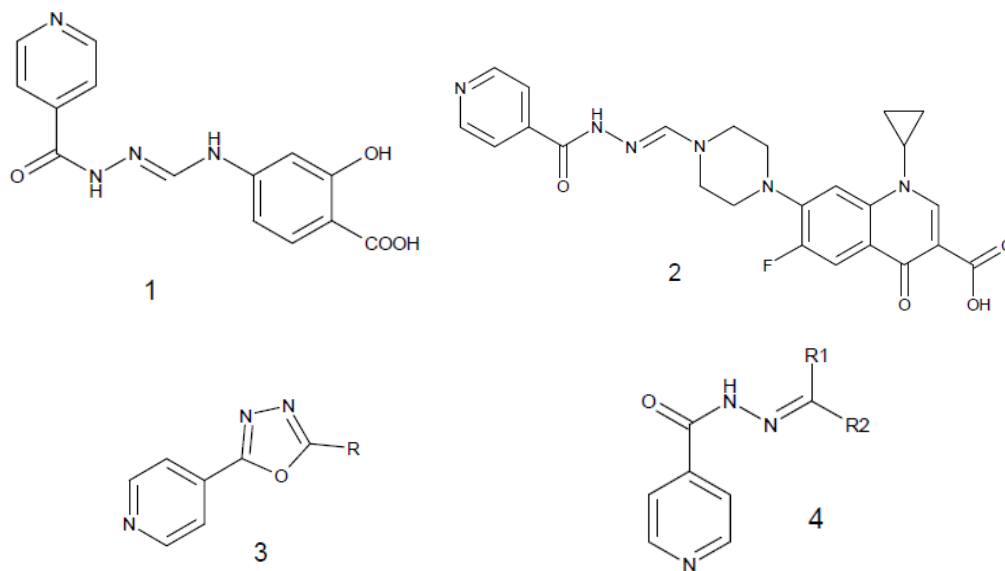
Figure 2.4. Tuberculosis drugs-and their mechanism of action

2.2.1. Isoniazid derivatives

One of the strategies frequently used in medicinal chemistry to develop new drugs is “hybridization”, a method that has been proposed particularly for new anti-TB drugs. An example is the design of molecules based on INH or PZA, incorporating NR1R2 groups derived from a second anti-TB molecule or possibly other nucleophilic groups to provide anti-TB activity. With special interest compounds 1 and 2 (figure 2.5.) were obtained.

These could be considered prodrugs because they contain two conventional drugs that are bound by a CH fragment. Although the results of activity are very similar to those presented by INH and PZA, the hydrolysis of new compounds ensures prolonged release of the active drugs [92].

A variety of compounds derived from INH that include mostly a hydrazine fragment have been determined. Following this strategy and considering the inclusion of an oxadiazole moiety, Navarrete et al, developed new agents with high anti-TB activity (3, figure 2.5). Due to the substitution in 5-position on the oxadiazole ring, the compounds obtained showed high lipophilicity, hypothesizing that this lipophilicity could facilitate passage of these compounds through the *M. tuberculosis* bacterial membrane [93]. Also, structural modification of the hydrazide moiety on INH (4, figure 2.5) provided lipophilic adaptations of the drug that blocked the N-acetylation process, obtained high levels of *in vitro* activity against *M. tuberculosis* and macrophages infected, as well as low toxicity [94].



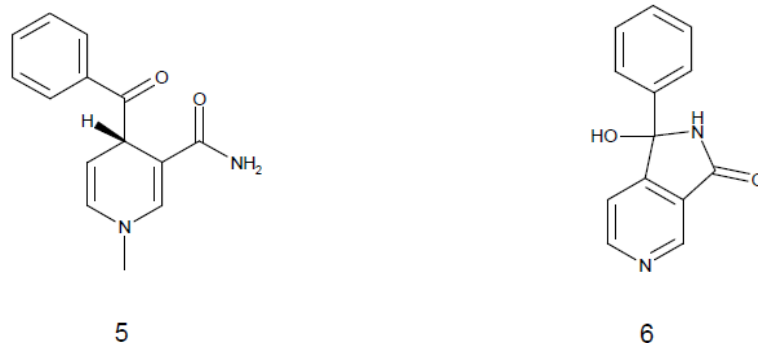


Figure 2.5. Structure of compounds derivatives of anti-TB first line drugs.

Another strategy in drug design is the formation of molecules that mimic the natural substrate of an enzyme. Delaine et al designed a new series of bi-substrate-type inhibitors based on a covalent association between molecules mimicking the INH substrate and the NAD cofactor that could provide compounds with a high affinity and selectivity for the INH catalytic site (5 and 6, figure 2.5). In these compounds, the authors determined that incorporating a lipophilic component into the nicotinamide hemiamidal frame work provides more active derivatives [95].

2.2.2. Ethambutol derivatives

Amino alcohols that include EMB, which is used for pharmacological TB treatment, are an important class of compounds with various applications. This compound has been widely studied determining that the 1, 2-ethylenediamine moiety is the EMB pharmacophore, possibility due to chelate bond formation with divalent metal ions such as copper. Based on EMB, a second-generation agent has been developed, a compound called SQ109 (7, figure 2.6), which is being tested in clinical trials. It is a drug that exhibits potent activity against *M.tuberculosis* strains, including multidrug resistant strains *in vitro* and *in vivo*. Unfortunately, SQ109 has poor bioavailability of only 12% and 3.8% in rats and dogs, respectively. Studies indicate that this compound undergoes oxidation, epoxidation and *N*-dealkylation, which cause its low bioavailability; therefore

strategies have been designed to improve its bioavailability minimizing this first-pass effect. Prodrugs based on carbamate groups are a good option for reducing this effect. Considering this Meng and colleagues developed a new series of analogues based on carbamate prodrugs of SQ109 (8, figure 2.6) that provide good chemical stability as substrates of plasma esterase. The results of bioavailability of these compounds show a five-fold increase of the SQ109 reference compound [96].

Alternatively, Zhang has carried out the synthesis of new analogues of S2824 (9, figure 2.6), a second-generation compound derived from EMB. The results show that new analogues with a homopiperazine ring (10, figure 2.6) have high *in vitro* activity against both sensitive and drug-resistant *M. tuberculosis* strains [97].

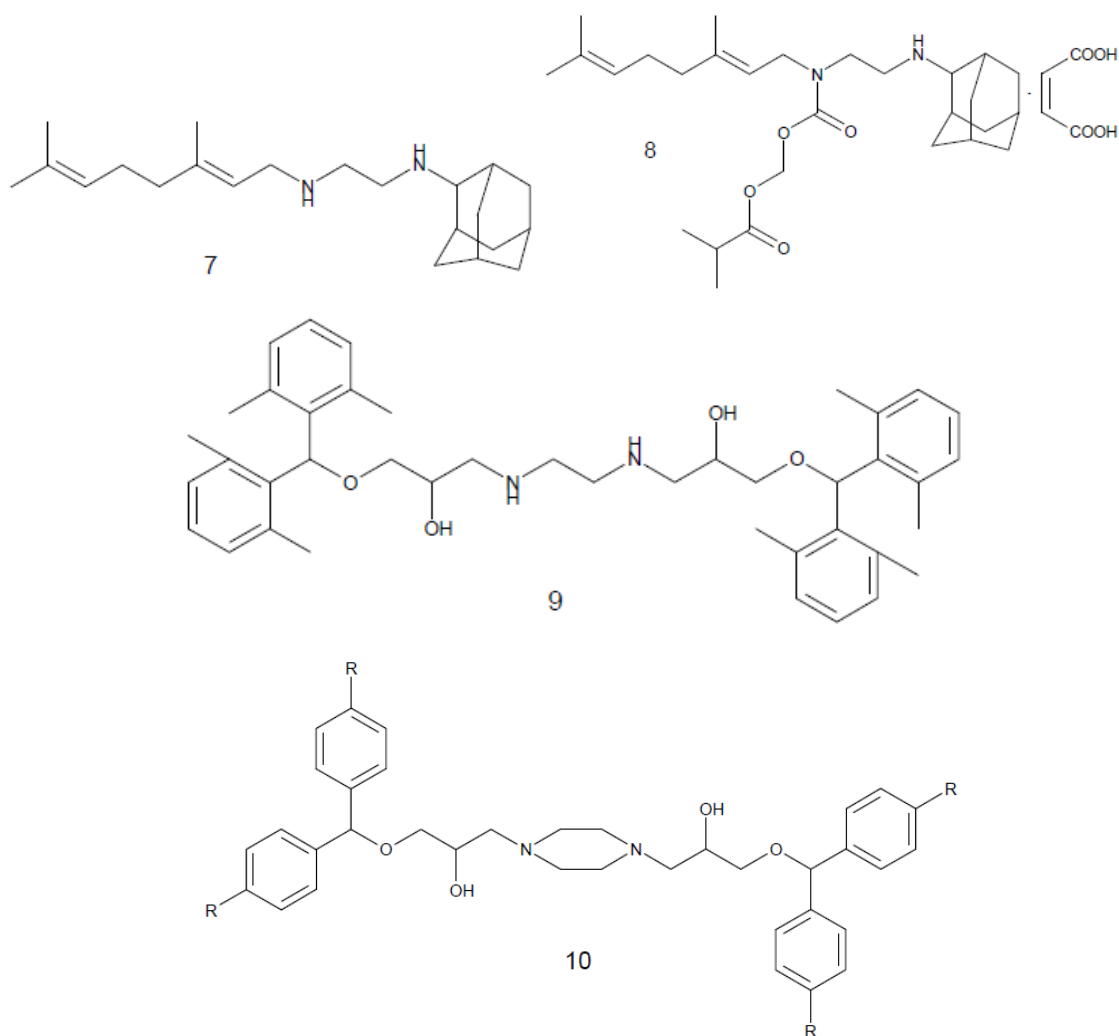


Figure 2.6. Structure of SQ109 and analogs

In the design of new 1, 2-diamine derivatives (11, figure 2.7) compounds with 35 times more activity than EMB have been synthesized. Interestingly, studies show that they do not have the same target as EMB. An SAR analysis has determined that the presence of a β -hydroxy group on the amine increases anti-TB activity; however, the distance between oxygen and nitrogen atoms in EMB are the same as between both atoms in the hydroxyl ethyl amine suggesting a good relationship between both structures (12, figure 2.7). In a new series of EMB analogs obtained by Cunico et al, it was determined that the sulfonamide moiety reduces activity against *M. tuberculosis*, and that the amino alcohol moiety on hydroxy ethyl sulfonamide is crucial for anti-TB activity, where the presence of a carbamate moiety leads to a loss of activity. Consistent with this, it has been reported that if compounds lose the basicity of the amino group (12, figure 2.7); this results in a loss of activity [98]. Finally, EMB has served as a proposal for tripartite hybridization (chloroquine, isoxyl and ethambutol) for the development of new anti-TB agents (13, figure 2.7), which exhibit high activity against *M. tuberculosis* [99].

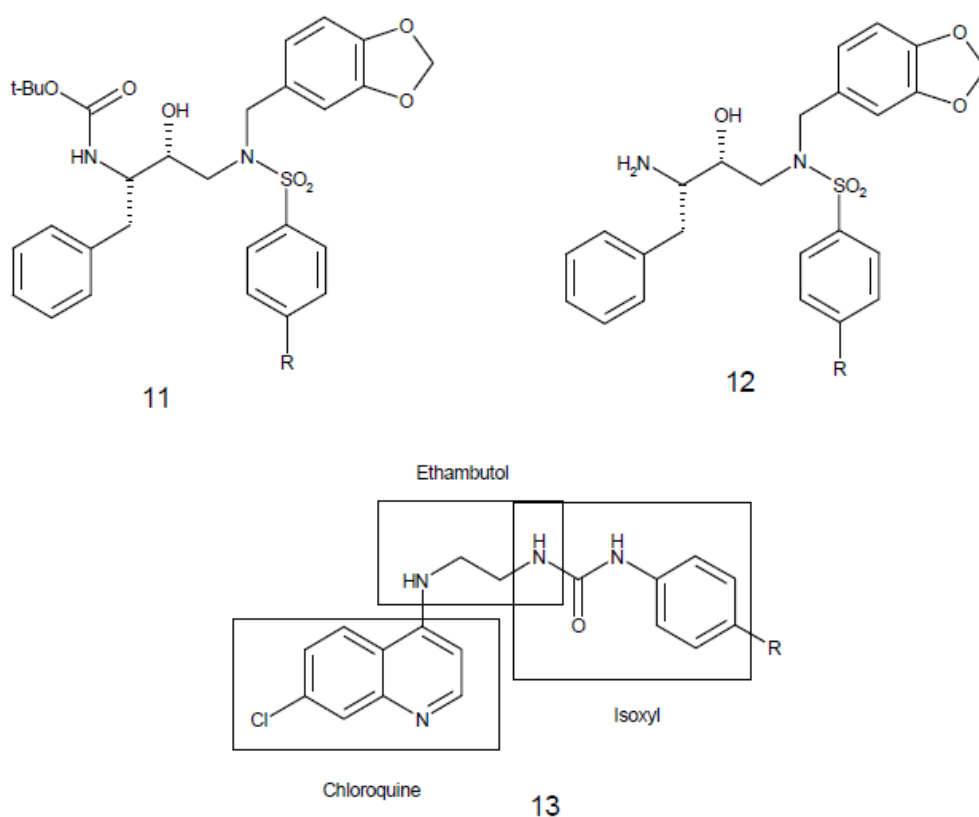


Figure 2.7. Ethambutol analogs as anti-TB agents

2.2.3. Salicylanilides derivatives

Salicylanilides (SAL) derivatives have been of great interest in medicinal chemistry, although their mechanism of action still unknown. It is postulated that they serve as epidermal growth factor receptor protein kinase (EGFR PTK) inhibitors. Such compounds have generally been designed to compete with adenosine triphosphate (ATP) in binding with the catalytic domain of tyrosine kinase. Recent studies specify that selective inhibitors of interleukin-12 p40 production also have a specific role in the initiation, expansion, and control of the cellular response to TB. Following the development of SAL derivatives, Imramovský's group obtained a series of compounds (14, figure 2.8) with activity similar to INH. Through a SAR study, they established that positions R1 and R2 showed Cl and Br atoms that are necessary for high activity against TB and that the benzyl and isopropyl substituent at R3 increases activity [100].

In addition, in various SAL derivatives that have been developed it has been shown that electron withdrawing groups on the salicyloyl ring and hydrophobic groups on the anilindering, as well as the 2-hydroxy group, are essential for optimal antimicrobial effect. Halogen substituted SAL in both parties maintains the requirements and forms of more active derivatives that show anti-TB activity. However, its unsuitable physical properties led to the generation of prodrugs of SAL derivatives with better bioavailability, and due to a high degree of lipophilicity, more efficient transport through *M. tuberculosis* cell membranes.

Considering this, Imramovský and colleagues obtained compounds (15, figure 2.8) with interesting activity against *M. tuberculosis*. They showed a level of inhibition of 89% - 99% and an MIC of 3.13 µg/mL. Although, they demonstrated that lipophilicity is a secondary parameter in anti-TB activity, they also demonstrated that in these compounds the stereo isomer effect is important for anti-TB activity; however, in this case the difference is not determined for individual R/S isomers [92].

Using the hybridization strategy, Ferriz et al obtained a new series of derivatives with SAL and carbamate groups, which have been used as antibacterial and antiviral agents. Thus the hybridization of two moieties could produce a new series with changes in their pharmacokinetic and pharmacodynamic properties. Ferriz et al postulated that carbamate could be protecting these molecules against first-pass metabolism, increasing their activity profile. The series obtained show that Cl atoms at 3 and 4-position on the aniline ring increase *M. tuberculosis* biological activity. Interestingly, the presence of an alkyl chain also increases the biological activity of these compounds, which suggests the importance of carbamate group (16, figure 2.8). Although these kinds of compounds are consistent with the Lipinski rules, it is speculated that due to their high lipophilicity, these molecules have high permeability, making their release more effective [101]. Another strategy using SAL derivatives has been the formation of cyclic derivatives, which could serve as antibacterial agents with a dual inhibition system. Thus, following this design strategy a new series of benzoxazinediones derivatives was obtained, where a thioxo group replaced one or two oxo groups. The substitution of an oxo group by the thioxo

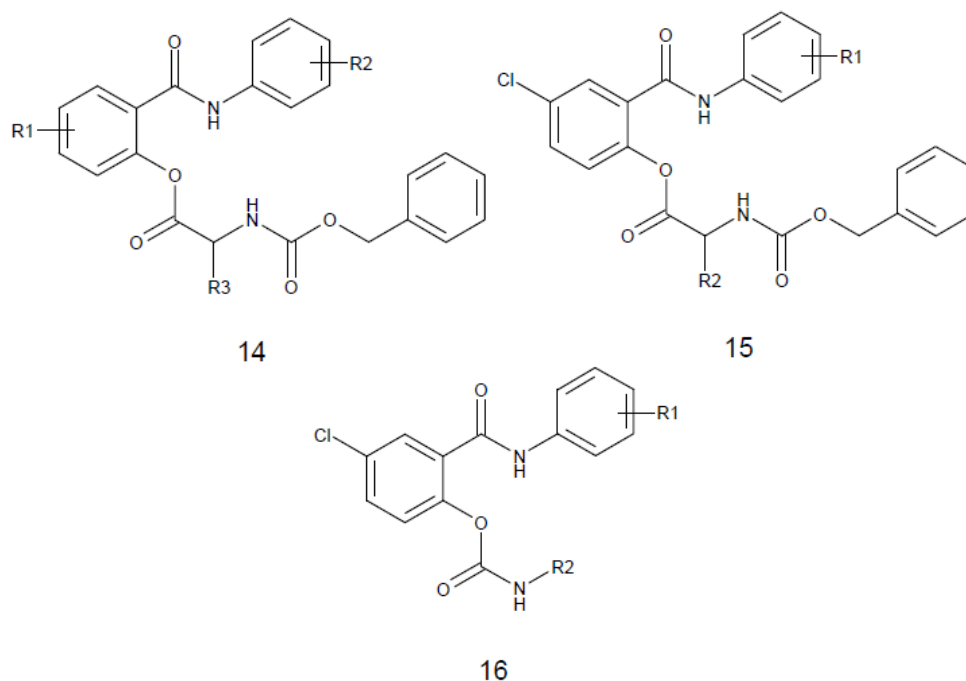


Figure 2.8. General structure of salicylanilides derivatives

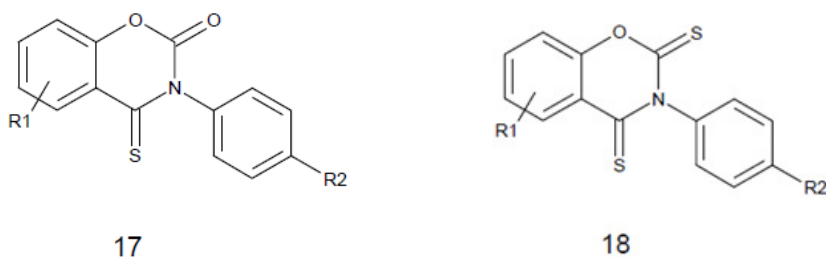


Figure 2.9. General structure of 1, 3-benzoxazine derivatives.

group (17, figure 2.9) strongly increased anti-TB activity, although a second substitution with the thioxo group had only a small effect on activity (18, figure 2.9) [102].

2.2.4. Quinoline derivatives

A quinoline ring is one of the moieties frequently used in new drug design. It has been considered a pharmacophore for the design of anti-TB agents. Diarilquinoline, denominated TMC207 (19, figure 2.10), is an adenosine ATP synthase inhibitor that is one of the most important quinoline derivatives with anti-TB activity. TMC207 is currently in Phase II clinical trials. Also, butanamide has been established as an important pharmacophore with good antibacterial activity and the carbohydrazone moiety is also known as a pharmacophore group. Based on the above, the design of new quinoline derivatives with active carbohydrazone and butanamide moieties in 3 and 4-position, respectively, has been carried out. The SAR study of these compounds shows that the presence of a trifluoromethyl group at 8-position increases activity; however, the introduction of a fluoro group in 6-position partially decreases activity (20, figure 2.10) considering these type of compounds nontoxic [103]. Following the development of mefloquine analogs (21, figure 2.10) in a series of compounds (22, figure 2.10), good anti-TB activity has been attributed to the presence of pharmacologically active heterocyclic groups such as pyrazole, imidazole, and indole rings on the quinoline ring.

Surprisingly, compounds with a heteroaromatic pyrazole ring have activity against resistant strains, which can be attributed to the presence of substituents (electron donating groups) that stabilize the pyrazole ring, making the quinoline ring a more active entity [104].

The conformational restriction-like strategy in flexible drugs is extensively used in medicinal chemistry. This helped determine steric requirements of receptor-drug interaction and identification of new structures with high efficiency and selectivity. Based on this, Goncalves et al studied the conformational restriction of the piperidinyl ring of mefloquine through the construction of an oxazolidine ring and different substituents on the phenyl ring (23, figure 2.10).

Conformational restriction showed that the introduction of an oxazolidine core in themefloquine structure enhances anti-TB activity. Although, the activity of these compounds are affected by substituents on the aromatic ring bound to C-17 of the oxazolidenyl nucleus.

Compounds that show hydroxyl or methoxyl groups, which are both electron donors and capable of forming strong hydrogen bonds, in general are active. In contrast, with one exception, compounds with nitro or halogenated groups (electron withdrawing groups and capable of forming only weak hydrogen bonds), are inactive [105]. Thus, mefloquine has been used to design anti-TB agents. Modifications in previous reports included introduction of a hydrazone linker into mefloquine at 4-position, substitution of a piperidine with a piperazine ring and extension of the basic terminus of the piperazine ring at 4-position.

Additionally, isoxazole is emerging as one of the most powerful hits in high-through put screening (HTS) against *M. tuberculosis*. Both types of compounds show an aromatic ring, a two-atom linker and a five or six member ring. Hybridization strategies have been the basis for the design of new chemical entities by Mao et al (24, figure 2.10). One problem that has been detected in this type of compounds is poor penetration of acid derivatives through the *M.tuberculosis* cell wall. It is suggested that these compounds

may act as prodrugs when ester derivatives generate acid derivatives (24, figure 2.10). SAR studies of these compounds show that when a methyl group replaces a trifluoromethyl group, it is 10 times less active, suggesting that electronic effects may play an important role in anti-TB activity. Additionally, steric effects can affect anti-TB activity. Subsequently, making use of drug design strategies, the authors included ester bioisosteres, such as amides and oxadiazole, although none of these bioisosteres showed better activity than ester derivatives.

It was determined that 2 and 8-trifluoromethyl groups on quinoline ring (24, figure 2.10) are essential for anti-TB activity against replicative bacteria [106]. Isoxazole derivatives have also been reported as anti-TB agents, in particular compound 25 (figure 2.11) with an activity of 2.9 μM , which is comparable to INH and (RIF) [107]. Thus, quinoline and oxazole ring hybridization has been used to develop a series of new anti-TB agents (26, figure 2.11) which have good activity due to the presence of arylsubstituents at 2-position on quinoline ring. SAR studies show that the introduction of a 1, 3-oxazole ring significantly increases activity, obtaining compounds that are more potent than INH [108]. In search of a new moiety that confers anti-TB activity with low cytotoxicity, Yang and colleagues reported methoxybenzofuro (2, 3-b) quinoline derivatives (27, figure 2.11), compounds that have a potent *M. tuberculosis* growth inhibition of 99% at low concentrations (0.20 $\mu\text{g/mL}$) and very low cytotoxicity against VERO cells with an Inhibitor concentration 50 (IC_{50}) value of > 30.00 $\mu\text{g/mL}$ [110].

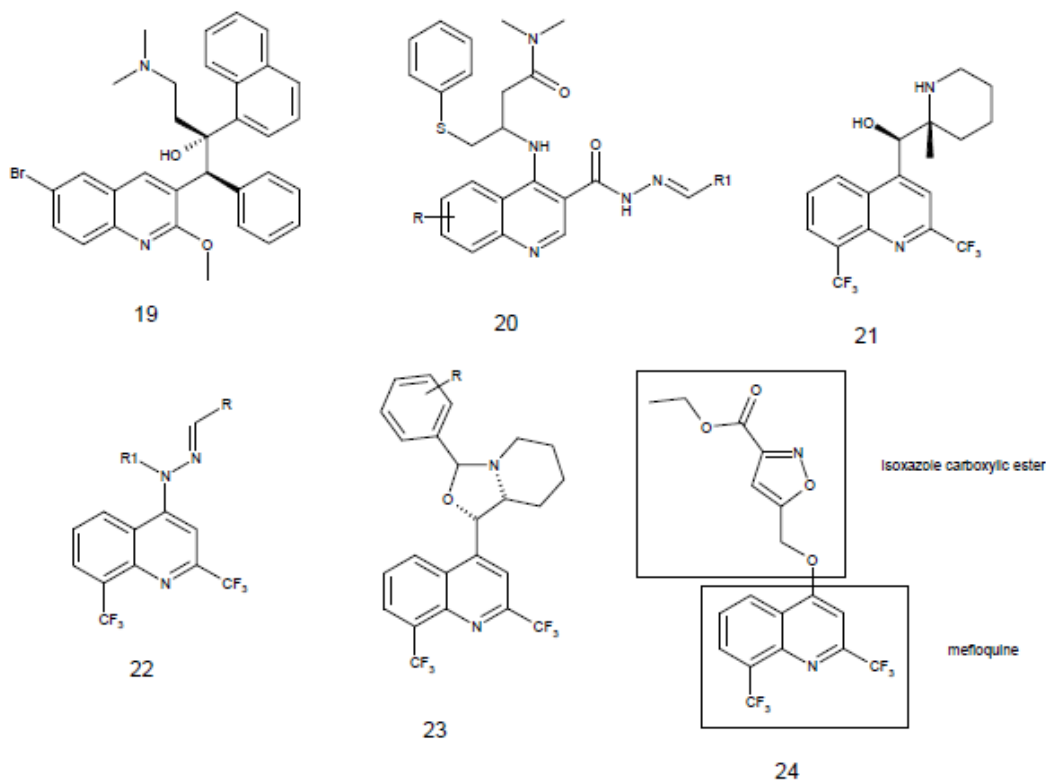


Figure 2.10. Quinoline as scaffold for designing new anti-TB agents

Several studies have analyzed modifications in the quinolone ring, mainly at 3, 6 and 7-position. Wube et al proposed a new strategy for anti-TB agent development. They made a modification in the 2-position, including an aliphatic side chain with various degrees of unsaturation, lengths chains, and double bond positions (28, figure 2.11). Their results showed that increasing the chain length enhances anti-TB activity, showing optimal activity with 14C atoms. If there is an increase of more carbon atoms in the chain, activity decreases dramatically. This behavior has also been described for ciprofloxacin derivatives where lipophilicity could play an important role in anti-TB activity. Other research has determined that the saturated aliphatic chain has less activity than

unsaturated analogues. This means that unsaturation of an aliphatic chain is an essential structure for in vitro anti-TB activity [111].

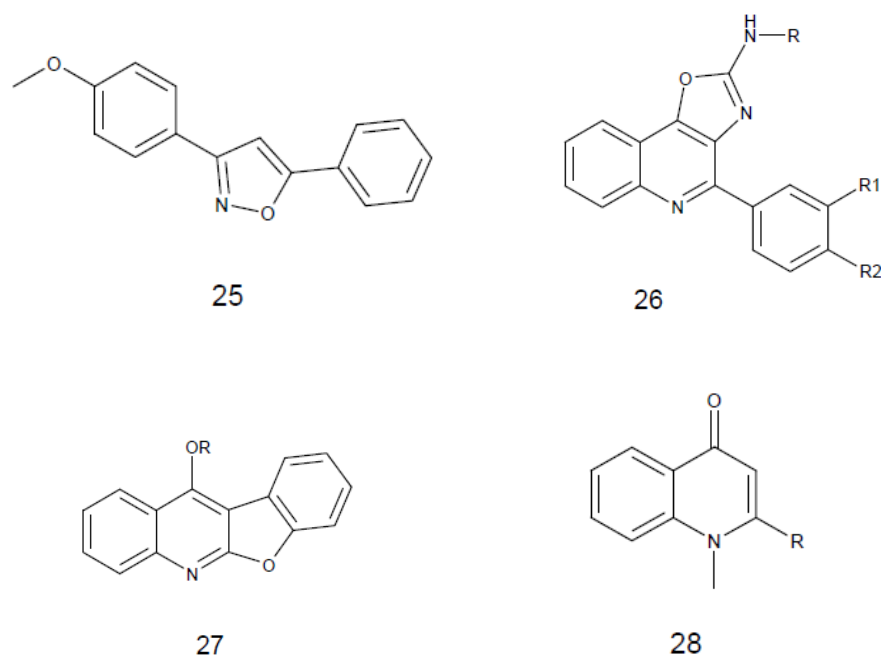


Figure 2.11. Quinoline and oxazole derivatives as anti-TB agents

On the other hand, both phenazine and quinoxaline rings are considered bioisosteres of the quinoline ring. In this focus, phenazine derivatives are a class of useful compounds for new anti-TB agent development, particularly Tubermicyn B and Clofazimine (phenazine derivatives). Likewise, De Logu et al developed new agents that show activity (29, figure 2.12) in a concentration range of 0.19 to 3.12 mg/L against *M. tuberculosis*-resistant clinical isolates. Interestingly, they found that this series of compounds were ineffective in inhibiting the growth of INH resistant strains. Compounds that had exocyclic groups, which confer different lipophilic and electronic properties, but with a size similar to INH, such as the phenylamide methyl lipophilic group in 4-position, were the most active. In contrast, the same group at 3-position reduced activity 100-fold. Also, phenazine derivatives with electron withdrawing groups in 2 and 3-position have values with similar biological activity.

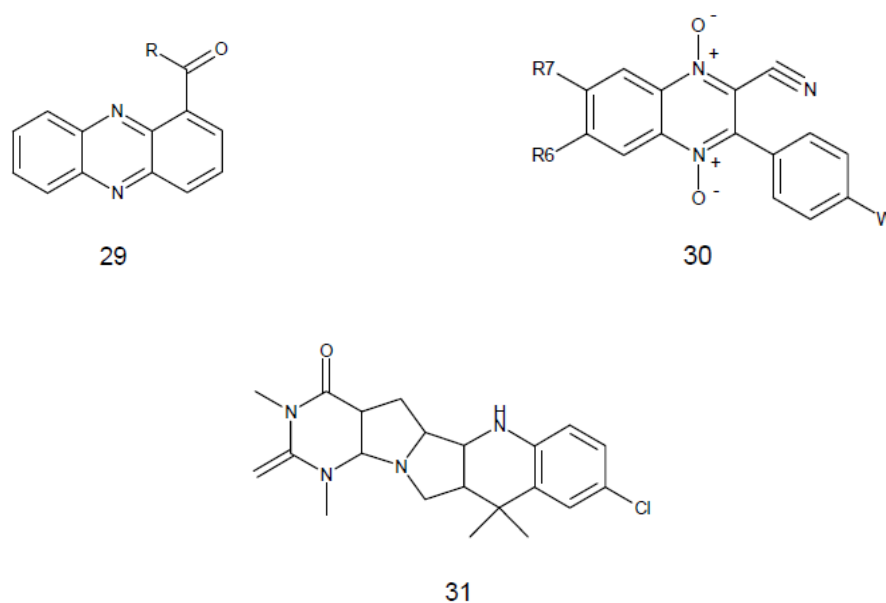


Figure 2.12. General structure of phenazine-1-carboxamides, quinoline and quinoxaline derivatives.

These results show the importance of the aryl moiety as a pharmacophore for phenazine carboxamide anti-TB agents. While phenazine's mechanism of action is still unknown, it is hypothesized that it could act as a cellular superoxide dismutase inhibitor.

We know that the compound Lomofungin (1-carbomethoxy-5-formyl-4, 6, 8-trihydroxyphenazine) is capable of inhibiting DNA-dependent RNA polymerase, with both options being possible mechanisms of action of phenazine derivatives [112]. Quinoxalines are compounds with a broad spectrum of biological activities. Quinoxaline-*N* oxide derivatives are known as *M. tuberculosis* bioreductor agents. In this type of compounds missing *N*-oxide groups have led to the loss of anti-TB activity. In this sense, Monge's group developed over 500 derivatives of quinoxaline (30, figure 2.12), demonstrating the importance of this group for generating a new class of anti-TB drugs. Interestingly, this research group determined that the quinoxaline compounds obtained have activity on non-replicating bacteria, which could lead to shorter anti-TB therapies [113].

Finally, a compound denominated ER-2 is a new analogue of quinoline derivatives (31, figure 2.12) that is a gyrase supercoiling inhibitor that has potency similar to Ciprofloxacin with a minimum inhibitory concentration 90 (MIC90) of 0.5 $\mu\text{g/mL}$ [114].

2.2.5. Azoles derivatives

One of the most important strategies for effective anti-TB agent design has been the development of cell wall biosynthesis inhibitors. Azole derivatives have shown interesting anti-TB antimicrobial activity, inhibiting the bacteria by blocking lipid biosynthesis and/or additional mechanisms. Thus, by hybridization of 1, 2, 4-triazoles and a thiazole moiety, new anti-TB agents were discovered (32, figure 2.13). These molecules with a highly electronegative part at the sulfhydryl groups have emerged as new anti-TB compounds. Particularly, Schiff bases derivatives probably due to its ability to increase penetration into the bacterial cell [115].

Benzimidazole is an important pharmacophore in drug discovery. Gill et al propose 1,2,3-triazole and benzimidazole ring hybridization as design strategies of new anti-TB agents. They have also considered the use of electron withdrawing groups in the benzimidazole ring, which are present in molecules with anti-TB activity. They obtained compound 33 (figure 2.13) that could be considered a lead series. Their optimization led to determine that substitutions with electron withdrawing groups produce a loss of anti-TB activity [116]. A new strategy of hybridization between benzimidazole and a 1, 2, 4-triazole ring has obtained a series of compounds (34, figure 2.13). Using a SAR study, it was determined that these compounds enhance biological activity by increasing electronegativity of the molecule, but surprisingly when a trifluoromethyl group (high electronegativity) was introduced, it produced a substantial loss of activity, which could be due to a delay in intracellular transport [117]. Following with the use of a benzimidazole ring as a drug design, Klimešova and cols replaced a nitrogen atom with a corresponding oxygen atom (isosteric) (35, figure 2.13) to obtain a series of benzyl sulfanyl benzoxazole derivatives. They consider alkyl sulfanyl derivatives of pyridine, benzimidazole and tetrazole as new anti-TB agents, which present anti-TB activity due to

the presence of the alkyl sulfanyl group bound to an electron deficient carbon atom in the heterocycle ring. Thus, a SAR study of these compounds indicates that anti-TB activity is attributed to the presence of a benzyl moiety at 2-position on the benzoxazole ring, denoting that anti-TB activity is not affected by electron withdrawing or electron donating substituents on the benzyl moiety. It is important to note that the presence of two nitro groups on benzyl led to the most active compound (MIC 2 $\mu\text{mol/L}$), which may be related to compounds such as PA-824 and OPC-67683, that also show nitro groups. Research postulated as a mechanism of action the generation of active species that act on biochemical targets. Additionally, regression coefficient values for log P show that anti-TB activity increases when lipophilicity decreases [117].

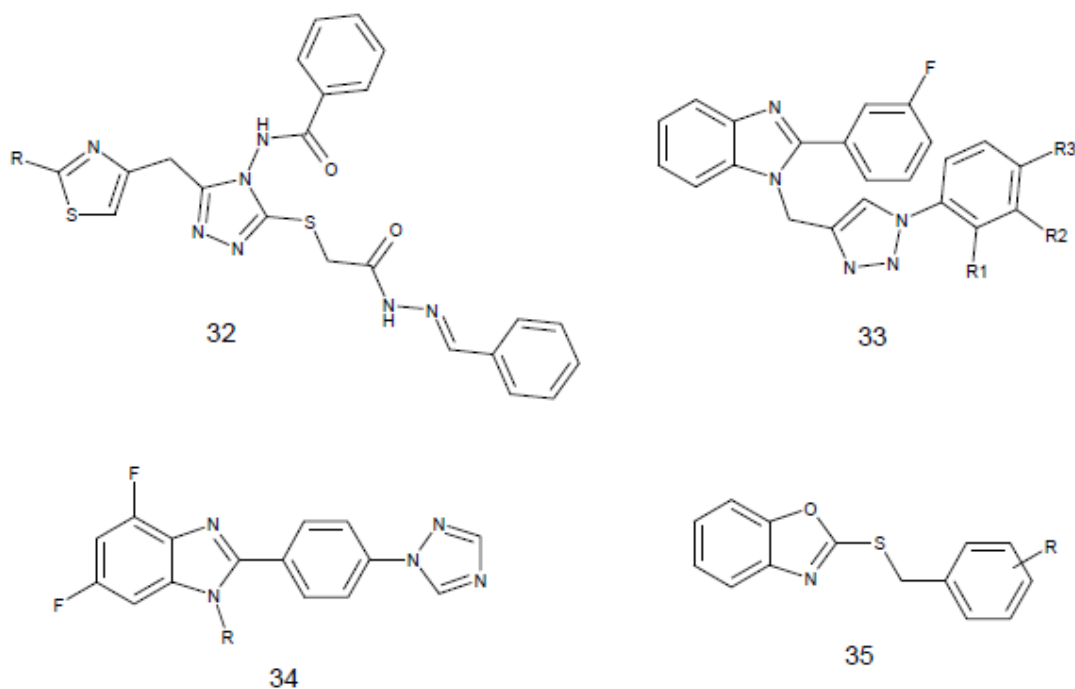


Figure 2.13. Triazole and benzimidazole scaffold for designing new anti-TB agents

Another strategy using 1, 2, 4-triazole and 1, 3, 4-thiadiazole rings, led to the development of new anti-TB agents (36, figure 2.13). Guzeldemerci et al obtained compounds that inhibit 90% *M. tuberculosis* with a concentration greater than 6.25 $\mu\text{g/mL}$. In addition, the benzothiazole moiety has been recognized for anti-TB design.

Both benzothiazole and 1, 2, 4-triazole moiety were considered to obtain new structures based on hybridization (37, figure 2.13). Benzothiazole derivatives with 4-methoxy groups showed the best anti-TB activity; however, compounds obtained by hybridization with the 1, 2, 4-triazole-benzothiazole moiety with the best activity were those with an electron withdrawing substituent (Cl) on the benzothiazole ring [119].

Another moiety considered in anti-TB agent design has been isopropylthiazole. Based on this a series of isopropylthiazole derived triazolothiadiazoles, triazolo thidiazines derivatives, and mannich bases were developed. The SAR study of the thiadiazoles series (38, figure 2.13) shows that these compounds have excellent activity against *M. tuberculosis* when they have fluorinated (highly electronegative) substituents that increase molecule lipophilicity, producing hydrophobic molecule interactions with specific binding sites on either receptors or enzymes [120].

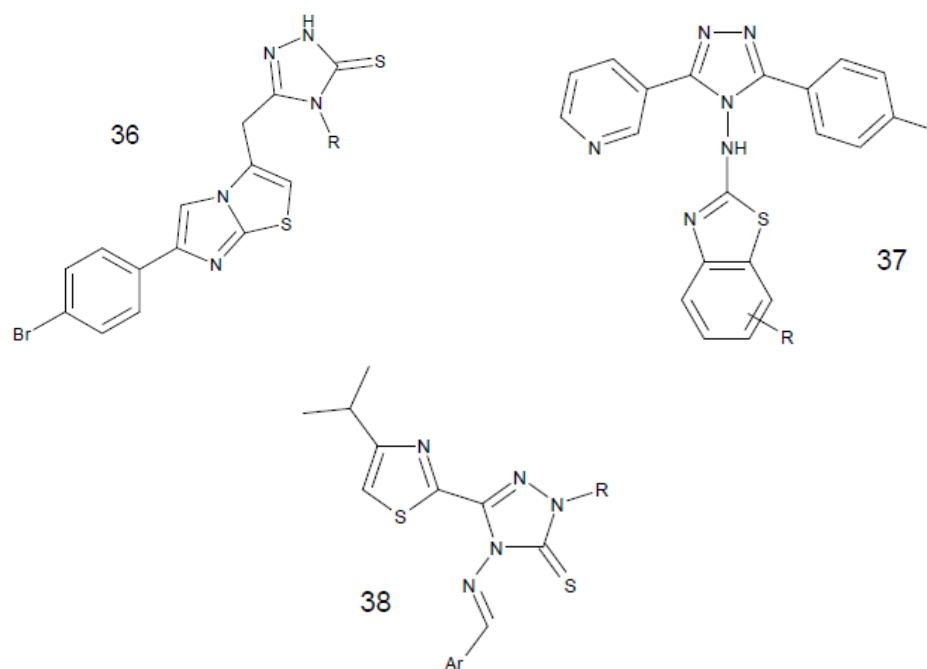


Figure 2.14. Triazole derivatives as anti-TB agents

One of the strategies employed in the development of new drugs is *in silico* screening based on drug structure, structural data of protein and a virtual library of compounds. With this strategy Izumizono et al identified 5 classes of compounds that have an affinity for the active site of enoyl-acyl carrier protein reductase. They determined that these compounds share a structural skeleton of dibenzofuran, acetoamide, triazole, furyl and methoxy phenyl groups (figure 2.14) that completely inhibit *M. vanbaalenii* growth with no toxic effect on mammalian cells. Binding mode prediction determined that compounds 39, 40 and 41 form common hydrogen bonds with amino acid Lys 165 of the active site of the reductase protein. Lys 165 is an amino acid residue that is known to form hydrogen bonds with INH. This shows that hydrogen bond formation with Lys 165 tends to be effective in the design of new drugs. In drug-interaction, the triazole group of compound 39 forms hydrogen bonds with the active site, and the methoxy and sulfonyl groups in compound 40 and the sulfonyl group in compound 41, respectively, form hydrogen bonds with Lys 165 [121].

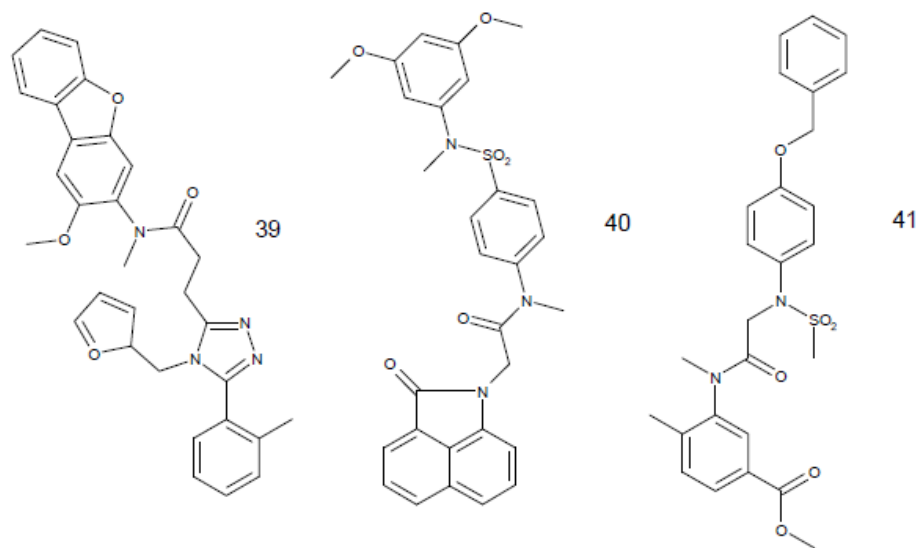


Figure 2.15: Dibenzofurane, triazole, methylphenyl and acetamide moiety in compounds with anti-TB activity.

Other derivatives of azoles are pyrazoles. Their activity has been tested against *M. tuberculosis*. SAR studies show that the presence of a *para*-chloro benzoyl moiety in C4-position on the pyrazole ring is essential for anti-TB activity. Results of a series of pyrazole derivatives, generally show that cyclohexylthio substituted pyrazole derivatives are more active than aryl thio substituted systems. An excellent activity is presented when a *para*-nitro phenylthio ring is incorporated on a pyrazole ring (42, figure 2.15) [122].

Thiazoles are compounds that contains sulfur and nitrogen atom in its structure, and have been the basis of clinically used compounds. Therefore Samadhiya and colleagues consider it a basis of anti-TB agent design. In one study, which synthesized a series of new thiazoles (43, figure 2.15), it was demonstrated through SAR analysis that compounds with nitro groups show greater biological activity on *M. tuberculosis* than compounds with Cl and Br atoms, although these derivatives (Cl and Br) have better activity than other compounds.

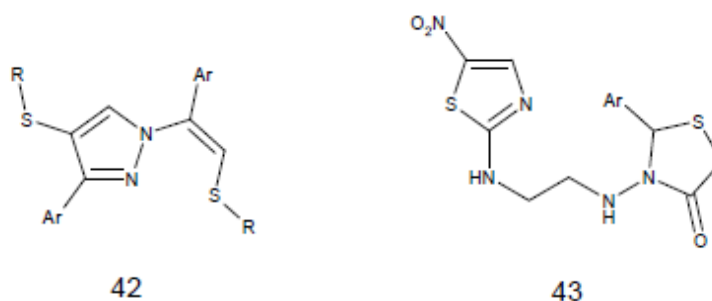


Figure 2.16. General structure of pyrazoles and thiazoles derivatives as anti-TB agents

Finally, they found that the activity of the compound depends on the nature of the substituent groups (electron withdrawing) with the following sequence $\text{NO}_2 > \text{Cl} > \text{Br} > \text{OCH}_3 < \text{OH} > \text{CH}_3$ [123]. On the other hand, hybridization of Spiro compound and pyrrolo (2,1-b) thiazole, an unusual ring with different biological properties, particularly permitted the obtention of pyrrolothiazoles derivatives (44, figure 2.16) that present a MIC of $0.007 \mu\text{M}$ against *M.tuberculosis*, being more potent than INH and Ciprofloxacin [124].

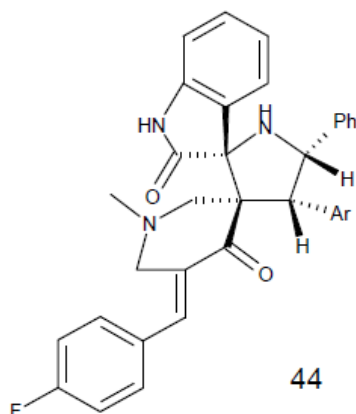


Figure 2.17. Spiro-pyrrolothiazoles derivative with anti-TB activity

2.2.6. Hydrazides/hydrazones derivatives

Hydrazide/hydrazone is a class of compounds that have been considered for new anti-TB drug design. An example is diflunisal, a hydrazide/hydrazone derivative, which has dual effect acting with antimicrobial/anti-inflammatory properties. Furthermore, in thiazolyl hydrazone derivatives, SAR studies have found that substitutions on the phenyl ring affect anti-TB activity (45, figure 2.17) [125]. Another example of a thiazolyl hydrazine is compound 46 (figure 2.17), which has high anti-TB activity with an IC_{50} of 6.22 $\mu\text{g/mL}$ and low toxicity ($CC_{50} > 40 \mu\text{g/mL}$). Here, a pyridyl moiety plays a direct role related to anti-TB activity [126]. Pyridine is a moiety known in the design of anti-TB agents. Considering this, and using hybridization technique, Sankar et al developed a series of compounds with potential anti-TB activity (47, figure 2.17), although in many cases as this, the use of this technique did not produce any agent with excellent activity against *M. tuberculosis* [127].

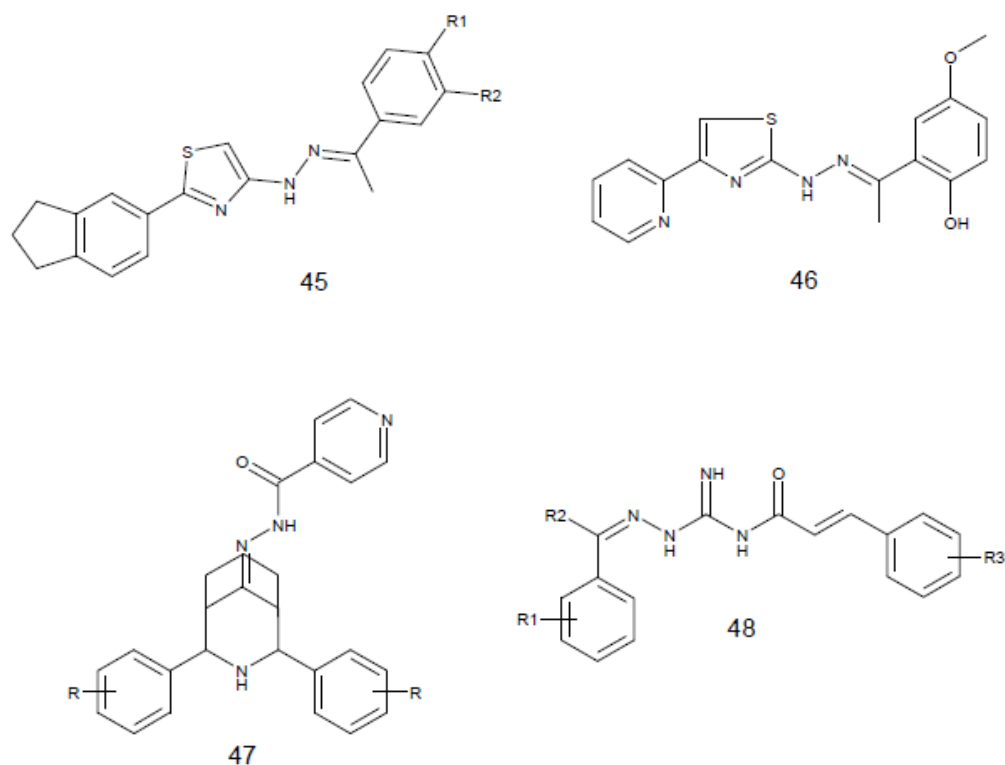


Figure 2.18. Hydrazone derivatives as anti-TB agents

New designs have been made by molecular hybridization of E-cinamic acid and guanlyl hydrazones. Based on an empirical analysis of SAR, Bairwa and colleagues determined that electronic and steric parameters have an important role in the activity of these compounds on *M. tuberculosis* (48, figure 2.17). They remain the basis of new anti-TB agents [128].

2.2.7. Nitrogen heterocyclic derivatives

Purines are an important group in the design of anti-TB agents. In these compounds (49, figure 2.18), activity depends on the substituents present in C2, C6 and N9 of the purine ring [129]. In 6, 9-disubstituted purine derivatives, activity increases substantially when a Cl atom is introduced in the 2-position. Interestingly, purine derivatives with thienyl

substituents exhibit better activity in non-replicating bacteria, although in these compounds a Cl atom in 2-position is not beneficial for activity. Additionally, it has been determined that purine N-9 is important for activity, in the case of purine C-8, an atom can be exchanged without losing activity and a change in purine N-7 results in a loss of activity, although there are 7-deazapurines derivatives (50, figure 2.18) that could be compared with RIF [130].

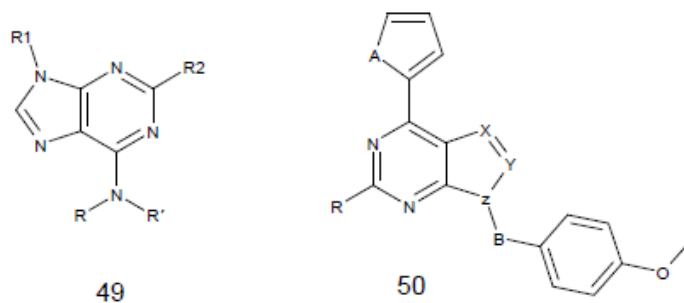


Figure 2.19. Purine derivatives as anti-TB agents

Heterocycles with one nitrogen atom, especially pyrimidines have potential therapeutic applications as anti-TB agents, but there are few reports. For this reason, the design of new pyrimidine derivatives is a viable option (51, figure 2.19). However, neither compound has an activity comparable to reference drugs, although it has been described that the substituent nature in 2-position can modulate cytotoxic activity [131].

On the other hand, thymidine monophosphate kinase of *M. tuberculosis* (TMPKmt) is a prominent target for the development of anti-TB drugs. TMPK is the last specific enzyme for TTP synthesis and is a key enzyme in *M. tuberculosis* metabolism. This enzyme is different from human enzyme analogs (22% homology). TMPK inhibitors have been developed with single or multiple chemical modifications of the pyrimidine moiety and thymidylate sugar. In particular benzyl-thymine derivatives have been remarkable TMPK inhibitors, which has led to the proposal of new modifications such as: chain length in *para*-position on the benzyl ring, saturation of the alkyl chain, functionalization of the chain group and substitution at 5-position of the core base. This has led to more selective

compounds on TMKP that correspond to benzyl-pyrimidines substituted by a chain length of 4 carbons and a terminal carboxylic acid function. Docking of molecule 52 (figure 2.19) on TMPKmt showed that the hydrogen of the thymine and acid group can interact with Arg95 [132].

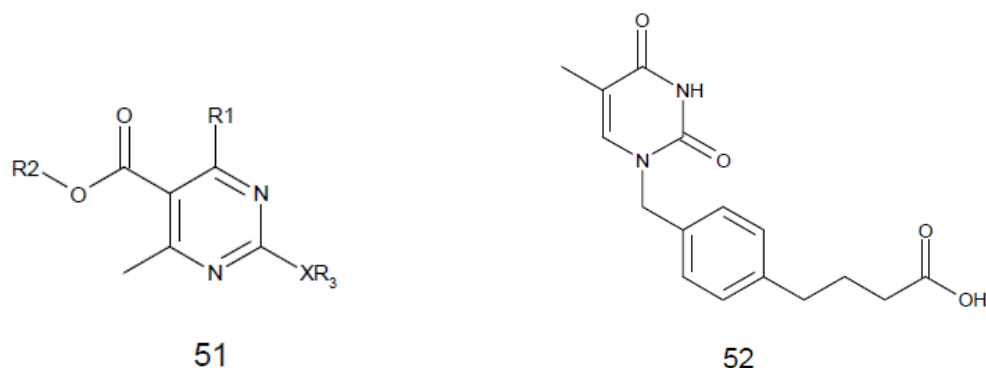


Figure 2.20 .General structures of pyrimidine derivatives as anti-TB agents.

Pyridine derivatives have also been described as anti-TB agents, an example is compound 53 (figure 2. 20), which presents inhibitory activity with an IC₅₀ value of 0.38 μM, suggesting that its possible mechanism of action is through glutamine synthetase inhibition. This would be the first inhibitor compound not derived from amino acids [133]. Another series of pyridine derivatives were developed by Fassihi et al who synthesized compound 54 (figure 2.20), a potent anti-TB agent with activity similar to RIF. The results of these compounds showed that an imidazole group as a substituent is equivalent to a nitro phenyl group, which has been reported in anti-TB agents derived from 1, 4-dihydropyridinecarboxamides [134].

Another important heterocyclic for the design of anti-TB agents is the pyridazine moiety. In these compounds a relationship between Br, Cl and CH₃ substituents, respectively, with Brand vinyl has been found with a favorable anti-TB activity. In these compounds there is an influence of the substituents X in *para*-position on the aromatic ring, where the activity is increased in the following order: CH₃ < Cl < Br with the activity being affected by the R1 substituents, where the most active compounds have a CH₃ group (55, figure 2.21) [135]

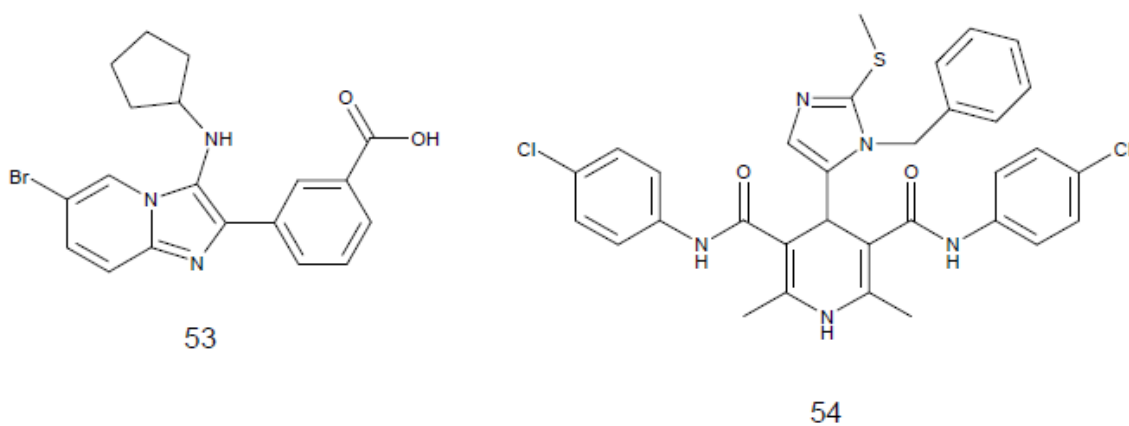


Figure 2.21. Pyridine derivatives with potential activity anti-TB

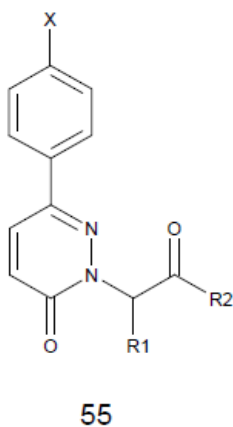


Figure 2.22. N-substituted-pyridazinones derivatives

2.2.8. Thiazine derivatives

Indumathi et al [136] synthesized a facile (*L*)-proline-catalysed green synthesis of highly functionalized [1, 4]-thiazines demonstrated good antimycobacterial activity (Figure 2.22). It was reported that ng MeN-thiazines, and PhCH₂N-thiazines series, showed an equal activity. HN-thiazines showed a higher activity than MeN-thiazines, and PhCH₂N. A general trend emerges, the order of activity being: HN-thiazines>MeN-thiazines>

PhCH₂N-thiazines. This can probably be ascribed to enhancement of the activity of the thiazine pharmacophore by either the hydrogen donor property of the thiazines which is available only in NH thiazines or accessibility of lone pair of electrons on the nitrogen for hydrogen bonding interactions or both. The enhanced steric congestion at nitrogen in MeN- and PhCH₂N-thiazines could also diminish the accessibility of lone pair of electrons on the nitrogen lowering their activity relative to the HN-thiazines. General structure is as shown below.

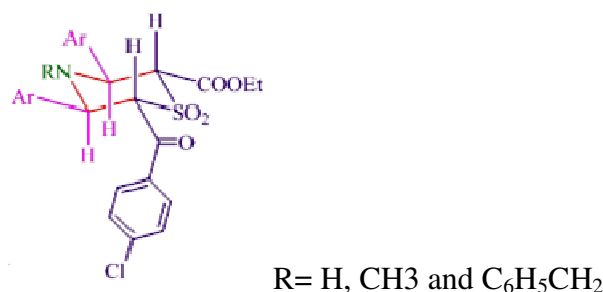


Figure 2.23. N-substituted- thiazines derivatives

The HN-thiazines with *para*-methoxy and *para*-nitro phenyl group showed the highest activity against MTB. When the nitro group is either at the *ortho*- or *meta*- position of the phenyl ring of HN-thiazines, the activity is diminished relative to the *para*-nitro analog, showing that the activity is sensitive to the position of the substituent in the aryl ring. The HN-thiazine with *para*-NMe₂ group showed much less activity than that with either *para*-NO₂ or *para*-MeO group, suggesting that besides electronic effects other factors also influence the activity. Among the halogenated HN-thiazines, it is found that the order of activity is: 2, 4-dichloro > 4-chloro > 3-fluoro. Among the heteroaryl compounds, the [1, 4]-thiazine with 2-furyl group is found to be twice as active as the 2-thienyl group. When the aryl ring in HN-thiazine is phenyl, 1-naphthyl or *para*-dimethylaminophenyl, the activity is diminished. The most active thiazine against MTB is 11 and 75 times more active than ethambutol and pyrazinamide respectively, while its activity is 2 and 6 times less than that of isoniazid and rifampicin respectively.

These compounds also exhibited MDR –TB activity. The thiazine with *para*-nitro group showed the highest activity against MDR-TB, being 67, 6, and 90, 597 times higher than that of isoniazid, rifampicin, ethambutol and pyrazinamide respectively. The activity of the compounds against MDR-TB is significantly influenced by the substituent in the aryl ring of the thiazines, the order of activity being: (4-O₂NC₆H₄) > (4-H₃COC₆H₄) > (4-H₃CC₆H₄) > (4-ClC₆H₄).

2.2.9. Other derivatives

Several studies indicate that thiosemicarbazone derivatives can be used in TB therapy and prophylaxis. Previous studies of 1H-2-thiosemicarbazone indolinone derivatives indicate that halogenation of R1, elongation of the alkyl chain in R2, substitutions of the alkyl chain in R2 with cyclohexyl or phenyl, and the presence of a substituent in R3, are more efficient for increasing anti-TB activity, while R1 substitutions with a nitro group produce the most active compounds. The presence of a morpholine ring in Schiff bases substituted in R1 with a nitro group also has a significant impact on anti-TB activity. The results of biological activity of this new series indicate that the elongation of the alkyl chain increases activity.

This enhanced activity is related to lipophilicity properties and confirmed by values of LogP compounds. Also, replacement of the alkyl chain in R2 and phenyl unsubstituted cyclohexyl has led to more active compounds (56, figure 2.23). The absence of substitutions at N1 on the indole ring and increased lipophilicity appear to be responsible for high activity against *M. tuberculosis* [137]. An example of thiosemicarbazone-derived compounds that have exhibited important anti-TB activity with an IC₅₀ value of 2.59 uM/mL is compound 57 (figure 2.23) [138].

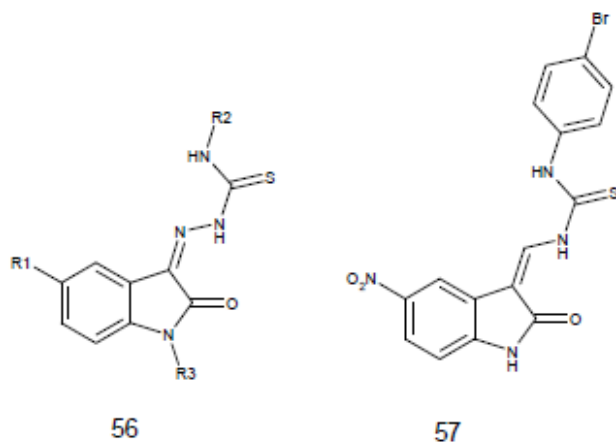


Figure 2.24. General structure of 1H-indole-2, 3-dione 3-thiosemicarbazone with anti-TB activity

Other moieties used in the design of anti-TB agents are phenazine and benzothiadiazine. In particular, benzothiadiazine 1, 1-dioxide constituents are an important class of anti-TB agents (58, figure 2.24). A SAR study of this series of compounds indicates that the furan/thiophene group linked to benzothiadiazine through a methylene bridge exhibits good activity against TB. It is important to point out that a conjugated thiophene derivative shows moderate activity and is enhanced when it presents a nitrofuran group. However, elimination of the methylene group with a carbonyl group leads to a dramatic loss of activity. Finally, Kamalet al postulated piperazine-benzothiadiazine with methylene linkage (59, figure 2.24) as an attractive moiety for the design of anti-TB agents [139].

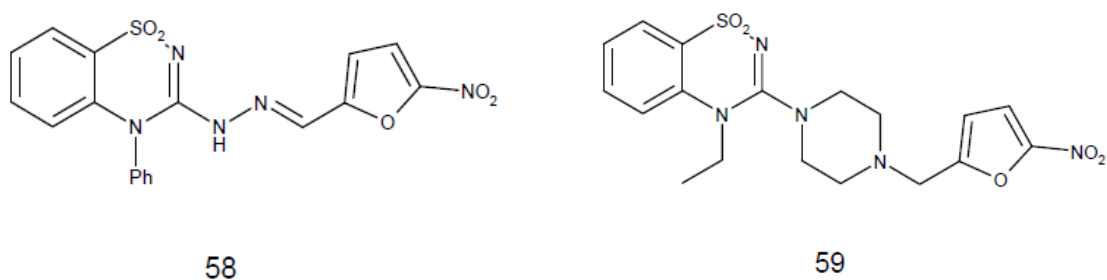


Figure 2.25. Benzothiadiazine derivatives as anti-TB agents

The creation of a hybrid compound has been a frequent strategy for the design of anti-TB agents. One example is compound 60 (figure 2.25), formed from dibenzofuran and 2, 2-dimethylpyran subunits. SAR studies and modifications of benzofurobenzopyran have demonstrated less active compounds such as compound 61 (figure 2.25), where the furan B ring is replaced by an ether linker, a single carbon-carbon bond, a carbonyl group, a hydroxymethylene or a methylene group. Even modifications such as acylation and bromination in 5-position on the C ring have produced inactive compounds, thus, it has been suggested as a basis for the pharmacophore structure of compound 60. In this sense, Terenzi et al has carried out the synthesis of more derivatives of compound 60, finding that substitutions with a hydroxy, methoxy, or halogen group on benzofurobenzopyran increases anti-TB activity. Although, hydroxy compounds with good activity showed, unfortunately, cytotoxic activity on VERO cells. Halogenated compounds with a Cl or Br atom in 8, 9 and 11-position, exhibit increased potency compared with compound 60. SAR analysis shows that electronic effects of substituents on the A ring play a dramatic role in anti-TB activity. In addition, potency was significantly decreased when the A ring was substituted by an electron withdrawing group. In contrast, electron donating group substitutions such as hydroxy or methoxy show a significant increase in activity (62, figure 2.25). While all compounds showed a possible mechanism of action of interaction with lipid biosynthesis of the *M. tuberculosis* cell wall, a specific compound was an epoxy-mycolate synthesis inhibitor [140].

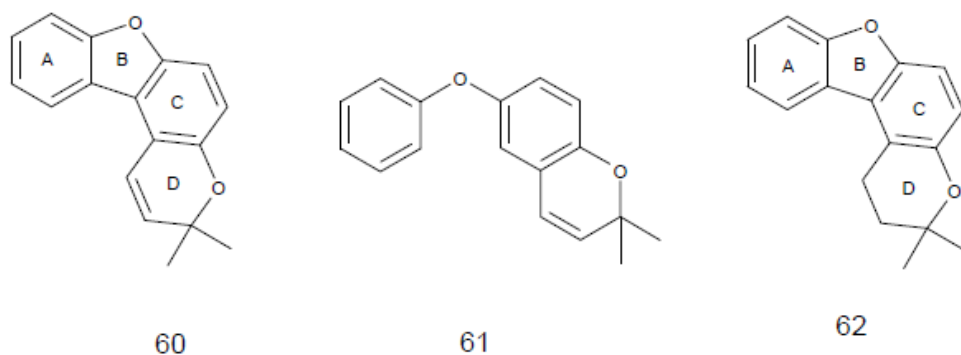
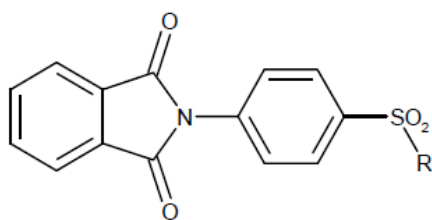


Figure 2.26. Structure of benzofurobenzopyrane as anti-TB agents

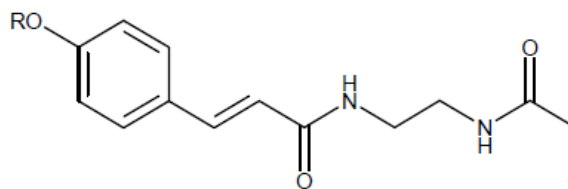
Other compounds containing a phthalimide moiety have been described as biophoroto design new prototypes of drug candidates with different biological activities. It has been shown that hybridization of both phthalimide (Thalidomide) and sulfonamide (Dapsone) moiety leads to compounds with activity against *M. leprae*. In this sense, the design of new products such as anti-TB agents is interesting. SAR study of a series of derivatives showed that if the pyrimidine ring is substituted in any position or changed by an isosteric, this decreases activity on *M. tuberculosis*. Amino group substitutions by another phthalimide ring also lead to a decrease in anti-TB activity (63, figure 2.26). Modifications in the pyridine ring decrease anti-TB activity. Introduction of a phthalimide group by molecular hybridization did not produce compounds with an activity similar to INH; however, it allows for compounds with MIC values similar to PZA [141].



63

Figure 2.27. Phthalimide derivatives as anti-TB agent

Among families of compounds that act as inhibitors of the FAS-II system we can mention diphenyl ether systems that interact with enzyme-cofactor binary complex, but, recently new compounds such as indols, benzofuran and cinnamic acid derivatives have been reported. Development of new cinnamic acid derivatives would focus on more specific FAS-II inhibitors. From a series of compounds developed (figure 2.27) it was determined that addition of an alkyl chain increases anti-TB activity. The best results are associated with an acceptable lipophilicity parameter that appears when a geranyl chain is incorporated. This led to compound 64, the most active substance with an MIC of 0.1 $\mu\text{g}/\text{mL}$ [142]. It has also been shown that amide derivatives of fatty acids have anti-TB activity.



64

Figure 2.28.Cinnamic derivatives

Due to their nature these compounds are designed to penetrate bacterial cells, which can be useful for studying the mechanism of INH resistance as this can also be due to factors such as mutations in unknown genes, decreased permeability, or increased efflux [143].

2.3. Drugs in clinical trials

In drug design, bicyclic nitroimidazofurane derivatives that have anti-TB activity, such as CGI-17341 (65, figure 2.28) have been developed; however, this compound is mutagenic. This has led to the development of PA-824 (66, figure 2.28) [144-146], which is currently in phase II clinical studies and has a long half-life [147]. Its mechanism of action is to inhibit *M. tuberculosis* cell wall lipids and protein synthesis; however, it also inhibits non-replicating bacteria.

Additionally, it was reported that PA-824 is a prodrug that is metabolized by *M. tuberculosis* before exercising its effect and may involve bioreduction of aromatic nitro groups to generate a radical intermediate nitro [148-150]. Drug resistance has been shown to be mediated by the loss of a specific glucose-6-phosphate dehydrogenase enzyme or of its deazaflavin cofactor F420, which may provide electrons for the reductive reaction. SAR of nitroimidazo [2, 1-b] oxazine series is found in fig. 2.28[147].

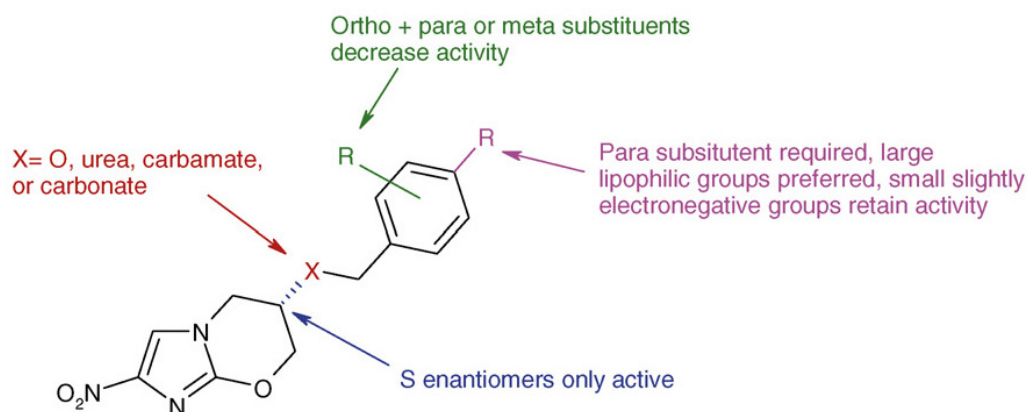
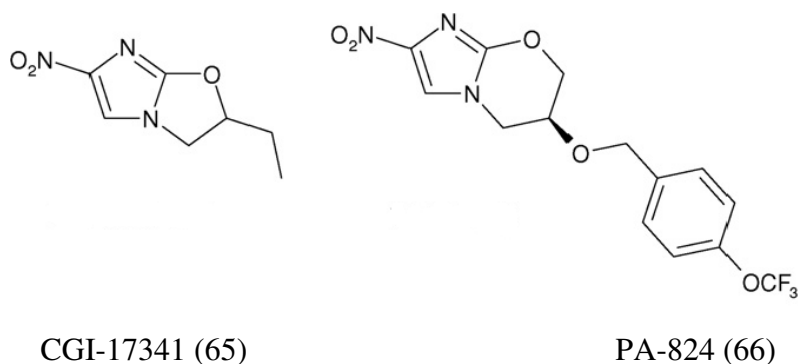


Figure 2.29. In vitro anti-TB structure activity relationships (SAR) of the nitroimidazo [2, 1-b] oxazine series

The interest in derived oxazoles as anti-TB compounds led to the development of OPC-67683 (67, figure 2.29)[151], which has excellent activity in vitro in sensitive and resistant *M.tuberculosis* strains and does not show cross-resistance to any current first-line drugs, with the evidence that infrequent and low dosing may be effective. The long half-life of OPC-67683, the lack of metabolism by CYP enzymes and its efficacy in immune compromised mice suggest that this drug may be useful for the treatment of co-infected TB/HIV patients [151,152].

Its mechanism of action involves inhibition of the synthesis of keto-mycolic, and methoxy-mycolic acid, although is possible another possible mechanism of action or interaction with another drug target in *M. tuberculosis*. OPC-67683 also acts as a prodrug, since *M. tuberculosis* metabolizes it and produces as a product desnitroimidazooxazole metabolite.

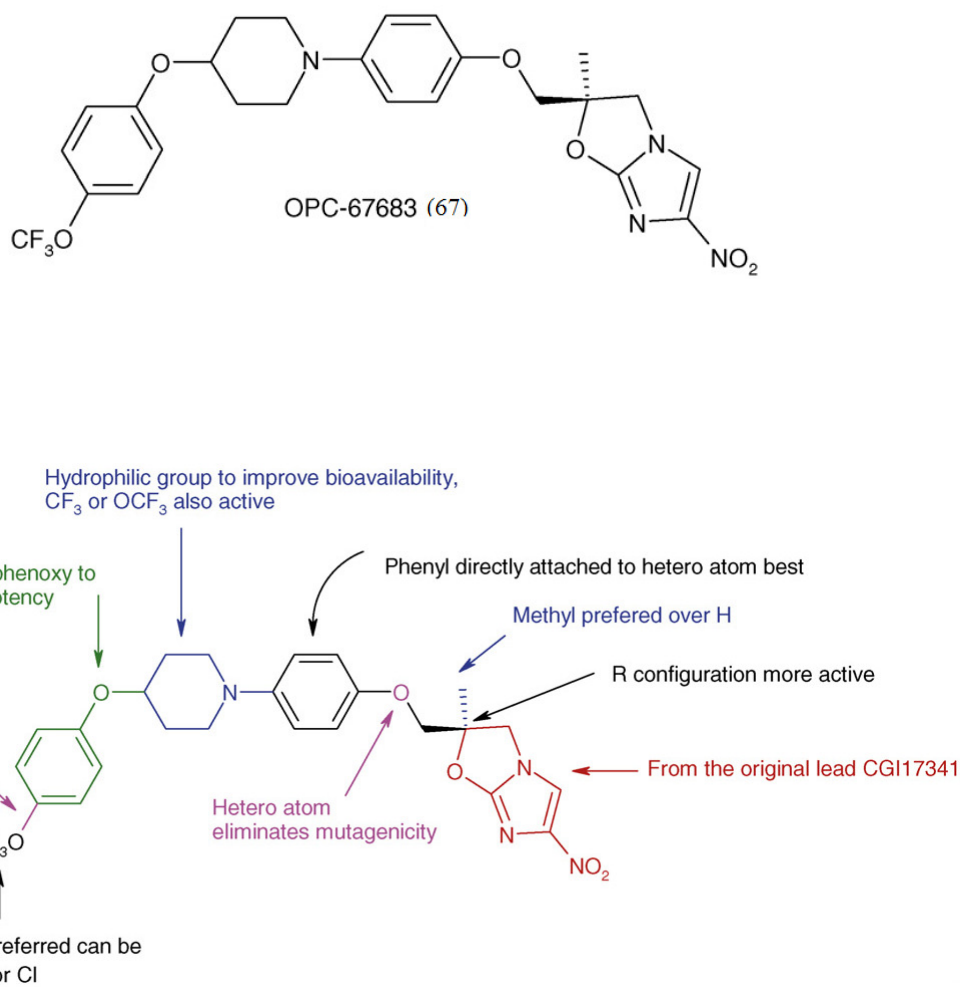


Figure 2.30. Summary of the SAR in the nitroimidazo [2, 1-b] oxazole series

TMC207 (68, figure 2.30) is a quinoline derivative with potent anti-TB activity in susceptible, MDR and XDR strains, with no cross-resistance to current first-line drugs [153-156]. It appears that TMC207 has greater potency against mutated drug resistant

strains than to fully susceptible isolates. Whilst TMC207-resistant *M.tb* strains have appeared, they remain fully susceptible to other anti-TB drugs such as RIF, INH, SM and EMB. The use of TMC207 alone appears to be at least as effective as a combination of RIF, INH and PZA and more effective than RIF alone in mouse models. TMC207 has a potent sterilising ability in guinea pigs, being 100 times more effective than the conventional combination of RIF, INH and PZA. TMC207 has been determined to be well absorbed orally in humans, with a long half-life, which explains the effectiveness of single weekly dosing in mice. TMC207 is metabolised by CYP3A4 and, therefore, when it is administered with RIF its levels decrease significantly, making TMC207 likely to be incompatible with anti-retrovirals.

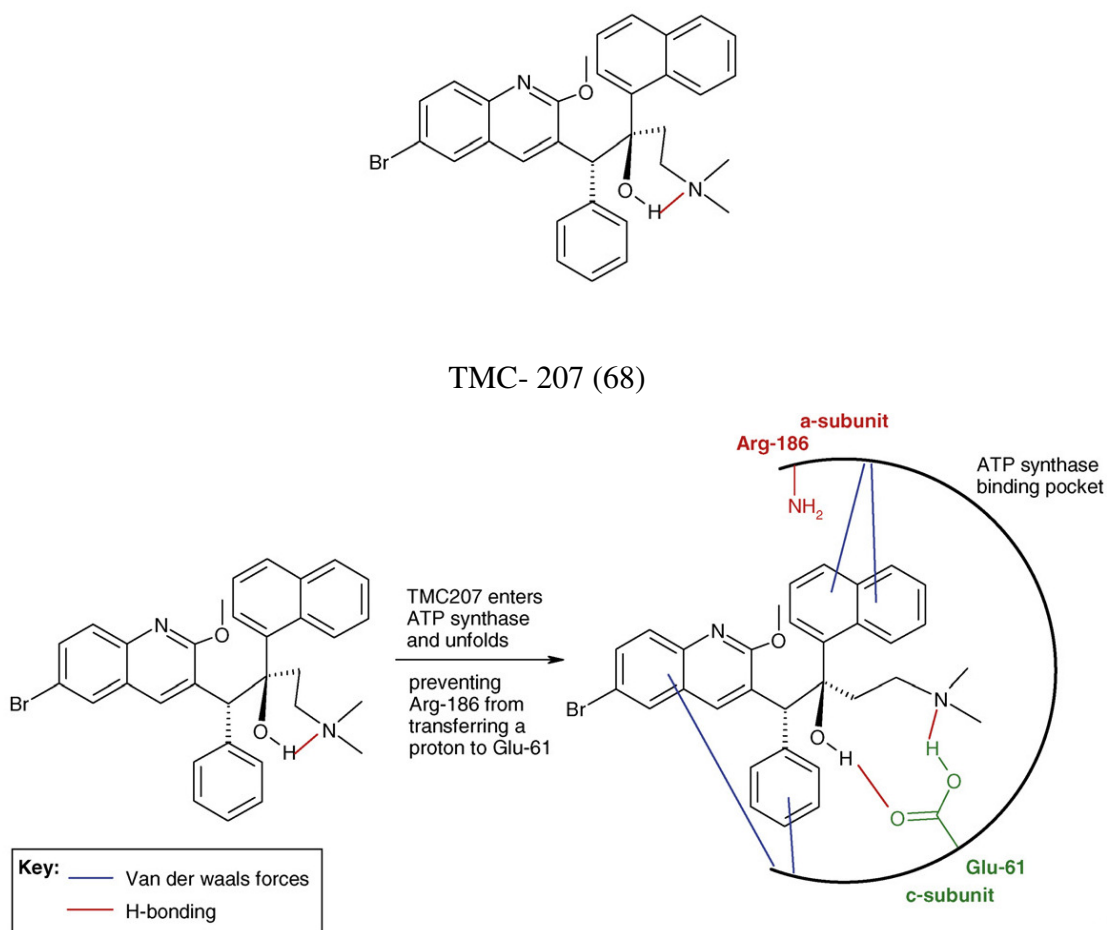


Figure 2.31. Diagram showing the interactions between TMC207 and the binding site of *M.tb* ATP synthase

It is well absorbed in humans with a long half-life and is currently in phase II clinical studies. PhaseIIa clinical trials have demonstrated that TMC207 is well tolerated in patients, with an appropriate activity against M.tb. although lower than RIF or INH monotherapy. Its mechanism of action involves inhibition of ATP synthase that binds the M. tuberculosis membrane and there is a synergistic effect between TMC207 and PZA.

Other compounds with very promising anti-TB activity are LL-3858 and OPC-37306 (69 and 70, figure 2.31) [157-160]. Some other examples of anti-TB compounds in clinical trials are showed in table 1 [161-162].

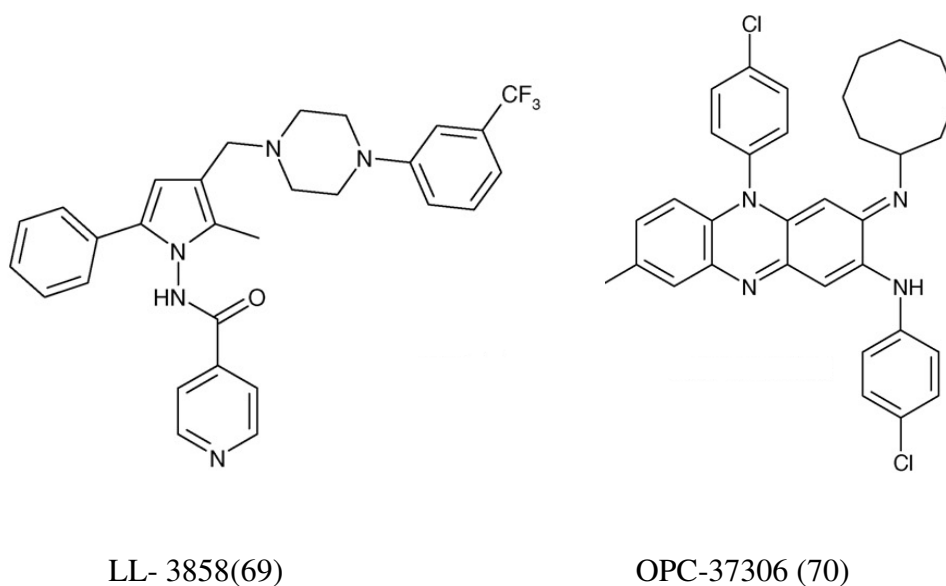


Figure 2.32. Structures of few promising anti-TB

Many new antibiotic candidates are chemical molecules reengineered from old drug classes discovered decades ago. This approach has identified new TB drugs from existing antibacterial drug classes and either involved there design of accessible scaffolds to improve their antimycobacterial potencies or, more directly, the repositioning of known antibacterial drugs with good antimycobacterial activity for testing in TB clinical trials (Table 2.1 & 2.2). During re-engineering of known scaffolds, chemical modifications are introduced into the core structure that may lead to improved bactericidal activities, better

resistance profiles, safety, tolerability or superior pharmacokinetic/ pharmacodynamic properties. Figure 2.32 depicts the existing drugs and NCE's at various stages of development.

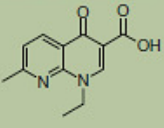
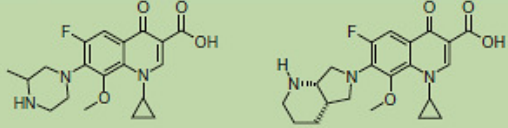
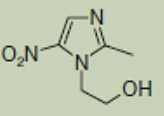
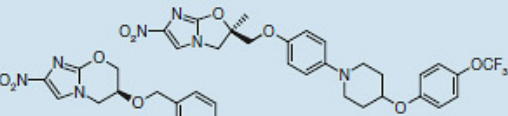
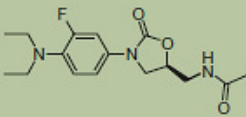
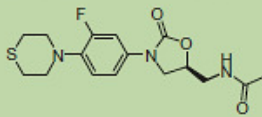
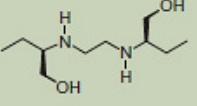
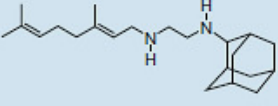
Antibiotic class	Parent scaffold	Derivatized scaffolds
Fluoro-quinolones	 Nalidixic acid	 Gatifloxacin Moxifloxacin
Nitro-imidazoles	 Metronidazole	 PA-824 OPC-67683
Oxazolidinones	 Linezolid	 PNU-100480
1,2-ethylene diamine	 Ethambutol	 SQ109

Table 2.1: Remodelling the existing antibacterial drug classes.

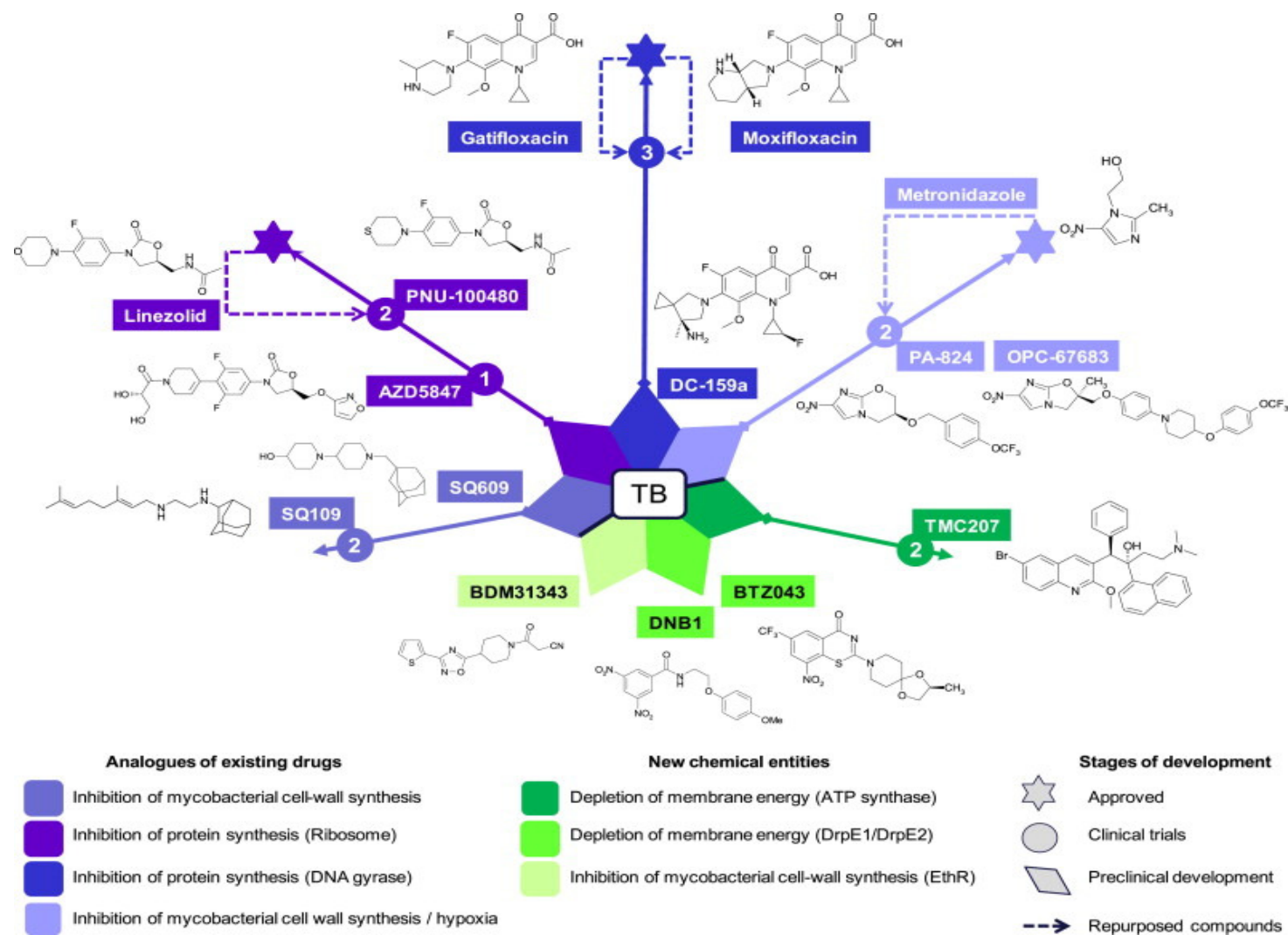


Figure 2.33. Existing and NCE's at various stages of development

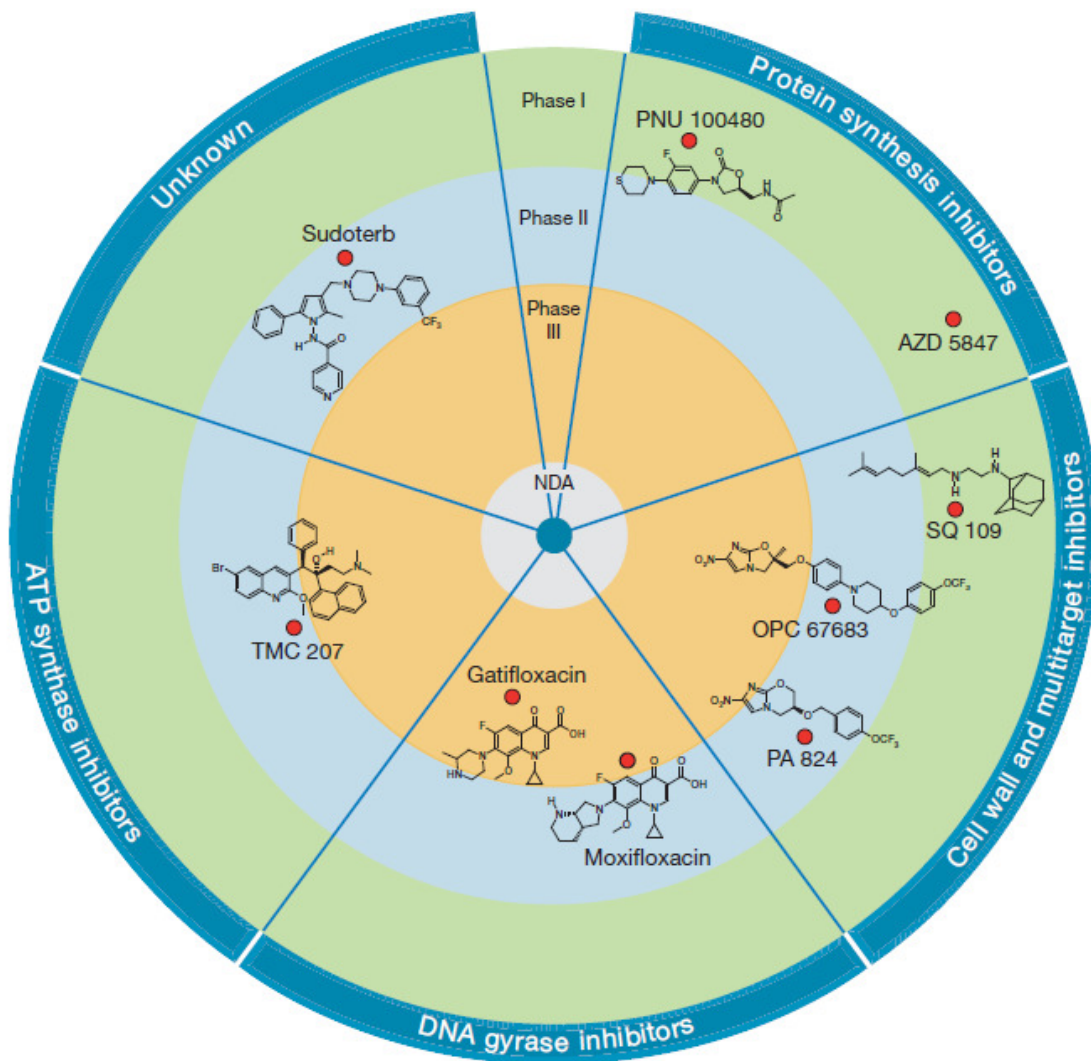


Figure 2.34. A bull's-eye representation of the current clinical pipeline for TB

Each drug candidate is shown with its current clinical phase of development along with the target family. TMC207 is in phase IIB trials for MDR-TB and in phase IIA trials for drug-Susceptible TB. The structure of AZD-5847 has not been disclosed. NDA is a new drug application (for regulatory approval).

Table 2.2: Some compounds under clinical trials along with the funding agencies

Compound	Funding	Target	Mechanism of action	Resistance mechanisms	Clinical trial phase
a) Nitroimidazoxacines					
PA-824	GATB	F420 dependent nitroreductase	Inhibition of proteins and cellwall biosynthesis	Rv0407, Rv3547, Rv3261 and Rv3262 mutations	II
OPC-67683	Otsuka	Nitroreductase	Inhibition of mycolic acid and cell wall biosynthesis	Rv3547 mutations	II
b) Fluoroquinolones					
Moxifloxacin	Bayer, CDC, NIH, FDA	DNA gyrase	Inhibition of DNA biosynthesis	<i>gyrA</i> mutations	III
Gatifloxacin	NIH	DNA gyrase	Inhibition of DNA biosynthesis	<i>gyrA</i> mutations	III
c) Diarilquinolines					
TMC207	Tibotec	F1F0 ATP sintetase	Inhibition of ATPsynthesis anddisruption ofmembrane potential	<i>atpE</i> mutations	III
d) Oxazolidinones					
Linezolid	NIH, Pfizer	Ribosome	Inhibition of protein biosynthesis	rRNA 23S mutations	Pre-trial
e) Dietilamins					
SQ109	Sequella	Unknown	Inhibition of cellwall biosynthesis	Unknown	I/II
f) Pirrols					
LL3858	Lupin	Unknown	Unknown	Unknown	I

Chemical tailoring of existing drugs or drug classes has led to the identification of new molecules with potent antimycobacterial activities. The oxazolidinones also include the

recently discovered AZD-5847, the structure of which has not been disclosed yet and is therefore not listed here. SQ109, an orally active cell-wall-targeting diamine antibiotic, identified via combinatorial chemistry approaches, is currently being tested in humans.

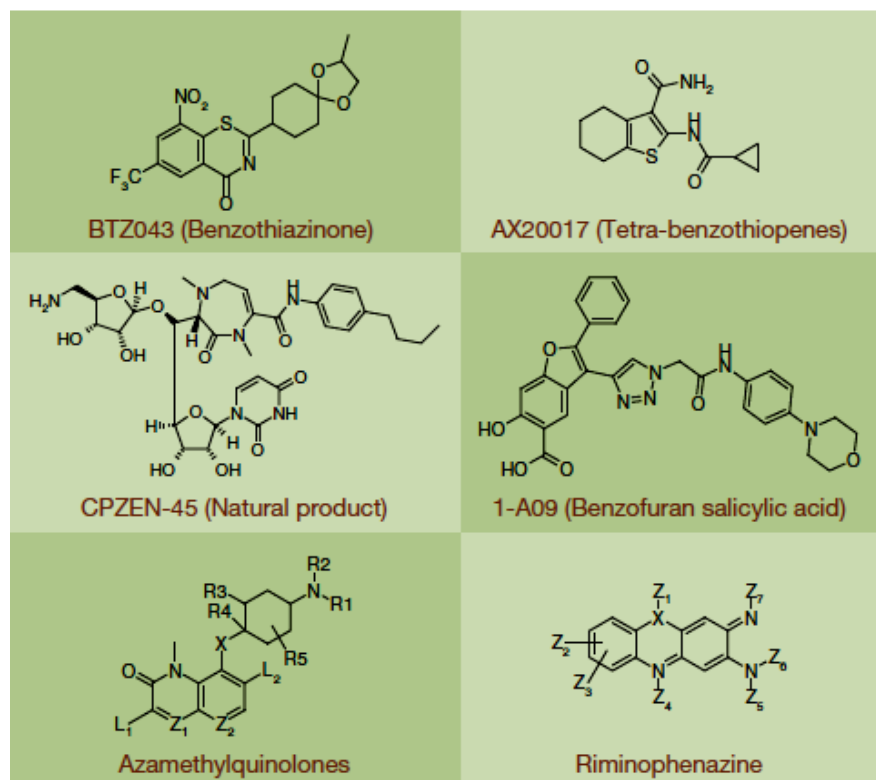


Figure 2.34. Representative underexplored and new chemical scaffolds.

Some of the chemical structures shown are mentioned in the text. CPZEN-45, streptomyces-derived natural product, is a semi-synthetic nucleoside antibiotic from the caprazamycin family with TB activity. Re-engineering of riminophenazine's chemical scaffold can lead to interesting energy metabolism inhibitors with the potential to kill non-replicating bacilli. Azamethylquinolones have demonstrated activity on mycobacteria and further chemical optimization may lead to interesting lead candidates hopefully with better resistance profiles. However, a recent kinase library screen in *E. coli* led to the identification of a pyrido pyrimidine scaffold as a competitive inhibitor of the ATP binding site of acetyl-coenzyme-A carboxylase. For mycobacteria, the search for kinase inhibitors with potent in vitro bactericidal activity has not been successful,

although chemical optimization towards the uniquely conserved ATP-binding pockets of protein kinaseG did identify a new chemical scaffold, tetra-hydro-benzothiophene (AX20017), but with activity restricted to infected macrophages (Figure 2.34). A related concept within bacterial research is to identify inhibitors of bacterial virulence factors or host targets that can modulate pathogen survival inside the infected cells. Recently, it was revealed that the innate immune response within macrophages can be modulated by specifically inhibiting the mycobacterial tyrosine phosphatase (mtpB), which blocks host ERK1/2 and P38 signalling and promotes intramacrophage survival of mycobacteria.

Chapter 3-

Objective and plan of work

3.1 Objective and Rationale for the design of proposed compounds

The main objective of the proposed work is to design and synthesize novel 1, 3 and 1, 4-thiazine derivatives for the treatment of tuberculosis and also evaluate the possible pharmacokinetic properties.

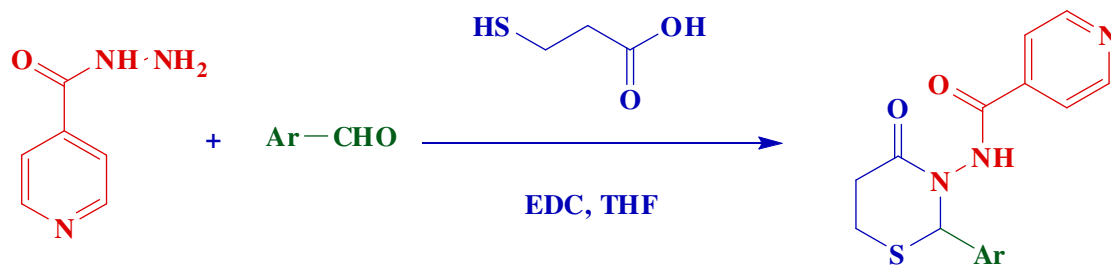
The incidence of TB infection has steadily risen in the past decade, and this increase can be attributed to a similar increase in human immunodeficiency virus (HIV) infection [163]. The association of TB and HIV infections is so dramatic that in some cases nearly two-thirds of the patients diagnosed with TB are also HIV-1 seropositive [164]. Furthermore, numerous studies have shown that TB is a cofactor in the progression of HIV infection [165]. The reemergence of TB infection is further complicated by an increase in cases that are resistant to conventional antitubercular drug therapy. Not only does the increasing rate of multidrug-resistant TB create problems for the treatment but also the costs are exploding. Thus, new drugs are necessary to overcome the current problems of therapy.

3.2 Plan of work

Various substituted Thiazines have been synthesized and tested for their antitubercular activity. The present work comprises of the synthesis of the following

3.2.1. [1, 3]-Thiazine derivatives

3.2.1.1. Design and synthesis of 1, 3-Thiazine derivatives [166]



R= (sub) heteroaryl; Ar= (sub) phenyl, heteroaryl; R₁= H, alkyl, halogen etc.

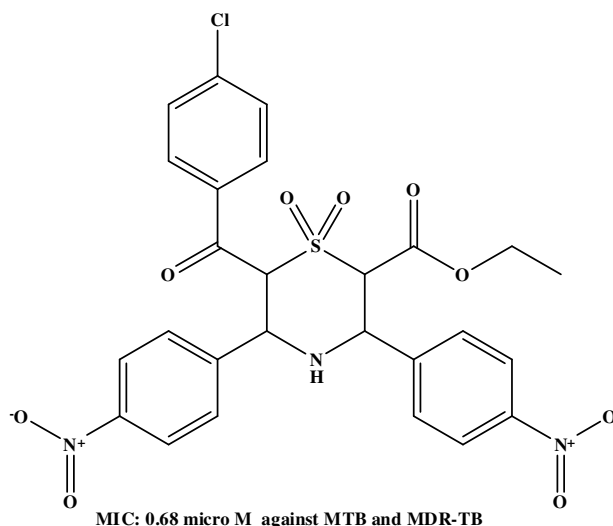
3.2.1.2. 1, 3-Thiazine derivatives were evaluated for the following tests

1. In vitro antimycobacterial activity against *M. tuberculosis* H37RV
2. Cytotoxicity
3. Pharmacokinetics, tissue distribution and excretion of compound most active compound.
4. Interaction of most active compound with other drugs

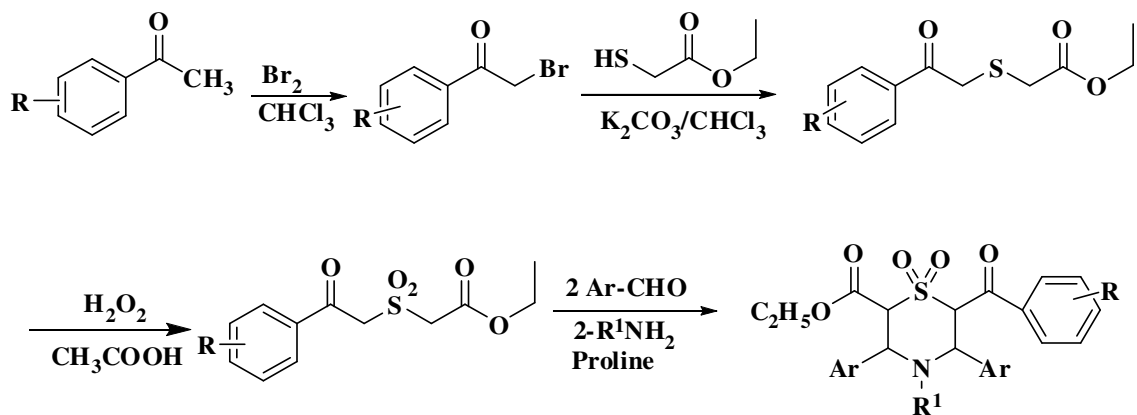
3.2.2. [1, 4]-Thiazine derivatives

3.2.2.1. Design and synthesis of 1, 4-Thiazine derivatives [136]

Earlier we reported anti-tubercular ethyl 6-(4-chlorobenzoyl)-3, 5-di (4-nitrophenyl)-1, 1-dioxo-1, 4-thiazinane-2-carboxylate, which inhibited *in vitro* *M. tuberculosis* H37Rv (MTB) with minimum inhibitory concentration of 0.68 μ M [136].



In the course of screening to discover new compounds employed in the chemotherapy of tuberculosis, in this proposal we are planning to synthesize some novel 1, 3 and 1, 4-thiazine derivatives for the treatment of TB.



R = H, Cl, CH₃, etc.; Ar = (sub) phenyl, heteroaryl; R¹ = (sub) heteroaryl

3.2.2.2. 1, 4-Thiazine derivatives were evaluated for the following tests

1. *In vitro* antimycobacterial activity against *M. tuberculosis* H₃₇RV
2. In-vitro enzyme assay (chorismate mutase)
3. Cytotoxicity assay
4. In-vitro dormant antimycobacterial activity
5. 3D QSAR models generation and PLS analysis

Chapter 4

1. 3-Thiazine derivatives as anti-tubercular agents

Chapter 4.1

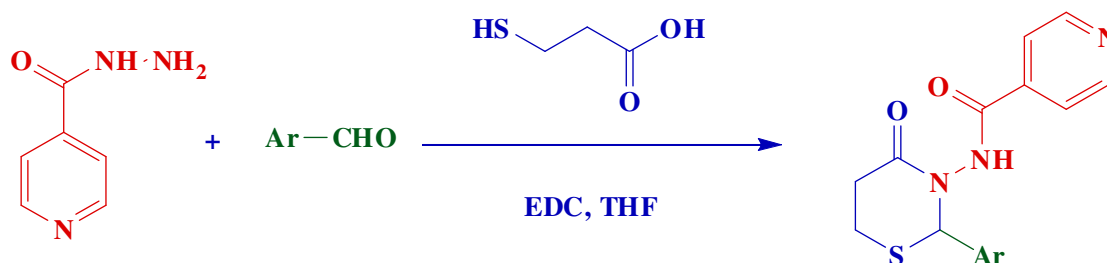
Synthesis and biological screening

This chapter illustrates the novel INH analogs being incorporated in the 1, 3-thiazinan scaffold T. Srivastava et al have earlier reported the dicyclohexylcarbodiimide mediated synthesis of 4-thiazolidinones and metathiazanones, by one-pot three component condensation of amine, bezaldehyde, mercaptopropinoic acid in the ratio of 1:2:3 to give the desired product in quantitative yield [166]. In continuation of our efforts in discovering new leads for antimycobacterial activities, we tried to extend the above work by replacing the amine with isoniazid. Though reaction went smoothly for simple amines, our initial effort to synthesize the isoniazid analog of metathiazanones resulted in very poor yield as majority of the product was found in the filtered residue along with dicyclohexyl urea formed as the side product of the reaction. Purification of the resultant residue by column chromatography gave the desired product in very low yield.

4.1.1. Chemistry

A series of 32 molecules were synthesized. The synthesis of the target molecules were achieved as illustrated in Scheme 1.

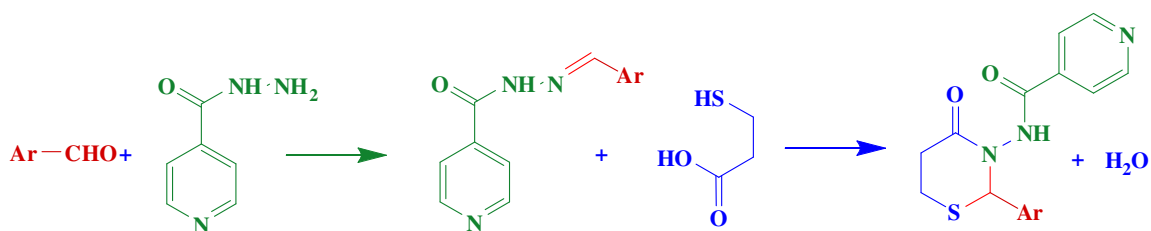
Synthesis of N (Aryl-4-oxo-1, 3-thiazinan-3yl) isonicotinamide:



Scheme 4.1.1. Formation of [1, 3]-thiazines

As previously reported, the reaction involves the addition of sulfur nucleophile to the imine centre followed by attack of the nitrogen on the carboxylic moiety with the expulsion of water giving the cyclized product. In *N, N'*-Dicyclohexylcarbodiimide (DCC) [166] mediated synthesis of thiazolidinones, carbodiimide enhances the activation

of the carboxyl group of an adduct obtained by the sulfur addition to the imine thereby facilitating cyclization. Keeping this in mind we decided to set a trial with 1-ethyl-3-(3-dimethylaminopropyl) carbodiimide (EDC) as the activating carbodiimide for the synthesis of metathiazanones, as the corresponding urea formed as side product during the course of the reaction would be highly water soluble and can be easily eliminated by simple workup. The reaction not only gave the desired product in quantitative yield but also with desired purity. It was observed that as reported in the case of DCC mediated cyclization, addition of EDC in ice cold conditions gives better yields as compared with the reaction carried out at ambient temperature.



Scheme 4.1.2. Mechanism for the formation of [1, 3]-thiazines

To explore the scope and limitations of these conditions a series of 32 aromatic and heterocyclic aldehydes containing electron-withdrawing groups (such as nitro, halogens) or electron-donating groups (such as methoxy, methyl etc) were employed and as apparent from the Table 4.1.1, they were found to react well to give the corresponding N-aryl-4-oxo-1, 3-thiazinan-3-yl) isonicotinamide in good to excellent yields (50- 95%).

INH was dissolved in THF and the reaction mixture was cooled to 0°C, the corresponding aldehyde was then added drop wise, followed by 3-mercaptopropionic acid and 1-ethyl-3-(3-dimethylaminopropyl) carbodiimide, the reaction mixture was then slowly warmed to room temperature and stirred at room temperature for another 5-6 hours (monitored by TLC for completion), it was then quenched with water and worked up to give the desired metathiazanones in quantitative yield.

4.1.2. Methodology

All commercially available chemicals and solvents were used without further purification. TLC experiments were performed on alumina-backed silica gel 40 F254 plates (Merck, Darmstadt, Germany). The plates were illuminated under UV (254 nm) and molybdinic acid. Melting points were determined using Buchi B-540 and are uncorrected. Elemental analyses were carried out on an automatic Flash EA 1112 Series, CHN Analyzer (Thermo). All ¹H and ¹³C NMR spectra were recorded on a Bruker AM-300 (300.12 MHz, 75.12 MHz), BrukerBioSpin Corp, Germany. Molecular weights of unknown compounds were checked by LCMS 6100B series Agilent Technology.

In a typical procedure, the corresponding aldehyde (2.0 mmol) was added to an ice cold solution of Isoniazid (1.0 mmol) in THF. The reaction mixture was stirred at 0°C for another 5-10 min. Mercaptopropionic acid (3.0 mmol) was then added drop wise to the reaction mixture while maintaining the temperature at 0°C, followed by the addition of 1-Ethyl-3-(3-dimethylaminopropyl) carbodiimide (EDC) (1.3 mmol). The reaction mixture was then slowly warmed to room temperature and stirred at room temperature for 5-6 hours (monitored by TLC for completion). The reaction mixture was evaporated to dryness; water (10 ml) was added to the residue and extracted with dichloromethane (2 x 15 ml). The combined organic layer was then successively washed with 5% aq. citric acid (2x10 ml), water (1x10 ml), 5% aq. sodium hydrogen carbonate (1x15 ml) and finally washed with brine (1x15 ml), dried over anhydrous Na₂SO₄ and evaporated under reduced pressure to give the desired product. The crude product was then further purified either by recrystallisation from ethanol- ethyl acetate mixture (7:3 v/v) or by column chromatography.

4.1.3. Characterization of Compounds

The purity of compounds 1–32 was checked by TLC and elemental analysis. Both analytical and spectral data (¹H NMR, ¹³C NMR, and mass spectra) of all the synthesized compounds were in full agreement with the proposed structures [173]. Lipophilicity of the synthesized derivatives and that of the parent compound, INH, are

expressed in terms of their logP values (Table 4.1.1). These values were computed with a routine method called calculated logP (ClogP) using ChemBioDraw Ultra 11.0 software. Chemical shifts are reported in ppm (δ) with reference to internal standard TMS. The signals are designated as follows: s, singlet; d, doublet; dd, doublet of doublets; t, triplet; m, multiplet.

N-(4-oxo-2-phenyl-1, 3-thiazinan-3-yl) isonicotinamide (1):

White solid; M.P - 146-148; Yield (87%); Anal.Calcd for $C_{16}H_{15}N_3O_2S$: C, 61.32; H, 4.82; N, 13.41. Found: C, 60.93 H, 4.87; N, 13.79. 1H NMR (300 MHz, $CDCl_3$): δ 2.78–2.96 (m, 4H, CH_2CH_2), 5.73 (s, 1H, CH), 7.09-7.23 (m, 5H, ArH of phenyl), 7.72 - 8.81(m, 4H, ArH of pyridyl), 8.19 (s, 1H, NH). ^{13}C NMR (75MHz, $CDCl_3$): δ 170.9, 163.8, 149.8, 140.2, 138.6, 128.7, 127.9, 126.3, 122.9, 63.7, 38.6, 31.9. MS m/z : 313.09 [M^+].

N-(4-oxo-2-o-tolyl-1, 3-thiazinan-3-yl) isonicotinamide (2):

White solid;M.P - 111-113; Yield (83%);Anal.Calcd for $C_{17}H_{17}N_3O_2S$: C, 62.36; H, 5.23; N, 12.83 Found: C, 62.56; H, 5.06; N, 12.61. 1H NMR (300 MHz, $CDCl_3$): δ 2.31(s, 3H, CH_3), 2.74–2.94 (m, 4H, CH_2CH_2), 5.79 (s, 1H, CH), 6.99-7.11 (m, 4H, ArH of phenyl), 7.79 - 8.91(m, 4H, ArH of pyridyl), 8.31 (s, 1H, NH). ^{13}C NMR (75MHz, $CDCl_3$): δ 171, 163.9, 149.7, 140.3, 139, 136.6, 128.9, 126.9, 125.1, 122.8, 57.4, 38.2, 31.8, 18.3. MS m/z : 327.10 [M^+].

N-(4-oxo-2-m-tolyl-1, 3-thiazinan-3-yl) isonicotinamide (3):

White solid;M.P - 170-172; Yield (69%);Anal.Calcd for $C_{17}H_{17}N_3O_2S$: C, 62.36; H, 5.23; N, 12.83 Found: C, 62.46; H, 5.63; N, 12.69. 1H NMR (300 MHz, $CDCl_3$): δ 2.33 (s, 3H, CH_3), 2.71–2.89 (m, 4H, CH_2CH_2), 5.76 (s, 1H, CH), 6.85-7.21 (m, 4H, ArH of phenyl), 7.73 - 8.89(m, 4H, ArH of pyridyl), 8.17 (s, 1H, NH). ^{13}C NMR (75MHz, $CDCl_3$): δ 171.1, 163.8, 149.6, 140.1, 138.8, 137.9, 130.4, 128.6, 127.9, 125.4, 122.6, 64.5, 38.4, 31.7, 25.1. MS m/z : 327.10 [M^+].

N-(4-oxo-2-p-tolyl-1, 3-thiazinan-3-yl) isonicotinamide (4);

White solid; M.P - 126--128; Yield (71%); Anal. Calcd for C₁₇H₁₇N₃O₂S: C, 62.36; H, 5.23; N, 12.83 Found: C, 62.21; H, 5.69; N, 12.49. ¹H NMR (300 MHz, CDCl₃): δ 2.34(s, 3H, CH₃), 2.73–2.94 (m, 4H, CH₂CH₂), 5.77 (s, 1H, CH), 6.91-7.09 (m, 4H, ArH of phenyl), 7.79 - 8.91(m, 4H, ArH of pyridyl), 8.19 (s, 1H, NH). ¹³C NMR (75MHz, CDCl₃): δ 171.2, 164, 149.7, 140.4, 137.2, 136.8, 128.9, 128.6, 122.9, 63.9, 38.5, 31.7, 24.3. MS *m/z*: 327.10 [M⁺].

N-(2-(4-methoxyphenyl)-4-oxo-1, 3-thiazinan-3-yl) isonicotinamide (7):

White solid; M.P - 166-168; Yield (84%); Anal. Calcd for C₁₇H₁₇N₃O₃S: C, 59.46; H, 4.99; N, 12.24. Found: C, 59.39; H, 4.93; N, 12.21. ¹H NMR (300 MHz, CDCl₃): 2.69–2.83 (m, 4H, CH₂CH₂), 3.71(s, 3H, OCH₃) 5.74 (s, 1H, CH), 6.71-7.03 (m, 4H, ArH of phenyl), 7.89 - 8.97(m, 4H, ArH of pyridyl), 8.13 (s, 1H, NH) ¹³C NMR (75MHz, CDCl₃): δ 171.4, 164.2, 159.3, 149.9, 140.7, 131.5, 129.7, 122.6, 113.9, 64.1, 56.1, 38.4, 31.6. MS *m/z*: 343.10 [M⁺].

N-(2-(3, 4, 5-trimethoxyphenyl)-4-oxo-1, 3-thiazinan-3-yl) isonicotinamide (8):

Off White solid; M.P - 176-178; Yield (81%); Anal. Calcd for C₁₉H₂₁N₃O₅S: C, 56.56; H, 5.25; N, 10.42. Found: C, 56.69; H, 5.1; N, 10.24. ¹H NMR (300 MHz, CDCl₃): 2.71–2.85 (m, 4H, CH₂CH₂), 3.79 (s, 3H, OCH₃), 3.82 (s, 6H, 2*OCH₃), 5.81 (s, 1H, CH), 6.16 (d, 1H, ArH of phenyl), 6.18 (d, 1H, ArH of phenyl), 7.85 - 8.93(m, 4H, ArH of pyridyl), 8.21 (s, 1H, NH). ¹³C NMR (75MHz, CDCl₃): δ 171.4, 164.3, 150.8, 149.9, 140.8, 137.3, 133.1, 122.6, 105.9, 64.7, 56.7, 56.5, 38.3, 31.7. MS *m/z*: 403.12 [M⁺].

N-(2-(4-hydroxy-3-methoxyphenyl)-4-oxo-1, 3-thiazinan-3-yl) isonicotinamide (9):

Yellow solid: M.P - 133-135; Yield (75%); Anal. Calcd for C₁₇H₁₇N₃O₄S: C, 56.81; H, 4.77; N, 11.69. Found: C, 56.87; H, 4.67; N, 11.21. ¹H NMR (300 MHz, CDCl₃): 2.78–2.91 (m, 4H, CH₂CH₂), 3.7 (s, 3H, OCH₃), 5.83 (s, 1H, CH), 6.5-6.74 (m, 3H, ArH of phenyl), 7.89 - 8.95 (m, 4H, ArH of pyridyl), 8.23 (s, 1H, NH). ¹³C NMR (75MHz, CDCl₃): δ 171.1, 163.9, 152.1, 149.9, 144.6, 140.9, 132.5, 122.7, 122.1, 116.4, 113.9, 64.3, 56.3, 38.1, 31.8. MS *m/z*: 359.09 [M⁺].

N-(2-(3-hydroxyphenyl)-4-oxo-1, 3-thiazinan-3-yl) isonicotinamide (11):

Off white solid; M.P - 107-109; Yield (74%); Anal.Calcd for C₁₆H₁₅N₃O₃S: C, 58.34; H, 4.59; N, 12.76. Found: C, 58.14; H, 4.79; N, 12.71. ¹H NMR (300 MHz, CDCl₃): 2.75–2.91 (m, 4H, CH₂CH₂), 5.85 (s, 1H, CH), 6.59-6.92 (m, 4H, ArH of phenyl), 7.89 - 8.95 (m, 4H, ArH of pyridyl), 8.30 (s, 1H, NH). ¹³C NMR (75MHz, CDCl₃): δ 171.3, 164.1, 158.1, 149.7, 141.1, 140.6, 131.1, 122.7, 121.7, 114.1, 64.4, 38.3, 31.9. MS *m/z*: 329.08 [M⁺].

N-(2-(3-(dimethylamino) phenyl)-4-oxo-1, 3-thiazinan-3-yl) isonicotinamide (13):

Pale yellow solid; M.P - 148-150; Yield (80%); Anal.Calcd for C₁₈H₂₀N₄O₂S: C, 60.65; H, 5.66; N, 15.72. Found: C, 60.5; H, 5.86; N, 15.89. ¹H NMR (300 MHz, CDCl₃): 2.73–2.89 (m, 4H, CH₂CH₂), 3.1 (s, 6H, 2*N-CH₃) 5.82 (s, 1H, CH), 6.54-6.92 (m, 4H, ArH of phenyl), 7.81 - 8.86 (m, 4H, ArH of pyridyl), 8.24 (s, 1H, NH). ¹³C NMR (75MHz, CDCl₃): δ 171.3, 164, 149.7, 148.9, 141.1, 140.7, 129.6, 122.8, 118.3, 113.5, 112.1, 63.8, 41.2, 38.1, 31.6. MS *m/z*: 356.13 [M⁺].

N-(2-(4-isopropylphenyl)-4-oxo-1, 3-thiazinan-3-yl) isonicotinamide (14):

White solid; M.P - 123-125; Yield (91%); Anal.Calcd for C₁₉H₂₁N₃O₂S: C, 64.20; H, 5.95; N, 11.82. Found: C, 64.30; H, 6.01; N, 11.91. ¹H NMR (300 MHz, CDCl₃): 1.36-1.41 (d, 6H, 2*CH₃), 2.69–2.87 (m, 4H, CH₂CH₂), 3.26–3.35 (m, 1H, CH), 5.81 (s, 1H, CH), 6.91-7.09 (m, 4H, ArH of phenyl), 7.79 - 8.91(m, 4H, ArH of pyridyl), 8.19 (s, 1H, NH). ¹³C NMR (75MHz, CDCl₃): δ 171.4, 164.1, 149.1, 147.1, 140.6, 135.9, 129.1, 126.1, 123.1, 63.8, 38.6, 36.2, 31.4, 24.1. MS *m/z*: 355.14 [M⁺].

N-(2-(4-(benzyloxy) phenyl)-4-oxo-1, 3-thiazinan-3-yl) isonicotinamide (17):

White solid; M.P - 189-190; Yield (84%); Anal.Calcd for C₂₃H₂₁N₃O₃S: C, 65.85; H, 5.05; N, 10.02. Found: C, 65.89; H, 4.99.; N, 9.97. ¹H NMR (300 MHz, CDCl₃): δ 2.79–2.87 (m, 4H, CH₂CH₂), 5.21(s, 2H, CH₂) 5.80 (s, 1H, CH), 6.8-7.01(m, 4H, ArH of phenyl), 7.43-7.54 (m, 5H, ArH Of benzyl), 7.91-8.87(m, 4H, ArH of pyridyl), 8.3 (s, 1H, NH, D₂O exchangeable). ¹³C NMR (75MHz, CDCl₃): δ 171.1, 163.9, 158.3, 148.9, 141.1,

138.8, 130.3, 128.2, 127.1, 125.2, 124.1, 120.8, 114.12, 70.1, 63.7, 38.2, 31.5MS *m/z*: 419.13 [M⁺].

N-(2-(3-nitrophenyl)-4-oxo-1, 3-thiazinan-3-yl) isonicotinamide (19):

Pale yellow solid; M.P - 186-188; Yield (71%); Anal.Calcd for C₁₆H₁₄N₄O₄S: C, 53.62; H, 3.94; N, 15.63. Found: C, 53.39; H, 3.69; N, 15.73. ¹H NMR (300 MHz, CDCl₃): δ 2.71–2.88 (m, 4H, CH₂CH₂), 5.83 (s, 1H, CH), 7.4-8.84 (m, 8H, ArH of phenyl & pyridyl), ¹³C NMR (75MHz, CDCl₃): δ 171.2, 164.1, 149.3, 148.7, 141.1, 140.7, 134.9, 129.8, 124.3, 122.9, 119.3, 62.9, 38.4, and 31.7.MS *m/z*: 358.07 [M⁺].

N-(2-(4-chlorophenyl)-4-oxo-1, 3-thiazinan-3-yl) isonicotinamide (21):

White solid; M.P-161-163; Yield (65%); Anal.Calcd for C₁₆H₁₄ClN₃O₂S: C, 55.25; H, 4.06; N, 12.08. Found: C, 55.32; H, 4.13; N, 12.34. ¹H NMR (300 MHz, CDCl₃): δ 2.76–2.91 (m, 4H, CH₂CH₂), 5.84 (s, 1H, CH), 7.01-7.26 (m, 4H, ArH of phenyl), 7.8 - 8.91 (m, 4H, ArH of pyridyl), 8.31 (s, 1H, NH). ¹³C NMR (75MHz, CDCl₃): δ 171.4, 164.1, 149.6, 140.7, 137.5, 131.9, 130.1, 128.3, 123.1, 63.8, 38.1, 31.4.MS *m/z*: Found [M+H *m/z*: %] 347.5, 100; 349.05, 37.2

N-(2-(2-bromophenyl)-4-oxo-1, 3-thiazinan-3-yl) isonicotinamide (23):

White solid; M.P-157-159; yield (67%); Anal.Calcd for C₁₆H₁₄BrN₃O₂S: C, 48.99; H, 3.60; N, 10.71. Found: C, 49.12; H, 3.63; N, 10.9. ¹H NMR (300 MHz, CDCl₃): 2.71–2.91 (m, 4H, CH₂CH₂), 5.85 (s, 1H, CH), 6.99-7.33 (m, 4H, ArH of phenyl), 7.81 - 8.89(m, 4H, ArH of pyridyl), 8.25 (s, 1H, NH). ¹³C NMR (75MHz, CDCl₃): 171.3, 163.9, 149.6, 142.1, 141, 131.8,131, 129.5, 127.7, 123.6, 122.4, 55.9, 38.1, 31.6.MS *m/z*: Found [M+H *m/z*: %] 391.00, 100; 393.05, 98.

N-(2-(4-fluorophenyl)-4-oxo-1, 3-thiazinan-3-yl) isonicotinamide (27):

White solid; M.P-183-185; Yield (60%); Anal.Calcd for C₁₆H₁₄FN₃O₂S: C, 57.99; H, 4.26; N, 12.68. Found: C, 58.13; H, 4.29; N, 12.78. ¹H NMR (300 MHz, CDCl₃): δ 2.78–2.94 (m, 4H, CH₂CH₂), 5.81 (s, 1H, CH), 6.91-7.13 (m, 4H, ArH of phenyl), 7.86 - 8.89

(m, 4H, ArH of pyridyl), 8.29 (s, 1H, NH). ¹³C NMR (75MHz, CDCl₃): 171.3, 164.2, 161.6, 149.8, 141.1, 134.8, 130.9, 123.1, 116.4, 63.7, 38.3, 31.8. MS *m/z*: 331.08 [M⁺].

N-(2-(4-(trifluoromethyl) phenyl)-4-oxo-1, 3-thiazinan-3-yl) isonicotinamide (30):

White solid; M.P-199-201; Yield (66%); Anal.Calcd for C₁₇H₁₄F₃N₃O₂S: C, 53.54; H, 3.70; N, 11.02. Found: C, 66.01; H, 4.89.; N, 9.37. ¹H NMR (300 MHz, CDCl₃): δ 2.81–2.97 (m, 4H, CH₂CH₂), 5.82 (s, 1H, CH), 7.03-7.33 (m, 4H,Ar), 7.89-8.91 (m, 4H, ArH of pyridyl) 8.3 (s, 1H, NH) ¹³C NMR (75MHz, CDCl₃): 171.2, 164.2, 149.7, 141.3, 140.2,129.8, 128.7, 125.1, 124.3, 122.2, 63.6, 38.2, 31.8. MS *m/z*: 381.08 [M⁺].

N-(2-(5-nitrofuran-2-yl)-4-oxo-1, 3-thiazinan-3-yl) isonicotinamide (32):

Brown solid; M.P-179-181; Yield (89%); Anal.Calcd for C₁₄H₁₂N₄O₅S: C, 48.27; H, 3.47; N, 16.08. Found: C, 48.21; H, 3.43; N, 16.12. ¹H NMR (300 MHz, CDCl₃): δ 2.81–2.93 (m, 4H, CH₂CH₂), 6.01 (s, 1H, CH), 6.81 (d, 1H, furfuryl), 7.61 (d, 1H, furfuryl) 7.91-9.01(m, 4H,ArH of pyridyl) 8.4 (s, 1H, NH) ¹³C NMR (75MHz, CDCl₃): 171.2, 164.1, 156.1, 151.5, 149.8,140.9, 123.1,115.4, 109.6, 63.9, 37.2, 27.8. MS *m/z*: 348.05 [M⁺].

4.1.2. Biological Screening and results

4.1.2.1 *In vitro* antimycobacterial Screening

All the compounds were screened for their *in vitro* antimycobacterial activity against log-phase cultures of MTB Middle brook 7H11 agar medium supplemented with OADC by agar dilution method similar to that recommended by the National Committee for Clinical Laboratory Standards for the determination of MIC in triplicate [167]. The MIC is defined as the minimum concentration of a compound required to completely inhibit the bacterial growth.

Test Protocol: Micro-organism: Mycobacterium tuberculosis H₃₇Rv ATCC 27294 was obtained from tuberculosis Research Centre, Chennai, India. Culture Media: Middle brook 7H11 agar with OADC growth supplement

Composition:

Middle brook 7H9 broth base	-	0.47 g
Distilled Water	-	90 mL
Glycerol	-	0.4 mL
Tween 80	-	0.2 mL
OADC growth supplement		
Bovine albumin fraction V	-	0.5 g
Oleic acid	-	0.02 mL
Dextrose	-	0.2 g
Sodium Chloride	-	0.085 g
Distilled Water	-	10 mL

Method (Agar dilution method)

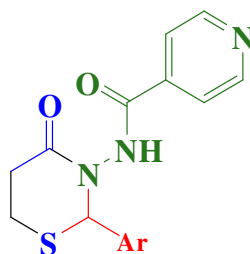
1. 2 fold serial dilutions of each test compound were dissolved in DMSO incorporated into Middlebrook 7H11 agar medium with OADC growth Supplement.
2. Inoculum of *M. tuberculosis* H₃₇Rv were prepared from fresh Middlebrook 7H11 agar slants with OADC growth supplement adjusted to 1mg/mL (wet weight) in Tween 80 (0.05%) saline diluted to 10⁻² to give a concentration of approximately 10⁷cfu/mL.
3. A 5 µL amount of bacterial suspension was spotted into 7H11 agar tubes containing 10- fold serial dilutions of drugs per mL.
4. The tubes were incubated at 37°C and final readings were recorded after 28 days.

The MIC's of the synthesized compounds along with the standard drug INH for comparison are reported in Table 4.1.1.

4.1.2.2. Cytotoxicity evaluation

The safety profile of compounds 1-32 was tested on human cancer cell lines HepG2 at the concentration of 25 μ M using the MTT method. Briefly, cells (2500/well) were seeded in 96-well plates and cultured for 24 hrs, followed by treatment with the compounds 1-32 for another 48 hrs. 20 μ L of 5 mg/ml MTT was added per well and incubated for another 2.5 hrs at 37°C. Then the supernatant fluid was removed and MTT formazan precipitate was dissolved in 150 μ L of DMSO, shaken mechanically for 15-20 min. The optical density of each well was measured at 570 nm, using a Perkin Elmer Victor 3 microplate spectrophotometer. The inhibitory rates at 20 μ M are given in Table 4.1.1, all the active compounds showed low toxicity in this assay and the most potent compound 17 exhibited good safety profile with inhibitory rates as low as 8.8%.

Table.4.1.1. Physical constants, anti-tubercular activity & cytotoxicity of the compounds



Comp No.	Ar	Yield (%)	Melting range (°C)	ClogP ^a	MIC μM ^b	HepG2 cell line % cytotox. ^c
1	phenyl	87	146-148	2.56	9.9	10.6
2	<i>o</i> -methyl phenyl	83	111-113	3.01	9.56	12.6
3	<i>m</i> -methyl phenyl	69	170-172	3.06	9.56	8.6
4	<i>p</i> -methyl phenyl	71	126-128	3.06	9.56	12.4
5	<i>o</i> -methoxy phenyl	89	151-153	2.45	9.08	15.2
6	<i>m</i> -methoxy phenyl	93	129-131	2.48	9.08	10.4
7	<i>p</i> -methoxy phenyl	84	166-168	2.48	4.54	12.6
8	<i>m,m',p</i> -trimethoxy phenyl	81	176-178	1.86	7.76	8.6
9	<i>p</i> -hydroxy-3-methoxy-phenyl	75	133-135	1.74	8.7	16.11
10	<i>o</i> -hydroxyl phenyl	72	98-100	1.84	18.98	8.6
11	<i>m</i> -hydroxyl phenyl	74	107-109	1.89	9.49	8.2
12	<i>p</i> -hydroxyl phenyl	76	121-123	1.89	18.9	10.7
13	<i>p</i> -dimethylamino phenyl	80	148-150	2.70	8.78	4.6
14	<i>p</i> -isopropyl phenyl	91	123-125	3.99	2.138	19
15	<i>o</i> -benzyloxy phenyl	84	181-183	2.25	0.24	10.6
16	<i>m</i> -benzyloxy phenyl	62	163-165	4.25	0.24	12.6
17	<i>p</i> -benzyloxy phenyl	84	189-190	4.25	0.12	8.8
18	<i>o</i> -nitro phenyl	68	169-171	2.22	2.12	28.8
19	<i>m</i> -nitro phenyl	71	186-188	2.30	0.56	28.6
20	<i>p</i> -nitro phenyl	53	194-196	2.30	1.11	32
21	<i>o</i> -chloro phenyl	61	155-157	3.27	1.15	20.6

22	<i>p</i> - chloro phenyl	65	161-163	3.27	0.575	26.8
23	<i>o</i> - bromo phenyl	67	157-159	3.42	0.25	22.2
24	<i>p</i> - bromo phenyl	81	142-144	3.42	0.50	18.4
25	<i>o</i> - fluoro phenyl	91	102-104	2.70	0.60	18.6
26	<i>m</i> - fluoro phenyl	71	131-133	4.25	0.60	16.4
27	<i>p</i> - fluoro phenyl	60	183-185	2.70	0.30	18.6
28	<i>o</i> -(trifluoromethyl) phenyl	74	191-193	3.42	0.52	24.2
29	<i>m</i> -(trifluoromethyl) phenyl	62	197-199	3.44	0.52	26.4
30	<i>p</i> -(trifluoromethyl) phenyl	66	199-201	3.44	0.13	20.6
31	<i>o</i> - furfuryl	70	172-174	1.74	41.2	18.6
32	<i>m'</i> -nitro furfur-2-yl	89	179-181	1.74	4.48	38.6
	Isoniazid	-	-	-0.66	0.36	10.0

^aCLog P was obtained from ChemBioDraw Ultra 11.0; ^bMIC- Minimum inhibitory concentration ^cIC₅₀ was determined at 20 μM

4.1.3. Discussion

Thirty two novel isoniazid analogues were prepared by one-pot three component condensations of isoniazid (INH), 3-mercaptopropionic acid and various aryl/heteroaryl aldehydes. The yields range from 52-93% and the purity of compounds was checked by TLC and elemental analysis. Log P values ranged from 1.74-4.25, lowest being comp 9 and highest being comp. 17 & 18. Because the later bears a bulky aromatic group.

In the MTB screening, all the compounds showed in vitro activity against MTB with MIC ranging from 0.12-41.2 μM. Thirteen compounds (15-17, 19, 22-30) inhibited MTB with less than 1 μM. When compared to standard first line drug INH (MIC of 0.36 μM); six compounds (15-17, 23, 27, 30) were more potent with MIC less than 0.36 μM. Compound N-(2-(4-(benzyloxy) phenyl)-4-oxo-1, 3-thiazinan-3-yl) isonicotinamide (17) inhibited MTB with MIC of 0.12 μM and was three times more potent than INH. The enhanced activity might be due to its hydrophobicity, ClogP of this compound 17 was 4.25 whereas parent compound INH was -0.66. With respect to structure anti-TB activity,

Compound 1, without any substituent on the phenyl rings, displayed an MIC of 9.9 μM and serves as the standard for potency comparison. Introduction of smaller electron donating groups in the phenyl ring 2-13 not alter the activity much; MIC ranging from 4.54-18.98 μM . Among them only 4-methoxy group (7) group enhances the activity twice and introduction of hydroxyl group is detrimental to activity. Introduction bulky groups like benzyloxy on the phenyl ring enhances the activity to 39-92 times with MIC of less than $<1 \mu\text{M}$. The enhanced activity might be due to its hydrophobicity, ClogP of this compounds 15-17 was 4.25 whereas standard compound 1 is 2.56. Introduction of electron withdrawing groups like nitro, halogen, and trifluoromethyl enhances the potency with MIC ranging from 0.13-2.12 μM . The order of activity among the electron withdrawing groups $\text{CF}_3 > \text{Br} > \text{F} > \text{Cl} > \text{NO}_2$. Replacement of phenyl with furan ring makes the compound less active but introduction of nitro group in the furan ring makes the compound 10 times more active with MIC of 4.48 μM .

Compound N-(2-(4-(benzyloxy) phenyl)-4-oxo-1, 3-thiazinan-3-yl) isonicotinamide – “Compound 17” inhibited MTB with MIC of 0.12 μM and was three times more potent than INH was selected for further studies. The most potent compound 17 was selected and assessed for its basic pharmacokinetic, tissue distribution and interaction studies.

4.2. Pharmacokinetics,

tissue distribution

and excretion of compound

N-(2-(4-(benzyloxy) phenyl)-4-oxo-

1,3-thiazinan-3-yl) isonicotinamide-

“Compound 17”

Compound N-(2-(4-(benzyloxy) phenyl)-4-oxo-1, 3-thiazinan-3-yl) isonicotinamide – “compound -17.” (Figure 4.2.1) inhibited MTB with MIC of 0.12 μ M and was three times more potent than INH was selected for further studies. The most potent compound compound 17 was selected and assessed for its basic pharmacokinetic and tissue distribution.

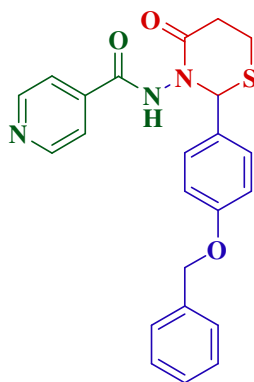


Figure: 4.2.1 Structure of compound 17.

Measurement of drug concentrations in biological matrices is an important aspect of discovery and development for those products containing new active substances. Such data may be required to support new applications in toxicokinetic, pharmacokinetic and distribution studies to make critical decisions supporting the safety and efficacy of a compound. It is therefore paramount that the applied bioanalytical methods used are well characterised, fully validated and documented to a satisfactory standard in order to yield reliable result. The main objective of method validation is to demonstrate the reliability of a particular method for the determination of an analyte concentration in a specific biological matrix, such as blood, plasma, tissue, accurately either in-vitro or in-vivo studies.

In the present chapter, a simple, robust and reproducible method has been developed and validated to estimate compound 17 concentrations in rat plasma. This method meets the requirements and provides high degree of accuracy, sensitivity and specificity by simple extraction using high performance liquid chromatography and detection by ultraviolet -

visible spectroscopy [174-177]. The applicability of the method has extended to quantitate compound 17 in various tissues. In addition, certain key validation experiments, such as accuracy, precision, recovery, stability studies (freeze– thaw, bench-top, in-injector and long-term), that were performed with each tissue matrix are reported.

4.2.1. Method Validation in plasma and tissue homogenates

A simple, robust and reproducible method has been developed and validated to estimate compound 17 concentrations in rat plasma. This method meets the requirements and provides high degree of accuracy, sensitivity and specificity by simple extraction using high performance liquid chromatography and detection by ultraviolet - visible spectroscopy.

4.2.1.1 Experimental Conditions:

A. Chemicals and reagents:

Test substance compound 17(Figure: 4.2.1) was synthesized at Drug research laboratory, BITS PILANI Hyderabad Campus. β -naphthol, Phosphated buffer saline and Ammonium acetate were supplied by Sigma Chemicals. Acetonitrile (HPLC grade) and Methanol (HPLC grade) were supplied by Sigma-Aldrich. The reagents Glacial acetic acid and ethyl acetate were of HPLC grade.

B. Instrumentation and Chromatographic conditions

Analyses were performed on a reverse phase HPLC (Perkin Elmer LC system equipped with Flexar quarternary pump along with peltier controlled Flexar auto-sampler and Flexar PDA) on Brownlee Analytical C18 column (4.6 x 150 mm, 3 μ m, Perkin Elmer Corporation, U.S.A) column. The mobile phase used is a mixture of 0.01 M ammonium acetate (pH = 4.5) and acetonitrile mixture (62:38, v/v) delivered at 1 mL/min. Plasma concentration time data of the analyte were analyzed by non-compartmental method using WinNonlin Version 5.1 (Pharsight Corporation, Mountain View, CA).

C. Preparation of stocks and standard

Primary stock solutions of compound 17 and IS for preparation of standard and quality control (QC) samples were prepared by weighing separately. The primary stock solutions (1.0 mg/mL) of the analyte and IS were prepared in methanol and stored at -20°C, which were found to be stable for one month (data not shown).

D. Preparation of calibration and quality control samples

Appropriate dilutions were made in methanol for compound 17 to produce working stock solutions of 2.5, 4.0, 6.0, 8.0, 10, 20, 40, 60 µg/ml on the day of analysis and these stocks were used to obtain a calibration curve (CC). Another set of working stock solutions was made in methanol (from primary stock) at 50, 9, 3 and 2.5 µg/mL, of which 50 and 9 µg/mL were used for QC high and QC medium respectively. Whereas working stock solutions at 3 and 2.5 µg/mL were used for QC low and lower limit of quantitation (LLOQ) of compound 17, respectively. A working solution of IS (100 µg/mL) was also prepared in methanol. Calibration samples were prepared by spiking 100 µL of control rat plasma with the appropriate amount of analyte (10 µL) and IS (20 µL) on the day of analysis. Samples for the determination of recovery, precision and accuracy were prepared by spiking control rat plasma in bulk at appropriate concentrations (0.25, 0.3, 0.9 and 5 µg/mL as LLOQ, LQC, MQC and HQC for compound 17). Aliquots of 100 µL volumes were taken into different tubes and depending on the nature of experiment, samples were stored at $-80 \pm 10^{\circ}\text{C}$ until analysis.

E. Extraction procedure for biosamples

The recovery of compound 17 and IS from plasma and various tissue homogenates was determined by comparing the responses of the analytes extracted from replicate QC samples (n = 4) with the response of analyte from the neat samples at equivalent concentrations. Recoveries was determined at low and high quality control concentrations, whereas the recovery of the IS was determined at a single concentration of 20.0 µg/mL.

Following removal of each tissue from the second group of dissected rat, the tissues were put into the physiological saline to exclude the remaining blood stain. Tissues were dried using fibreless tissue paper, weighed and cut into small pieces using a surgical blade. Tissue homogenate was made using phosphate buffer saline (pH 7.4) under ice with a homogenizer. All tissues were diluted five times with phosphate buffer saline.

Liquid - liquid extraction method was used for the extraction of compound 17 in biosamples. To each of plasma and tissue samples, IS solution (20 μ L) equivalent to 20 μ g was added mixed for 15 sec on a cyclomixer; followed by extraction with 1.7 ml of suitable extraction solvent viz. plasma with ethyl acetate, stomach and blood with mixture of an equivolume mixture of ethyl acetate and dichloromethane. The mixture was vortexed for 2 min and centrifugated for 4 min at 3200 rpm. The organic layer (1.4 mL) was separated and evaporated to dryness at 50°C using a gentle stream of nitrogen. The residue was reconstituted in 150 μ L of the reconstitution solvent (0.01M ammonium acetate: acetonitrile: 62:38, v/v) and 10 μ L was injected onto HPLC system at 315 nm (λ_{max} of the analyte). From rest of the tissues the analyte and IS was recovered by simple protein precipitation process.

F. Specificity and selectivity

The specificity of the method was evaluated by analyzing rat plasma and tissue from six different batches of rat to demonstrate the potential interferences at LC peak region at for the IS and analyte.

G. Calibration curve

Calibration curves were acquired by plotting the peak area ratio of the compound 17 to that of IS against the nominal concentration of calibration standards. Plasma samples were (0.25, 0.4, 0.6, 0.8, 1, 2, 4 and 6 μ g/ml) prepared by spiking 100 μ L of blank plasma with 10 μ L of standard stock solution and 10 μ L of IS 200 μ g/mL. Standard tissue samples were prepared in similar manner with appropriate blank tissues. The acceptance criterion for each back-calculated standard concentration was $\pm 15\%$ deviation from the nominal value except at LLOQ, which was set at $\pm 20\%$.

H. Precision and accuracy

Inter / intra assay precision and accuracy was determined by analyzing six replicates at four different QC levels as described above on four different days. The criteria for acceptability of the data included accuracy within $\pm 15\%$ deviation (S.D) from the nominal values and a precision of within $\pm 15\%$ relative standard deviation (R.S.D), except for LLOQ, where it should not exceed $\pm 20\%$ of S.D.

I. Stability experiments

The stability of compound 17 and IS in the injection solvent was determined periodically by injecting replicate preparations of processed samples up to 24 h (in auto-sampler at 4°C) after the initial injection. The ratio of peak-areas of the compound 17 and IS obtained at initial cycle were used as the reference to determine the relative stability of the compound 17 at subsequent points. Stability of compound 17 in the biomatrix after 10 h (bench top) exposure at ambient temperature ($25 \pm 2^\circ\text{C}$) was determined at two concentrations in six replicates. Freezer stability of the compound 17 in biomatrix was assessed by analyzing the low and high QC samples stored at $-80 \pm 10^\circ\text{C}$ for at least 30 days. The stability of compound 17 in biomatrix following repeated three freeze-thaw cycles (stored at $-80 \pm 10^\circ\text{C}$ between cycles) was assessed using QC samples spiked with analyte. Samples were processed as described above. Samples were considered to be stable if assay values were within the acceptable limits of accuracy (i.e., $\pm 15\%$ S.D) and precision (i.e., $\pm 15\%$ R.S.D).

4.2.1.2 Results and discussion

A. Specificity and selectivity

A typical chromatogram for the biomatrix (free of analyte and IS) and spiked with analyte at LLOQ and IS are shown in the Figure 4.2.2 to 4.2.5. No interfering peaks from endogenous compounds are observed at the retention times of analyte and IS. The retention time of compound 17 and IS were 10.5 and 8.5 min, respectively. The total chromatographic run time was only 13 mins.

B. Recovery

The extraction recoveries of the compound 17 from biomatrix were calculated by comparing the response of biological samples spiked with the analyte and extracted with a suitable solvent to that of standard solutions of equivalent concentration. The results of the comparison of neat standards vs biological samples extracted standards were estimated for compound 17 at low, mid, high QC concentrations and peak area ratios (analyte/internal standard) were used for the calculations. The mean recovery of > 91% was found in plasma and >75% in other tissue homogenates. The recovery of IS at 20.0 $\mu\text{g/mL}$ was 96.5%.

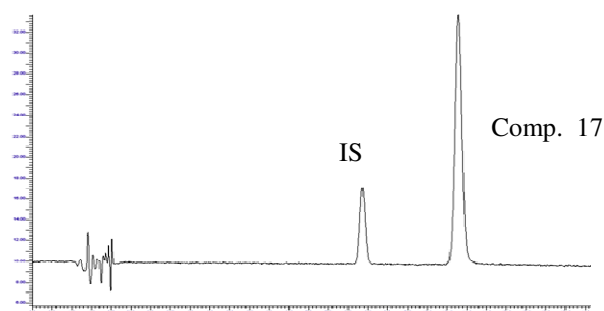


Figure 4.2.2. Standard chromatogram

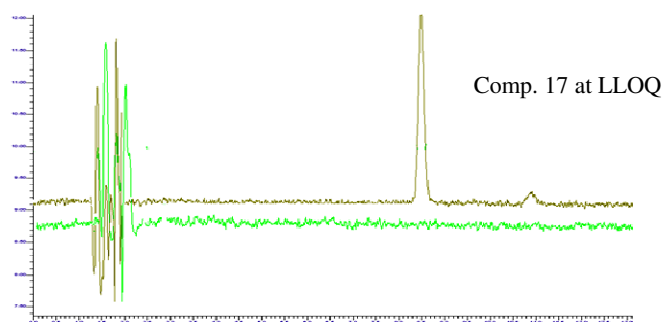


Figure 4.2.3. Specificity chromatogram in plasma

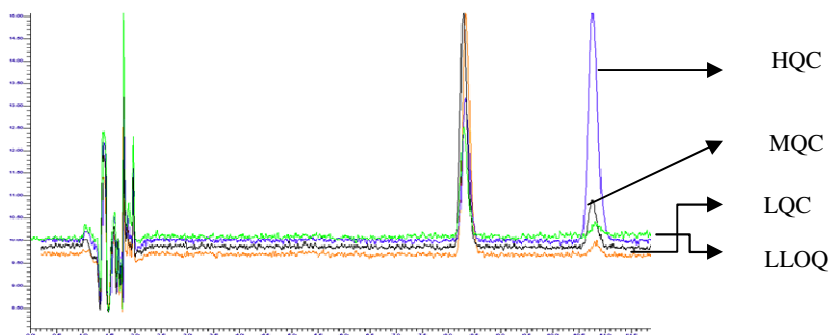


Figure 4.2.4. Quality control standards in plasma

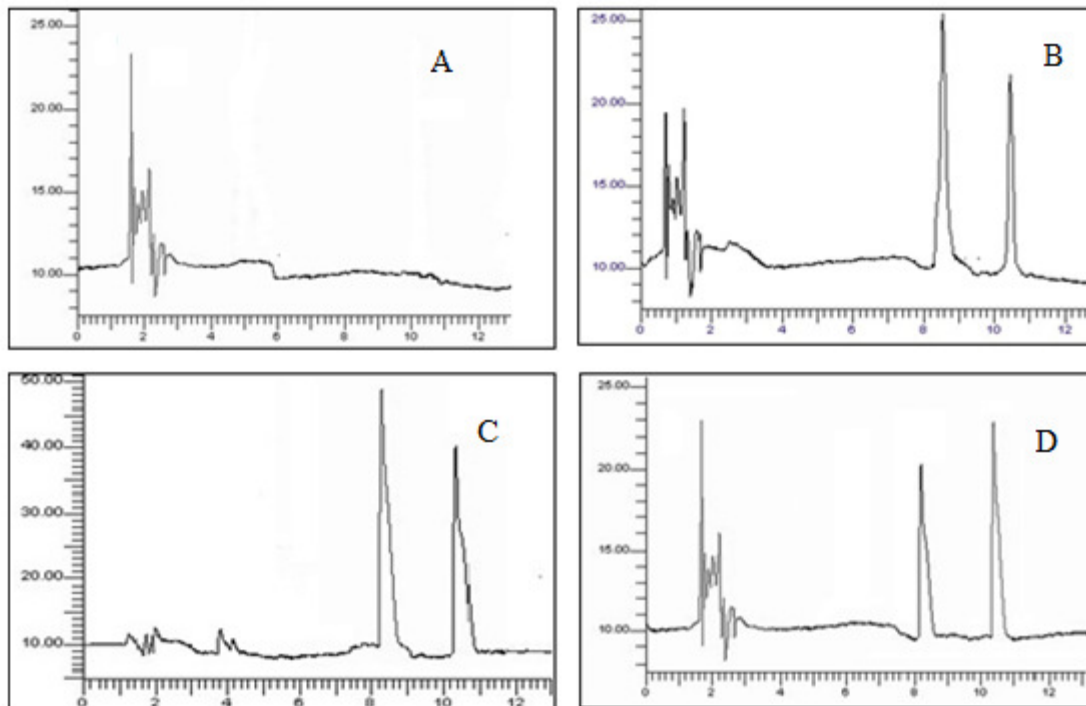


Figure 4.2.5. Blank tissue (A); Blank tissue spiked with compound 17 and IS (B); Rat liver tissue sample obtained after 2 h after 50 mg/kg oral dose of compound 17 (C); Rat lung tissue sample obtained after 2 h after 50 mg/kg oral dose of compound 17 (D)

C. Calibration curve

The calibration curve was prepared by determining the best fit of peak-area ratios (peak area analyte/peak area IS) versus concentration, and fitted to the equation $y = mx + c$.

The average regression ($n = 4$) for compound 17 was found to be >0.99 . Calibration curve were obtained without weighing factor. The linearity range, regression equation, percent accuracy observed for the mean and back calculated concentrations for BITS -17 in each of the matrix is given in Table 4.2.1.

D. Precision and accuracy

The method provides accuracy and precision for the determination of compound 17. The accuracy, intra- and inter-assay precision was determined by analyzing six replicates of

QC samples at four concentrations. Table 4.2.2 gives a summary of the recoveries for rat biological samples spiked with different concentrations of compound 17. The intra day precision ranged from 0.86 to 6.22 and inter day precision ranges from 0.71 to 4.83 for all the biological samples. The results demonstrated the reproducibility of the devised method.

E. Stability

The stability was predicted at LQC and HQC concentrations in a battery of stability tests viz., in-injector, bench-top, repeated three freeze/thaw cycles and at $-80 \pm 10^\circ\text{C}$ for 20 days (Table 4.2.3 to 4.2.5). These results indicate that the analyte was stable in-injector (24 h), bench top (room temperature for 10 h), after freeze thaw condition (3 cycles). The results were also proved that the analyte are stable for 20 days in biological samples.

Table 4.2.1. Linear regression of peak areas and concentration for compound 17 in biological sample

Sample	Linearity range $\mu\text{g/ml}$	Slope	Intercept	r^2	Accuracy range
Plasma	0.25 - 6	0.273	0.0101	0.9995	99.59 - 101.90
Blood	0.25 - 4	0.458	0.0226	0.9993	98.18 - 101.19
Lung	0.4 - 4	0.415	0.0210	0.9999	99.37 - 100.01
Liver	0.6 - 5	0.274	0.0510	0.9990	99.48 - 101.77
Heart	0.4 - 6	0.317	0.0060	0.9988	98.34 - 101.89
Small intestine	0.6 - 6	0.273	0.0541	0.9991	99.22 - 101.03
Large intestine	0.25 - 2	0.430	0.0218	0.9989	96.75 - 99.95
Brain	0.25 - 2	0.408	0.0700	0.9991	99.33 - 99.82
Stomach	0.25 - 2	0.521	0.0220	0.9994	97.92 - 101.19

Table 4.2.2. Intra day and inter day precision and accuracy of compound 17 from
Biological samples

Biological sample	Intra day				Inter day			
	Nominal (µg/ml)	Obtained (µg/ml)	Accuracy (%)	% CV	Obtained (µg/ml)	Accuracy (%)	% CV	
Plasma	LLOQ	0.25	0.259	103.71	1.86	0.256	102.51	3.33
	LQC	0.30	0.318	105.89	2.97	0.312	104.07	3.61
	MQC	0.90	0.967	107.40	1.95	0.920	102.23	3.80
	HQC	5.00	4.792	95.84	1.48	4.987	100.00	3.05
Blood	LLOQ	0.25	0.248	99.15	0.90	0.251	100.21	1.22
	LQC	0.30	0.296	98.77	1.50	0.299	99.53	2.57
	MQC	0.70	0.698	99.69	0.91	0.700	100.07	0.94
	HQC	3.00	3.045	101.50	1.58	3.023	100.92	1.38
Lung	LLOQ	0.40	0.407	101.70	1.60	0.400	100.12	2.21
	LQC	0.50	0.500	100.06	1.25	0.502	100.36	1.15
	MQC	0.90	0.901	100.09	1.83	0.902	100.20	1.00
	HQC	3.00	3.022	100.73	1.68	3.044	101.40	1.39
Liver	LLOQ	0.60	0.618	103.08	1.23	0.604	100.59	1.92
	LQC	0.70	0.691	98.74	1.39	0.699	99.83	1.14
	MQC	1.50	1.502	100.11	1.42	1.501	100.03	0.71
	HQC	5.00	4.976	99.53	1.21	5.012	100.43	1.15
Heart	LLOQ	0.40	0.399	99.84	1.26	0.402	100.42	1.62
	LQC	0.50	0.492	98.46	1.44	0.496	99.23	2.14
	MQC	1.50	1.499	99.94	1.14	1.500	100.00	0.90
	HQC	5.00	4.922	98.44	2.04	4.949	99.21	1.57
Small intestine	LLOQ	0.60	0.608	101.39	1.25	0.592	98.67	2.95
	LQC	0.70	0.681	97.31	1.41	0.688	98.34	1.83
	MQC	1.50	1.493	99.55	1.43	1.493	99.51	1.16
	HQC	5.00	4.975	99.50	1.21	5.029	100.69	1.13
Large intestine	LLOQ	0.25	0.261	103.71	0.86	0.251	100.05	2.78
	LQC	0.30	0.309	103.01	1.94	0.301	100.26	2.98
	MQC	0.70	0.752	107.48	0.90	0.717	102.40	4.46
	HQC	3.00	3.071	103.66	1.25	3.038	101.61	1.78
Brain	LLOQ	0.25	0.238	95.29	1.30	0.246	98.23	2.88
	LQC	0.30	0.303	101.05	6.22	0.298	99.36	4.83
	MQC	0.70	0.697	99.60	1.75	0.699	99.87	2.16
	HQC	1.50	1.497	99.81	3.69	1.498	99.99	2.09
Stomach	LLOQ	0.25	0.248	99.15	0.90	0.250	99.97	1.61
	LQC	0.30	0.296	98.77	1.50	0.299	99.66	2.25
	MQC	0.70	0.698	99.69	0.91	0.701	100.11	0.93
	HQC	3.00	3.045	101.50	1.58	3.010	100.16	1.97

Accuracy (%), [(Obtained concentration/nominal concentration) x 100]; CV (%), coefficient of variation [(S.D./mean) x 100].

Table 4.2.3. Stability data of compound 17 quality controls in Plasma

	Mean \pm SD ^a ($\mu\text{g/ml}$)	Accuracy ^b (%)
Low QC		
Third freeze thaw	97.34 \pm 2.65	97.34
10 h (bench top)	96.49 \pm 3.509	96.49
24 h (in injector)	100.32 \pm 0.317	100.17
Dry Extract (12 h)	97.51 \pm 2.486	97.51
60 days at-80°C	94.68 \pm 5.322	94.68
High QC		
Third freeze thaw	99.41 \pm 0.59	99.41
10 h (bench top)	98.17 \pm 1.830	98.17
24 h (in injector)	99.98 \pm 0.018	99.98
Dry Extract (12 h)	97.98 \pm 0.021	97.98
60 days at-80°C	99.87 \pm 0.132	99.87

QC, quality Control

^aBack –Calculated plasma concentrations

^b(Mean assayed concentration/ mean assayed concentration at 0 h i.e., fresh samples) x 100

Table 4.2.4. Stability data of compound 17 quality controls in Liver, lungs, heart and brain*

Biological Sample	Liver		Lung		Heart		Brain	
	Mean \pm SD ^a ($\mu\text{g/ml}$)	Accuracy ^b (%)	Mean \pm SD ^a ($\mu\text{g/ml}$)	Accuracy ^b (%)	Mean \pm SD ^a ($\mu\text{g/ml}$)	Accuracy ^b (%)	Mean \pm SD ^a ($\mu\text{g/ml}$)	Accuracy ^b (%)
Low QC								
Third freeze thaw	0.699 \pm 0.005	99.24	0.501 \pm 0.008	99.59	0.502 \pm 0.010	100.16	0.302 \pm 0.007	104.12
8 h (bench top)	0.704 \pm 0.004	100.17	0.504 \pm 0.008	99.79	0.506 \pm 0.003	101.15	0.303 \pm 0.007	98.29
24 h (in injector)	0.703 \pm 0.004	99.88	0.503 \pm 0.905	99.54	0.498 \pm 0.005	100.63	0.292 \pm 0.009	94.88
20 days at -80°C	0.695 \pm 0.005	98.89	0.500 \pm 0.006	99.07	0.504 \pm 0.003	101.85	0.295 \pm 0.005	95.62
High QC								
Third freeze thaw	5.006 \pm 0.062	101.39	3.089 \pm 0.002	101.79	5.089 \pm 0.108	102.65	1.559 \pm 0.019	103.54
8 h (bench top)	5.084 \pm 0.058	100.43	3.039 \pm 0.042	98.79	5.085 \pm 0.072	102.34	1.523 \pm 0.029	99.33
24 h (in injector)	5.094 \pm 0.056	100.61	3.035 \pm 0.035	98.63	4.922 \pm 0.139	99.06	1.491 \pm 0.005	97.24
20 days at -80°C	5.066 \pm 0.062	98.94	3.083 \pm 0.021	100.20	5.050 \pm 0.065	101.64	1.527 \pm 0.042	99.62

QC, quality Control

^aBack –Calculated plasma concentrations

^b(Mean assayed concentration/ mean assayed concentration at 0 h i.e., fresh samples) x 100

Table 4.2.5. Stability data of compound 17 quality controls in stomach, blood, large intestine, small intestine

Biological Sample	Stomach		Blood		Large intestine		Small intestine	
	Mean ± SD ^a (µg/ml)	Accuracy ^b (%)	Mean ± SD ^a (µg/ml)	Accuracy ^b (%)	Mean ± SD ^a (µg/ml)	Accuracy ^b (%)	Mean ± SD ^a (µg/ml)	Accuracy ^b (%)
Low QC								
Third freeze thaw	0.298 ± 0.006	97.76	0.304 ± 0.002	104.04	0.308 ± 0.010	103.03	0.699 ± 0.005	102.98
8 h (bench top)	0.302 ± 0.004	99.13	0.297 ± 0.006	97.69	0.308 ± 0.008	103.75	0.704 ± 0.004	103.66
24 h (in injector)	0.300 ± 0.005	98.48	0.300 ± 0.005	98.48	0.290 ± 0.007	97.66	0.678 ± 0.004	99.87
20 days at -80°C	0.305 ± 0.003	101.49	0.295 ± 0.005	96.80	0.310 ± 0.005	103.40	0.695 ± 0.005	100.94
High QC								
Third freeze thaw	3.214 ± 0.056	106.56	3.095 ± 0.052	102.83	3.070 ± 0.052	103.03	5.009 ± 0.047	99.76
8 h (bench top)	3.095 ± 0.113	102.62	3.046 ± 0.050	101.02	3.071 ± 0.063	100.23	5.084 ± 0.058	101.27
24 h (in injector)	2.938 ± 0.047	97.43	2.938 ± 0.047	97.43	3.089 ± 0.051	100.81	5.052 ± 0.056	100.62
20 days at -80°C	2.969 ± 0.046	97.48	3.028 ± 0.054	100.40	3.113 ± 0.049	101.60	5.066 ± 0.062	100.10

QC, quality Control

^aBack –Calculated plasma concentrations

^b(Mean assayed concentration/ mean assayed concentration at 0 h i.e., fresh samples) x 100 Parameter

4.2.2. Pharmacokinetic Study

Pharmacokinetics is the study of the way the body deals with the absorption, distribution, metabolism, and excretion of drugs under investigation expressed in mathematical terms. Absorption, distribution, metabolism, and excretion (ADME) studies in discovery and exploratory development stages of drugs are conducted to assess the metabolism and excretion of a radiolabeled drug following a single administration (intravenous or oral) to rodents (rats or mice), nonrodents (dogs or monkeys), special species such as rabbits, and humans. These studies will evaluate the exposures of the parent compound and its metabolites in animals and humans for validation of toxicological species, (2) identify the major metabolic pathways in humans to support drug–drug interaction studies and (3) establish the rate and route of excretion of a drug candidate, and in addition, (4) provide metabolism data of drugs for regulatory filing.

In this present chapter basic pharmacokinetic parameters have been established in rats using a previous validated method as described in section 5.1. The drug is administered by oral and iv routes and the bioavailability is established. The bioavailability is a pharmacokinetic term that describes the rate and extent to which the active drug ingredient is absorbed from a drug product and becomes available at the site of drug action. However, drug concentrations usually cannot be readily measured directly at the site of action. Therefore, most bioavailability studies involve the determination of drug concentration in the blood. The bioavailability of a drug product often determines the therapeutic efficacy of that product since it affects the onset, intensity and duration of therapeutic response of the drug

4.2.2.1. Experimental Conditions:

Male Wistar rats, ~3 months of age and weighing between 200-250 g were used in this study following the approval from ethics committee for animal use. The two oral formulations (50mg/kg) constituted of a suspension of drug firstly, in sodium CMC and tween 80. Second formulation constituted of cremophore ELP, sodium CMC and SLS.

The animals were fasted overnight (~14 h) and had free access to water throughout the experimental period. Animals were provided with standard diet 3 h post-dosing. The formulation for intravenous administration (10 mg/kg) was prepared with propylene glycol, cremophore ELP, N-methyl-pyrrolidone in normal saline. The rats were anaesthetized in ether and blood samples (~0.5mL, were collected from retro-orbital plexus into microfuge tube (containing 20 µL of saturated EDTA) at 0.5, 1, 1.5, 2, 3, 5, 8, 10 and 24 h post-dosing. Plasma was harvested by centrifuging the blood using micro centrifuge at 6000 rpm for 5 min. Rat plasma (100 µL) samples were spiked with IS and processed as described in section 4.2.1.

Pharmacokinetic parameters [168,170,171,178] were calculated by employing a non-compartmental analysis (Gibaldi and Perrier, 1982). The peak plasma concentrations (C_{max}) and the corresponding time (T_{max}) were directly obtained from the raw data. The area under the plasma concentration vs. time curve upto the last quantifiable time point, AUC (0-t) was obtained by a linear and log-linear trapezoidal summation. The AUC (0-t) extrapolated to infinity (i.e. AUC (0-∞)) by adding the quotient of C_{last}/K_{el}, where C_{last} represents the last measurable time concentration and K_{el} represents the apparent terminal rate constant. K_{el} was calculated by the linear regression of the log-transformed concentrations of the drug in the terminal phase. The half-life (t_{1/2}) of the terminal elimination phase was obtained using the relationship $t_{1/2} = 0.693/K_{el}$ by non-compartmental method were evaluated by using WinNonlinTM Enterprise, Version: 5.3.

4.2.2.2. Results and discussion

The concentration of compound 17 in a plasma sample was determined by the same method as described in section 4.2.1. Plasma concentration time data of the analyte were analyzed by non-compartmental method. The basic pharmacokinetic parameters assessed were half life (t_{1/2}), elimination rate constant (K_{el}), mean plasma clearance (CL) and mean volume of distribution (V_d) as reported in Table 4.2.6. After a single i.v. bolus dose of 10 mg/kg body weight, compound 17 has a low elimination half life of 1.14 h in systemic circulation. The drug is cleared from the body at a rate of 22.48 ml/kg/min

which indicates the rate of clearance is medium (calculated based on the overall body extraction ratio). The volume of distribution (1.99 L) was found to be moderate.

Post oral administration of a single dose of 50 mg/kg body weight the peak concentration was achieved in 1.31 ± 0.06 and 1.0 ± 0.12 $\mu\text{g/mL}$ with formulation one and two, respectively. The plasma levels then declined rapidly with formulation one and the levels sustained with the second one (Fig 4.2.6).

Table 4.2.6. Pharmacokinetic parameters of compound 17 following oral and intravenous administration

	Compound 17			Isoniazid	
	Oral		Intravenous ^c	Oral	Intravenous
	Form 1 ^a	Form 2 ^b			
Dose (mg/kg)	50	50	10	50	10
AUC _(0-t) ($\mu\text{g}\cdot\text{hr/mL}$)	5.87 ± 0.24	11.61 ± 0.28	7.50 ± 0.94	197.09 ± 7.99	684 ± 5.5
C_{max}/C_0 ($\mu\text{g/mL}$)	1.31 ± 0.06	1.0 ± 0.12	5.29 ± 1.41	52.33 ± 1.28	298.2 ± 3.18
T_{max} (hr)	3.00	2.00	-	2.00	-
Kel (1/hr)	-	-	0.62 ± 0.10	-	0.24 ± 0.002
$t_{1/2}$ (hr)	-	-	1.14 ± 0.20	-	2.88 ± 0.13
V_d (lit/kg)	-	-	1.99 ± 0.49	-	0.026 ± 0.002
Cl(ml/kg/min)	-	-	22.48 ± 0.16	-	0.21 ± 0.001
Bioavailability (%)	16.7	33.02		17.36	

^a Formulation 1- sodium CMC and tween 80;

^b Formulation 2- cremophore ELP, sodium CMC and SLS

^cpropylene glycol, cremophore ELP, N-methyl-pyrrolidone in normal saline

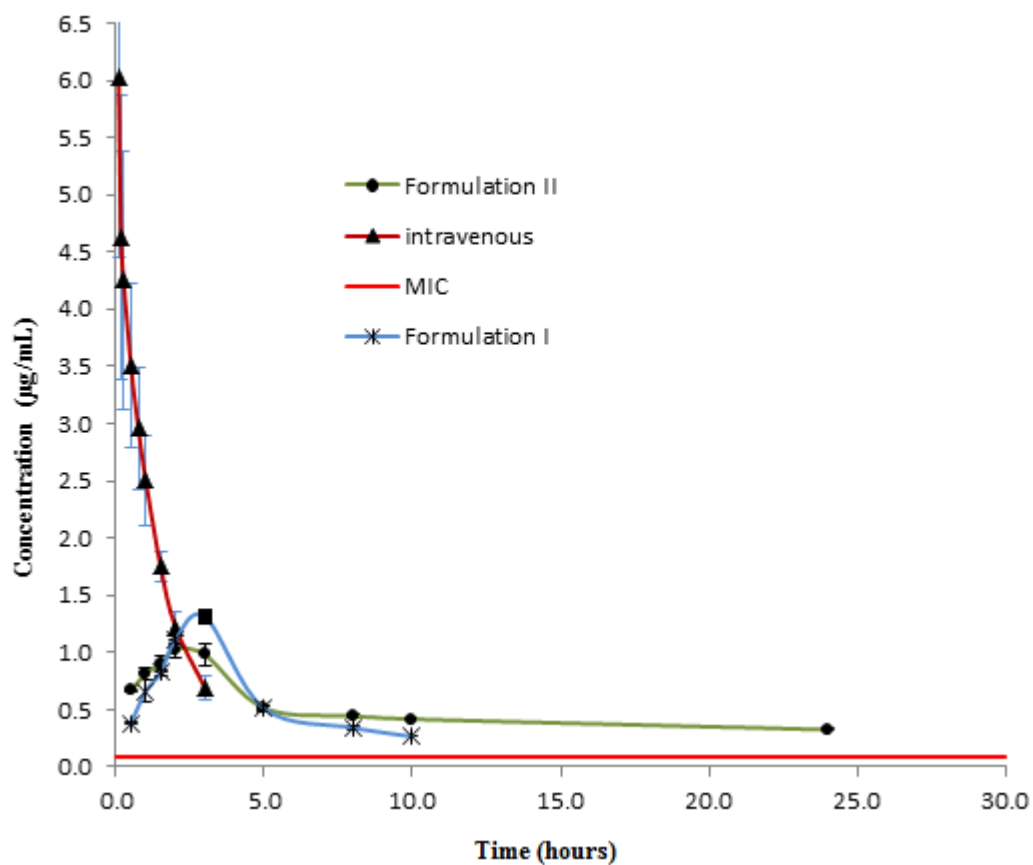


Figure 4.2.6. Concentration time profile of compound 17 after oral and intravenous administration

The oral bioavailability also increased from 16.7% to 33%. The concentration time profiles of both the formulations were well above the levels the MIC values of the compound (Figure 4.2.6). The low systemic bioavailability of the compound can be attributed to its very poor aqueous solubility in the gastrointestinal fluids, therefore low and delayed absorption.

4.2.3. Tissue Distribution Study

Tissue distribution studies are essential in providing information on distribution and accumulation of the compound and/or metabolites, especially in relation to potential sites of action; this information may be useful for designing toxicology and pharmacology studies and for interpreting the results of these experiments. Consideration should be given to measuring unchanged compound and/or metabolites in organs and tissues in which extensive accumulation occurs or if it is believed that such data may clarify mechanisms of organ toxicity.

A tissue distribution study performed after oral administration will provide the concentration of an NCE in various tissues relative to the circulatory levels of the NCE, and this aids in mapping tissue to plasma ratios during drug absorptive, distributive and elimination phases. The outcome of such key experiments will provide information regarding the propensity (or lack of it) to accumulate in tissue (s). By estimating the concentrations in plasma and other tissues, one can establish the tissue/plasma ratio, which will help the researcher to use plasma as a surrogate to assess the levels in other tissues during pharmacology, PK/PD, toxicokinetic studies, etc. In the present section the tissue distribution was established after oral administration of compound -17.

4.2.3.1. Experimental Conditions:

The tissue distribution study was performed in overnight (~12 h) fasted healthy male Wistar rats (n = 6, weight range 200–240 g) following the approval from the ethics committee for animal use [179-182]. During the fasting time animals had free access to water. Compound -17 was administered to rats by oral administration at a dose of 50 mg/kg (in the form of a suspension, prepared using cremophore ELP, sodium CMC and SLS). At each time point, viz. 1 h (during the initial absorption phase), 2 h (around C_{max}) and 5 and 8 h (elimination phase), two rats were sacrificed and various tissues (heart, lung, liver, stomach, small intestine, large intestine and brain along with blood and plasma) were collected separately from each animal. These were dried and weighed

accurately. Individual tissues were cut into small pieces and homogenized using optimum volume of chilled phosphated buffer saline by tissue homogenizer.

Tissue homogenate samples (50 mL) were spiked with IS solution and processed as described in the 'extraction procedure for biosamples' section. The standard curve was generated using individual tissue homogenates. Along with respective samples, QC samples at low, medium and high concentrations spiked in respective blank tissue homogenates were assayed in duplicate and were randomly distributed among standard calibrators and unknown samples in the analytical run; not more than 33% of the QC samples were greater than $\pm 15\%$ of the nominal concentration.

4.2.3.2 Results and discussion

There is a wide tissue distribution of compound 17 in rats after oral administration, shown in Figure 4.2.7. Drug concentrations in highly perfused tissues were highest after 2 hours post dosing except for stomach Table 4.2.7. Comprises of the tissue to plasma ratios, assessing the tissue-plasma ratio, the plasma could be used as a surrogate to determine the concentrations of compound 17 in other tissues in a pharmacodynamic and toxicokinetic study. Comparing the distribution profiles, the maximum concentration was in intestine as the drug has low absorption due to its poor solubility. Presence of drug concentrations significantly above MIC levels (Figure 4.2.8) in brain till 5 hours and in lungs at 2 hours post administration signifies that brain and lungs could be good therapeutic targets for the drug.

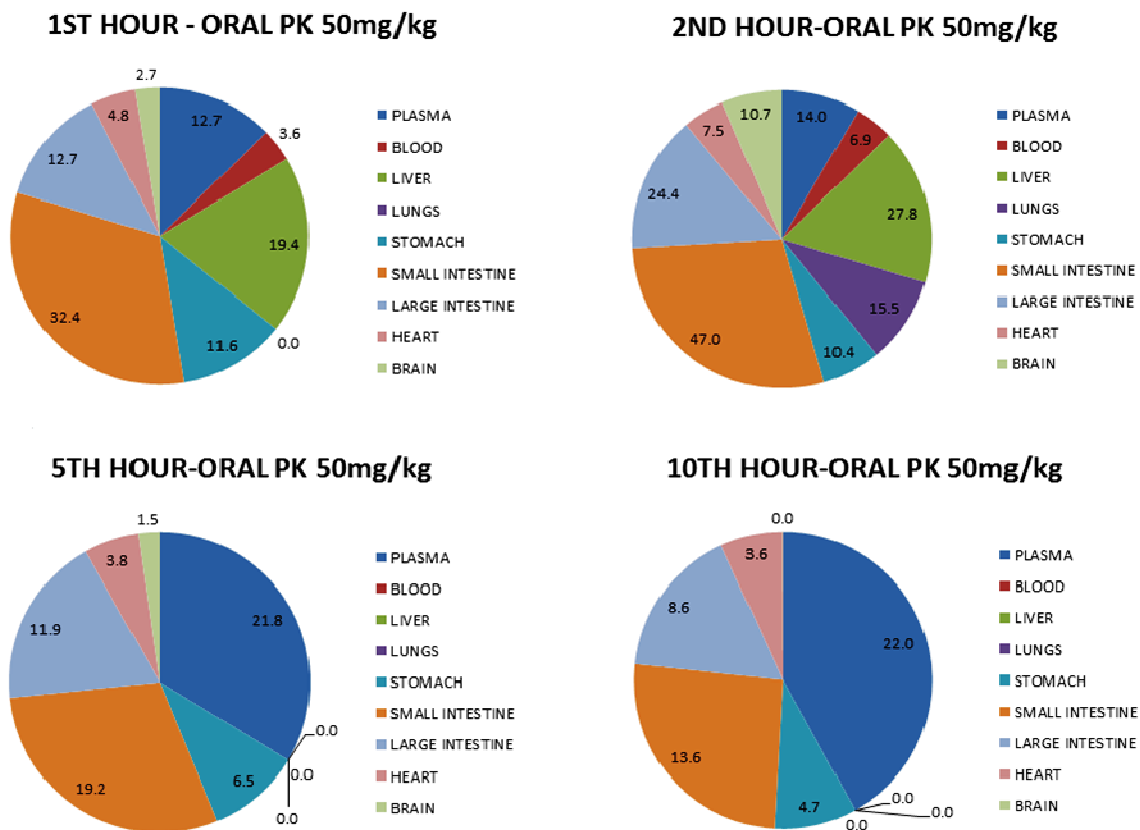


Figure 4.2.7. Pie chart representation of drug distribution at different time points after oral administration of compound 17(50mg/kg)

Table 4.2.7: Biological sample concentrations ($\mu\text{g/ml}$) of compound 17 at various time points along with ratios (tissue to plasma)

Sample	1h	Ratio	2h	Ratio	5h	ratio	10h	ratio
Plasma	0.80	NA	1.50	NA	0.70	NA	0.50	NA
Blood	0.20	NA	0.40	NA	0.00	NA	0.00	NA
Lung	0.00	0.00	0.90	0.60	0.00	0.00	0.00	0.00
Liver	1.20	1.50	1.70	1.10	0.00	0.00	0.00	0.00
Heart	0.30	0.40	0.50	0.30	0.20	0.30	0.20	0.40
Small intestine	2.00	2.60	2.90	1.90	1.20	1.60	0.80	1.60
Large intestine	0.80	1.00	1.50	1.00	0.70	1.00	0.50	1.00
Brain	0.20	0.20	0.60	0.40	0.10	0.10	0.00	0.00
Stomach	0.70	0.90	0.60	0.40	0.40	0.50	0.30	0.50

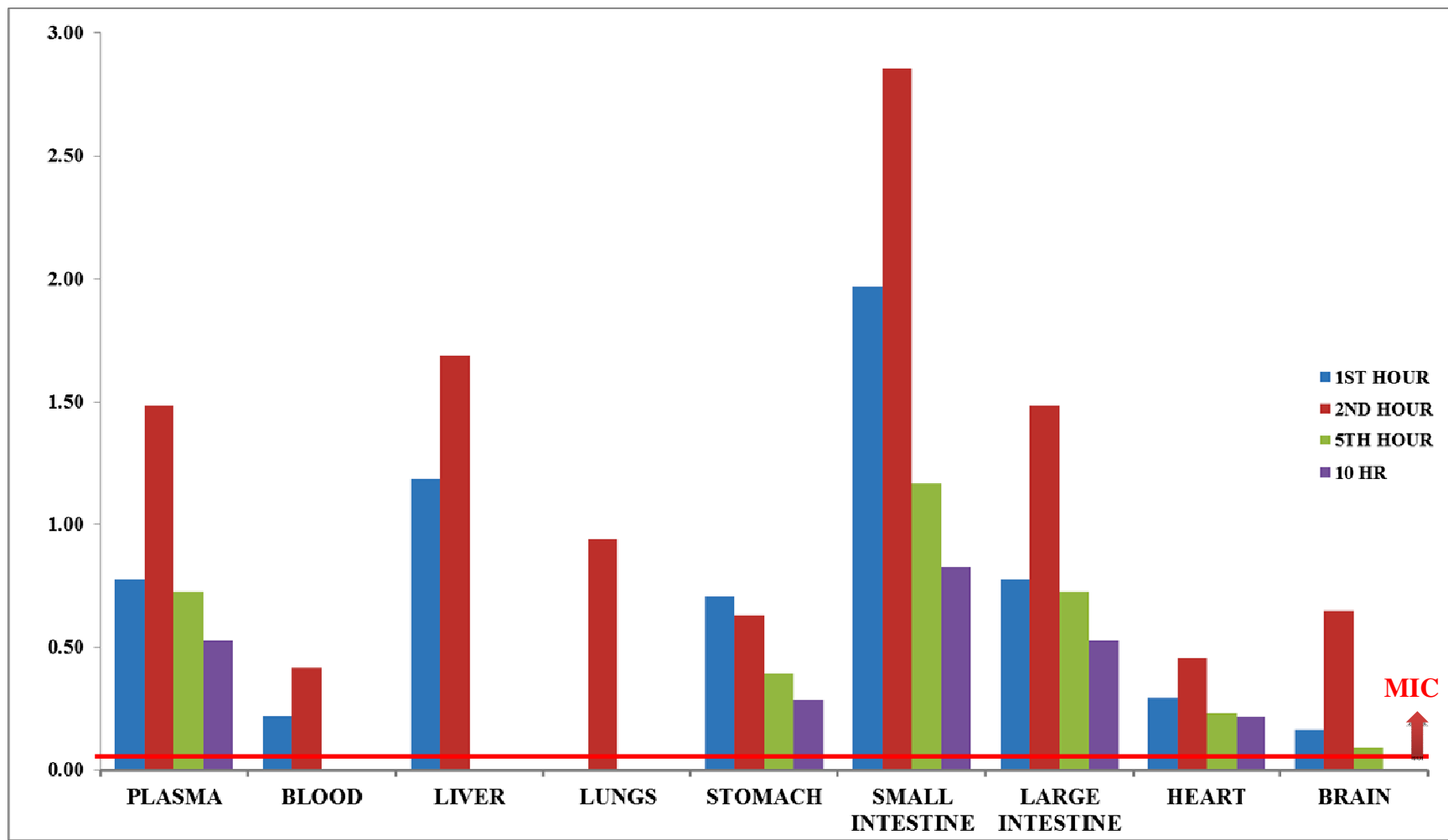


Figure 4.2.8. Bar graph representation of drug distribution after oral administration of compound 17(50mg/kg)

4.2.4. Excretion

Excretion is the process of eliminating waste metabolic products, the major route of which is renal (urinary) excretion via the kidneys. The major non-metabolic routes of clearance (CL_{tot}) include bile and urinary elimination of unchanged compounds. The excretion with sweat, faeces and expired air as well as the ability of compounds to be excreted into breast milk and transferred to neonates may also be significant. Different routes of excretion and the organs include Bile through the liver, urine through the kidneys, feces through the intestines, expired air through the lungs, sweat through the skin, saliva through the mouth, milk through breasts and hair. The major routes of excretion are by renal and faecal excretion.

Elimination of substances by the kidneys into the urine is the primary route of excretion of drugs. The primary function of the kidney is the excretion of body wastes and harmful chemicals. Three processes are involved in urinary excretion: filtration, secretion, and reabsorption. Approximately one-fourth of the cardiac output circulates through the kidney, the greatest rate of blood flow for any organ. A considerable amount of the blood plasma filters through the glomerulus into the nephron tubule. This results from the large amount of blood flow through the glomerulus, the relatively large pores (40 angstrom, an angstrom is one one-hundred millionth of a centimeter) in the glomerular capillaries, and the hydrostatic pressure of the blood. Small molecules, including water, readily pass through the sieve-like filter into the nephron tubule. Both lipid-soluble and polar substances will pass through the glomerulus into the tubule filtrate. Binding to plasma proteins will influence urinary excretion. Polar substances usually do not bind with the plasma proteins and thus can be filtered out of the blood into the tubule filtrate. In contrast, substances extensively bound to plasma proteins remain in the blood. Secretion, which occurs in the proximal tubule section of the nephron, is responsible for the transport of certain molecules out of the blood and into the urine. Secretion occurs by active transport mechanisms that are capable of differentiating among compounds on the basis of polarity.

Elimination of toxicants in the faeces occurs from two processes: excretion in bile, which then enters the intestine, and direct excretion into the lumen of the gastrointestinal tract. The biliary route is an important mechanism for fecal excretion of xenobiotics and is even more important for the excretion of their metabolites. This route generally involves active secretion rather than passive diffusion. However, the most likely substances to be excreted via the bile are comparatively large, ionized molecules, such as large molecular weight (greater than 300) conjugates. Once a substance has been excreted by the liver into the bile, and subsequently into the intestinal tract, it can then be eliminated from the body in the faeces, or it may be reabsorbed. Since most of the substances excreted in the bile are water-soluble, they are not likely to be reabsorbed as such. However, enzymes in the intestinal flora are capable of hydrolyzing some glucuronide and sulfate conjugates, which can release the less-polar compounds that may then be reabsorbed.

Another way that xenobiotics can be eliminated via the faeces is by direct intestinal excretion. While this is not a major route of elimination, a large number of substances can be excreted into the intestinal tract and eliminated via faeces. Some substances, especially those which are poorly ionized in plasma (such as weak bases), may passively diffuse through the walls of the capillaries, intestinal submucosa and into the intestinal lumen to be eliminated in the faeces. Intestinal excretion is a relatively slow process and is therefore an important elimination route only for those xenobiotics that have slow biotransformation, or slow urinary or biliary excretion. Increasing the lipid content of the intestinal tract can enhance intestinal excretion of some lipophilic substances.

Excretion studies are essential in providing information on estimating the excretion pattern of the compound and/or metabolites, this information may be useful for designing toxicological and pharmacological studies and for interpreting the results of these experiments. Consideration should be given to measuring unchanged compound and/or metabolites in the body by which extensive accumulation occurs or if it is believed that such data may clarify mechanisms of organ toxicity.

4.2.4.1. Experimentation

A. Collection of Excreta [4]

Blank samples of male Wistar Rats were kept in metabolic cage (figure 4.2.9) which is specially designed for the collection of urine and faeces separately. The urine was collected for every 12 hours in a day, measured and stored in a freezer at -80 °C. The pellets of faeces were collected for every 12 hours in a day in a petridish carefully. The pellets were freeze dried in a lyophilizer at a temperature of -80 °C. Then the dried faeces was weighed accurately and stored in freezer at -80 °C.



Figure 4.2.9. Metabolic cage

Drug samples of male Wistar rats, ~3 months of age and weighing between 190-200 g were used in this study. The animals were fasted overnight (~12 h) and had free access to water throughout the experimental period. BITS17 was dosed at a dose of 50 mg/kg body weight through oral route. The formulation was prepared using 0.25% sodium CMC, 5% Sodium Lauryl sulphate, and 10% Cremophore ELP. The urine and faeces were collected separately for every 12 hours in a day. Urine was measured and stored in a freezer at -80 °C. Faeces was liophilised as describe above before transferring into the freezer.

B. Instrumentation and Chromatographic conditions

Analyses were performed on a reverse phase HPLC (Perkin Elmer LC system equipped with Flexar quarternary pump along with peltier controlled Flexar auto-sampler and Flexar PDA) on Brownlee Analytical C18 column (4.6 x 150 mm, 3 μ m, Perkin Elmer Corporation, U.S.A) column. The mobile phase used is a mixture of 0.01 M ammonium acetate (pH = 4.5) and acetonitrile mixture (62:38, v/v) delivered at 1 mL/min.

4.2.4.2. Results and Discussion

Following a single oral dose, a total of 51.51 % of the dose was excreted over a period of 24 hr post-dose. The majority (50.54 %) was recovered in faeces within 24 hr following dose administration. Only less was recovered from urine accounting for 1.01 % of the dose administered. The individual and mean recovery (expressed as a percent of the dose administered) in urine, faeces, are presented in Tables 4.2.8. Corresponding graphical representations are presented in Figures 4.2.10.

Table 4.2.8: Cumulative Individual and Mean Recovery in Excreta of Male Wistar Rats Following Oral Administration of compound 17 at 50 mg/kg

Sample	Time(hrs)	Rat 1	Rat 2	Rat 3	Rat 4	Mean	SD	% CV
Urine	0-12	1.06	1.05	0.88	1.03	1.01	0.08	8.38
	12 -24	-	-	-	-	-	-	-
	Subtotal	1.06	1.05	0.88	1.03	1.01	0.08	8.38
Feaces	0-12	52.86	43.38	55.45	47.3	49.75	5.44	10.93
	12 -24	0.97	0.64	1.17	0.4	0.80	0.34	43.04
	Subtotal	53.83	44.02	56.62	47.7	50.54	5.73	11.33

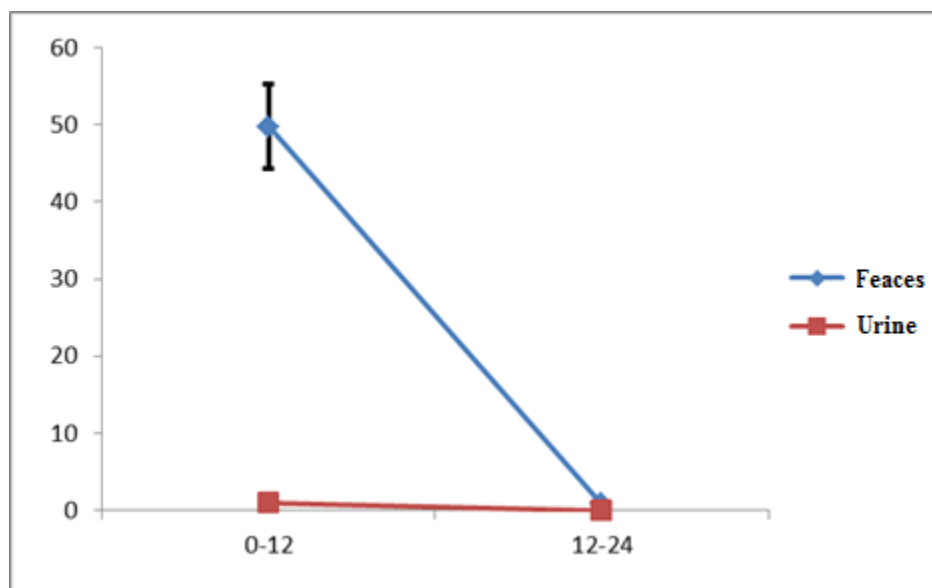


Figure 4.2.10. Mean Cumulative Recovery in Excreta Following a Single dose administration of compound 17 to Male Wistar Rats at a Target Dose of 50 mg/kg

4.2.5. CONCLUSION

It can be inferred from the excretion data that approximately 50-60 % of the drug administered orally is excreted unchanged in the faeces. The results of tissue distribution studies provided supportive evidence as equivalent amounts of drug was recovered from the large intestine in unchanged form. There is likelihood that the drug did not undergo enterohepatic recirculation as the corresponding pattern was neither observed in plasma levels nor the tissue levels. Very less amount of drug was recovered from urine which indicates that either the urinary excretion in the unchanged form is low or the drug might have undergone extensive metabolism in the body (Study of metabolites yet to be performed).

*4.3. Interaction of compound
N-(2-(4-(benzyloxy) phenyl)-4-
oxo-1,3-thiazinan-3-yl)
isonicotinamide – “Compound 17”
with other drugs*

Drug-drug interactions occur when one therapeutic agent either alters the concentration (pharmacokinetic interactions) or the biological effect of another agent (pharmacodynamics interactions). Pharmacokinetic drug-drug interactions can occur at the level of absorption, distribution, or clearance of the affected agent. Many drugs are eliminated by metabolism. The microsomal reactions that have been studied the most involve cytochrome P (CYP) 450 family of enzymes, of which a few are responsible for the majority of metabolic reactions involving drugs. These include the isoforms CYP1A2, CYP2C9, CYP2C19, CYP2D6, and CYP3A4 [183,184].

4.3.1. DISTRIBUTION OF CYP ENZYMES

Cytochrome P450 enzymes are found in practically all tissues, with highest abundance and largest number of individual CYP forms present in the liver. CYPs reside also in the intestine, lung, kidney, brain, adrenal gland, gonads, heart, nasal and tracheal mucosa, and skin. (Figure.4.3.1) The content of drug-metabolizing CYPs is much lower in other tissues. Extra hepatic metabolism may have clinically significant local effects, systemic metabolic clearance of drugs occurs in the liver with a significant contribution by the gut wall in special cases. P450 enzymes can be found throughout the body, particularly at interfaces, such as the intestine, nasal epithelia, and skin. The liver and the intestinal epithelia are the predominant sites for P450-mediated drug elimination and are also the sites worth considering in most detail with respect to drug-drug interactions.

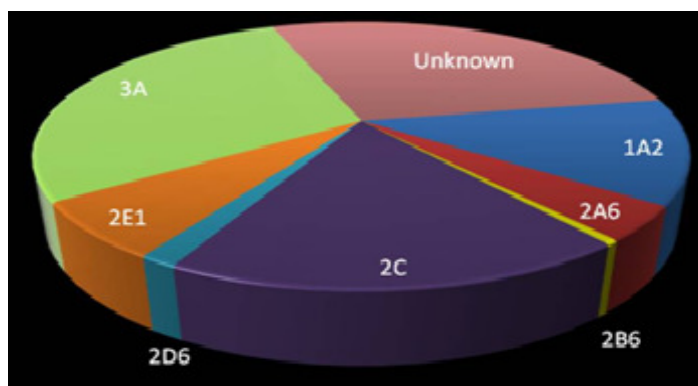


Figure.4.3.1. Relative abundance of CYP450 enzymes in liver

Although P450 enzymes have been well characterized in many other tissues, it is unlikely that these play a significant role in the overall elimination of drugs [185].

4.3.2. MECHANISM OF PHARMACOKINETIC DRUG-DRUG INTERACTION

Enzyme inhibition refers to the decrease in metabolic enzyme activity due to the presence of an inhibitor. Drug metabolism by CYP450 can be inhibited by any of the following three mechanisms: competitive inhibition, noncompetitive inhibition and uncompetitive inhibition. Inhibition of enzyme activity may result in higher concentrations and/or prolonged half-life of the substrate drug, which enhances the potential for toxic side effects. The clinical significance of a specific drug-drug interaction depends on the degree of accumulation of the substrate and the therapeutic window of the substrate.

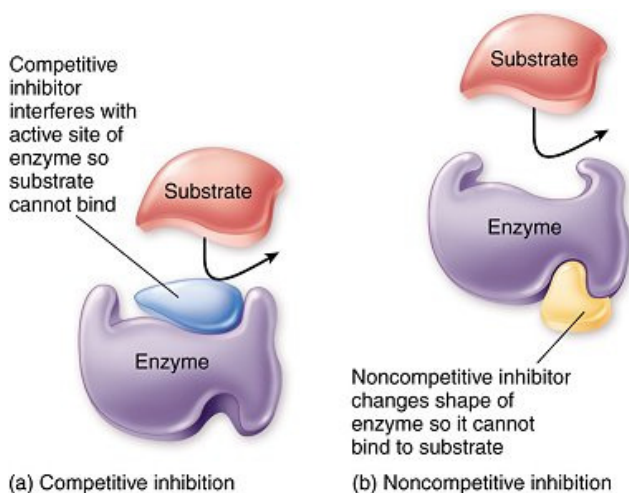


Figure.4.3.2. Mechanisms of enzyme Inhibition

Enzyme induction is associated with an increase in enzyme activity thus speed up the oxidation and clearance of a drug. For drugs that are substrates of the isoenzyme induced, the effect is to lower the concentration of these substrates. The clinical consequence of the presence of an inducing agent and the resultant decrease in concentration of the substrate may mean a loss of efficacy. It is rather difficult to predict the time-course of

enzyme induction because of several factors, including the drug half-life and enzyme turnover, which determine the time-course of induction. These include inducer-specific aspects such as the potency of the inducer, the dose and the concentration of the inducer needed for the induction to occur, the duration of the exposure needed for the induction to happen, the metabolic properties of the inducer, the length of the exposure to the inducer, the duration of the induction once the inducer is withdrawn, the route of the exposure (e.g. orally, topically or by inhalation), and the anatomical location of the CYP enzymes induced (e.g. intestine, skin or lung) [186,187] .

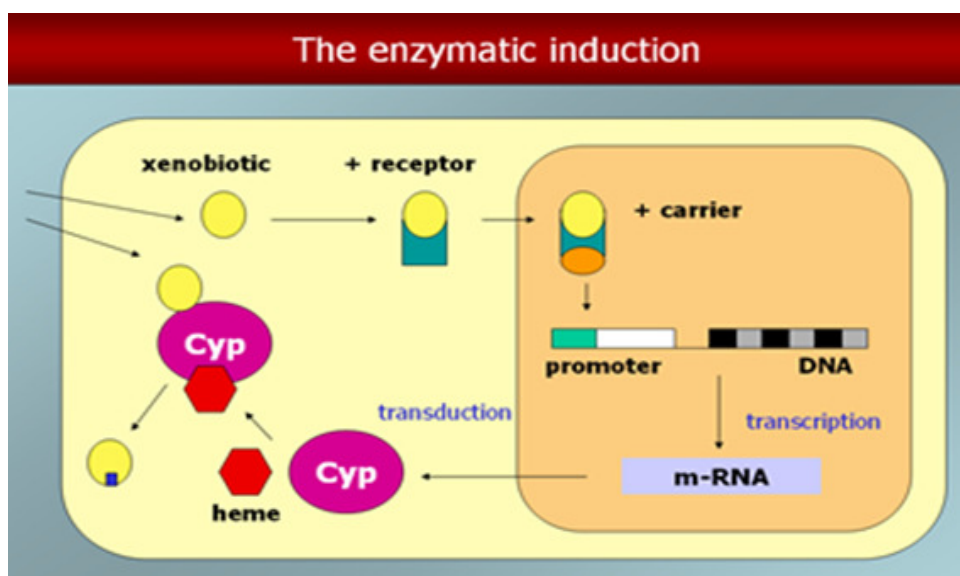


Figure.4.3.3. Mechanism of enzyme induction

4.3.3. ROLE OF *IN VIVO* ANIMAL STUDIES

Whenever feasible, drug metabolism should be investigated in human tissues, cells, or subcellular fractions as interspecies and intraspecies differences in drug-metabolizing enzymes limit the ability to extrapolate between experimental animals and humans. However, animal species may provide useful models in which to determine whether a new chemical species generated *in vitro* by human liver microsomes produces pharmacological or toxicological effects *in vivo* and how these compare with the effects of the parent compound. Knowledge of comparative drug metabolism in humans and

animals can play a useful role in the rational selection of animal models for toxicology studies. Major discrepancies in the metabolism of a drug between laboratory test species and humans diminish the predictive value of toxicology data obtained from these animals [188].

CYP isoforms catalyze the oxidation and reduction of a variety of endogenous compounds and these facilitate the excretion of xenobiotics. Approximately 40 genes code for specific isoforms in the rat genome with four major subfamilies of CYP isoforms in rat liver exhibiting different but somewhat overlapping substrate specificities. The CYP isoforms in rats are mainly CYP2C11 and CYP3A2. Although the composition and relative proportions of specific CYP isoforms are different in humans and rats, there is strong catalytic and regulatory conservation of the subfamilies among the rat isoforms and their human orthologs.

Anti-tubercular drugs are never used alone but are often given concomitantly with drugs prescribed for other diseases. We have therefore reviewed the potential interactions of compound 17 important metabolizing enzymes and with other drugs which interact with CYP450 enzymes [189,190]. These interaction studies have been performed in animals to check the possible drug drug interactions and the alterations in the pharmacokinetic parameters can be used to interpret the study. Usually such parameters include C_{max}, T_{max} and AUC, CL and the terminal half-life. The C_{min} has been found to be closely related to clinical efficacy or safety. C_{min} determination and interpretation based on this data becomes significantly important. So the animals were dose with NCE and the drugs under investigation alterations in the pharmacokinetic parameters were determined.

4.3.4. General methodology adopted for experimentation

A. Administration of compound 17 and test compound

Male Wistar rats, ~3 months of age and weighing between 190-200 g were used in this study. For Oral pharmacokinetic study, the animals were fasted overnight (~14 h) and had free access to water throughout the experimental period. The formulation was

prepared using 0.25% sodium CMC, 5% Sodium Lauryl sulphate, and 10% Cremophore ELP. The rats were anaesthetized in ether and blood samples (~1.00 mL) were collected from retro-orbital plexus into microfuge tube (containing 10 µL of saturated EDTA) at 0, 5, 1, 1.5, 2.0, 2.0 3.0, 5.0, 8.0, 10 and 24 hours post-dosing.

Animals were grouped into 3 groups with n = 4 in first two groups and last group n = 8 animals each. First group received only compound 17, second received only the test drug (drug used to study the drug - drug interaction) and the third group received the combination of both compound 17 and the test drug. The third group animals were bled using sparsing technique (Table: 4.3.1) so as to facilitate the volume of sample required for analysis. All the animals receiving compound 17 were tested at 50 mg/kg body weight. Dose used for the test was simple scaled down to the animal dose from the marketed dose.

Table.4.3.1. Sparsing for pharmacokinetic study of Test Drug + compound 17

Time(hr)	Rat1	Rat2	Rat3	Rat4	Rat5	Rat6	Rat7	Rat8
0.5	x	x	x	x				
1				x	x	x	x	
1.5	x	x					x	x
2		x	x	x	x			
3					x	x	x	x
5	x		x	x		x		
8		x	x		x			x
10	x			x			x	x
24		x			x	x	x	

B. Chemicals and reagents:

Test substance compound 17 was synthesized at Drug research laboratory, BITS PILANI Hyderabad Campus. β -naphthol, and Ammonium acetate were supplied by Sigma

Chemicals. Acetonitrile (HPLC grade) and Methanol (HPLC grade) were supplied by Sigma-Aldrich. The reagents Glacial acetic acid and ethyl acetate were of HPLC grade.

C. Instrumentation and Chromatographic conditions

Analyses were performed on a reverse phase HPLC (Perkin Elmer LC system equipped with Flexar quarternary pump along with peltier controlled Flexar auto-sampler and Flexar PDA) on Brownlee Analytical C18 column (4.6 x 150 mm, 3 μ m, Perkin Elmer Corporation, U.S.A) column. The mobile phase used is a mixture of 0.01M ammonium acetate (pH = 4.5) and acetonitrile mixture (62:38, v/v) delivered at 1 mL/min. This above method was used to detect compound 17 and method used to detect is described under individual sections. Plasma concentration time data of the analyte were analyzed by non-compartmental method using WinNonlin Version 5.1 (Pharsight Corporation, Mountain View, CA).

D. Extraction procedure for biosamples

Liquid - liquid extraction method was used for the extraction of compound 17 from plasma. To the plasma, IS solution (20 μ L) equivalent to 20 μ g was added mixed for 15 sec on a cyclomixer; followed by extraction with 1.7 ml of ethyl acetate. The mixture was vortexed for 2 min and centrifugated for 4 min at 3200 rpm. Supernatant solvent of 1.4 ml was collected and kept in lyophiliser for evaporation of recovery solvent. The residue was reconstituted in 150 μ L of the reconstitution solvent (0.01M ammonium acetate: acetonitrile: 62:38, v/v) and 10 μ L was injected onto HPLC system at 315 nm (λ_{max} of the analyte). Chromatographic conditions and extraction procedure for biosamples was modified according to test drug used and are discussed under respective individual sections.

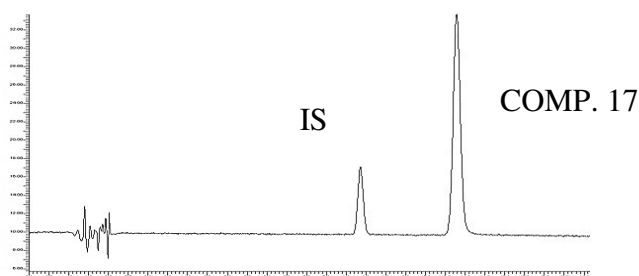


Figure.4.3.4. Chromatogram of compound 17 and IS

4.3.5. CYP 1A

CYP1A is expressed mainly in the liver and is not or weakly expressed in extrahepatic tissues in human, rat and mouse. The human cytochrome P450 enzyme CYP1A plays an important role in the metabolism of several clinically used drugs. It has to be emphasized that, besides smoking, concomitant intake of drugs which are inhibitors, inducers or even merely competing substrates for CYP1A represents one of the most prominent and frequent factors of influence on CYP1A activity [191-192].

4.3.5.1. ONDANSETRON (SUBSTRATE)

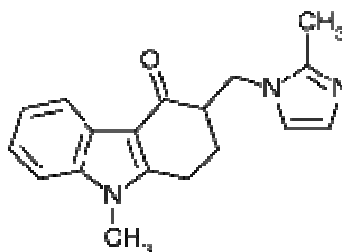


Figure.4.3.5. Ondansetron

Ondansetron is a selective 5-HT₃ receptor antagonist. Serotonin receptors of the 5-HT₃ type are present both peripherally on vagal nerve terminals and centrally in the chemoreceptor trigger zone of the area postrema because of which it is effectively used as an antiemetic (to treat nausea and vomiting). Nausea and vomiting symptoms are predominant during initial phases of anti-tubercular therapy which demands administration of anti emetics like Ondansetron. Therefore it is important to study the possible drug interactions when Ondansetron and compound 17 are co-administered.

A. Ondansetron metabolism:

Ondansetron is extensively metabolized in humans, with approximately 5% of a radio labeled dose recovered as the parent compound from the urine. The primary

metabolic pathway is hydroxylation on the indole ring followed by glucuronide or sulfate conjugation. Hepatic oxidative metabolism accounts for more than 95% of Ondansetron clearance from the body. The major excreted metabolites are conjugates of 7-hydroxy or 8-hydroxyondansetron, which appear to contribute little to the activity of the parent drug. Because of large intersubject variability in clearance and the relative safety of Ondansetron, adjustments in Ondansetron dosing based on age or gender alone are not recommended. Although some nonconjugated metabolites have pharmacologic activity, these are not found in plasma at concentrations likely to significantly contribute to the biological activity of Ondansetron. Ondansetron is a substrate for human hepatic cytochrome P-450 enzymes CYP1A [192].

B. Bioanalytical method for Ondansetron:

The mobile phase used in the method was Acetonitrile and ammonium acetate (pH = 4.0) as non-polar and polar phases respectively in proportions using reverse phase HPLC at 310nm (λ_{max} of Ondansetron). The finally developed gradient method consisted of % change in Acetonitrile with respect to time (0.01→10 min: 27%; 10.01→20.00 min: 40%; 20.01→25 min: 27%). Ondansetron, IS and compound 17 were eluted at 6.4, 16.2 and 20.1 mins respectively.

For the purpose of analysis, a validated method has been taken from the literature and required modifications have been done to suit the specifications of the analysis for combination samples. This method has been confirmed for by repeated linearity range. Accuracy and precision for the newly developed method have been established at 0.5µg/ml.

Table.4.3.2. Mini Validation of Ondansetron

LINEARITY RANGE (µg/ml)	0.5 – 20 ($r^2 = 0.9989$)
ACCURACY (n=6)	102.42%
PRECISION (n=6)	1.36%

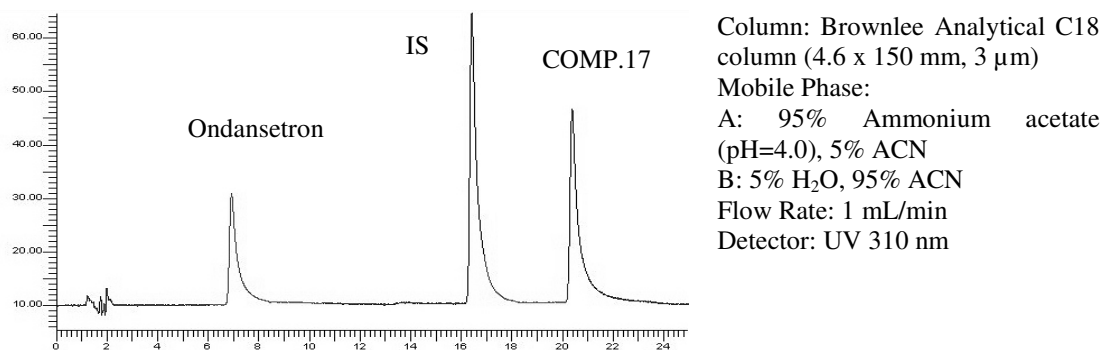


Figure.4.3.6. A typical chromatogram of Ondansetron, IS and compound 17.

Table.4.3.3. Pharmacokinetic parameters of compound 17 administered with ondansetron

Parametres (n=4)	Comp. 17 alone [#]	Comp. 17 with ondansetron [*]	p value (Unpaired t-test) $\alpha = 0.05$	Significant difference Between the parametres
AUC _(0-t) μ g.hr/ml	11.61 \pm 0.28	9.35 \pm 0.85	5.54	Yes
C _{max} (μ g/ml)	1.03 \pm 0.07	2.59 \pm 0.17	8.64	Yes
T _{max} (hr)	2.00 \pm 0.00	2.00 \pm 0.00	-	-

Note: t = [#]24h *10h

Table.4.3.4. Pharmacokinetic parameters of ondansetron administered with compound 17

Parametres (n=4)	Ondansetron Alone [#]	ondansetron with Comp.17*	p value (Unpaired t-test) $\alpha = 0.05$	Significant difference Between the parametres
AUC _(0-t) $\mu\text{g}\cdot\text{hr}/\text{ml}$	13.22 \pm 0.44	5.78 \pm 0.69	17.46	Yes
Cmax ($\mu\text{g}/\text{ml}$)	2.72 \pm 0.03	1.43 \pm 0.31	7.80	Yes
Tmax (hr)	2.00 \pm 00	3.00 \pm 00	-	-

Note: t = [#]10h *8h

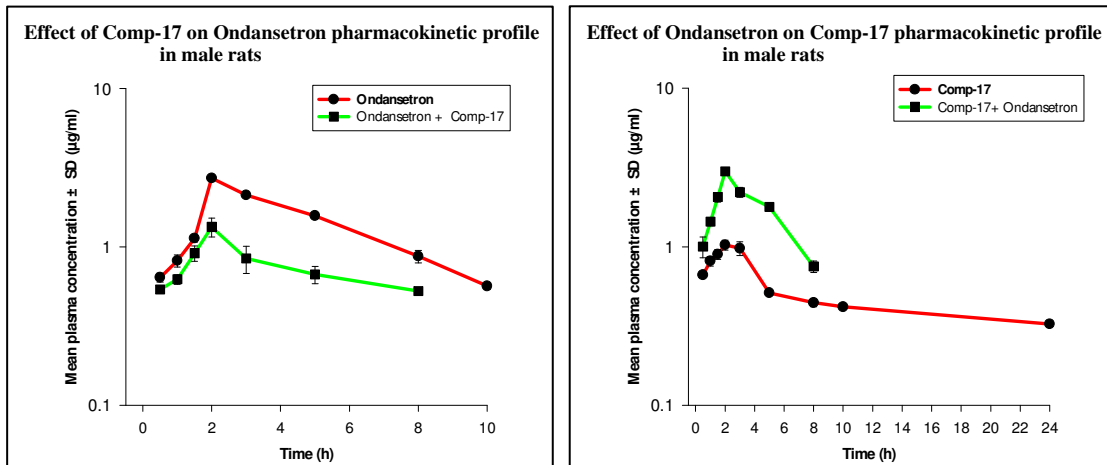


Figure 4.3.7. Log linear Concentration time profile of Ondansetron and in combination with compound 17

C.Results

Both the compounds were well tolerated by the animals. The pharmacokinetic parameters are listed in table 4.3.3 & 4.3.4. The difference between mean values for the parameters which characterise the AUC, C_{max}, were significant when compound 17 was administered with/without ondansetron. AUC values (11.61 ± 0.28 vs 9.35 ± 0.85 $\mu\text{g}\cdot\text{hr}/\text{ml}$), C_{max} values of compound 17 (1.03 ± 0.07 vs 2.59 ± 0.17 $\mu\text{g}/\text{ml}$) before and after the ondansetron treatment had a significant effect ($p= 0.05$). Time to attain peak plasma concentrations (T_{max}) remained unchanged.

The difference between mean values for the parameters which characterise the AUC, C_{max}, were significant when ondansetron was administered with/without compound 17. AUC values (13.22 ± 0.44 vs 5.78 ± 0.69 $\mu\text{g}\cdot\text{hr}/\text{ml}$), C_{max} values were (2.73 ± 0.03 vs 1.43 ± 0.31 $\mu\text{g}/\text{ml}$) before and after the compound 17 treatment had a significant effect ($p= 0.05$). Time to attain peak plasma concentration (T_{max}) was also prolonged (2.00 vs 3.00hr).

4.3.5.2. CIPROFLOXACIN (INHIBITOR)

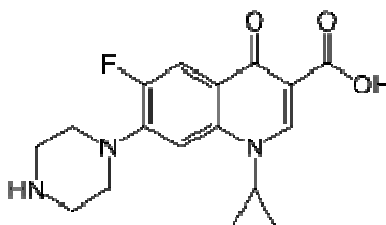


Figure 4.3.8.Ciprofloxacin

Ciprofloxacin is an antimicrobial broad-spectrum antibiotic which belongs to fluoroquinolone group. It is a second-generation fluoroquinolone antibacterial. It kills bacteria by interfering with the enzymes that cause DNA to rewind after being copied, which stops synthesis of DNA and of protein. Ciprofloxacin can alter and be altered by the metabolism and effects of other drugs, resulting in some significant drug-drug

interactions that may affect the musculoskeletal, central nervous, renal, and other systems. For this reason, it has been selected for studying its interactions with compound 17.

A. Ciprofloxacin Metabolism:

An alternative explanation for the 'loss' of ciprofloxacin from the systemic site may be an extensivemetabolism of the drug. The piperazinyl ring seems to be the centre of metabolism; the ring may become oxidized (M2), opened (MI), formylated or sulphated.

B. Bio analytical method development:

The mobile phase used in the method was Acetonitrile, methanol and 0.25% orthophosphoric acid adjusted to pH = 3 with TEA. The finally developed gradient method consisted of % change in B as acetonitrile, C as methanol with respect to time (0.01→1 min: 0% B, 10% C; 1.01→4.5 min: 20% B, 30% C; 4.51→6.0 min: 25% B, 25% C; 6.01→12.50 min: 50% B, 20% C; 12.51→17.5 min: 85% B, 5% C, 17.51→20 min: 0% B, 0% C). The analysis was performed using reverse phase HPLC at 340nm (λ_{max} of Ciprofloxacin). Ciprofloxacin, IS and compound 17 were eluted at 5.9, 10.1 and 11.5 respectively. For the purpose of analysis, a validated method has been taken from the literature and required modifications have been done to suit the specifications of the analysis for combination samples. This method has been confirmed for by repeated linearity range. Accuracy and precision for the newly developed method have been established at 0.5µg/ml.

Table.4.3.5. Mini Validation of Ciprofloxacin

LINEARITY RANGE (µg/ml)	0.5 – 20 ($r^2 = 0.9991$)
ACCURACY (n=6)	101.273
PRECISION (n=6)	1.70

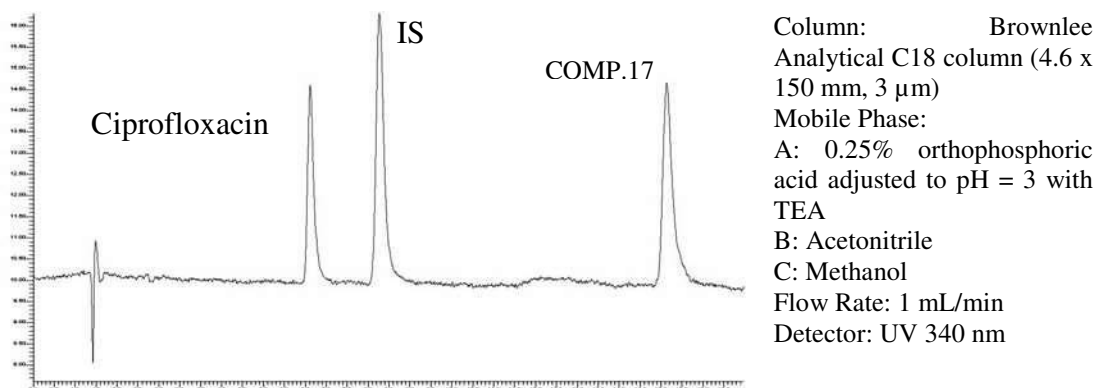


Figure 4.3.9.A typical chromatogram of Ciprofloxacin, IS and compound 17

Table.4.3.6. Pharmacokinetic parameters of compound 17 with Ciprofloxacin

Parametres (n=4)	Comp.17 alone [#]	Comp. 17 with Ciprofloxacin*	p value (Unpaired t-test) $\alpha = 0.05$	Significant difference Between the parameters
AUC _(0-t) μ g.hr/ml	11.61 \pm 0.28	13.41 \pm 0.61	6.29	Yes
Cmax (μ g/ml)	1.03 \pm 0.07	2.99 \pm 0.09	38.19	Yes
Tmax (hr)	2.00 \pm 0.00	2.00 \pm 0.00	-	-

Note: t = [#]24h *8h

Table.4.3.7. Pharmacokinetic parameters of Ciprofloxacin with compound 17

Parametres (n=4)	Ciprofloxacin Alone [#]	Ciprofloxacin with Comp.17*	t value (Unpaired t-test) $\alpha =0.05$	Significant difference Between the parameters
AUC _(0-t) $\mu\text{g.hr/ml}$	11.36 \pm 0.16	6.35 \pm 0.66	18.11	Yes
Cmax ($\mu\text{g/ml}$)	1.05 \pm 0.02	1.08 \pm 0.07	38.19	Yes
Tmax (hr)	2.00 \pm 0.00	3.00 \pm 0.00	-	-

Note: t = [#]28h *10h

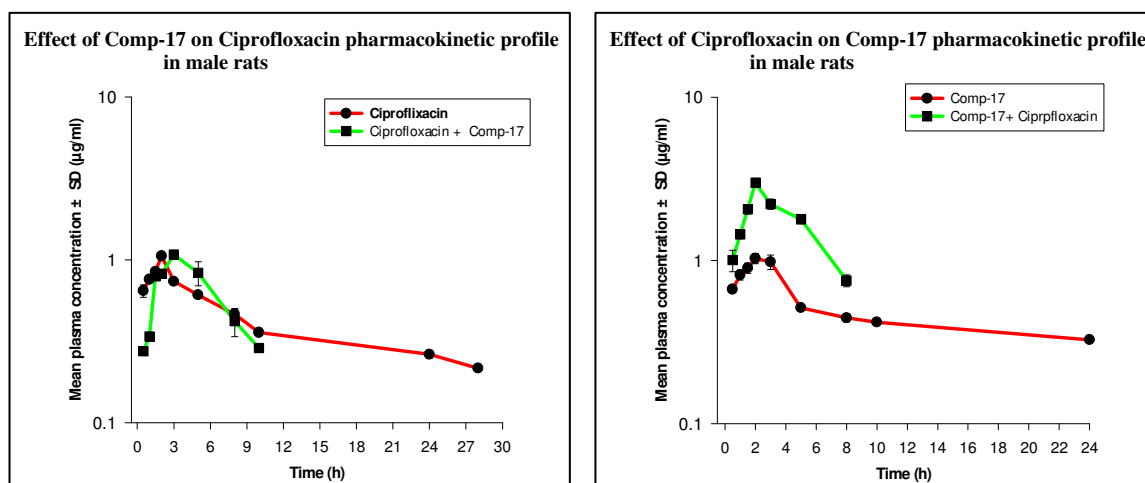


Figure 4.3.10. Log linear Concentration time profile of ciprofloxacin and compound 17

C. Results

Both the compounds were well tolerated by the animals. The pharmacokinetic parameters are listed in table 4.3.7 & 4.3.8. The difference between mean values for the parameters which characterise the AUC, C_{max}, were significant when compound 17 was administered with/without Ciprofloxacin. AUC values (11.61 ± 0.28 vs 13.41 ± 0.61 $\mu\text{g}\cdot\text{hr}/\text{ml}$), C_{max} values of compound 17 (1.03 ± 0.07 vs 2.99 ± 0.09 $\mu\text{g}/\text{ml}$) before and after the Ciprofloxacin treatment had a significant effect ($p= 0.05$). Time to attain peak plasma concentrations (T_{max}) remained unchanged.

The difference between mean values for the parameters which characterise the AUC, C_{max}, were significant when Ciprofloxacin was administered with/without compound 17. AUC values (11.36 ± 0.16 vs 6.35 ± 0.66 $\mu\text{g}\cdot\text{hr}/\text{ml}$), C_{max} values were (1.05 ± 0.02 vs 1.08 ± 0.07 $\mu\text{g}/\text{ml}$) before and after the compound 17 treatment had a significant effect ($p= 0.05$). Time to attain peak plasma concentration (T_{max}) was also prolonged (2.00 vs 3.00 hr).

4.3.6. CYP2C

The CYP2C subfamily is the most complex subfamily of the P450s found in human and animal species with several different isoforms. In human, the CYP2C family is involved in the metabolism of about 16% of drugs currently on the market. CYP2C9 is the major form, accounting 60% of total human CYP2C. In addition to liver, CYP2C mRNA is also detected in the kidney, testes, adrenal gland, prostate, ovary and duodenum. CYP2C9 metabolizes many clinically important drugs [193,194].

4.3.6.1. GLIPIZIDE (SUBSTRATE)

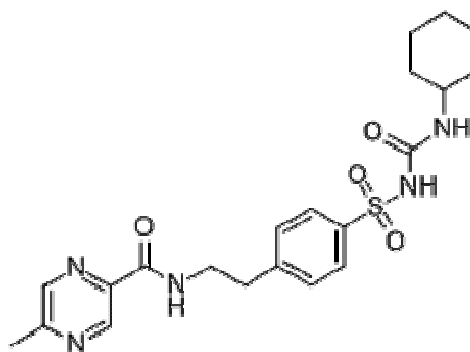


Figure 4.3.11. Glipizide

Glipizide is an oral medium-to-long acting anti-diabetic drug from the sulfonylurea class. It is classified as a second generation sulfonylurea, which means that it undergoes enterohepatic circulation. Mechanism of action is produced by blocking potassium channels in the beta cells of the islets of Langerhans. By partially blocking the potassium channels, it will increase the time the cell spends in the calcium release stage of cell signaling leading to an increase in calcium. The increase in calcium will initiate more insulin release from each beta cell. Since diabetes is a common disease found in majority of the population, co administration of anti-diabetic drugs with tuberculosis therapy is very frequent. Therefore it has been selected to study the drug interactions with compound 17.

A. Metabolism of Glipizide

Metabolites are mainly represented by hydroxy-cyclohexyl derivatives and are eliminated predominantly in the urine. The major metabolites of glipizide are products of aromatic hydroxylation and have no hypoglycemic activity. A minor metabolite which accounts for less than 2% of a dose, an acetylaminoethyl benzenederivatives which are reported to have 1/10 to 1/3 as much hypoglycemic activities as the parent compound.

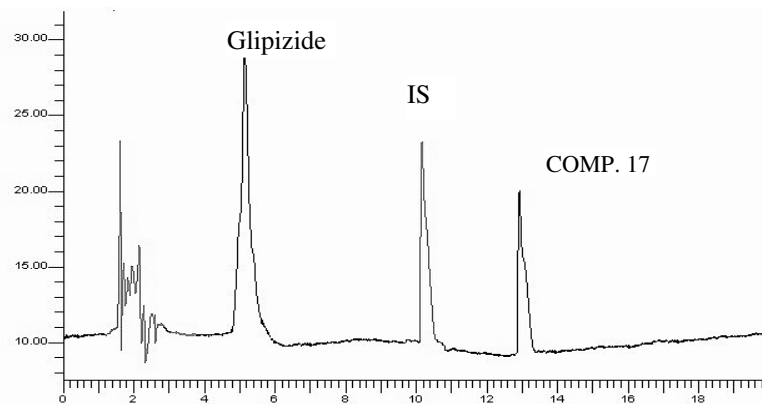
B. Bio analytical method development

The mobile phase used in the method was Methanol and ammonium formate (pH = 3) as non polar and polar phases respectively. The finally developed gradient method consisted of % change in Methanol with respect to time ((0.01→12 min: 55%; 12.01→17.00 min: 80%; 17.01→22.5 min: 55%). Analysis was performed using reverse phase HPLC at 230nm (λ_{max} of Glipizide). Glipizide, IS and compound 17 were eluted at 6.6, 8.2 and 15.2mins, respectively.

For the purpose of analysis, a validated method has been taken from the literature and required modifications have been done to suit the specifications of the analysis for combination samples. Thus a linearity range, accuracy and precision for the newly developed method have been established.

Table 4.3.8. Mini Validation of Glipizide

LINEARITY RANGE	0.8 – 20 ($r^2 = 0.993$)
ACCURACY (n=6)	101.63%
PRECISION (n=6)	0.68%



Column: Brownlee Analytical C18 column (4.6 x 150 mm, 3 μ m)
 Mobile Phase:
 A: 95% Ammonium acetate (pH 3.0), 5% MeOH
 B: 5% H₂O, 95% MeOH
 Flow Rate: 1 mL/min
 Detector: UV 230 nm

Figure 4.3.12. A typical chromatogram of Glipizide, IS and compound 17.

Table 4.3.9. Pharmacokinetic parameters of compound 17 with Glipizide

Parametres (n=4)	Comp.17 alone [#]	Comp. 17 with Glipizide*	p value (Unpaired t-test) $\alpha = 0.05$	Significant difference Between the parameters
AUC _(0-t) μ g.hr/ml	11.61 \pm 0.28	8.40 \pm 3.42	1.868	No
Cmax (μ g/ml)	1.03 \pm 0.07	2.97 \pm 0.62	6.30	Yes
Tmax (hr)	2.00 \pm 0.00	1.00 \pm 0.00	-	-

Note: t = [#]24h *5h

Table 4.3.10. Pharmacokinetic parameters of Glipizide with compound 17

Parametres (n=4)	Glipizide Alone [#]	Glipizide with Comp. 17*	t value (Unpaired t-test) $\alpha = 0.05$	Significant difference Between the parameters
AUC _(0-t) $\mu\text{g.hr/ml}$	73.82 \pm 3.60	462.19 \pm 95.99	8.086	Yes
Cmax ($\mu\text{g/ml}$)	7.53 \pm 0.28	45.57 \pm 14.06	5.41	Yes
Tmax (hr)	3.00 \pm 0.00	5.00 \pm 0.00	-	-

Note: t = [#]24h *24h

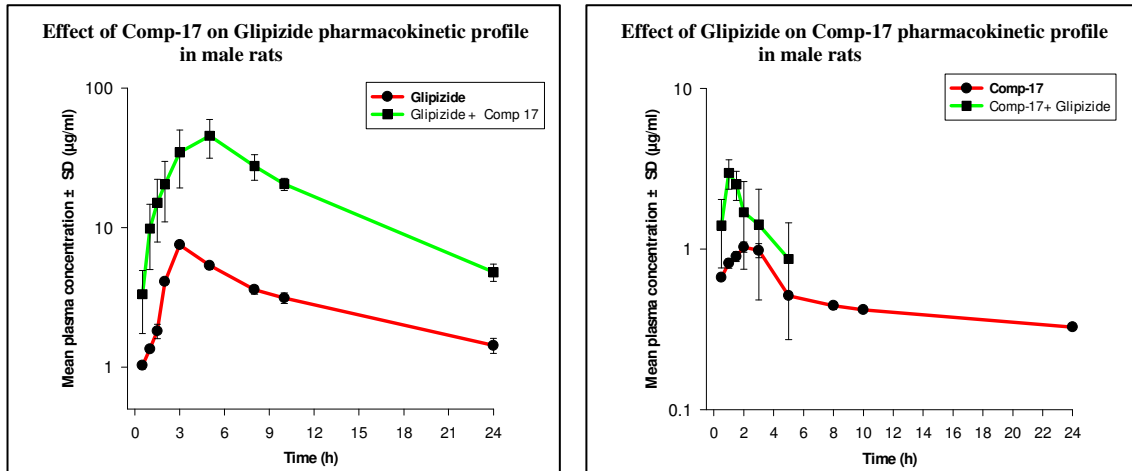


Figure 4.3.13. Log linear Concentration time profiles of glipizide and compound 17

C. Results

Both the compounds were well tolerated by the animals. The pharmacokinetic parameters are listed in table 4.3.11 & 4.3.12. The difference between mean values for the C_{max} was significant and mean exposure values (AUC) were not significant when compound 17 was administered with/without glipizide. AUC values (11.61 ± 0.28 vs 8.40 ± 3.42 $\mu\text{g}\cdot\text{hr}/\text{ml}$), C_{max} values of compound 17 (1.03 ± 0.07 vs 2.97 ± 0.62 $\mu\text{g}/\text{ml}$) before and after the glipizide treatment was tested at 95% confidence limits. Time to attain peak plasma concentrations (T_{max}) remained unchanged.

The difference between mean values for the parameters which characterise the AUC, C_{max}, were significant when glipizide was administered with/without compound 17. AUC values (73.82 ± 3.60 vs 462.19 ± 95.99 $\mu\text{g}\cdot\text{hr}/\text{ml}$), C_{max} values were (7.53 ± 0.28 vs 45.57 ± 14.06 $\mu\text{g}/\text{ml}$) before and after the compound 17 treatment had a significant effect ($p = 0.05$). Time to attain peak plasma concentration (T_{max}) was also prolonged (3.00 vs 5.00 hr).

4.3.6.2. RANITIDINE (INHIBITOR)

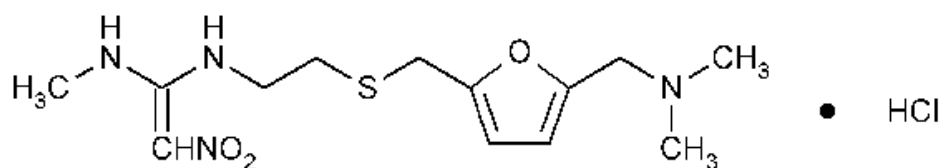


Figure 4.3.14. Ranitidine

It is a histamine H₂-receptor antagonist that inhibits stomach acid production. It is commonly used in treatment of peptic ulcer disease (PUD) and gastro-esophageal reflux disease (GERD). Ranitidine is also used along side fexofenadine and other antihistamines for the treatment of skin conditions such as hives. Ranitidine, like other drugs that reduce

stomach acid, may interfere with the absorption of drugs. Thus the study of interaction with compound 17 is very important [195, 196]

A. Metabolism of ranitidine:

Ranitidine is metabolized to the N-oxide, S-oxide, and N-desmethyl metabolites, accounting for approximately 4%, 1%, and 1% of the dose, respectively.

B. Bio analytical method development:

The mobile phase used in the method was acetonitrile and potassium dihydrogen phosphate at pH=6.5 as non polar and polar phases respectively. The finally developed gradient method was consist of % change in Acetonitrile with respect to time (0.01→4.00 min: 15%; 4.01→13.00 min: 47%; 13.01→16 min: 15%). Analysis was performed using reverse phase HPLC at 330 nm (λ_{max} of Ranitidine). Ranitidine, IS and compound 17 were eluted at 4.2mins, 12mins and 13.6 mins respectively.

For the purpose of analysis, a validated method has been taken from the literature and required modifications have been done to suit the specifications of the analysis for combination samples. Thus a linearity range, accuracy and precision for the newly developed method have been established.

Table.4.3.11. Mini Validation of Ranitidine

LINEARITY RANGE	0.25 – 6 ($r^2 = 0.9997$)
ACCURACY (n=6)	102.12
PRECISION (n=6)	1.33

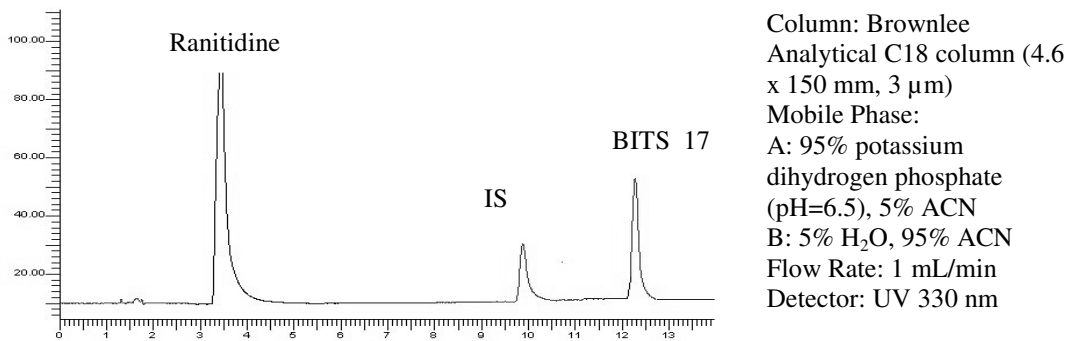


Figure 4.3.15. A typical chromatogram of Ranitidine, IS and compound 17

Table.4.3.12. Pharmacokinetic parameters of compound 17 with Ranitidine

Parametres (n=4)	Comp.17 alone [#]	Comp. 17 with Ranitidine*	p value (Unpaired t-test) $\alpha = 0.05$	Significant difference Between the parametres
AUC _(0-t) $\mu\text{g.hr/ml}$	11.61 \pm 0.28	14.32 \pm 0.77	6.626	Yes
Cmax ($\mu\text{g/ml}$)	1.03 \pm 0.07	2.37 \pm 0.18	5.83	Yes
Tmax (hr)	2.00 \pm 00	3.00 \pm 00	-	-

Note: t = [#]24h *10h

Table.4.3.13. Pharmacokinetic parameters of Ranitidine with compound 17.

Parametres (n=4)	Ranitidine Alone [#]	Ranitidine with Comp.17*	t value (Unpaired t-test) $\alpha =0.05$	Significant difference Between the parametres
AUC _(0-t) $\mu\text{g.hr/ml}$	5.14 \pm 0.17	3.92 \pm 0.16	2.325	No
Cmax ($\mu\text{g/ml}$)	0.8 \pm 0.07	1.04 \pm 0.06	5.41	Yes
Tmax (hr)	2.00	3.00	-	-

Note: t = [#]8h *8h

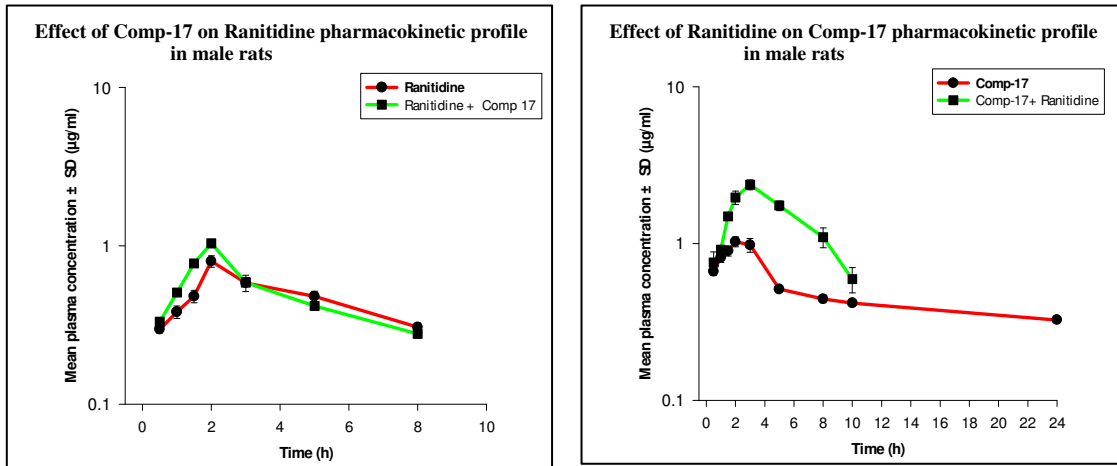


Figure 4.3.16. Log linear concentration time profile of ranitidine and compound 17

C. Results

Both the compounds were well tolerated by the animals. The pharmacokinetic parameters are listed in table 4.3.15 & 4.3.16. The difference between mean values for the parameters which characterise the AUC, C_{max}, were significant when ranitidine was administered with/without compound 17. AUC values (11.61 ± 0.28 vs 14.32 ± 0.77 $\mu\text{g}\cdot\text{hr}/\text{ml}$), C_{max} values were (1.03 ± 0.07 vs 2.37 ± 0.18 $\mu\text{g}/\text{ml}$) before and after the ranitidine treatment had a significant effect ($p= 0.05$). Time to attain peak plasma concentration (T_{max}) was also prolonged (2.00 vs 3.00 hr).

The difference between mean values for the C_{max} was significant and mean exposure values (AUC) were not significant when ranitidine was administered with/without compound 17. AUC values (5.14 ± 0.17 vs 3.92 ± 0.16 $\mu\text{g}\cdot\text{hr}/\text{ml}$), C_{max} values of compound 17 (0.8 ± 0.07 vs 1.04 ± 0.06 $\mu\text{g}/\text{ml}$) before and after the ranitidine treatment was tested at 95% confidence limits. Time to attain peak plasma concentrations (T_{max}) was also prolonged (2.00 vs 3.00 hr).

4.3.7. CYP3A

CYP3A is involved in the oxidation of the largest range of substrates of all the CYPs. As a result, CYP3A is present in the largest quantity of all the CYPs in the liver. Most drugs undergo deactivation by CYP3A, either directly or by facilitated excretion from the body. Also, many substances are bioactivated by CYP3A to form their active compounds, and many protoxins being toxicated into their toxic forms. The P450 3A subfamily is highly inducible and can be inhibited by numerous drugs [196]. It has been estimated that CYP3A metabolizes about half of all drugs on the market. Because many other commonly used drugs are moderate-to-potent inhibitors of CYP3A, it is not surprising that drug toxicity of CYP3A substrates due to inhibition of CYP3A is relatively common. CYP3A also is sensitive to enzyme induction, and a number of drugs are known to be CYP3A inducers. The enzyme is involved in the biotransformation of approximately 50% of therapeutic drugs currently on the market, although its content in the liver is only 30% of total P450. CYP3A is expressed in liver, stomach, lung, intestine and renal tissue [198, 199].

4.3.7.2. ATORVASTATIN (SUBSTRATE)

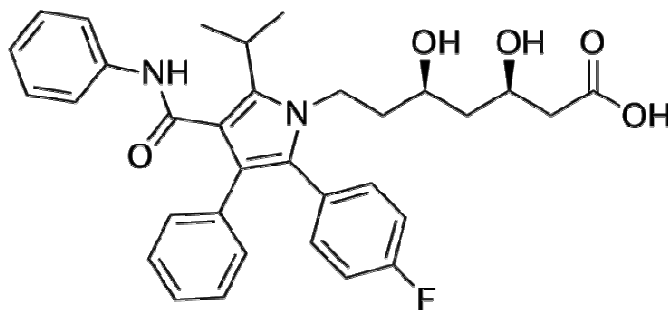


Figure 4.3.17. Atorvastatin

Atorvastatin is a member of the drug class known as statins, used for lowering blood cholesterol. It also stabilizes plaque and prevents strokes through anti-inflammatory and other mechanisms. Like all statins, atorvastatin works by inhibiting HMG-CoA reductase,

an enzyme found in liver tissue that plays a key role in production of cholesterol in the body. Statins, 3-hydroxy-3-methylglutaryl coenzyme A (HMG-CoA) reductase inhibitors, are extremely effective in the treatment of dyslipidemia. They have been shown to reduce the risk of major coronary outcomes and all cause mortality. Statins that undergo phase I metabolism by the CYP3A4 isoenzyme are referred to as statin 3A substrates. Following hepatocyte entry and metabolism (phase I and II), statins exert their cholesterol inhibitory effect and are subsequently eliminated. For most statins, elimination occurs through biliary excretion, PV is partially eliminated by renal excretion. Inhibition of statin metabolism (phase I or II) and/or active membrane transporters (influx or efflux) may result in elevated plasma concentrations and has the potential to increase the risk for statin-related adverse events. Coronary diseases are very frequent in most of the patients taking anti tubercular therapy. Therefore the interaction of compound 17 with atorvastatin has been studied.

A. Metabolism of atorvastatin:

Atorvastatin undergo significant metabolism via the cytochrome P450 3A4 (CYP3A4) isozymes. Bile is the major route of drug-derived excretion, accounting for 73% of the oral dose, respectively. The remaining drug can be recovered in the feces; only trace amounts are excreted in urine. Major forms were the para- and ortho-hydroxy metabolites, a glucuronide conjugate of ortho-hydroxy atorvastatin, and unchanged atorvastatin. Two minor metabolites are β -oxidation products.

B. Bio analytical method development:

The mobile phase used in the method was Acetonitrile, methanol and ammonium acetate (pH = 5) as non polar and polar phases respectively. The finally developed gradient method consisted of % change in B as Buffer : acetonitrile in the ratio 5:95, C as buffer : methanol in the ratio 10 : 90 and D as water with respect to time (0.01→2 min: 0% B, 0% C, 0% D; 2.01→6 min: 0% B, 10% C, 0% D; 6.01→9 min: 20% B, 30% C, 0% D; 9.01→12 min: 20% B, 25% C, 5% D; 12.01→14 min: 50% B, 20% C, 0% D, 14.01→18 min: 85% B, 5% C, 0% D, 18.01→21 min: 0% B, 0% C, 0% D). Analysis was

performed using reverse phase HPLC at 241nm (λ_{max} of atorvastatin). Atorvastatin, IS and compound 17 were eluted at 17.2, 8 and 12 mins.

For the purpose of analysis, a validated method has been taken from the literature and required modifications have been done to suit the specifications of the analysis for combination samples. Thus a linearity range, accuracy and precision at 10 $\mu\text{g/ml}$ for the newly developed method have been established.

Table.4.3.14. Mini Validation of Atorvastatin

LINEARITY RANGE ($\mu\text{g/ml}$)	10 – 250 ($r^2 = 0.9997$)
ACCURACY (n=6)	105.27%
PRECISION (n=6)	1.58%

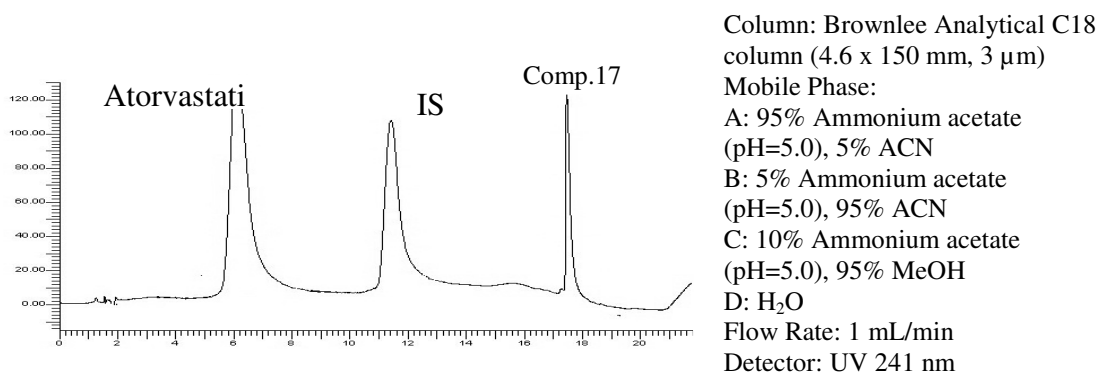


Figure 4.3.18. A typical chromatogram of Atorvastatin, IS and compound 17.

Table.4.3.15. Pharmacokinetic parameters of compound 17 with Atorvastatin

Parametres (n=4)	Comp.17 alone [#]	Comp. 17 with Atorvastatin*	p value (unpaired t- test) $\alpha =0.05$	Significant difference Between the parametres
AUC _(0-t) $\mu\text{g.hr/ml}$	11.61 \pm 0.28	10.08 \pm 0.32	7.23	Yes
Cmax ($\mu\text{g/ml}$)	1.03 \pm 0.07	2.35 \pm 0.04	32.70	Yes
Tmax (hr)	2.00 \pm 00	3.00 \pm 00	-	-

Note: t = [#]24h *8h

Table.4.3.16. Pharmacokinetic parameters of Atorvastatin with compound 17

Parametres (n=4)	Atorvastatin Alone [#]	Atorvastatin with Comp. 17*	t value (Unpaired t-test) $\alpha =0.05$	Significant difference Between the parameters
AUC _(0-t) $\mu\text{g.hr/ml}$	100.31 \pm 7.23	309.73 \pm 13.51	27.32	Yes
Cmax ($\mu\text{g/ml}$)	21.07 \pm 0.13	62.53 \pm 2.22	37.70	Yes
Tmax (hr)	3.00	3.00	-	-

Note: t = [#]8h *10h

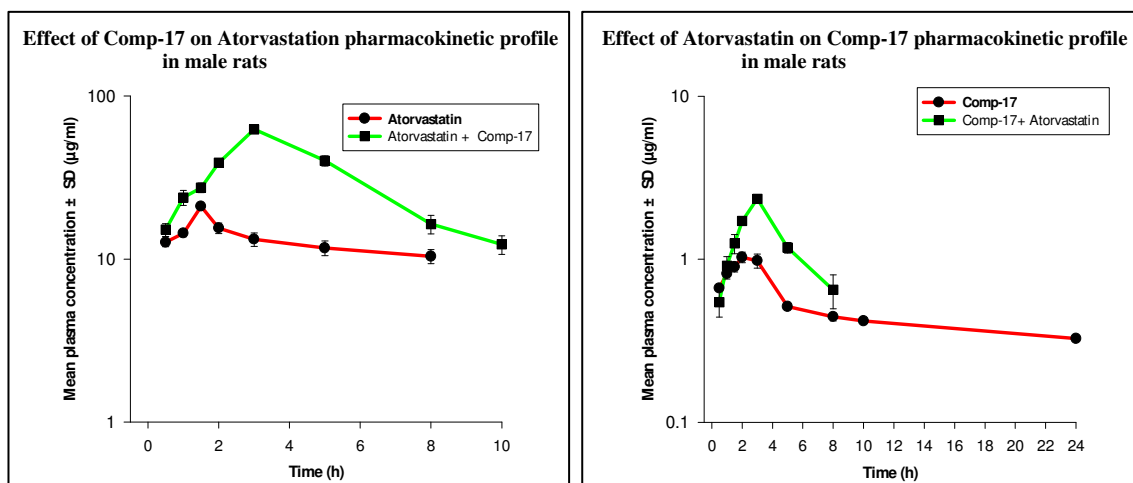


Figure 4.3.19. Log linear Concentration time profiles of atorvastatin and compound 17

C. Results

Both the compounds were well tolerated by the animals. The pharmacokinetic parameters are listed in table 4.3.19 & 4.3.20. The difference between mean values for the parameters which characterize the AUC, C_{max}, were significant when compound 17 was administered with/without atorvastatin. AUC values (11.61 ± 0.28 vs 10.08 ± 0.32 $\mu\text{g}\cdot\text{hr}/\text{ml}$), C_{max} values of compound 17 (1.03 ± 0.07 vs 2.35 ± 0.14 $\mu\text{g}/\text{ml}$) before and after the atorvastatin treatment had a significant effect ($p = 0.05$). Time to attain peak plasma concentration (T_{max}) was also prolonged (2.00 vs 3.00 hr).

The differences between mean values for the parameters which characterize the AUC, C_{max}, were significant when atorvastatin was administered with/without compound 17. AUC values (100.31 ± 7.23 vs 309.73 ± 13.51 $\mu\text{g}\cdot\text{hr}/\text{ml}$), C_{max} values were (21.07 ± 0.13 vs 62.53 ± 2.22 $\mu\text{g}/\text{ml}$) before and after the compound 17 treatment had a significant effect ($p = 0.05$). Time to attain peak plasma concentration (T_{max}) remained unchanged.

4.3.7.2. KETOCONAZOLE (INHIBITOR)

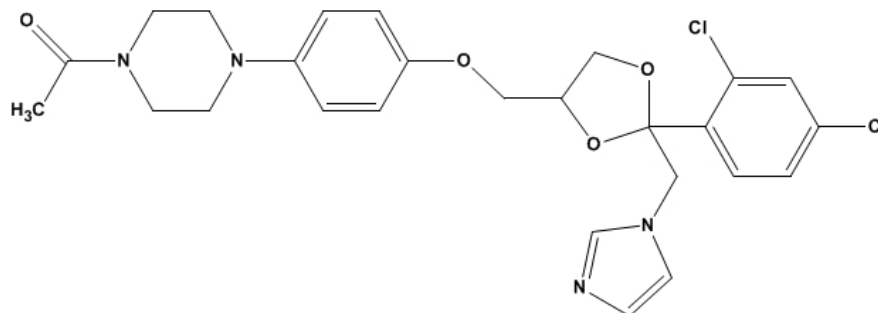


Figure 4.3.20. Ketoconazole

Ketoconazole is an antifungal drug with therapeutic efficacy in prostate cancer and other benign and malignant neoplastic conditions. Ketoconazole inhibits cytochrome P450 dependent enzyme 11-hydroxylase activity, which suppresses testosterone production leading to inhibition of testosterone-dependent prostate cancer cell growth. Intriguingly, the receptors that are affected by ketoconazole are phylogenetically related and all are involved in xenobiotic metabolism indicating that perhaps there is subclass specificity with which ketoconazole mediates its activity.

A. Metabolism of ketoconazole:

N-deacetyl ketoconazole (DAK) is a major initial metabolite in mice, which, like lipophilic 4-alkylpiperazines, is susceptible to successive oxidative attacks on the N-1 position producing ring-opened dialdehydes. Deactivation of KT yields a major product, DAK, for further metabolism by microsomal monooxygenases that seem to be Flavin Mono Oxidase related.

Mechanism of inhibition by ketoconazole:

Drug metabolism is controlled by a class of orphan nuclear receptors (NRs), which regulate expression of genes such as CYP (cytochrome) 3A4 and MDR-1 (multi-drug

resistance-1), that are involved in this process. Xenobiotic-mediated induction of CYP3A4 and MDR-1 gene transcription is inhibited by ketoconazole. Ketoconazole mediates its effect by inhibiting the activation of NRs, human pregnenolone X receptor and constitutive androstene receptor, involved in regulation of CYP3A4 and MDR-1. Ketoconazole represses the coordinated activation of genes involved in drug metabolism, by blocking activation of aspecific subset of NRs [200]. Due to its nonspecific interaction with various xenobiotics, this drug has been selected to study the drug interactions with compound 17.

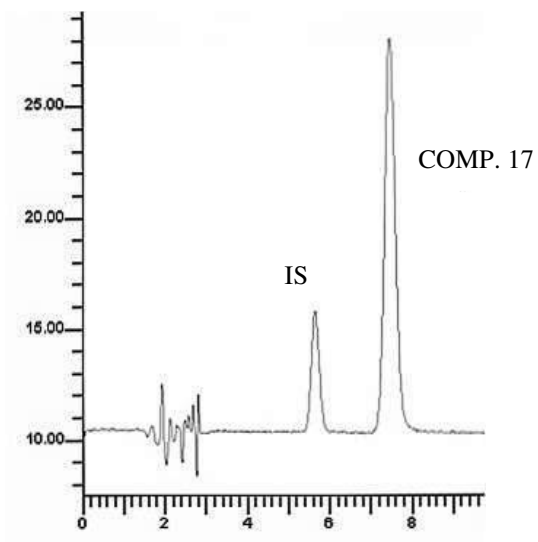
B. Bio analytical method development:

The mobile phase used in the method was Acetonitrile and ammonium acetate pH 6.8 as non-polar and polar phases respectively in the ratio of 50:50 using reverse phase HPLC at 231 nm (λ_{max} of Ketoconazole). Ketoconazole and IS were eluted at 5.2 mins and 8.5 mins respectively.

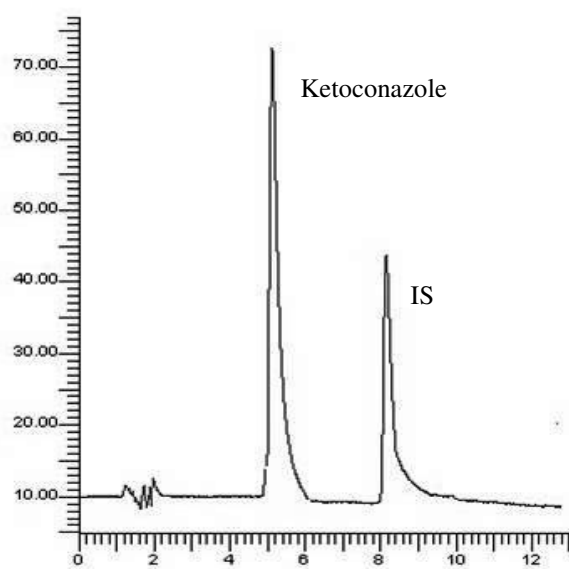
For the purpose of analysis, a validated method has been taken from the literature and required modifications have been done to suit the specifications of the analysis for combination samples. Thus a linearity range, accuracy and precision for the newly developed method have been established.

Table.4.3.17. Linearity and precision of Ketoconazole

LINEARITY RANGE ($\mu\text{g/ml}$)	0.25 – 6 ($r^2 = 0.999$)
ACCURACY (n=6)	102.47
PRECISION (n=6)	1.50



Column: Brownlee Analytical C18 column
 (4.6 x 150 mm, 3 μ m)
 Mobile Phase:
 A: 62% 0.01M ammonium acetate (pH 6.5)
 B: 38% ACN
 Flow Rate: 1 mL/min
 Detector: UV 315 nm



Column: Brownlee Analytical C18
 column (4.6 x 150 mm, 3 μ m)
 Mobile Phase:
 A: 50% ammonium acetate (pH 6.8),
 B: 50% ACN
 Flow Rate: 1 mL/min
 Detector: UV 231 nm

Figure 4.3.21. Atypical chromatograms of Ketoconazole, IS and Compound 17.

Table.4.3.18. Pharmacokinetic parameters of Compound 17 with Ketoconazole

Parametres (n=4)	Comp.17 alone [#]	Comp. 17 with Ketoconazole*	p value (Unpaired t-test) $\alpha =0.05$	Significant difference Between the parametres
AUC _(0-t) $\mu\text{g.hr/ml}$	11.61 \pm 0.28	11.75 \pm 0.47	0.527	No
Cmax ($\mu\text{g/ml}$)	1.03 \pm 0.07	2.25 \pm 0.15	14.07	Yes
Tmax (hr)	2.00 \pm 00	3.00 \pm 00	-	-

Note: t = [#]24h *10h

Table.4.3.19. Pharmacokinetic parameters of Ketoconazole with Compound 17

Parametres (n=4)	Ketoconazole Alone [#]	Ketoconazole with Comp. 17*	t value (Unpaired t-test) $\alpha =0.05$	Significant difference Between the parameters
AUC _(0-t) $\mu\text{g.hr/ml}$	12.87 \pm 1.88	11.03 \pm 0.56	1.85	No
Cmax ($\mu\text{g/ml}$)	2.67 \pm 0.36	3.39 \pm 0.62	1.99	No
Tmax (hr)	3.00	2.00	-	-

Note: t = [#]10h *8h

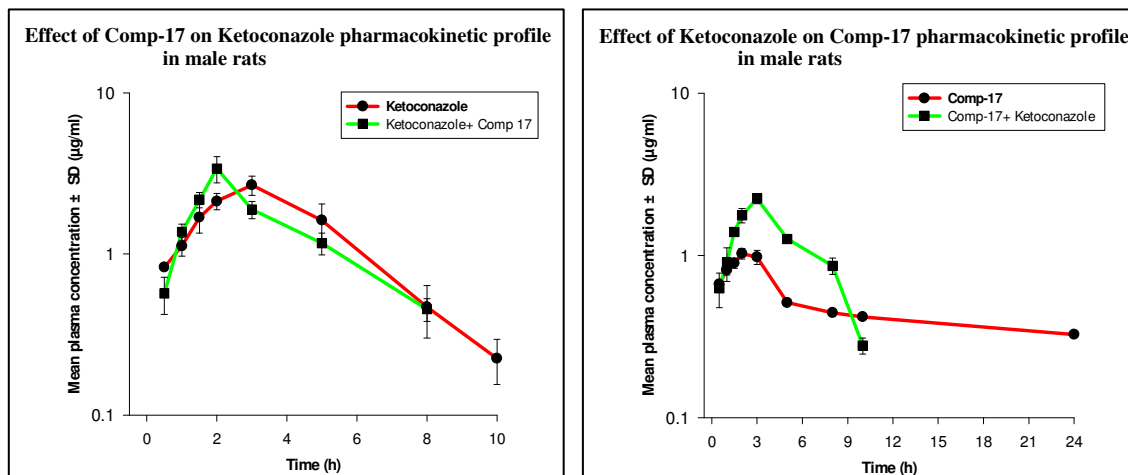


Figure 4.3.22. Log linear Concentration time profiles of ketoconazole and Compound 17

C. Results:

Both the compounds were well tolerated by the animals. The pharmacokinetic parameters are listed in table 4.3.22 & 4.3.23. The difference between mean values for the parameters which characterise the AUC, C_{max}, were significant when ketoconazole was administered with/without compound 17. AUC values (11.61 ± 0.28 vs 11.75 ± 0.47 $\mu\text{g}\cdot\text{hr}/\text{ml}$), C_{max} values were (1.03 ± 0.07 vs 2.25 ± 0.15 $\mu\text{g}/\text{ml}$) before and after the ketoconazole treatment had a significant effect ($p= 0.05$). Time to attain peak plasma concentration (T_{max}) was also prolonged (2.00 vs 3.00 hr).

The difference between mean values for the C_{max} was significant and mean exposure values (AUC) were not significant when ketoconazole was administered with/without compound 17. AUC values (12.87 ± 1.88 vs 11.03 ± 0.56 $\mu\text{g}\cdot\text{hr}/\text{ml}$), C_{max} values of compound 17 (2.67 ± 0.36 vs 3.39 ± 0.62 $\mu\text{g}/\text{ml}$) before and after the ketoconazole treatment was tested at 95% confidence limits. Time to attain peak plasma concentrations (T_{max}) was also prolonged (3.00 vs 2.00 hr).

4.3.8. Discussion:

The plasma concentrations of compound 17 were altered by the administration of ondansetron (substrate) and ciprofloxacin (inhibitor) indicating that the metabolism of compound 17 is mediated through 1A enzyme. There is a slight decrease in compound 17 levels and 2 fold decrease in the ondansetron levels indicating that the deactivation being increased by compound 17 (hetero activation of compound 17(?) and/or any increase in the free fraction). It was also seen that the metabolism of compound 17 may be suppressed by a ciprofloxacin, thereby increased plasma concentrations of compound 17, possibly by inhibition of the enzyme CYP1A. This could probably lead to clinically significant adverse events of the coadministered drug concomitant use of compound 17 and ciprofloxacin in rats, a similar drug-drug interaction may occur in human, although the isoforms of CYP enzymes are different. Caution should be exercised about the dose of compound 17 when treated with CYP 1A inhibitors.

There is a marked increase (six fold) in the glipizide levels in presence of compound 17 showing that CYP2C levels can affect the metabolism of sulfonylureas, showing that compound 17 inhibits 2C9 metabolism. Results suggest that increased levels of glipizide can induce hypoglycemia. Caution should be exercised about the dose of glipizide when treated with compound 17. Though the plasma concentration of compound 17 was not altered in the presence of glipizide and ranitidine but there was two fold increase in the peak plasma concentration with ranitidine. The ranitidine (metabolism - N-oxide (66-76%) and S-oxide (13-18%) by FMO and desmethylranitidine by CYP2C19, 1A2 and 2D6,) levels were unaltered with compound 17.

The present study clearly showed that the plasma concentrations of compound 17 were unaltered by the administration of atorvastatin and ketoconazole indicating that the metabolism of compound 17 is not a mediated through 3A enzyme. But the plasma concentrations of atorvastatin were enhanced with the concomitant administration of compound 17. Lyophilic HMG-CoA reductase inhibitors, such as simvastatin,

lovastatin, and atorvastatin, are metabolized by CYP3A4 in the liver or small intestine. Increase in plasma concentration of HMG-CoA reductase inhibitor indicates the possibility of inhibition of the enzyme CYP3A. In present study, it is possible to consider that the metabolism of atorvastatin may be suppressed by a compound 17, possibly by inhibition of the enzyme CYP3A by later. These results suggest that the increased HMG-CoA reductase inhibitors increase the incidence of rhabdomyolysis in patients. Levels of ketoconazole (metabolized by FMO's to N-deacetylated product) are unaltered indicating that compound 17 does not interfere with its metabolism.

There is a difference in CYP isoforms that exist in humans and rats. Rats do not possess CYP3A4, but CYP3A1, 3A2, 3A9, and 3A18 as the CYP3A subfamily. CYP3A2 plays an important role in drug metabolism in rats, and may metabolize atorvastatin. However, it is uncertain whether HMGCoA reductase inhibitors can be metabolized by CYP3A2 in rats. Other enzyme 1A, 2C are present in rats.

4.3.9 Conclusion

A major component of the safety assessment process is to identify, at the earliest stage possible, the potential for toxicity in humans. Though human CYPs differ from rodent CYPs in both isoform composition and catalytic activities, xenobiotic metabolism by male rats can reflect human metabolism. Because concomitant use of xenobiotics which are either substrates or inhibitors of the CYP 450 enzymes studied in specific with that of compound-17 showed alterations in their metabolism in male Wistar rats as discussed above, a similar drug-drug interaction between them may occur in human, although the isoforms of CYP are different. We should use caution about the dose of these drugs in patients when co administered with compound 17. Thus, understanding the mechanism underlying drug interactions is useful, not only in preventing drug toxicity or adverse effects, but also in devising safer therapies for disease.

Chapter 5.0

1. 4-Thiazine derivatives as antitubercular agents

Earlier in this lab (*L*)-proline-catalysed green synthesis of highly functionalized [1, 4]-thiazines and the results of their evaluation for *in vitro* antimycobacterial activity against *M. tuberculosis* H37Rv (MTB). The choice of (*L*)-proline as catalyst in this transformation is based on the fact that, besides being an abundant and inexpensive amino acid, it is known to catalyse diverse organic transformations, both enantio- and non enantioselective ones such as aldol [201], Mannich [202], Michael [203], Diels Alder/Knoevenagel [204], unsymmetric Biginelli [205] and tandem [206] reactions. The efficiency of (*L*)-proline in diverse organic transformations is ascribable to multiple catalytic roles it can play, such as an acid or a base and both, as a nucleophile and its ability to form enamine/enaminium intermediates upon reaction with carbonyl/ α & β -unsaturated carbonyl compounds. This work is a continuation to design newer antibacterial agents to obtain a lead series for 1, 4-thiazines with tractable SAR and potencies better than the previously reported derivatives.

5.1. Chemistry

The target compounds synthesized in this study were designed for a SAR study. It was understood that retaining the thiazine pharmacophore was very important for activity and any modification there resulted in either reduced or no activity [126]. In the light of these findings, it was decided to extend the previously reported thiazines by converting into their corresponding amides, which was achieved by treating the scaffold moiety with various acid chlorides in presence of a suitable base. This would give a clear understanding on the influence of various substituents in determining the anti-tubercular activity; viz hydrophilicity, lipophilicity electron withdrawing, electron donation properties and also steric factors were taken into consideration. Also an effort has been made to study the role of substituent on acetophenone part of the thiazine moiety in activity determination, by using chloro, methyl and unsubstituent acetophenone as precursor for synthesis. Thus the following library (Scheme 5.1) was designed for the study.

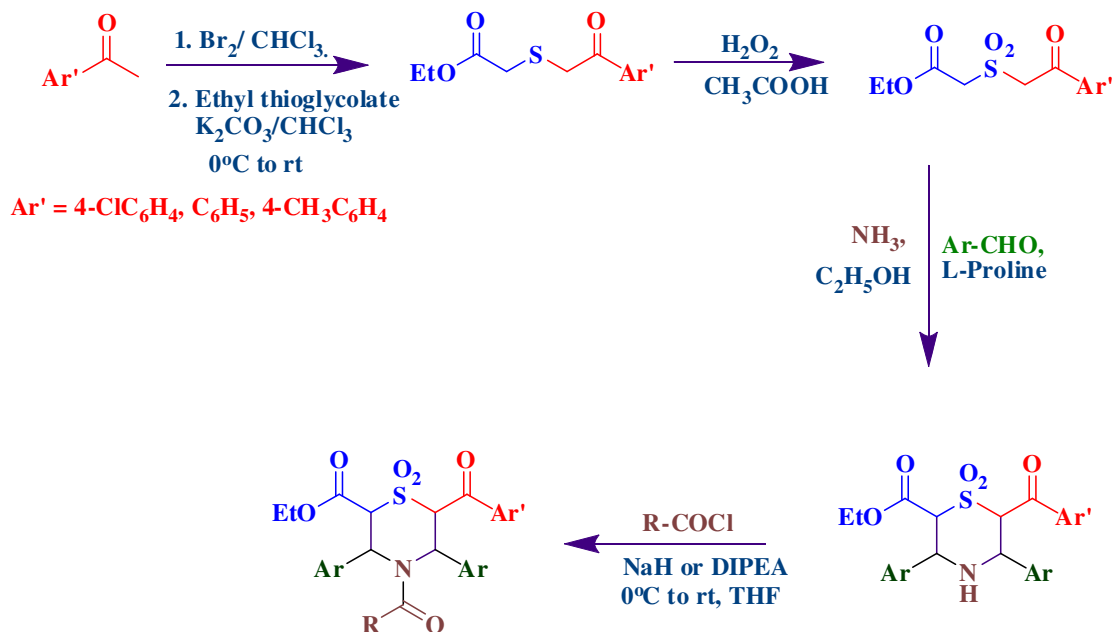
The synthetic sequence used to prepare the title compound is outlined in Scheme 1. The sulfone was achieved in three steps as previously reported by Reddy et al [207] from commercially available substituted acetophenone, by first converting them into the corresponding phenacyl bromide with bromine/acetic acid, followed by alkylation with ethylthioglycolate in presence of a base. The sulfide formed was further oxidized to the corresponding sulfone using excess of hydrogen peroxide at ambient temperature. All the steps went smoothly giving the desired product in quantitative yield. The sulfone was further converted into the corresponding thiazine by a protocol involving L-Proline-catalyzed one pot three component reactions of the sulphone, corresponding aldehyde and ammonia as previously reported by us [136]. This facile transformation presumably occurs via a one-pot domino sequence of enamine formation/iminium intermediate/Michael addition which ultimately forms thiazines in good yields via the intra-molecular Mannich type reaction. The mechanism for the formation of [1, 4]-thiazines derivatives is described in Scheme 5.2.

Though the L- proline catalysed cyclisation is essentially non-enantioselective, but a chiral HPLC analysis of a representative final molecule '7' revealed a very low enantiomeric excess of 4.9 %. The non enantioselectivity as explained in our previous work is probably due to the existence of the eniminium intermediate in two conformations and each of which probably facilitates subsequent Michael addition of the amine on opposite faces of the eniminium functionality, from the side opposite to that of the carboxyl group of proline due to steric interaction with the incoming Michael donor, the amine. The final library was achieved by converting the thiazine into the corresponding amides by treating the scaffold moiety with appropriate acid chlorides in presence of either sodium hydride or DIPEA as base. All the reaction in the final step were monitored at regular intervals by LC-MS and immediately purified by preparative HPLC, as it was observed that the leaving the reaction mixture for longer intervals led to the decomposition of products or too many side products, especially when sodium hydride was used as base. Though the final reactions were very tricky and required repeated trials and purification but we could achieve all the compounds with desired purity. Libraries of 52 amide derivatives were prepared using the above method for the

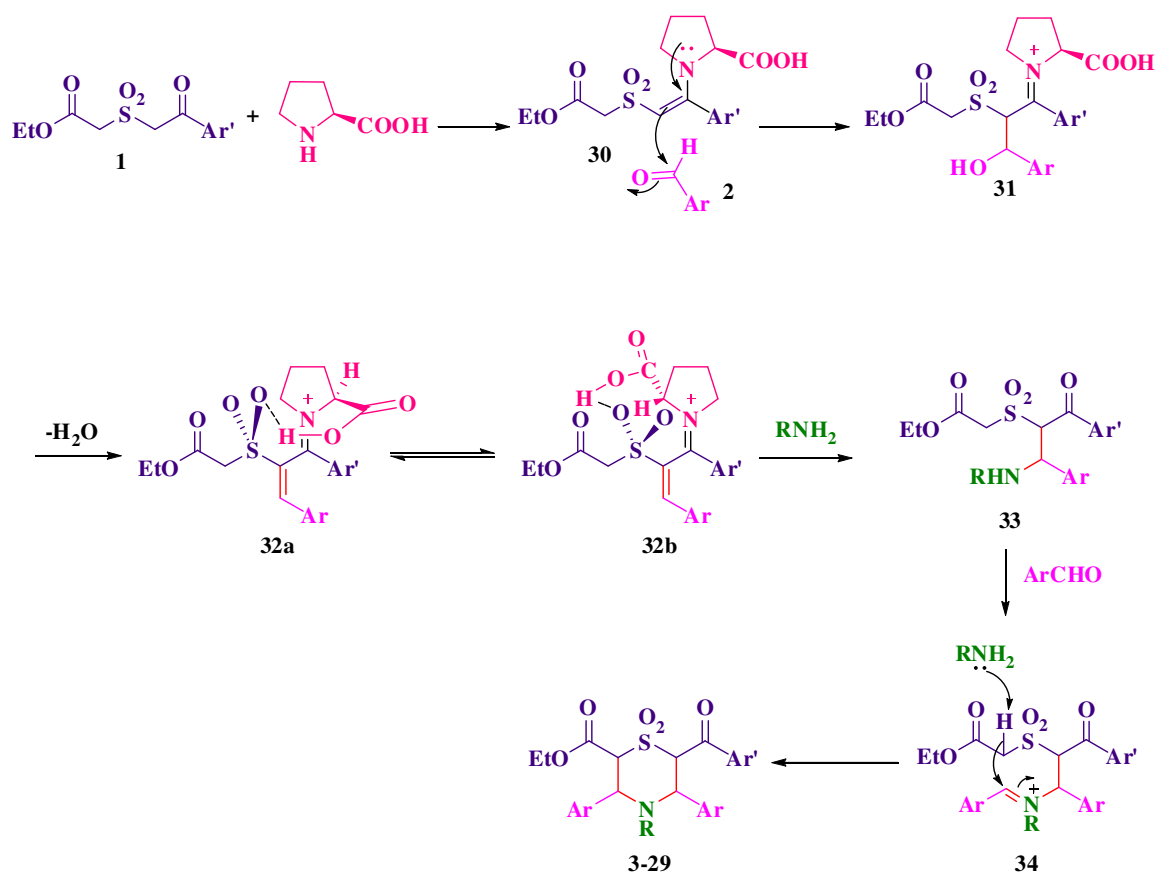
present study; further optimization of these hits is in progress. Both analytical and spectral data (^1H NMR, ^{13}C NMR, and mass spectra) of all the synthesized compounds were in full agreement with the proposed structures.

5.1.1. Methodology

All the reagents were purchased from Aldrich. All the solvents were freshly distilled before use. Melting points were determined using Buchi B-540 and are uncorrected. The homogeneity of the compounds was monitored by thin layer chromatography (TLC) on silica gel 40 F254 (Merck, Darmstadt, Germany) coated on aluminum plates, visualized by UV light and KMnO_4 solution. Elemental analyses were carried out on an automatic Flash EA 1112 Series, CHN Analyzer (Thermo). All ^1H and ^{13}C NMR spectra were recorded on a Bruker AM-300 (300.12 MHz, 75.12 MHz), Bruker Bio Spin Corp, Germany. Molecular weights of unknown compounds were checked by LCMS 6100B series Agilent Technology. Chemical shifts are reported in ppm (δ) with reference to.



Scheme 5.1: Synthesis of [1,4]-thiazines derivatives



Scheme 5.2. Mechanism for the formation of [1,4]-thiazines

internal standard TMS. The signals are designated as follows: s, singlet; d, doublet; dd, doublet of doublets; t, triplet; m, multiplet

General procedure for the synthesis of target molecule:

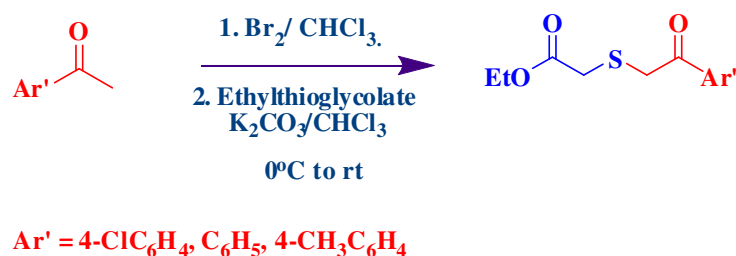
The target molecule was achieved in a five step process from commercially available substituted acetophenone or phenacyl bromide as depicted in Scheme 1.

5.1.2. Synthesis of Ethyl-2-(2-oxo-2-Aryl ethylthio) acetate:

Bromine (1mmol) was added drop wise to a vigorously stirred ice cold solution of the substituted acetophenone (1mmol) in acetic acid (40 ml) while marinating the internal

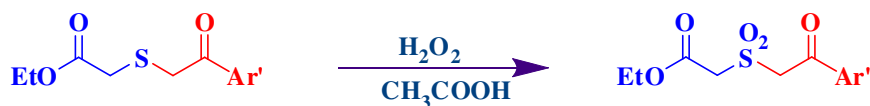
temperature of the reaction below 20°C. The reaction mixture was then stirred at 0°C for another 2-3 hour (monitored by TLC for completion). The solid obtained was then filtered, washed with aqueous ethanol and dried. The crude product was further purified by recrystallisation from ethanol, to give the corresponding phenacyl bromide as white solid.

Ethyl thioglycolate (1 mmol) in chloroform was added drop wise to a solution of the above obtained phenacyl bromide and K₂CO₃ (50 mol %) in chloroform at 0°C. The reaction mixture was slowly warmed to room temperature (rt) and stirred at rt (monitored by TLC for completion). The reaction mixture was then filtered; the organic phase was washed successively with water (25 mL), dried over anhydrous Na₂SO₄ and concentrated in vacuum to afford the desired sulphide in quantitative yield.



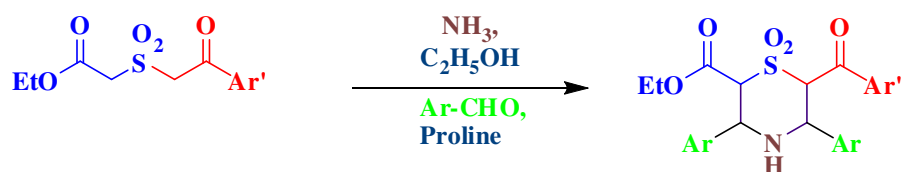
5.1.3. Synthesis of ethyl 2-[(2-oxo-2-arylethyl) sulfonyl] acetate:

To the above obtained sulphide in acetic acid, was added H₂O₂ (50%) in excess amount. The reaction mixture was then stirred at rt for 24 hours (monitored by TLC for completion). The reaction mixture was poured into ice-water and the solid separated was filtered, led to the sulfone.



5.1.4. Synthesis of ethyl 6- (sub: benzoyl)-1, 1-dioxo-3, 5-diaryl-1, 4-thiazinane-2-carboxylates:

The synthesis was achieved by a one pot three component reaction of the corresponding sulfone, aldehyde and ammonia in ratio 1:2:1 in presence of green catalyst L-proline as previously reported by our group. In a typical procedure to a solution of ethyl 2-[(2-oxo-2-arylethyl) sulfonyl] acetate (1.6 mmol) in ethanol at rt was added L-proline (30 mol%), and ammonia (1.6mmol). The reaction mixture was then allowed to stand at rt for about 3-4 hrs wherein the product start precipitating out. The solid thus obtained was filtered and the crude re-crystallised from ethanol: ethylacetate mixture (7:3) to afford the desired product as white to off white solid in quantitative yield.



Ethyl 6-(4-chlorobenzoyl)-3,5 di(4-nitrophenyl)-1,1-dioxo-1,4-thiazinane-2-carboxylate:

Pale yellow solid; M.P 173°C; Yield (90%). ^1H NMR (300 MHz, DMSO- d_6) δ 1.09 (t, 3H, $J = 7.2\text{Hz}$ - CH_3 of $\text{COOCH}_2\text{CH}_3$), 2.79 (s, NH, br), 4.02-4.16 (m, 2H, - CH_2 of $\text{COOCH}_2\text{CH}_3$), 4.90 (d, 1H, $J=10.5\text{ Hz}$, H2), 5.01 (d, 1H, $J=10.5\text{ Hz}$, H3), 5.10 (d, 1H, $J=10.3\text{ Hz}$, H5), 6.01 (d, 1H, $J=10.3\text{ Hz}$, H6), 7.42-8.29 (m, 12H, ArH). ^{13}C NMR (75MHz, DMSO- d_6) δ c 186.3, 160.5, 146.8, 146.6, 144.5, 140.0, 134.2, 129.8, 129.6, 128.5, 128.2, 128.1, 126.8, 122.6, 69.3, 68.7, 61.6, 60.7, 60.3, 12.8. Anal. Calcd for $\text{C}_{26}\text{H}_{22}\text{ClN}_3\text{O}_9\text{S}$: C, 53.11; H, 3.77; N, 7.15. Found: C, 53.16 H, 3.82; N, 7.21 MS m/z : 587.08 (100%) [$\text{M}+1$] 587.08, [$\text{M}+2$] 589.07, [$\text{M}+3$] 588.08.

Ethyl 6-(4-chlorobenzoyl) -1,1-dioxo-3,5 diphenyl-1,4-thiazinane-2-carboxylate:

White solid; M.P 140°C; Yield (90%). ¹H NMR (300 MHz, CDCl₃): δH1.06 (t, 3H, J=7.1Hz -CH₃ of COOCH₂CH₃), 2.01 (s, NH, br), 4.05-4.12 (m, 2H, -CH₂ of COOCH₂CH₃), 4.37 (d, 1H, J=10.7 Hz, H2), 4.80 (d, 1H, J=10.7 Hz, H3), 5.01 (d, 1H, J=10.2 Hz, H5), 5.23 (d, 1H, J=10.2 Hz, H6), 7.18-7.81 (m, 14H, ArH). ¹³CNMR (75MHz, CDCl₃): δc 187.0, 161.5, 141.2, 138.3, 138.2, 136.0, 130.7, 129.6, 129.4, 129.3, 128.4, 128.3, 73.6, 73.0, 63.1, 62.8, 62.3, 14.2.

Anal.Calcd for C₂₆H₂₄ClNO₅S: C, 62.71; H, 4.86; N, 2.81. Found: C, 62.77 H, 4.91; N, 2.79 MS m/z: 497.11 (100%) [M+1] 497.11, [M+2] 499.10, [M+3] 498.11.

Ethyl 6-(4-chlorobenzoyl)-3,5 di (4-methylphenyl) -1,1- dioxo- 1,4 -thiazinane -2-carboxylate:

White solid; M.P153°C; Yield (87%). ¹H NMR (300 MHz, DMSO-d₆) δH1.10 (t, 3H, J=7.1Hz -CH₃ of COOCH₂CH₃), 2.06 (s, NH, br), 2.26 (s, 3H, -CH₃),), 2.34 (s, 3H, -CH₃), 4.07-4.16 (m, 2H, -CH₂ of COOCH₂CH₃), 4.37 (d, 1H, J=10.6 Hz, H2), 4.69 (d, 1H, J=10.6 Hz, H3), 4.91 (d, 1H, J=10.3 Hz, H5), 5.28 (d, 1H, J=10.3 Hz, H6), 7.02-7.89 (m, 12H, ArH). ¹³CNMR (75MHz, CDCl₃): δc 187.0, 161.3, 140.9, 138.4, 138.1, 135.6, 135.2, 134.9, 130.4, 129.3, 129.1, 128.9, 128.8, 127.6, 73.0, 71.9, 64.6, 63.7, 62.4, 21.6, 21.3, 13.9. Anal.Calcd for C₂₈H₂₈ClNO₅S: C, 63.93; H, 5.37; N, 2.66. Found: C, 64.01 H, 5.36; N, 2.68 MS m/z: 525.14 (100%) [M+1] 525.14, [M+2] 527.13, [M+3] 526.14.

Ethyl 6-(benzoyl)-3,5 di(4-nitrophenyl)-1,1-dioxo-1,4-thiazinane-2-carboxylate:

Yellow solid; M.P 155°C; Yield (83%). ¹H NMR (300 MHz, DMSO-d₆) δH0.98 (t, 3H, J=6.9Hz -CH₃ of COOCH₂CH₃), 2.37 (s, NH, br), 3.97-4.08 (m, 2H, -CH₂ of COOCH₂CH₃), 4.69 (d, 1H, J=10.2 Hz, H2), 4.87 (d, 1H, J=10.3 Hz, H3), 5.02 (d, 1H, J=10.0 Hz, H5), 5.79 (d, 1H, J=10.1 Hz, H6), 7.39-8.27 (m, 13H, ArH). ¹³CNMR (75MHz, DMSO-d₆) δc 185.9, 160.2, 146.7, 146.5, 144.0, 137.9, 133.2, 128.4, 128.2, 127.7, 127.6, 125.8, 125.9, 122.4, 69.1 68.6, 61.3, 60.3, 60.0, 12.9. Anal.Calcd for C₂₆H₂₃N₃O₉S: C, 56.41; H, 4.19; N, 7.59. Found: C, 56.37; H, 4.13; N, 7.57. MS m/z: 553.11[M+].

Ethyl 6-(benzoyl) -1,1-dioxo-3,5 diphenyl-1,4-thiazinane-2-carboxylate:

White solid; M.P 157°C; Yield (87%). ¹H NMR (300 MHz, CDCl₃): δH 1.04 (t, 3H, J=7.2 Hz -CH₃ of COOCH₂CH₃), 2.10 (s, NH, br), 3.96-4.06 (m, 2H, -CH₂ of COOCH₂CH₃), 4.32 (d, 1H, J=10.7 Hz, H2), 4.69 (d, 1H, J=10.7 Hz, H3), 4.91 (d, 1H, J=10.3 Hz, H5), 5.10 (d, 1H, J=10.2 Hz, H6), 7.16-7.93 (m, 15H, ArH). ¹³C NMR (75 MHz, CDCl₃): δc 186.7, 161.1, 138.2, 138.1, 137.4, 133.4, 129.7, 129.5, 129.3, 129.2, 128.5, 128.3, 73.7, 72.9, 63.0, 62.5, 62.1, 13.9. Anal. Calcd for C₂₆H₂₅NO₅S: C, 67.37; H, 5.44; N, 3.02. Found: C, 67.33; H, 5.40; N, 3.00. MS m/z: 463.15 [M⁺].

Ethyl 6-(benzoyl)-3,5 di(4-methylphenyl)-1,1-dioxo-1,4-thiazinane-2-carboxylate:

Pale white solid; M.P 157°C; Yield (85%). ¹H NMR (300 MHz, DMSO-d₆) δH 1.09 (t, 3H, J=7.1 Hz -CH₃ of COOCH₂CH₃), 2.11 (s, NH, br), 2.24 (s, 3H, -CH₃), 2.35 (s, 3H, -CH₃), 4.03-4.10 (m, 2H, -CH₂ of COOCH₂CH₃), 4.41 (d, 1H, J=10.7 Hz, H2), 4.74 (d, 1H, J=10.7 Hz, H3), 4.93 (d, 1H, J=10.2 Hz, H5), 5.32 (d, 1H, J=10.2 Hz, H6), 6.99-7.93 (m, 13H, ArH). ¹³C NMR (75 MHz, CDCl₃): δc 186.9, 161.4, 138.5, 138.2, 137.9, 135.5, 135.1, 133.4, 129.2, 129.0, 128.9, 128.5, 127.7, 72.9, 71.0, 64.8, 63.6, 62.5, 21.5, 21.3, 14.0. Anal. Calcd for C₂₈H₂₉NO₅S: C, 68.41; H, 5.95; N, 2.85. Found: C, 68.39; H, 5.91; N, 2.83. MS m/z: 491.18 [M⁺].

Ethyl 6-(4-toluoyl)-3,5 di(4-nitrophenyl)-1,1-dioxo-1,4-thiazinane-2-carboxylate:

Pale yellow solid; M.P 155°C; Yield (79%); ¹H NMR (300 MHz, CDCl₃) δH 1.0 (t, 3H, J=7.1 Hz -CH₃ of COOCH₂CH₃), 2.29 (s, 3H, -CH₃), 2.67 (s, NH, br), 4.02-4.12 (m, 2H, -CH₂ of COOCH₂CH₃), 4.78 (d, 1H, J=10.4 Hz, H2), 4.95 (d, 1H, J=10.3 Hz, H3), 5.09 (d, 1H, J=10.3 Hz, H5), 5.87 (d, 1H, J=10.2 Hz, H6), 6.87-8.24 (m, 12H, ArH). ¹³C NMR (75 MHz, CDCl₃) δc 186.3, 160.5, 146.7, 146.5, 144.4, 142.7, 133.7, 128.3, 128.1, 127.8, 127.7, 126.1, 126.6, 122.9, 69.0, 68.5, 61.4, 60.7, 60.1, 23.8, 13.1. Anal. Calcd for C₂₇H₂₅N₃O₉S: C, 57.14; H, 4.44; N, 7.40. Found: C, 57.12; H, 4.39; N, 7.37. MS m/z: 567.13 [M⁺].

Ethyl 6-(4-toluoyl) -1,1-dioxo-3,5 diphenyl-1,4-thiazinane-2-carboxylate:

White solid; M.P 157°C; Yield (83%). ¹H NMR (300 MHz, CDCl₃): δH 1.03 (t, 3H, J=7.1 Hz -CH₃ of COOCH₂CH₃), 2.16 (s, NH, br), 2.33 (s, 3H -CH₃), 3.99-4.10 (m, 2H, -CH₂ of COOCH₂CH₃), 4.31 (d, 1H, J=10.7 Hz, H2), 4.72 (d, 1H, J=10.8 Hz, H3), 4.94 (d, 1H, J=10.3 Hz, H5), 5.15 (d, 1H, J=10.3 Hz, H6), 6.93-7.56 (m, 14H, ArH). ¹³CNMR (75 MHz, CDCl₃): δc 186.9, 161.4, 143.2, 138.3, 138.2, 134.3, 129.9, 129.6, 129.4, 129.3, 128.5, 128.4, 73.6, 73.1, 63.0, 62.7, 62.1, 22.9, 14.0. Anal. Calcd for C₂₇H₂₇NO₅S: C, 67.90; H, 5.70; N, 2.93. Found: C, 67.93; H, 5.72; N, 2.91. MS m/z: 477.16 [M+].

Ethyl 6-(4-toluoyl)-3,5 di(4-methylphenyl)-1,1-dioxo-1,4-thiazinane-2-carboxylate:

White solid; M.P 157°C; Yield (87%). ¹H NMR (300 MHz, DMSO-d₆) δH 1.10 (t, 3H, J=7.1 Hz -CH₃ of COOCH₂CH₃), 2.09 (s, NH, br), 2.27 (s, 3H, -CH₃), 2.33 (s, 3H, -CH₃), 2.37 (s, 3H, -CH₃), 4.10-4.18 (m, 2H, -CH₂ of COOCH₂CH₃), 4.39 (d, 1H, J=10.6 Hz, H2), 4.73 (d, 1H, J=10.6 Hz, H3), 4.97 (d, 1H, J=10.3 Hz, H5), 5.39 (d, 1H, J=10.3 Hz, H6), 6.83-7.47 (m, 12H, ArH). ¹³CNMR (75 MHz, CDCl₃): δc 187.0, 161.1, 143.2, 138.3, 138.0, 135.4, 135.2, 134.0, 129.5, 129.3, 128.9, 128.7, 127.8, 73.0, 72.0, 64.5, 63.2, 62.5, 21.7, 21.4, 21.2, 13.7. Anal. Calcd for C₂₉H₃₁NO₅S: C, 68.89; H, 6.18; N, 2.77. Found: C, 68.92; H, 6.178; N, 2.80. MS m/z: 505.19 [M+].

5.1.5. Final Library:

The final library (Table 5.1) was achieved by either using Method A or Method B. All the reactions were regularly monitored by LCMS and immediately purified in order to avoid decomposition of the product/ reduce the side products.

Method A: To solution of the corresponding thiazine (1 mmol) in dry dichloromethane at 0°C was added drop wise DIPEA (2 mmol) and stirred for 5-7 mins. Acid chloride (1.2 mmol) was then added to the reaction mixture at 0°C. The reaction mixture was slowly warmed to room temperature (rt) and stirred at rt (monitored by LCMS). Water was added to the reaction mixture and the layers separated, the organic layer was washed with

brine, dried over anhydrous Na_2SO_4 and evaporated in vacuo. The crude was immediately purified by preparative HPLC to get the desired product.

Method B: To a suspension of sodium hydride (1mmol) in dry THF was added drop wise a solution of the corresponding thiazine in THF at 0°C . The reaction mixture was slowly warmed to rt and stirred at rt for 30 min. Acid chloride (1.2mmol) was then added to the reaction mixture at 0°C and the reaction mixture was stirred at rt (monitored by LCMS). The reaction mixture was quenched with saturated ammonium chloride, extracted with dichloromethane, washed with brine, dried over anhydrous Na_2SO_4 and evaporated in vacuo. The crude was immediately purified by preparative HPLC to get the desired product.

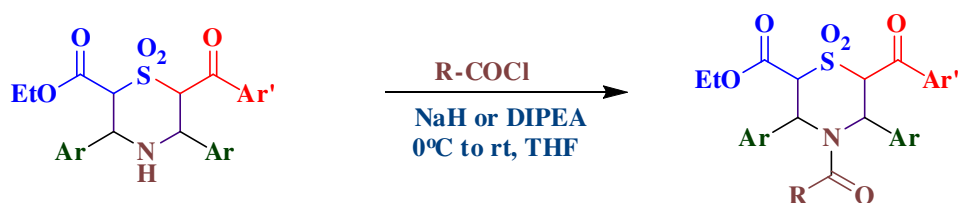
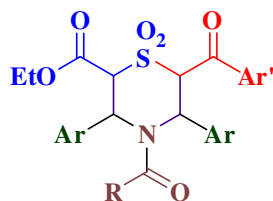


Table 5.1. Structure and Physical constants, of [1, 4]-thiazines



Comp.No	Ar'	Ar	R	Formula	% yield	LogP ^a	Mol. Wt	Melting range (°C)
1	<i>p</i> -tolyl	phenyl	cyclohexyl	C ₃₄ H ₃₀ ClNO ₆ S	57	5.61	587.23	136-138
2	<i>p</i> -tolyl	phenyl	phenyl	C ₃₄ H ₃₁ NO ₆ S	53	5.53	581.19	122-124
3	phenyl	phenyl	<i>p</i> -tolyl	C ₃₄ H ₃₁ NO ₆ S	56	5.53	581.19	177-179
4	phenyl	<i>p</i> -nitrophenyl	cyclohexyl	C ₃₃ H ₃₃ N ₃ O ₁₀ S	48	ND	663.19	134-136
5	<i>p</i> -chlorophenyl	phenyl	phenyl	C ₃₃ H ₂₈ ClNO ₆ S	57	5.60	601.09	116-118
6	phenyl	phenyl	phenyl	C ₃₃ H ₂₉ NO ₆ S	67	5.04	567.17	162-164
7	<i>p</i> -chlorophenyl	<i>p</i> -nitrophenyl	<i>p</i> -tolyl	C ₃₄ H ₂₈ ClN ₃ O ₁₀ S	59	ND	705.12	200-202
8	<i>p</i> -chlorophenyl	<i>p</i> -nitrophenyl	phenyl	C ₃₃ H ₂₆ ClN ₃ O ₁₀ S	67	ND	691.10	226-228
9	<i>p</i> -chlorophenyl	<i>p</i> -nitrophenyl	methyl	C ₂₈ H ₂₄ ClN ₃ O ₁₀ S	41	ND	629.09	187-159
10	<i>p</i> -tolyl	<i>p</i> -nitrophenyl	cyclohexyl	C ₃₄ H ₃₅ N ₃ O ₁₀ S	50	ND	677.18	127-129
11	phenyl	phenyl	cyclohexyl	C ₃₃ H ₃₅ NO ₆ S	55	5.12	573.22	151-153

Comp.No	Ar'	Ar	R	Formula	% yield	LogP ^a	Mol. Wt	Melting range (°C)
12	phenyl	phenyl	methyl	C ₂₈ H ₂₇ NO ₆ S	40	3.15	505.58	130-132
13	phenyl	phenyl	<i>p</i> -nitrophenyl	C ₃₃ H ₂₈ N ₂ O ₈ S	51	ND	612.16	118-120
14	phenyl	phenyl	<i>p</i> -chlorophenyl	C ₃₃ H ₂₈ ClNO ₆ S	60	5.60	601.13	146-148
15	phenyl	<i>p</i> -tolyl	<i>p</i> -tolyl	C ₃₆ H ₃₅ NO ₆ S	49	6.50	609.22	174-176
16	phenyl	<i>p</i> -tolyl	phenyl	C ₃₅ H ₃₃ NO ₆ S	53	6.02	595.20	159-161
17	phenyl	<i>p</i> -tolyl	cyclohexyl	C ₃₅ H ₃₉ NO ₆ S	41	6.09	601.25	148-150
18	phenyl	<i>p</i> -tolyl	methyl	C ₃₀ H ₃₁ NO ₆ S	47	4.12	533.19	148-150
19	phenyl	<i>p</i> -tolyl	<i>p</i> -chlorophenyl	C ₃₅ H ₃₂ ClNO ₆ S	56	ND	629.16	203-205
20	phenyl	<i>p</i> -nitrophenyl	<i>p</i> -tolyl	C ₃₄ H ₂₉ N ₃ O ₁₀ S	66	ND	671.10	110-112
21	phenyl	<i>p</i> -nitrophenyl	phenyl	C ₃₃ H ₂₇ N ₃ O ₁₀ S	73	ND	657.14	156-158
22	phenyl	<i>p</i> -nitrophenyl	<i>p</i> -nitrophenyl	C ₃₃ H ₂₆ N ₄ O ₁₂ S	66	ND	702.10	184-186
23	phenyl	<i>p</i> -nitrophenyl	<i>p</i> -chlorophenyl	C ₃₃ H ₂₆ ClN ₃ O ₁₀ S	62	ND	691.10	214-216
24	phenyl	<i>p</i> -tolyl	<i>p</i> -nitrophenyl	C ₃₅ H ₃₂ N ₂ O ₈ S	54	ND	640.19	153-155
25	<i>p</i> -chlorophenyl	phenyl	<i>p</i> -tolyl	C ₃₄ H ₃₀ ClNO ₆ S	55	6.09	615.13	120-122
26	<i>p</i> -chlorophenyl	phenyl	methyl	C ₂₈ H ₂₆ ClNO ₆ S	43	3.70	539.21	126-128
27	<i>p</i> -chlorophenyl	phenyl	cyclohexyl	C ₃₃ H ₃₄ ClNO ₆ S	51	5.68	607.18	124-126
28	<i>p</i> -chlorophenyl	<i>p</i> -nitrophenyl	cyclohexyl	C ₃₃ H ₃₂ ClN ₃ O ₁₀ S	53	ND	697.15	191-193

Comp.No	Ar'	Ar	R	Formula	% yield	LogP ^a	Mol. Wt	Melting range (°C)
29	<i>p</i> -chlorophenyl	<i>p</i> -nitrophenyl	<i>p</i> -chlorophenyl	C ₃₃ H ₂₅ Cl ₂ N ₃ O ₁₀ S	63	ND	725.06	168-170
30	<i>p</i> -chlorophenyl	<i>p</i> -tolyl	cyclohexyl	C ₃₅ H ₃₈ ClNO ₆ S	51	6.65	635.21	164-166
31	<i>p</i> -chlorophenyl	phenyl	<i>p</i> -nitrophenyl	C ₃₃ H ₂₇ ClN ₂ O ₈ S	57	ND	646.17	131-133
32	<i>p</i> -tolyl	phenyl	<i>p</i> -nitrophenyl	C ₃₄ H ₃₀ N ₂ O ₈ S	57	ND	626.17	151-153
33	<i>p</i> -tolyl	<i>p</i> -tolyl	cyclohexyl	C ₃₆ H ₄₁ NO ₆ S	46	6.58	615.27	211-213
34	<i>p</i> -tolyl	phenyl	<i>p</i> -chlorophenyl	C ₃₄ H ₃₀ ClNO ₆ S	62	6.09	615.15	164-166
35	<i>p</i> -tolyl	phenyl	<i>p</i> -tolyl	C ₃₅ H ₃₃ NO ₆ S	57	6.02	595.20	97-99
36	<i>p</i> -tolyl	<i>p</i> -tolyl	phenyl	C ₃₆ H ₃₅ NO ₆ S	55	6.50	609.22	124-126
37	<i>p</i> -tolyl	<i>p</i> -tolyl	<i>p</i> -chlorophenyl	C ₃₆ H ₃₄ ClNO ₆ S	50	7.06	643.18	174-176
38	<i>p</i> -tolyl	<i>p</i> -tolyl	methyl	C ₃₁ H ₃₃ NO ₆ S	44	4.61	547.20	211-215
39	<i>p</i> -tolyl	phenyl	methyl	C ₂₉ H ₂₉ NO ₆ S	42	3.63	519.17	142-144
40	<i>p</i> -tolyl	<i>p</i> -nitrophenyl	<i>p</i> -chlorophenyl	C ₃₄ H ₂₈ ClN ₃ O ₁₀ S	59	ND	705.12	191-194
41	<i>p</i> -tolyl	<i>p</i> -tolyl	<i>p</i> -tolyl	C ₃₅ H ₃₇ NO ₆ S	63	6.99	623.23	168-171
42	<i>p</i> -tolyl	<i>p</i> -nitrophenyl	<i>p</i> -nitrophenyl	C ₃₄ H ₂₈ N ₄ O ₁₂ S	61	ND	716.14	165-168
43	<i>p</i> -chlorophenyl	<i>p</i> -tolyl	methyl	C ₃₀ H ₃₀ ClNO ₆ S	40	4.68	567.15	131-133
44	<i>p</i> -chlorophenyl	<i>p</i> -tolyl	<i>p</i> -tolyl	C ₃₆ H ₃₄ ClNO ₆ S	63	7.06	643.18	171-174
45	<i>p</i> -chlorophenyl	4-tolyl	phenyl	C ₃₅ H ₃₂ ClNO ₆ S	51	6.58	629.16	187-190

Comp.No	Ar'	Ar	R	Formula	% yield	LogP	Mol. Wt	Melting range (°C)
46	phenyl	<i>p</i> -nitrophenyl	methyl	C ₂₈ H ₂₅ N ₃ O ₁₀ S	40	ND	595.10	151-153
47	<i>p</i> -chlorophenyl	<i>p</i> -tolyl	<i>p</i> -nitrophenyl	C ₃₅ H ₃₁ ClN ₂ O ₈ S	57	ND	674.15	191-194
48	<i>p</i> -tolyl	<i>p</i> -nitrophenyl	phenyl	C ₃₄ H ₂₉ N ₃ O ₁₀ S	67	ND	671.16	188-191
49	<i>p</i> -tolyl	<i>p</i> -tolyl	<i>p</i> -nitrophenyl	C ₃₆ H ₃₄ N ₂ O ₈ S	54	ND	654.20	146-149
50	<i>p</i> -tolyl	<i>p</i> -nitrophenyl	methyl	C ₂₉ H ₂₇ N ₃ O ₁₀ S	43	ND	609.23	150-153
51	<i>p</i> -tolyl	<i>p</i> -nitrophenyl	<i>p</i> -tolyl	C ₃₅ H ₃₁ N ₃ O ₁₀ S	67	ND	685.17	171-173
52	<i>p</i> -chlorophenyl	phenyl	<i>p</i> -chlorophenyl	C ₃₃ H ₂₇ Cl ₂ NO ₆ S	57	6.16	635.11	169-171

^aCLog P was obtained from ChemBioDraw Ultra 11.0; ND: not determined

5.1.6. Characterization of the Compounds

Ethyl 4-(cyclohexoyl)-6-(4-toluoyl) - 3, 5-phenyl-1, 1-dioxo-1, 4,-thiazinane-2-carboxylate (1)

White solid; M.P: 137°C; Yield (57%). ¹H NMR (300 MHz, CDCl₃): δH 1.06 (t, 3H, J=7.1Hz -CH₃ of COOCH₂CH₃), 1.27-1.69 (m,10H, -CH₂ of cyclohexoyl), 2.21-2.23 (m,1H,-CH of cyclohexoyl), 2.35 (s, 3H, -CH₃ of toluoyl), 4.01-4.04 (m,2H,-CH₂ of COOCH₂CH₃), 4.77 (d, 1H, J=10.6 Hz, H₂), 5.09 (d, 1H, J=10.6 Hz, H₃), 5.21 (d, 1H, J=10.2 Hz, H₅), 5.34 (d, 1H, J=10.2 Hz,H₆), 6.89-7.83 (m, 14H, ArH). ¹³CNMR (75MHz, CDCl₃): δc 186.9, 170.2, 161.4, 143.4, 138.3, 138.1, 134.3, 129.8, 129.6, 129.4, 129.2, 128.5, 128.1, 65.7, 63.7, 63.0, 55.4, 54.6, 33.0, 28.4, 26.1, 23.2, 14.0. Anal.Calcd for C₃₄H₃₀ClNO₆S: C, 69.48; H, 6.35; N, 2.38. Found: C, 69.50; H, 6.34; N, 2.40. MS m/z: 587.23 [M+].

Ethyl 4-(4-toluoyl)-6-(benzoyl) - 3, 5-diphenyl-1, 1-dioxo-1, 4,-thiazinane-2-carboxylate (3)

White solid; M.P: 178°C; Yield (56%). ¹H NMR (300 MHz, CDCl₃): δH 1.06 (t, 3H, J=7.2Hz -CH₃ of COOCH₂CH₃), 2.31 (s, 3H, -CH₃ of toluoyl), 4.05-4.13 (m,2H,-CH₂ of COOCH₂CH₃), 4.73 (d, 1H, J=10.7 Hz, H₂), 5.03 (d, 1H, J=10.6 Hz, H₃), 5.17 (d, 1H, J=10.3 Hz, H₅), 5.33 (d, 1H, J=10.3 Hz, H₆), 7.26 – 7.73 (m, 20H, ArH). ¹³CNMR (75MHz, CDCl₃): δc 187.0, 167.3, 161.5, 141.9, 138.5, 138.4, 137.9, 133.7, 132.3, 130.4, 129.6, 129.5, 129.3, 129.2, 129.1, 128.6, 128.3, 128.1, 66.3, 63.9, 63.2, 57.4, 54.5, 23.1, 14.1. Anal.Calcd for C₃₄H₃₁NO₆S: C, 70.20; H, 5.37; N, 2.41. Found: C, 70.17; H, 5.33; N, 2.39. MS m/z: 581.19 [M+].

Ethyl 4-(cyclohexoyl)-6-(benzoyl) - 3, 5-di (4-nitrophenyl)-1, 1-dioxo-1, 4,-thiazinane-2-carboxylate (4)

Pale yellow solid; M.P: 135°C; Yield (48%) ¹H NMR (300 MHz, CDCl₃): δH 1.04 (t, 3H, J=7.2Hz -CH₃ of COOCH₂CH₃), 1.33-1.69 (m,10H, -CH₂ of cyclohexoyl), 2.29-2.34 (m, 1H,-CH of cyclohexoyl) 4.04-4.13 (m,2H,-CH₂ of COOCH₂CH₃), 5.07-5.21 (m, 3H, H₂, H₃, H₅) 5.79 (d, 1H, J=10.3 Hz, H₆), 7.31-8.16 (m, 12H, ArH). ¹³CNMR (75MHz,

CDCl₃): δ_c 186.1, 170.7, 160.1, 146.8, 146.7, 144.2, 138.3, 133.4, 128.4, 128.1, 126.4, 123.0, 66.1, 64.3, 60.1, 56.0, 55.1, 54.6, 33.9, 30.1, 26.2, 12.9. Anal.Calcd for C₃₃H₃₃N₃O₁₀S: C, 59.72; H, 5.01; N, 6.33. Found: C, 59.77; H, 4.99; N, 6.31. MS m/z: 663.19 [M+].

Ethyl 4-(benzoyl)-6-(4-chlorobenzoyl) - 3, 5-diphenyl-1, 1-dioxo-1, 4,-thiazinane-2-carboxylate (5)

Pale whites solid; M.P: 117°C; Yield (57%). ¹H NMR (300 MHz, CDCl₃): δ_H 1.06 (t, 3H, J=7.1Hz -CH₃ of COOCH₂CH₃), 4.01-4.09 (m,2H,-CH₂ of COOCH₂CH₃), 4.67 (d, 1H, J=10.6 Hz, H2), 4.89 (d, 1H, J=10.6 Hz, H3), 5.03 (d, 1H, J=10.3 Hz, H5), 5.27 (d, 1H, J=10.4 Hz, H6), 7.27 – 7.87 (m, 19H, ArH). ¹³CNMR (75MHz, CDCl₃): δ_c 187.0, 167.2, 161.5, 141.2, 138.4, 138.3, 137.2, 135.7, 130.6, 130.3, 129.6, 129.4, 129.3, 129.2, 128.6, 128.4, 128.3, 66.4, 64.2, 63.0, 57.3, 54.6, 14.0. Anal.Calcd for C₃₃H₂₈ClNO₆S: C, 65.83; H, 4.69; N, 2.33. Found: C, 65.81 H, 4.71; N, 2.29 MS m/z: 601.09 (100%) [M+1] 601.13, [M+2] 603.13, [M+3] 602.14.

Ethyl 4-(cyclohexoyl)-6-(4-toluoyl) - 3, 5-di (4-nitrophenyl)-1, 1-dioxo-1, 4,-thiazinane-2-carboxylate (10)

Orange solid; M.P: 128°C; Yield (50%).¹H NMR (300 MHz, CDCl₃): δ_H 1.07 (t, 3H, J=7.2Hz -CH₃ of COOCH₂CH₃), 1.34-1.72 (m,10H, -CH₂ of cyclohexoyl), 2.31-2.37 (m, 4H,-CH of cyclohexoyl& -CH₃ of toluoyl) 4.05-4.15 (m,2H,-CH₂ of COOCH₂CH₃), 5.10 (d, 1H, J=10.5 Hz, H2), 5.18 (d, 1H, J=10.5 Hz, H3), 5.23 (d, 1H, J=10.2 Hz, H5), 5.86 (d, 1H, J=10.2 Hz, H6), 6.89-8.15,(m, 12H, ArH). ¹³CNMR (75MHz, CDCl₃): δ_c 186.3, 170.8, 160.3, 147.0, 146.9, 144.1, 142.8, 134.1, 128.5, 128.2, 126.7, 123.2, 66.3, 64.5, 60.1, 56.0, 55.2, 54.9, 34.0, 30.2, 26.3, 23.6, 13.1. Anal.Calcd for C₃₄H₃₅N₃O₁₀S: C, 60.26; H, 5.21; N, 6.20. Found: C, 60.23; H, 5.19; N, 6.19. MS m/z: 677.18 [M+].

Ethyl 4-(acetyl)-6-(benzoyl) - 3, 5-diphenyl-1, 1-dioxo-1, 4,-thiazinane-2-carboxylate (12)

Pale brown solid; M.P: 131°C; Yield (29%).¹H NMR (300 MHz, CDCl₃): δ_H 1.07 (t, 3H, J=7.1Hz -CH₃ of COOCH₂CH₃), 2.34 (s, 3H, -CH₃ of acetyl), 4.03-4.09 (m, 2H,-CH₂

of COOCH₂CH₃), 4.75 (d, 1H, J=10.6 Hz, H2), 5.21 (d, 1H, J=10.6 Hz, H3), 5.34 (d, 1H, J=10.4 Hz, H5), 5.43 (d, 1H, J=10.3 Hz, H6), 7.30 – 7.79 (m, 15H, ArH). ¹³CNMR (75MHz, CDCl₃): δc 187.0, 167.1, 161.3, 138.4, 138.3, 137.7, 133.6, 129.6, 129.3, 129.1, 129.0, 128.5, 128.1, 66.0, 63.7, 63.0, 54.8, 52.3, 24.4, 14.1. Anal.Calcd for C₂₈H₂₇NO₆S: C, 66.52; H, 5.38; N, 2.77. Found: C, 66.57; H, 5.33; N, 2.78. MS *m/z*: 505.58[M⁺].

Ethyl 4-(4-nitrobenzoyl)-6-(benzoyl) - 3, 5-diphenyl-1, 1-dioxo-1, 4,-thiazinane-2-carboxylate (13)

Yellow solid; M.P: 119°C; Yield (51%). ¹H NMR (300 MHz, CDCl₃): δH 1.06 (t, 3H, J=7.1Hz -CH₃ of COOCH₂CH₃), 4.06-4.14 (m,2H,-CH₂ of COOCH₂CH₃), 4.79 (d, 1H, J=10.7 Hz, H2), 5.24-5.37 (m, 2H, H3 & H5), 5.69 (d, 1H, J=10.3 Hz, H6), 7.29 – 8.21 (m, 19H, ArH). ¹³CNMR (75MHz, CDCl₃): δc 186.9, 167.3, 161.3, 151.4, 142.9, 138.5, 138.4, 137.8, 133.6, 130.2, 129.7, 129.5, 129.3, 129.2, 128.5, 128.2, 123.9, 66.3, 64.0, 63.0, 57.5, 54.5 14.1. Anal.Calcd for C₃₃H₂₈N₂O₈S: C, 64.69; H, 4.61; N, 4.57. Found: C, 64.71; H, 4.59; N, 4.54. MS *m/z*: 612.16 [M⁺].

Ethyl 4-(4-toluoyl)-6-(benzoyl) - 3, 5- di (4-methylphenyl)-1, 1-dioxo-1, 4,-thiazinane-2-carboxylate (15)

White solid; M.P: 175°C; Yield (49%). ¹H NMR (300 MHz, DMSO-d₆) δH 1.07 (t, 3H, J=7.0 Hz -CH₃ of COOCH₂CH₃), 2.26 (s, 3H, -CH₃),), 2.33 (s, 3H, -CH₃), 2.36 (s, 3H, -CH₃), 4.04-4.13 (m,2H,-CH₂ of COOCH₂CH₃), 4.66 (d, 1H, J=10.9 Hz, H2), 4.89 (d, 1H, J=10.9 Hz, H3), 5.13 (d, 1H, J=10.3 Hz, H5), 5.47 (d, 1H, J=10.4 Hz, H6), 7.32 – 7.91 (m, 17H, ArH). ¹³CNMR (75MHz, CDCl₃): δc 187.2, 167.4, 161.3, 142.3, 137.8, 137.6, 135.8, 135.6, 135.3, 133.5, 132.3, 129.3, 129.0, 128.6, 127.78, 127.7, 70.5, 69.4, 63.4, 62.5, 62.2, 21.7, 21.4, 21.3, 14.0. Anal.Calcd for: C₃₆H₃₅NO₆S: C, 70.91; H, 5.79; N, 2.30. Found: C, 70.93; H, 5.78; N, 2.32. MS *m/z*: 609.22 [M⁺].01.13 [M⁺]. Found: C, 66.57; H, 5.33; N, 2.78. MS *m/z*: 505.58 [M⁺].

Ethyl 4, 6-(benzoyl) - 3, 5-di (4-methylphenyl)-1, 1-dioxo-1, 4,-thiazinane-2-carboxylate (16)

Colourless solid; M.P 160°C; Yield (53%). ¹H NMR (300 MHz, DMSO-d₆) δH 1H NMR (300 MHz, DMSO-d₆) δH 1.06 (t, 3H, J=6.9 Hz -CH₃ of COOCH₂CH₃), 2.24 (s, 3H, -CH₃), 2.32 (s, 3H, -CH₃), 4.01-4.09 (m, 2H, -CH₂ of COOCH₂CH₃), 4.63 (d, 1H, J=10.9 Hz, H₂), 4.86 (d, 1H, J=10.9 Hz, H₃), 5.09 (d, 1H, J=10.4 Hz, H₅), 5.37 (d, 1H, J=10.4 Hz, H₆), 7.30 – 7.96 (m, 18H, ArH). ¹³CNMR (75MHz, CDCl₃): δc 187.2, 167.1, 161.4, 137.8, 137.6, 137.5, 135.6, 135.4, 135.2, 133.4, 130.4, 129.2, 129.0, 128.9, 128.6, 128.5, 128.4, 128.1, 127.4, 70.1, 67.9, 63.6, 62.5, 62.1, 21.7, 21.4, 13.9. Anal. Calcd for: C₃₅H₃₃NO₆S: C, 70.57; H, 5.58; N, 2.35. Found: C, 70.61; H, 5.59; N, 2.37. MS m/z: 595.20 [M+].

Ethyl 4-(4-chlorobenzoyl)-6-(benzoyl) - 3, 5-di (4-methylphenyl)-1, 1-dioxo-1, 4,-thiazinane-2-carboxylate (19)

White solid; M.P: 204°C; Yield (56%). ¹H NMR (300 MHz, CDCl₃): δH 1.10 (t, 3H, J=7.2Hz -CH₃ of COOCH₂CH₃), 2.24 (s, 3H, -CH₃), 2.34 (s, 3H, -CH₃), 3.99 - 4.08 (m, 2H, -CH₂ of COOCH₂CH₃), 4.73 (d, 1H, J=10.8 Hz, H₂), 5.09-5.17 (m, 2H, H₃ & H₅), 5.73 (d, 1H, J=10.3 Hz, H₆), 7.29 – 8.07 (m, 17H, ArH). ¹³CNMR (75MHz, CDCl₃): δc 187.0, 167.2, 161.3, 137.7, 137.5, 137.3, 135.8, 135.7, 135.6, 133.8, 133.5, 130.4, 129.3, 129.1, 128.7, 128.5, 127.3, 70.0, 68.3, 63.4, 62.7, 62.2, 21.5, 21.2, 13.5. Anal. Calcd for: C₃₅H₃₂ClNO₆S: C, 66.71; H, 5.12; N, 2.22. Found: C, 66.69; H, 5.10; N, 2.21. MS m/z: 629.16 (100%) [M+1] 629.16, [M+2] 630.17, [M+3] 631.16.

Ethyl 4-(4-toluoyl)-6-(benzoyl) - 3, 5-di (4-nitrophenyl)-1, 1-dioxo-1, 4,-thiazinane-2-carboxylate (20)

Pale yellow solid; M.P: 111°C; Yield (66%). ¹H NMR (300 MHz, CDCl₃) δH 1.04 (t, 3H, J=7.2Hz -CH₃ of COOCH₂CH₃), 2.26 (s, 3H, -CH₃ of toluoyl), 4.01-4.09 (m, 2H, -CH₂ of COOCH₂CH₃), 5.10 (d, 1H, J=10.4 Hz, H₂), 5.18 (d, 1H, J=10.7 Hz, H₃), 5.26 (d, 1H, J=10.2 Hz, H₅), 6.01 (d, 1H, J=10.4 Hz, H₆), 7.36-8.19 (m, 17H, ArH). ¹³CNMR (75MHz, CDCl₃) δc 186.3, 165.3, 160.2, 147.1, 146.9, 144.2, 141.7, 138.2, 133.5, 131.9, 128.4, 128.3, 128.2, 127.3, 126.2, 123.0, 65.5, 63.2, 60.1, 55.1, 53.4, 24.0, 13.0.

Anal.Calcd for C₃₄H₂₉N₃O₁₀S: C, 60.80; H, 4.35; N, 6.26. Found: C, 60.83; H, 4.37; N, 6.23. MS m/z: 671.10 [M+].

Ethyl 4, 6-di (benzoyl)-3, 5-di (4-nitrophenyl)-1, 1-dioxo-1, 4,-thiazinane-2-carboxylate (21)

Pale yellow solid; M.P: 157°C; Yield (73%). ¹H NMR (300 MHz, CDCl₃) δH 0.99 (t, 3H, J=7.0Hz -CH₃ of COOCH₂CH₃), 3.99-4.06 (m,2H,-CH₂ of COOCH₂CH₃), 5.21 (d, 1H, J=10.6 Hz, H2), 5.27 (d, 1H, J=10.3 Hz, H3), 5.34 (d, 1H, J=10.2 Hz, H5), 6.07 (d, 1H, J=9.8 Hz,H6), 7.29-8.12,(m, 18H, ArH). ¹³CNMR (75MHz, CDCl₃) δc 186.1, 164.9, 160.1, 146.8, 146.7, 144.2, 138.1, 137.0, 133.4, 129.0, 128.4, 128.2, 128.0, 127.3, 126.2, 123.0, 65.5, 63.2, 60.1, 55.1, 53.4, 13.0. Anal.Calcd for C₃₃H₂₇N₃O₁₀S: C, 60.27; H, 4.14; N, 6.39. Found: C, 60.31; H, 4.09; N, 6.37 MS m/z: 657.14 [M+].

Ethyl 4-(4-nitrobenzoyl)-6-(benzoyl) - 3, 5-di (4-methylphenyl)-1, 1-dioxo-1, 4,-thiazinane-2-carboxylate (24)

White solid; M.P: 154°C; Yield (54%). ¹H NMR (300 MHz, CDCl₃) : δH 1.10 (t, 3H, J=7.1Hz -CH₃ of COOCH₂CH₃), 2.25 (s, 3H, -CH₃), 2.35 (s, 3H, -CH₃), 4.06-4.14 (m, 2H,-CH₂ of COOCH₂CH₃), 4.72 (d, 1H, J=10.6 Hz, H2), 5.09-5.17 (m, 2H, H3 & H5), 5.68 (d, 1H, J=10.3 Hz, H6), 7.29 – 8.21 (m, 17H, ArH). ¹³CNMR (75MHz, CDCl₃): δc 187.1, 167.2, 161.3, 151.4, 142.8, 137.8, 137.6, 137.5, 135.7, 135.5, 133.5, 129.9, 129.3, 129.0, 128.7, 127.6, 124.4, 70.2, 69.5, 63.7, 62.6, 62.3, 21.7, 21.5, 13.9. Anal.Calcd for: C₃₅H₃₂N₂O₈S: C, 65.61; H, 5.03; N, 4.37. Found: C, 65.65; H, 5.05; N, 4.39 MS m/z: 640.19 [M+].

Ethyl 4-(4-toluoyl)-6-(4-chlorobenzoyl) - 3, 5-diphenyl-1, 1-dioxo-1, 4,-thiazinane-2-carboxylate (25)

White solid; M.P: 121°C; Yield (55%). ¹H NMR (300 MHz, CDCl₃) : δH 1.06 (t, 3H, J=7.1Hz -CH₃ of COOCH₂CH₃), 2.25 (s, 3H, -CH₃ of toluoyl), 4.03-4.11 (m, 2H, -CH₂ of COOCH₂CH₃), 4.71 (d, 1H, J=10.7 Hz, H2), 5.08 (d, 1H, J=10.8 Hz, H3), 5.18 (d, 1H, J=10.4 Hz, H5), 5.31 (d, 1H, J=10.3Hz, H6), 7.23 – 7.69 (m, 19H, ArH). ¹³CNMR (75MHz, CDCl₃): δc 187.1, 167.4, 161.6, 142.1, 141.3, 138.4, 138.3, 135.9, 132.4, 130.6,

129.6, 129.4, 129.2, 129.0, 128.5, 128.3, 128.0, 66.5, 64.0, 63.1, 57.2, 54.3, 22.9, 13.9. Anal.Calcd for C₃₄H₃₀ClNO₆S: C, 66.28; H, 4.91; N, 2.27. Found: C, 66.31 H, 4.89; N, 2.23 MS m/z: 615.15 (100%) [M+1] 615.15, [M+2] 617.15, [M+3] 616.15.

Ethyl 4-(cyclohexoyl)-6-(4-chlorobenzoyl) - 3, 5-di (4-nitrophenyl)-1, 1-dioxo-1, 4,-thiazinane-2-carboxylate (28)

Pale yellow solid; M.P: 192°C; Yield (53%). ¹H NMR (300 MHz, CDCl₃): δH 1.05 (t, 3H, J=7.2Hz -CH₃ of COOCH₂CH₃), 1.36-1.76 (m,10H, -CH₂ of cyclohexoyl), 2.31-2.36 (m, 1H,-CH of cyclohexoyl) 4.07-4.16 (m,2H,-CH₂ of COOCH₂CH₃), 5.09 (d, 1H, J=10.5 Hz, H₂), 5.16 (d, 1H, J=10.5 Hz, H₃), 5.24 (d, 1H, J=10.3 Hz, H₅), 5.92 (d, 1H, J=10.3 Hz, H₆), 7.33-8.18,(m, 12H, ArH). ¹³CNMR (75MHz, CDCl₃): δc 186.4, 170.9, 160.3, 146.9, 146.8, 144.1, 139.9, 134.5, 129.8, 129.6, 128.2, 126.7, 123.1, 66.3, 64.7, 60.2, 56.1, 55.3, 54.9, 34.2, 30.3, 26.4, 13.0. Anal.Calcd for C₃₃H₃₂ClN₃O₁₀S: C, 56.77; H, 4.62; N, 6.02. Found: C, 56.69 H, 4.61; N, 6.07 MS m/z: 697.15 (100%) [M+1] 697.15, [M+2] 699.15, [M+3] 698.15.

Ethyl 4-(4-chlorobenzoyl)-6-(4-chlorobenzoyl) - 3, 5-di (4-nitrophenyl)-1, 1-dioxo-1, 4,-thiazinane-2-carboxylate (29)

Pale yellow solid; M.P: 169°C; Yield (63%). ¹H NMR (300 MHz, CDCl₃): δ_H1.07 (t, 3H, J=7.2Hz -CH₃ of COOCH₂CH₃), 4.05-4.16 (m,2H,-CH₂ of COOCH₂CH₃), 5.13 (d, 1H, J=10.5 Hz, H₂), 5.23-5.35 (m, 2H, H₃ and H₅), 6.06 (d, 1H, J=10.3 Hz, H₆), 7.35-8.19 (m, 16H, ArH). ¹³CNMR (75MHz, CDCl₃): 186.3, 165.1, 160.4, 147.2, 147.0, 144.4, 140.3, 137.5, 134.6, 133.8, 129.8, 129.7, 129.5, 128.3, 128.1, 128.0, 126.6, 123.4, 68.1, 67.3, 61.5, 61.0, 60.3, 13.3. Anal.Calcd for C₃₃H₂₅Cl₂N₃O₁₀S: C, 54.55; H, 3.47; N, 5.78 Found: C, 54.59 H, 3.51; N, 5.71 MS m/z: 725.06 (100%) [M+1] 725.06, [M+2] 727.06, [M+3] 726.07.

Ethyl 4-(cyclohexoyl)-6-(4-toluoyl) - 3, 5-di (4-methylphenyl)-1, 1-dioxo-1, 4,-thiazinane-2-carboxylate (33)

Brown solid; M.P: 212°C; Yield (46%). ¹H NMR (300 MHz, CDCl₃): δH 1.11 (t, 3H, J=7.2Hz -CH₃ of COOCH₂CH₃), 1.27-1.63 (m, 10H, -CH₂ of cyclohexoyl), 2.24-2.36 (m,

10H, (1H -CH of cyclohexoyl& 6H -CH₃ of tolyl& 3H -CH₃ of toluoyl)) 3.99-4.10 (m, 2H, -CH₂ of COOCH₂CH₃), 4.74 (d, 1H, J=10.8 Hz, H2), 5.17 (d, 1H, J=10.8 Hz, H3), 5.29 (d, 1H, J=10.3 Hz, H5), 5.61 (d, 1H, J=10.3 Hz, H6), 6.83-7.54 (m, 12H, ArH). ¹³CNMR (75MHz, CDCl₃): δ_c 187.0, 170.2, 161.2, 143.3, 141.0, 137.7, 137.5, 135.8, 135.6, 134.0, 129.5, 129.2, 128.8, 127.7, 69.8, 68.5, 62.5, 62.0, 61.5, 48.0, 32.4, 28.0, 25.7, 21.7, 21.5, 21.4, 13.9. Anal. Calcd for: C₃₆H₄₁NO₆S: C, 70.22; H, 6.71; N, 2.27. Found: C, 70.26; H, 6.73; N, 2.31. MS m/z: 615.27 [M+].

Ethyl 4-(4-chlorobenzoyl)-6-(4-toluoyl) - 3, 5-diphenyl-1, 1-dioxo-1, 4,-thiazinane-2-carboxylate (34)

Off white solid; M.P: 165°C; Yield (62%). ¹H NMR (300 MHz, CDCl₃): δ_H 1.06 (t, 3H, J=7.1Hz -CH₃ of COOCH₂CH₃),), 2.35 (s, 3H, -CH₃ of toluoyl), 4.07- 4.14 (m, 2H, -CH₂ of COOCH₂CH₃), 4.77 (d, 1H, J=10.6 Hz, H2), 5.27-5.44 (m, 2H, H3 and H5), 5.72 (d, 1H, J=10.4 Hz, H6), 6.89 -7.87 (m, 18H, ArH). ¹³CNMR (75MHz, CDCl₃): δ_c 187.0, 167.1, 161.3, 143.5, 138.4, 138.3, 137.5, 134.2, 133.6, 130.4, 129.8, 129.6, 129.5, 129.4, 129.3, 128.5, 128.0, 66.5, 64.3, 62.9, 57.2, 54.3, 23.3, 14.1. Anal. Calcd for C₃₄H₃₀ClNO₆S: C, 66.28; H, 4.91; N, 2.27. Found: C, 66.31; H, 4.93; N, 2.28. MS m/z: 615.15 (100%) [M+1] 615.15, [M+2] 617.15, [M+3] 616.15

Ethyl 4, 6-(4-toluoyl) - 3, 5-diphenyl-1, 1-dioxo-1, 4,-thiazinane-2-carboxylate (35)

White solid; M.P: 98°C; Yield (57%). ¹H NMR (300 MHz, CDCl₃): δ_H 1.06 (t, 3H, J=7.1Hz -CH₃ of COOCH₂CH₃), 2.29 (s, 3H, -CH₃ of toluoyl), 2.36 (s, 3H, -CH₃ of toluoyl), 4.06-4.15 (m, 2H, -CH₂ of COOCH₂CH₃), 4.69 (d, 1H, J=10.7 Hz, H2), 4.93 (d, 1H, J=10.7 Hz, H3), 5.06 (d, 1H, J=10.3 Hz, H5), 5.28 (d, 1H, J=10.2 Hz, H6), 6.89 - 7.71 (m, 19H, ArH). ¹³CNMR (75MHz, CDCl₃): δ_c 187.0, 167.3, 161.4, 143.6, 142.2, 138.4, 138.3, 134.3, 132.4, 129.9, 129.6, 129.5, 128.6, 128.3, 128.1, 66.6, 64.1, 63.1, 57.5, 54.5, 23.6, 23.2, 14.0. Anal. Calcd for C₃₅H₃₃NO₆S: C, 70.57; H, 5.58; N, 2.35. Found: C, 70.61; H, 5.59; N, 2.34. MS m/z: 595.20 [M+].

Ethyl 4-(4-chlorobenzoyl)-6-(4-toluoyl) - 3, 5-di (4-nitrophenyl)-1, 1-dioxo-1, 4,-thiazinane-2-carboxylate (40)

Yellow solid; M.P: 192°C; Yield (59 %). ¹H NMR (300 MHz, CDCl₃): δ_H1.07 (t, 3H, J=7.1Hz -CH₃ of COOCH₂CH₃), 2.33 (s, 3H,-CH₃) 4.02-4.12 (m,2H,-CH₂ of COOCH₂CH₃), 5.11 (d, 1H, J=10.4 Hz, H₂), 5.17-5.28 (m, 2H, H₃ and H₅), 6.03 (d, 1H, J=10.2 Hz, H₆), 6.89-8.17 (m, 16H, ArH). ¹³CNMR (75MHz, CDCl₃): 186.2, 165.1, 160.4, 147.2, 147.0, 144.4, 142.8, 137.4, 134.2, 133.8, 129.5, 128.5, 128.3, 128.2, 128.0, 126.6, 123.3, 67.8, 67.1, 61.4, 61.0, 60.3, 23.7, 13.3 Anal. Calcd for C₃₄H₂₈ClN₃O₁₀S: C, 57.83; H, 4.00; N, 5.95. Found: C, 57.79; H, 3.7; N, 5.91. MS *m/z*: 705.12 (100%) [M+1] 705.12, [M+2] 706.12, [M+3] 707.12.

Ethyl 4-(4-nitrobenzoyl)-6-(4-toluoyl) - 3, 5-di (4-nitrophenyl)-1, 1-dioxo-1, 4,-thiazinane-2-carboxylate (42)

Orange solid; M.P: 167°C; Yield (61%). ¹H NMR (300 MHz, CDCl₃): δ_H1.08 (t, 3H, J=7.2Hz -CH₃ of COOCH₂CH₃), 2.36 (s, 3H,-CH₃) 4.08-4.18 (m,2H,-CH₂ of COOCH₂CH₃),5.21 (d, 1H, J=10.6 Hz, H₂), 5.35 (d, 1H, J=10.5 Hz, H₃), 5.47 (d, 1H, J=10.3 Hz, H₅), 6.15 (d, 1H, J=10.3 Hz,H₆), 6.92 - 8.29,(m, 16H, ArH). ¹³CNMR (75MHz, CDCl₃): δ_c 186.4, 165.3, 160.2, 150.2, 147.2, 147.0, 144.4, 142.9, 141.7, 134.2, 129.3, 128.5, 128.4, 128.2, 126.7, 123.6, 123.3, 123.2, 68.8, 67.5, 61.6, 60.5, 60.2, 23.8, 13.3. Anal.Calcd for C₃₄H₂₈N₄O₁₂S: C, 56.98; H, 3.94; N, 7.82. Found: C, 57.03; H, 3.91; N, 7.76 MS *m/z*: 716.14 [M⁺].

Ethyl 4-(acetyl)-6-(4-chlorobenzoyl) - 3, 5-di (4-methylphenyl)-1, 1-dioxo-1, 4,-thiazinane-2-carboxylate (43)

White solid; M.P: 132°C; Yield (39%). ¹H NMR (300 MHz, DMSO-d₆) δ_H1.07 (t, 3H, J=7.1Hz -CH₃ of COOCH₂CH₃), 2.21 (s, 3H, -CH₃ of acetyl), 2.28 (s, 3H, -CH₃), 2.33 (s, 3H, -CH₃), 4.05-4.13 (m,2H,-CH₂ of COOCH₂CH₃), 4.63 (d, 1H, J=11.0 Hz, H₂), 4.82 (d, 1H, J=11.0 Hz, H₃), 5.11 (d, 1H, J=10.5 Hz, H₅), 5.39 (d, 1H, J=10.6 Hz, H₆), 7.18-7.89 (m, 12H, ArH). ¹³CNMR (75MHz, CDCl₃): δ_c 187.0, 167.4, 161.3, 141.0, 137.7, 137.5, 135.6, 135.3, 134.6, 130.5, 129.3, 129.1, 128.8, 127.6, 70.0, 68.9, 62.4, 61.9, 60.9, 22.3, 21.6, 21.3, 13.9. Anal.Calcd for C₃₀H₃₀ClNO₆S: C, 63.43; H, 5.32; N, 2.47. Found: C,

63.47; H, 5.33; N, 2.43. MS *m/z*: 567.15 (100%) [M+1] 567.15, [M+2] 569.15, [M+3] 568.15

Ethyl 4-(acetyl)-6-(benzoyl) - 3, 5-di (4-nitrophenyl)-1, 1-dioxo-1, 4,-thiazinane-2-carboxylate (46)

Yellow solid; M.P: 152 °C; Yield (39%). ¹H NMR (300 MHz, , CDCl₃): δ_H1.07 (t, 3H, J=7.1Hz ,CH₃ of COOCH₂CH₃), 2.26 (s, -CH₃, acetyl), 4.03-4.12 (m,2H,-CH₂ of COOCH₂CH₃), 5.08 (d, 1H, J=10.3 Hz, H₂), 5.17 (d, 1H, J=10.5 Hz, H₃), 5.29 (d, 1H, J=10.3 Hz, H₅), 6.01 (d, 1H, J=10.3 Hz,H₆), 7.29-8.13 (m, 13H, ArH). ¹³CNMR (75MHz, CDCl₃) δ_c 185.6, 165.3, 160.1, 147.2, 147.1, 144.2, 138.3, 133.5, 128.4, 128.1, 126.4, 123.0, 65.7, 63.8, 60.3, 53.7, 53.0 24.1, 13.0. Anal.Calcd for C₂₈H₂₅N₃O₁₀S: C, 56.47; H, 4.23; N, 7.06. Found: C, 56.51; H, 4.22; N, 7.02. MS *m/z*: 595.10 [M⁺].

Ethyl 4-(4-nitrobenzoyl)-6-(4-chlorobenzoyl) - 3, 5-di (4-methylphenyl)-1, 1-dioxo-1, 4,-thiazinane-2-carboxylate (47)

White solid; M.P: 192°C ; Yield (57%). ¹H NMR (300 MHz, DMSO-d₆) δ_H1.09 (t, 3H, J=7.0Hz -CH₃ of COOCH₂CH₃), 2.27 (s, 3H, -CH₃), 2.33 (s, 3H, -CH₃), 4.08-4.17 (m, 2H,-CH₂ of COOCH₂CH₃), 4.68 (d, 1H, J=10.6 Hz, H₂), 4.93 (d, 1H, J=10.6 Hz, H₃), 5.19 (d, 1H, J=10.3 Hz, H₅), 5.63 (d, 1H, J=10.3 Hz, H₆), 7.31-8.29 (m, 16H, ArH). ¹³CNMR (75MHz, CDCl₃): δ_c 187.0, 167.3, 161.3, 151.6, 142.9, 141.0, 137.6, 137.4, 135.6, 135.4, 134.8, 130.6, 130.0, 129.3, 129.0, 128.8, 127.7, 124.2, 70.4, 69.3, 63.5, 62.7, 62.2, 21.6, 21.3, 13.9. Anal.Calcd for: C₃₅H₃₁ClN₂O₈S: C, 62.26; H, 4.63; N, 4.15. Found: C, 62.31; H, 4.67; N, 4.14. MS *m/z*: 674.15 (100%) [M+1] 674.15, [M+2] 675.15, [M+3] 676.15

Ethyl 4-(acetyl)-6-(4-toluoyl) - 3, 5-di (4-nitrophenyl)-1, 1-dioxo-1, 4,-thiazinane-2-carboxylate (50)

Orange solid; M.P: 151°C; Yield (43%). ¹H NMR (300 MHz, , CDCl₃): δ_H1.09 (t, 3H, J=7.1Hz ,CH₃ of COOCH₂CH₃), 2.29 (s, -CH₃, acetyl), 2.32 (s, 3H,-CH₃) 4.06-4.14 (m,2H,-CH₂ of COOCH₂CH₃), 5.11 (d, 1H, J=10.5 Hz, H₂), 5.27 (d, 1H, J=10.5 Hz, H₃), 5.36 (d, 1H, J=10.4 Hz, H₅), 6.01 (d, 1H, J=10.4 Hz,H₆), 6.94-8.18 (m, 12H, ArH).

¹³CNMR (75MHz, CDCl₃) δ_c 187.1, 166.0, 160.4, 147.3, 147.2, 144.3, 142.8, 134.2, 128.5, 128.2, 126.9, 123.3, 65.9, 63.8, 60.3, 53.9, 53.0, 23.7, 24.4, 13.2. Anal.Calcd for C₂₉H₂₇N₃O₁₀S: C, 57.14; H, 4.46; N, 6.89. Found: C, 57.17; H, 4.43; N, 6.90. MS *m/z*: 609.23 [M⁺].

Ethyl 4-(4-chlorobenzoyl)-6-(4-chlorobenzoyl) - 3, 5-diphenyl-1, 1-dioxo-1, 4,-thiazinane-2-carboxylate (52)

Off white solid; M.P^oC; Yield (57%). ¹H NMR (300 MHz, CDCl₃): δ_H 1.06 (t, 3H, J=7.1Hz -CH₃ of COOCH₂CH₃), 4.04 - 4.10 (m, 2H, -CH₂ of COOCH₂CH₃), 4.78 (d, 1H, J=10.6 Hz, H₂), 5.23-5.37 (m, 2H, H₃ and H₅), 5.59 (d, 1H, J=10.3 Hz, H₆), 7.26-7.93 (m, 18H, ArH). ¹³CNMR (75MHz, CDCl₃): δ_c 187.1, 167.1, 161.3, 141.1, 138.3, 138.1, 137.5, 135.8, 133.8, 130.7, 130.4, 129.6, 129.5, 129.4, 129.3, 128.4, 128.1, 66.3, 64.0, 63.0, 56.9, 54.2, 14.2. Anal.Calcd for C₃₃H₂₇Cl₂NO₆S: C, 62.27; H, 4.28; N, 2.20. Found: C, 62.23 H, 4.31; N, 2.24 MS *m/z*: 635.11 (100%) [M+1] 635.09, [M+2] 637.09, [M+3] 636.10

5.2. In-vitro biological activity:

5.2.1. In-vitro antimycobacterial activity

All compounds were screened for their *in vitro* antimycobacterial activity against log-phase cultures of *M. tuberculosis* H37Rv (ATCC27294) in Middle brook 7H11 agar medium supplemented with OADC by agar dilution method similar to that recommended by the National Committee for Clinical Laboratory Standards for the determination of MIC in triplicate [208]. The minimum inhibitory concentration (MIC) is defined as the minimum concentration of compound required to give complete inhibition of bacterial growth. The MIC's of the synthesized compounds along with the standard drugs for comparison are reported in Table 5.2.

Table 5.2. In-vitro antimycobacterial activity

Comp. No.	MTB MIC (μM)	Comp.No.	MTB MIC (μM)
1	10.63	30	39.3
2	85.96	31	19.32
3	21.49	32	39.92
4	2.35	33	40.6
5	20.76	34	20.29
6	88.08	35	41.97
7	0.57	36	82
8	72.24	37	9.7
9	79.36	38	91.3
10	2.3	39	96.23
11	43.58	40	4.42
12	98.9	41	40.08
13	10.2	42	34.88
14	10.38	43	39.3
15	20.5	44	38.81
16	20.98	45	39.67
17	41.55	46	20.99
18	93.7	47	9.26
19	9.92	48	9.31
20	37.22	49	19.09
21	38.01	50	20.51
22	8.9	51	9.11
23	18.06	52	19.32
24	19.51	Isoniazid	0.36
25	81.15	Rifampicin	0.12
26	46.29	Ethambutol	7.64
27	82.22	Pyrazinamide	50.77
28	17.9	Ciproflaxacin	9.41
29	8.6		

MTB :*M.Tuberculosis*

5.2.2. In-vitro enzyme assay:

The amino acid biosynthesis sequence provides important antibiotic targets if the organism is unable to scavenge for nutrients from the human host. A branching of this “shikimate pathway” occurs after the formation of chorismate; indeed, the name of this compound (suggested by an ecclesiastical authority) is derived from the Greek, meaning fork and its partitioning towards the individual aromatic products. This process is controlled by the activities of several chorismate-metabolizing enzymes. The whole shikimate pathway is essential for the *in vitro* viability of *M.tuberculosis* cell [209,210]. The chorismatase or CM (EC 5.4.99.5) catalyses the conversion of chorismate into prephenate and plays a key role in the biosynthesis of the essential aromatic amino acids such as tyrosine and phenylalanine. The catalyzed reaction is unique in nature because it is the only example of a pericyclic process i.e. a Claisen rearrangement in the primary metabolism step [211]. As only few enzymes are known to catalyze a pericyclic process, CM has generated considerable interest among enzymologists as well as bioorganic, medicinal and computational chemists, specifically with respect to the origins of its catalytic efficiency.

Protein expression and isolation:

The vector pET15 (b) / Rv1885c was transformed into BL21 (DE3) bacterial strain. For protein production, the transformed strain in LB media supplemented with 100 mg/ml ampicillin incubated at 37°C for 2-4 hrs at 120 rpm until OD reaches 0.6 at 600 nm. Now the culture was induced by 30 µM IPTG and incubated at 18°C overnight at 120 rpm. Pellet down the bacterial cells and suspend in lysis buffer (20% sucrose, 30 mM Tris pH-8.0, 1mM EDTA, 1 mM PMSF, 1 mM DTT). Shake this suspension at 150 rpm, 24°C for 10 mins. Centrifuge the suspension at 12000 rpm, 4°C for 15 mins. Resuspend the pellet in ice cold 5 mM MgSO₄ by shaking at 150 rpm, 4°C for 10 mins. Centrifuge at 12000 rpm, 4°C for 15 mins. The supernatant was buffered with 30 mM Tris pH-8.0 and store at -80°C.

Chorismate mutase activity was assayed for synthesized compounds at a concentration of 50 μ M by monitoring formation of phenylpyruvate by conversion of chorismate to prephenate plus phenyl pyruvate according to the method described previously with little modifications. Briefly the reaction mixture in a final volume of 50 μ l, 200 ng of enzyme in 50 mM Tris-HCl (pH 7.5), 0.5 mM EDTA, 0.1 mg/ml bovine serum albumin, and 10 mM mercaptoethanol along with and without test compound were incubated at 37°C for 15 min. Then reaction was initiated by adding 4 μ l of chorismic acid in order to get final concentration of 1 mM (sigma, C1761). The reaction was allowed to proceed at 37°C for 10 min and was terminated with 40 μ l of 1 N HCl. After a further incubation at 37°C for 10 min, 40 μ l of 2.5 N NaOH was added to convert prephenate to phenylpyruvate, which is formed in the enzymatic reaction. The absorbance of the phenylpyruvate was read at 320 nm. Non enzymatic conversion of chorismate to prephenate was recorded by measuring absorbance at 320 nm without enzyme for each reaction. Percent inhibition was calculated by following formula and its results are displayed in Table 5.3.

$$100 \times (C - T) \div C$$

where C- control and T- test compounds

Table 5.3. In-vitro enzyme assay

Comp. No.	Enzyme inhibition*	Comp. No.	Enzyme inhibition*
1	58.9	27	NT
2	NT	28	36.8
3	88	29	47.8
4	43.8	30	NT
5	42.6	31	46.8
6	NT	32	NT
7	54.5	33	NT
8	NT	34	56.7
9	NT	35	NT
10	48.2	36	NT
11	NT	37	42.1
12	NT	38	NT
13	42.1	39	NT
14	41.9	40	36.5
15	46.3	41	NT
16	52.4	42	NT
17	NT	43	NT
18	NT	44	NT
19	36.5	45	NT
20	NT	46	53
21	NT	47	50.6
22	48.6	48	53.3
23	42.1	49	53.5
24	51.6	50	54.2
25	NT	51	52.4
26	NT	52	50

*Enzyme inhibition studies were performed at 50 μ M concentration

5.2.3. Cytotoxicity assay:

Human embryonic kidney cells, HEK293T cells were procured from National Center for Cell Sciences, Pune, India. Cells were grown in DMEM, Supplemented with 10% heat inactivated fetal bovine serum (FBS), 100 IU/ml penicillin, 100 mg/ml streptomycin and 2 mM-glutamine and 20 ng/ml Amphotericin B. Cultures were maintained in a humidified atmosphere with 5% CO₂ at 37°C. The cells were subcultured twice each week, seeding at a density of about 2*10³ cells/ml. cell viability was determined by the trypan blue dye exclusion method.

The cells were treated with the synthesized compounds at different 5, 10, 25 µM concentrations. Control cells were supplemented with complete tissue culture medium containing the diluents control, that is, DMSO. This diluent was never present at > 0.1% final concentration and did not show any detectable effect. Cells were grown in a 96 well plate by seeding 5*10³ cells/ml and incubated at 37°C, 5% CO₂ for 24 h in a final volume of 200 µl. At 21 h, the medium was removed and 20 µl of MTT (5 mg/ml in PBS) was added. After 2 h incubation at 37°C, the plates were centrifuged at 2000 rpm, 2 min and the supernatant was removed without disturbing the formazan crystals. The crystals were dissolved in 100 µl of DMSO in each well and the plates were agitated for 1 min. This assay is based on the ability of metabolic active cells to reduce the tetrazolium salt MTT to water-soluble purple colored formazan compounds. The intensity of the formed dye, proportional to the number of metabolic active cells, was read at 590 nm using the Perkin Elmer victor TM3 multi plate reader. The results are shown in figure 5.1.

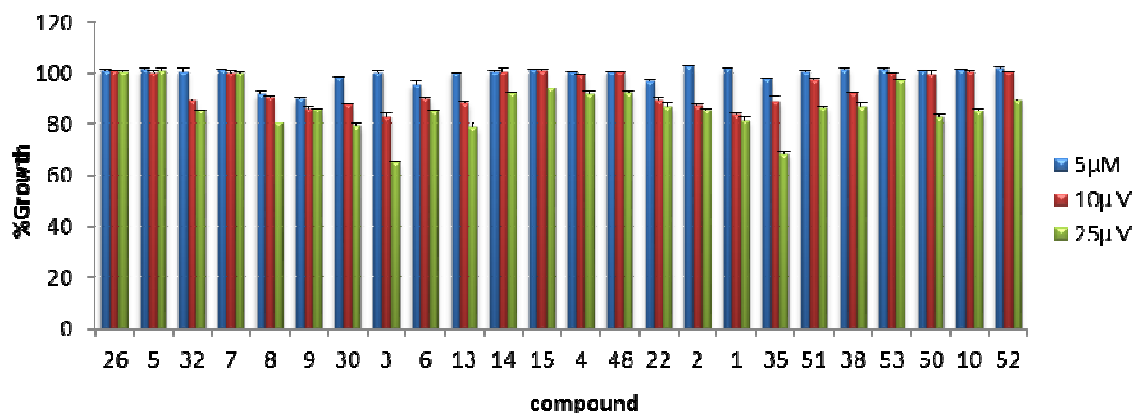


Figure.5.1: In-vitro cytotoxicity studies on HEK293T cell lines.

5.2.4. In-vitro dormant antimycobacterial activity

Latent TB infection is traditionally associated with the transition of bacilli to dormant state in response to non-optimal growth conditions in vivo and killing of dormant *M. tuberculosis* cells is a big challenge for the modern TB therapy. As non-replicating bacteria in vivo are less susceptible to antibiotics than actively growing bacteria, therefore the time needed for elimination of the pathogen is much longer.

The compound which showed good activity in the actively replicative MTB was also tested for their ability to affect viability of dormant ‘non-culturable’ *M. tuberculosis* cells and results are shown in Figure 5.2 with comparison of Isoniazid and Rifampicin. These ‘non-culturable’ cells possess a decreased ability to form colonies on standard solid media but they are potentially viable and may be transferred from dormant to active growing state by the special procedure of resuscitation. It was found that after treatment by several compounds cells were less able to recover from dormancy. The most prominent effect had the compound 7 which caused a ~2-log decrease in the viability of dormant cells after incubation with 10 μg/ml for 7 days. Although this compound may be regarded as the prominent compound for the development of derivatives which are more effective for dormant *M. tuberculosis* cells and latent. Latent TB infection is traditionally

associated with the transition of bacilli to dormant state in response to non-optimal growth conditions *in vivo* and killing of dormant *M. tuberculosis* cells is a big challenge for the modern TB therapy. As non-replicating bacteria *in vivo* are less susceptible to antibiotics than actively growing bacteria, therefore the time needed for elimination of the pathogen is much longer. This resistance to current available drugs is not conferred by genetic mechanisms and takes place due to changes in the physiological state of mycobacteria. Because of the absence of specific and high effective anti-latent TB drugs, traditional antibiotics such as isoniazid and rifampin are currently being used for latent TB curing but the effectiveness of such treatment of latent TB infection is controversial. To obtain dormant 'non-culturable' cells, *M. tuberculosis* bacilli were grown in potassium-deficient Sauton's medium supplemented with ADC and 0.05% of Tween-80 (37°C, 200 rpm). 'Non-culturability' was detected by inability of the cells to form colonies onto agar solidified Sauton's medium. Resuscitation of both treated and untreated NC cells was performed in liquid Sauton's medium, with the concentration of cells recovered from non-culturability being estimated by Most Probable Numbers (MPN) assay and with the use of statistical approaches [212].

The compound which showed good activity in the actively replicative MTB was also tested for their ability to affect viability of dormant 'non-culturable' *M. tuberculosis* cells and results are shown in figure 5.4 with comparison of Isoniazid and Rifampicin. These 'non-culturable' cells possess a decreased ability to form colonies on standard solid media but they are potentially viable and may be transferred from dormant to active growing state by the special procedure of resuscitation. It was found that after treatment by several compounds cells were less able to recover from dormancy. The most prominent effect had the compound 7 which caused a ~2-log decrease in the viability of dormant cells after incubation with 10 µg/ml for 7 days. Although this compound may be regarded as the prominent compound for the development of derivatives which are more effective for dormant *M. tuberculosis* cells and latent. Latent TB infection is traditionally associated with the transition of bacilli to dormant state in response to non-optimal growth conditions *in vivo* and killing of dormant *M. tuberculosis* cells is a big challenge for the modern TB therapy. As non-replicating bacteria *in vivo* are less susceptible to

antibiotics then actively growing bacteria, therefore the time needed for elimination of the pathogen is much longer. This resistance to current available drugs is not conferred by genetic mechanisms and takes place due to changes in the physiological state of mycobacteria. Because of the absence of specific and high effective anti-latent TB drugs, traditional antibiotics such as isoniazid and rifampin are currently being used for latent TB curing but the effectiveness of such treatment of latent TB infection is controversial.

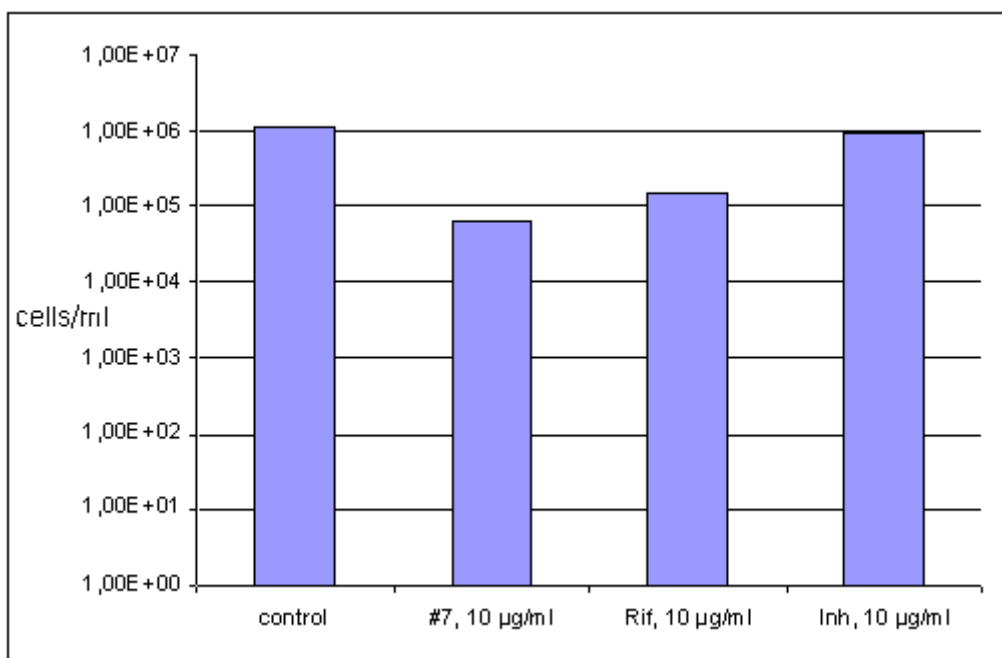


Figure 5.2. The effectiveness of the compound **7** for killing *M. tuberculosis* 'non-culturable' cells.

5.3. Atom based 3D QSAR methods

All computations for 3D QSAR development was carried out with PHASE 3.3 implemented in the Maestro 9.2 software package [213–215] (Schrodinger, LLC). Data set of synthesized compounds comprising of 41 molecules were collected and the respective MIC values were noted which further were converted into PMIC (-log MIC) values for QSAR development. All structures were drawn using 2D sketcher tab on Maestro graphical user interface. The LigPrep 2.5 [216] application from Schrodinger

software package was utilized to build and energetically minimize structures and to add hydrogens and generate stereoisomers at neutral pH 7 using ionizer subprogram. In the development of individual 3D QSAR approach, statistical analyses were performed using PHASE [217]. From the total 41 molecules, 28 of these were randomly chosen for training set and 13 (Table 5.4) were selected as test set, by using the “Automated Random Selection” option present in the PHASE application. For QSAR development, training set molecules were placed into regular grid of cubes, with each cube allotted zero or more “bits” to account for the different type of pharmacophore features in the training set that occupy the cube (1\AA^3). This representation gives rise to binary-valued occupation patterns that can be used as independent variables to create partial least-squares (PLS) factors 3D QSAR models.

5.3.1. 3D QSAR models generation, PLS and contour analysis

To provide superlative QSAR models and to exhibit reliable predictions for structure based activity, the generated 3D model should obey the limitations of internal statistical validation parameter boundaries [217]. Internal statistical validation by PLS analysis conferred important parameters obtained through LOO method. Individual 3D QSAR model developed has shown a good R^2 (LOO-cross validated value of training set) value of 0.981 which should be greater than 0.6. Model also displayed good predictive power with value of Q^2 (LOO-cross validated value for test set) of 0.68 which should be greater than 0.55. Standard deviation (SD) value of aligned compounds was shown lowest value 0.08 which should be below 0.3, with minimum root mean square error (RMSE) value of 0.24, and high value of variance ratio (F) 180. Predicted activities of each aligned compound versus experimental activities are presented in a scatter plot for both training and test sets (Figure 5.3) and the values are mentioned in table 2. In summary, all these values obtained were obeying the minimum limitations and demonstrated that the model generated was possessing good predictive capacity, which can be further correlated with the biological activity of individual compounds by using contour maps.

Contour maps obtained from the 3D QSAR model outlined the positions of important atoms that could enhance the bioactivity. By visualization of the 3D QSAR model in the context of most active and least active compounds, a clear correlation of the important moieties for activity are shown in Figure 5.4. In these representations, electron withdrawing favored red cube regions indicated the importance of p-nitro phenyl groups at position C-3 and C5 which is commonly present in all four most active compounds (4, 7, 10, and 40) as illustrated in figure 5.4a1. Absence of electron withdrawing groups at position C-3 and C5 in all the three least active ligands (12, 18, 39) with no overlapping of favored red cubes was observed, which indicated that the additional electron withdrawing groups could possibly increase the activity (figure 4b1). Overlapping of hydrophobic favored green cubes on bulky aryl groups at N-4 position (figure 5.4a2) of the four most active compounds (4, 7, 10, 40) was compared with the less overlapping of hydrophobic cubes (figure 5.4b2) on simple non bulky groups at N-4 position of least active compounds (12, 18, 39). These observations indicated that bulky hydrophobic or non-polar groups at N-4 position may increase activity. Negative ionic and positive ionic favored contour maps at C-3 and C5 positions are represented in cyan and purple cubes respectively (figure 5.4a3, b3) in the four most active compounds and 3 least active compounds indicating that p-NO₂ benzyl moieties were important in binding to the particular targets, absence and reduction of these groups at C-3 and C5 position showed decrease in activity.

Table 5.4. Aligned compounds for 3D QSAR study and their experimental and predicted biological activity

No	Comp. No.	pMIC Experimental	pMIC Predicted	Data set
1	3	4.668	4.674	training
2	4	5.629	5.739	training
3	5	4.683	4.656	training
4	6	4.055	4.050	training
5	7	6.244	6.090	training
6	9	4.100	4.212	test
7	10	5.638	5.201	test
8	11	4.361	4.386	training
9	12	4.005	3.980	training
10	13	4.991	4.996	training
11	15	4.688	4.451	test
12	16	4.678	4.415	test
13	17	4.381	4.420	training
14	18	4.028	4.006	training
15	21	4.419	4.367	training
16	22	5.051	4.789	test
17	23	4.743	4.651	training
18	24	4.71	4.729	training
19	25	4.091	4.125	training
20	26	4.335	4.167	test
21	28	4.747	4.755	training
22	29	5.066	5.424	test
23	30	4.406	4.581	test
24	32	4.399	4.719	test
13	17	4.381	4.420	training
14	18	4.028	4.006	training
15	21	4.419	4.367	training
16	22	5.051	4.789	test
17	23	4.743	4.651	training
18	24	4.71	4.729	training
19	25	4.091	4.125	training
20	26	4.335	4.167	test
21	28	4.747	4.755	training
22	29	5.066	5.424	test
23	30	4.406	4.581	test
24	32	4.399	4.719	test
25	33	4.391	4.375	training
26	34	4.693	4.567	training

27	35	4.377	4.401	training
28	36	4.086	4.074	training
29	38	4.040	4.123	test
30	39	4.017	4.070	training
31	40	5.355	5.348	training
32	41	4.397	4.419	test
33	42	4.457	4.528	training
34	44	4.411	4.569	test
35	45	4.402	4.406	training
36	46	4.678	4.721	training
37	47	5.033	5.004	training
38	48	5.031	4.972	training
39	49	4.719	4.876	test
40	51	5.04	5.266	training
41	52	4.714	4.663	training
25	33	4.391	4.375	training
26	34	4.693	4.567	training
27	35	4.377	4.401	training
28	36	4.086	4.074	training
29	38	4.040	4.123	test
30	39	4.017	4.070	training
31	40	5.355	5.348	training
32	41	4.397	4.419	test
33	42	4.457	4.528	training
34	44	4.411	4.569	test
35	45	4.402	4.406	training
36	46	4.678	4.721	training
37	47	5.033	5.004	training
38	48	5.031	4.972	training
39	49	4.719	4.876	test
40	51	5.04	5.266	training
41	52	4.714	4.663	training

Figure 5.3. Scatter plots plotted between Predicted vs. Observed activity of MTB inhibition by the best model obtained using 41 compounds

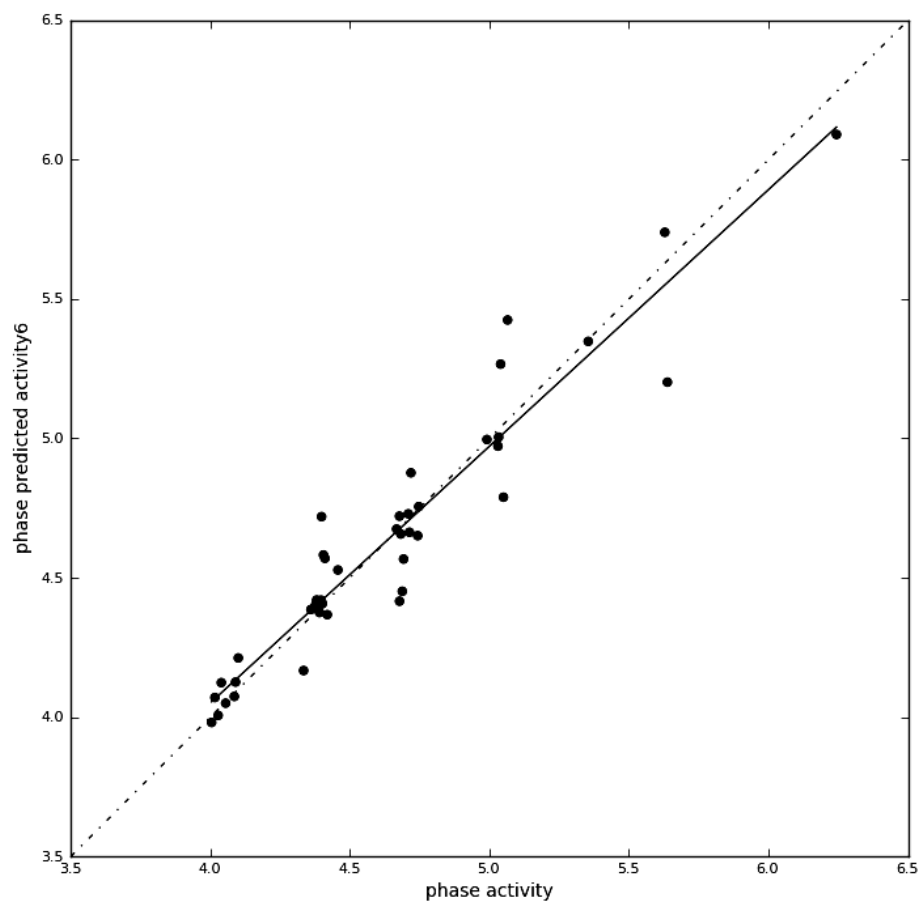
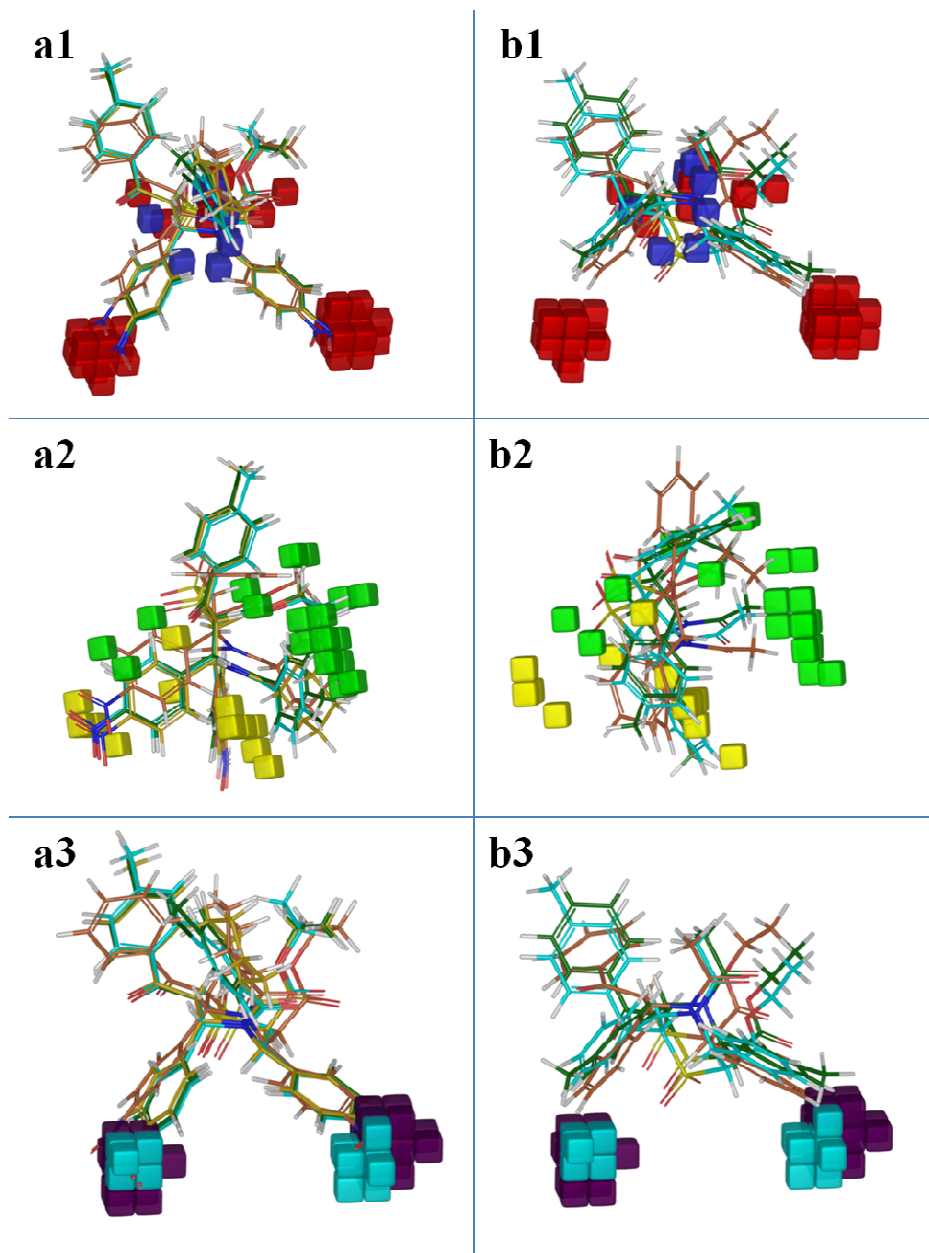


Figure.5.4 Illustration of the Phase QSAR map visualization on most active / inactive molecules



Legend: active compounds **4, 7, 10, 40** with their respective mapping of Electron withdrawing (a1) Hydrophobic (a2) combined positive and negative (a3). Secondly, least active compounds **12, 18, and 39** with their respective mapping of Electron withdrawing (b1) Hydrophobic (b2) combined positive and negative (b3). The visualization cubes are color coded as follows: red cubes are favored regions for electron withdrawing groups (a1, b1) blue cubes are disfavored regions (a1, b1). Hydrophobic favored green cubes (a2), and disfavored yellow cubes (b2). Negative ionic favored shown by cyan cubes (a3), positive ionic favored by purple cubes (b3). Most active compounds at a1, a2, a3 shown with orange carbons is compound 4, green is 7, yellow is 10, cyan is 40. Least active compounds at b1, b2, b3 shown with orange carbons is compound 12, green is 18, cyan is 39.

5.4. Discussion:

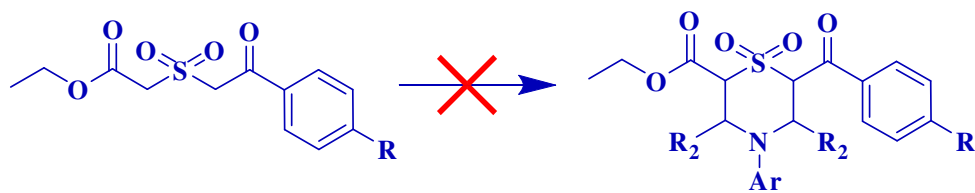
Encouraged by the promising results of the previous work on 1, 4 Thiazines by our group, further work was initiated in our lab with the goal of obtaining a lead series with tractable SAR and potencies better than the previously reported series. Considering the SAR inputs from the previous work, it was decided to modify the previously reported scaffold by substituting the N4 position of the thiazine scaffold by either alkylation or acylation with various alkyl/aryl halides or by converting into their corresponding amides by treatment with various acid chlorides. An attempt to prepare the corresponding urea, thiourea and sulphonamide was also designed.

Hence a library was designed and chemistry was taken for validation. First it was decided to synthesise the sulphone, which would be acting as scaffold template. The synthesis was achieved starting from acetophenone by first converting them to the corresponding phenacyl bromide with bromine and acetic acid. It was decided to start with acetophenone's having an electron withdrawing, electron donating and also without any substituent, which would help us in understanding the role of these substitution with respect to the activity. The so obtained phenacyl bromide was then alkylated with ethylthioglycolate in presence of a suitable base and then oxidising the alkylated product to their sulphone using excess of hydrogen peroxide. All the reaction went smoothly giving the desired products in quantitative yields. Our next attempt was the L-proline catalysed cyclisation using alkyl, aryl and heteroaryl amines to give the final product by the previously reported procedure from our group. Though the reaction went smoothly for aliphatic amines but the reaction was very sluggish with aromatic and heteroaryl amine resulting in a very messy TLC. Further analysis by LCMS revealed the absence of the desired mass. The one probable explanation which came in was the relatively low nucleophilicity of the aromatic amines especially the heteroaryl moieties would be the hindering the progress of the reaction. Also the heteroaryl moieties groups used in the synthesis (viz 2-amino-5-nitro thiazole, 2-amino-6-nitrobenzothiazole) had very low solubility which again didn't help in the progress of the reaction. Considering these

factors various trials were planned using various combination of base and solvents at various temperatures as mentioned below.

1. The first trial was performed using the previously reported procedure of L-proline catalysed reaction at room temperature using ethanol as solvent.

The TLC was very messy and LCMS revealed the absence of the desired mass. So it was decided to attempt various trials by replacing the catalyst L-proline with various other bases, while keeping the other conditions constant. Trials were performed by replacing L-proline with the following bases - Piperidine, pyridine, 4-dimethyl amino pyridine, piperazine, triethyl amine and diisopropyl amine. Though LCMS revealed the presence of the product in few cases but either the TLC was very messy or the product ratio was too low to be isolated, to proceed further.



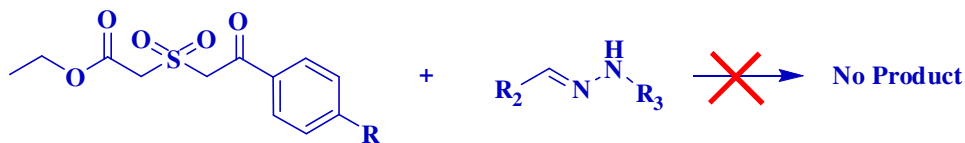
Ethanol/various other solvents, L-Proline/other reagents, ArNH₂, R₂CHO

2. To understand the effect of solvents in driving the reactions forward various trials were also performed with the above mentioned bases in various solvents like Tetrahydrofuran, DMSO, Methanol, Dimethyl formamide, Dimethyl acetamide, and also a combination of these solvents. Again these trials also didn't give us any conclusive results.

3. An attempt was also made to perform the reaction under catalytic amount of various Bronsted and Lewis acids, which also didn't help.

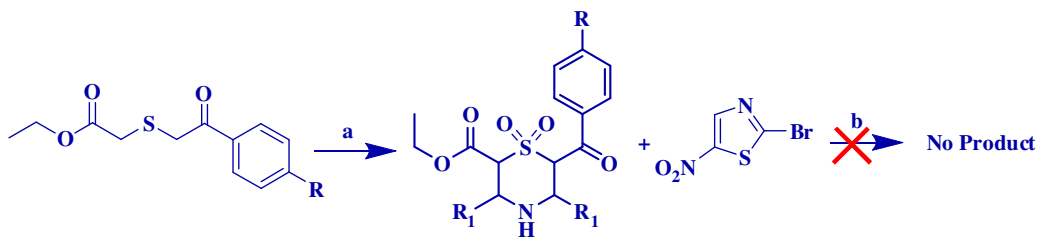
4. A thorough understanding of the mechanism of the reactions reveals that the facile transformation presumably occurs via a one-pot domino sequence of enamine formation/

iminium intermediate/ Michael addition which ultimately forms thiazines via the intramolecular Mannich type reaction. It was decided to perform this sequence once by one to understand the limiting factors. So first a iminium intermediate of the corresponding amine and aldehyde was prepared, which went smoothly. This intermediate was then allowed to react with scaffold (sulfone) to give the final product. Though the reactions worked for aliphatic amines, but didn't afford the desired product when aromatic/heterocyclic amines were used, which again helped us in understanding that the steric effect plays a very important role in driving/limiting the reaction forward.



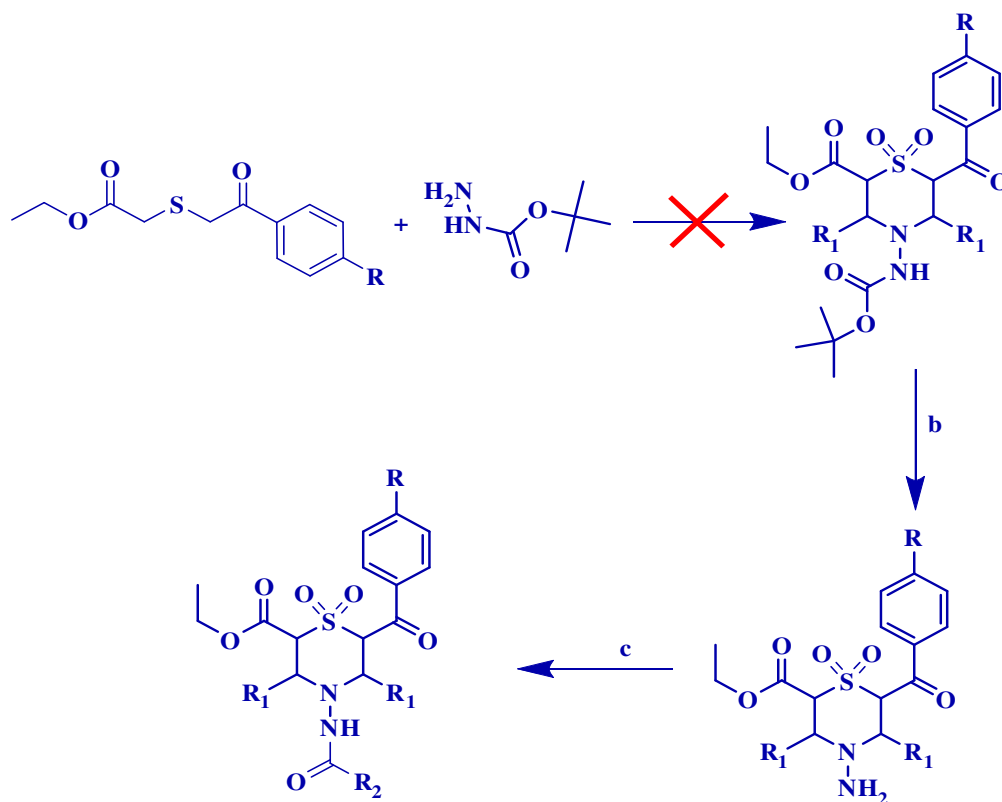
Ethanol, AcOH(cat), R₃NHNH₂, R₂CHO

5. An attempt was also performed by converting the corresponding sulphone into the thiazine by following the previously reported L-proline catalyzed cyclisation using ammonia as the amine source, which went smoothly as expected and the alkylating the N4 position so formed thiazine with various aromatic halides (synthesised via the diazotisation of various available amines, if it was not commercially available), which gave us the desired product but in very low yield (5-10%). Hence had to be dropped.



a. L-Proline, ethanol. R₁CHO, NH₃. b. base, DMF or THF

6. Considering all these factors into mind, a modification was suggested into the scheme by replacing the amine source in the cyclisation step with Boc protected hydrazine instead of ammonia/aliphatic amines to give modified thiazine (as shown in fig), and then deprotecting the Boc from the so formed thiazine, which could then be coupled with various groups to give a library of thiazine derivatives. But surprisingly the reaction didn't give us the desired product.



a. L-Proline, R_1 CHO, ethanol. b. HCl In dioxane c. R_2 COOH, EDCI.HCl, HOBT, DCM

The final library was achieved by converting the thiazine into the corresponding the amides by treating the scaffold moiety with appropriate acid chlorides in presence of either sodium hydride or DIPEA as base. The yields range from 40-73% and the purity of compounds was checked by TLC and elemental analysis. Log P values ranged from 3.15-

70.6. Analytical and spectral data (¹H NMR, ¹³C NMR, and massspectra) of all the synthesized compounds were in full agreement with the proposed structures.

All the 52 compounds screened showed promising *in vitro* activity against MTB with MIC ranging from 0.57-98.90 μM. Four compounds (**4**, **7**, **10** & **40**) inhibited MTB with less than 5 μM. Compound **7** (ethyl 4-(4-toluoyl)-6-(4-chlorobenzoyl) - 3, 5-di (4-nitrophenyl)-1, 1-dioxo-1, 4,-thiazinane-2-carboxylate) was found to be the most active compound *in-vitro* with MIC of 0.57 μM against log-phase culture of MTB, which is comparable to that of standard first line drug INH (MIC of 0.36 μM) and was thirteen times more potent than Ethambutol, sixteen times more potent than Ciprofloxacin and eighty nine times more potent than Pyrazinamide. In addition, four compounds (**4**, **7**, **10** & **40**) were found to be more active than Ethambutol (MIC of 7.64 μM) and eight compounds (**4**, **7**, **10**, **22**, **29**, **40**, **48**, & **51**) were more potent than Ciprofloxacin (MIC of 9.41 μM). Among the 52 derivatives screened, forty one compounds had more promising MIC than the first line drug Pyrazinamide with an MIC of 50.77 μM.

With respect to structure-TB activity relationship, the substitution at the phenyl ring attached to the C-6 of the thiazine ring did not have any significant influence in enhancing the activity. Whereas the substitution of electron withdrawing group (**4**, **7**, **10**, and **40**) to phenyl ring attached to the C-3 and C-5 of thiazine systems did significantly increase the activity as compared to the absence of any modifying group or electron donating groups. The influence of the groups attached to nitrogen (N-4) of the thiazines, viz. *p*-toluyl amide (**3**, **5**, **6**, **7**, **15**, **20**, **25**, **26**, **36**, **46** and **53**), benzoyl amide (**2**, **8**, **16**, **21**, **37**, **47** and **50**), cyclo hexyl amide(**1**, **4**, **11**, **17**, **28**, **29**, **31**, **34** and **41**), acetoyle (**9**, **12**, **18**, **27**, **39**, **40**, **44**, **45**, **48** and **52**) *p*-nitro benzoyl amide (**13**, **22**, **32**, **33**, **43**, **49** and **51**) and *p*-chloro benzoyl amide (**4**, **10**, **14**, **19**, **30**, **38**, **23**, **24**, **42** and **52**) on the anti-mycobacterial activity against MTB deserves comment. Compound **7** with a substitution of *p*-toluyl amide at N-4 and nitro substitution at C-3 /C-5 position exhibited maximum activity with a MIC of 0.57 μM. Compound **4**, **10** of cyclo hexyl amide series displayed a MIC of 2.35 and 2.30 μM respectively. Among the *p*-chloro benzoyl amide series, only one compound (**40**) (MIC = 4.42 μM) showed excellent activity. All the most active

compounds have different substitutions at N-4 position of thiazines namely *p*-toluyl amide, cyclo hexyl amide and *p*-chloro benzoyl amide but have common nitro group at C-3 /C-5 of thiazine system. Remaining compounds were moderately active. Benzoyl amide, *p*-nitro benzoyl amide showed moderate and acetyl series showed least activity (**12**, **18**, **38** and **39**). Overall increase in the activity may be attributed to the lipophilic moiety at N-4 position of thiazines, as this would have increased the permeability across the microbial membrane. This also explains why acetyl series has low activity probably due to decreased penetrability. Interestingly *p*-chloro benzoyl amide derivative showed better activity than *p*-nitro benzoyl one.

Few molecules of the series of substituted 1, 4-thiazine derivatives were tested for CM enzyme inhibition. The best molecular interaction with the CM enzyme inhibition was with a combination of benzyl substitution at C-6 and C-3/C-5 positions and *p*-toluoyl substitution at C-4 position of thiazine ring (compound **3**). The enzyme inhibitory activity brought by these structural modification, also correlated with an increase in the inhibition of the growth of *M. tuberculosis*. This is best explained with the compound **7** which showed moderate inhibitory property against CM and best inhibitory activity against *M. tuberculli* growth. Both these compounds had a common substituent of *p*-toluoyl at C4 position of thiazine ring. Compounds **1** & **34** also exhibited moderate inhibitory property and good MIC.

The cytotoxic effect of selected compounds on human embryonic kidney cells (HEK293) was evaluated by MTT assay using three different concentrations of molecules. there is not much significant difference in the growth of HEK293 cells with increasing dose. Substituting C-3 and C-5 position by $-\text{CH}_3$, $-\text{NO}_2$ groups along with various substitutions like $-\text{benzoyl}$, *p*-chloro benzoyl, *p*- nitro benzoyl, cyclohexoyl and *p*-toluoyl at N-4 position of thiazines did not show any significant cytotoxicity. Overall all the compounds did not exert any significant cytotoxicity.

The compound which showed good activity in the actively replicative MTB was also tested for their ability to affect viability of dormant 'non-culturable' *M. tuberculosis* cells

and results were compared with Isoniazid and Rifampicin. These 'non-culturable' cells possess a decreased ability to form colonies on standard solid media but they are potentially viable and may be transferred from dormant to active growing state by the special procedure of resuscitation. It was found that after treatment by several compounds cells were less able to recover from dormancy. The most prominent effect had the compound **7** which caused a ~2-log decrease in the viability of dormant cells after incubation with 10 µg/ml for 7 days. Although this compound may be regarded as the prominent compound for the development of derivatives which are more effective for dormant *M. tuberculosis* cells and latent forms.

Structure activity relationship reveals that the presence of electron withdrawing groups at C-3 /C-5 position of thiazine moiety brought about an increase in the activity and these results are well supported by 3D QSAR contour maps. 3D QSAR studies indicated that bulky hydrophobic or non-polar groups at N-4 position may increase activity. The negative ionic and the positive ionic contour maps show that p-NO₂ benzyl moieties were important in binding to the particular targets, absence and reduction of these groups at C-3 and C5 position showed decrease in activity.

5.5. Conclusion

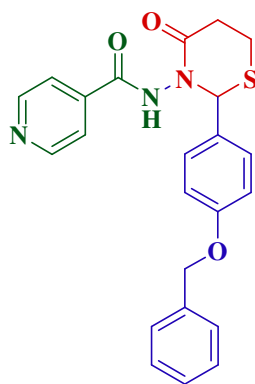
In the present study, a series of 52 substituted 1,4-thiazine derivatives with variations at N-4, C-6, C-3 and C-5 were synthesized and the structure–activity relationship was carried out around the parent compound. The most promising compound **7** is quite a modest candidate for the development of derivatives which are more effective for dormant *M. tuberculosis* cells and latent tuberculosis. The QSAR studies supported by the contour maps are also in line with the structure–activity relationship.

Although the strategy of targeting different substituents for better activity against *M.tuberculosis* and inhibitory property for CM, their cytotoxicity towards HEK293 cells precludes their development. With the contribution of molecular modeling we plan to

modify the chemical structure in order to gain more inhibitory activity against *M.tuberculosis* growth and CM, thereby compensate for the toxicity.

Chapter 6-
Summary and conclusion

- Totally 2 series of 84 compounds were synthesized out of which 32 compounds were from 1, 4-Thiazine derivatives and 52 compounds were from 1, 3-Thiazine derivatives.
- 1,3-Thiazine derivatives were prepared using one-pot three component condensations of isoniazid (INH), 3-mercaptopropionic acid and various aryl/heteroaryl aldehydes in the presence of EDC
- The purity of the compounds was ascertained by TLC, elemental analysis and their structures were elucidated by spectral data.
- All the compounds showed in vitro activity against MTB with MIC ranging from 0.12-41.2 μM
- The synthesized compounds were evaluated for cytotoxicity against human cancer cell lines HepG2. All the active compounds showed low toxicity and the most potent compound 17 exhibited good safety profile with inhibitory rates as low as 8.8%.
- Compound 17- N-(2-(4-(benzyloxy) phenyl)-4-oxo-1, 3-thiazinan-3-yl)isonicotinamide inhibited MTB with MIC of 0.12 μM and was three times more potent than INH.



- The pharmacokinetic studies of compound 17 in male wistar rats were found to be $t_{1/2}$, K_{el} , mean plasma clearance and mean volume of distribution 1.14 ± 0.20 h, 0.62 ± 0.10 h⁻¹, 1.35 ± 0.16 mg/h and 1.99 ± 0.49 L respectively. The bioavailability was found to be 33.02%.

- Tissue distribution studies reveals that compound 17 concentrations are significantly above MIC levels in brain till 5 hours and in lungs at 2 hours post administration signifies that brain and lungs could be good therapeutic targets for this compound.
- Approximately 50-60% of the compound 17 administered orally is excreted unchanged in the faeces and very less amount of drug is excreted from urine in unchanged form
- Interaction of compound 17 with other drugs indicate the following
 - (i) Presence of substrate and inhibitor of CYP 1A enzyme change the plasma concentrations of compound 17 probably indicates that the metabolism of compound 17 may be mediated through CYP 1A enzyme.
 - (ii) Change in the plasma concentrations of substrate of CYP 2C enzyme and CYP 3A, indicates that compound 17 may be inhibiting both the enzymes
- 1,4-thiazines derivatives were synthesized via one pot domino sequence in presence of green catalyst (L) proline
- The purity of the compounds was ascertained by TLC, elemental analysis and their structures were elucidated by spectral data.
- All the compounds showed in vitro activity against MTB with MIC ranging from 0.57-98.9 μM . The most active compound being compound 7
- Cytotoxicity evaluations of these compounds on HEK 293T cells showed that none of them were significantly cytotoxic
- Compound 7 also have the ability to affects the viability of dormant 'non-culturable' M. tuberculosis cells.
- 3D QSAR contour map supported the structure activity relationship of thiazine moiety revealing that the electron withdrawing group at the C-3 and C-4 positions resulted in increased activity.

Future perspectives

The present thesis work has given rise to novel 1, 3 and 1, 4 thiazine derivatives possessing antimicrobial activities in invitro models. Although all the synthesized have been found to process promising antitubercular activity, extensive studies have to be performed to prove the invivo efficacy, metabolism, formulation and toxicity. Further, with the help of molecular modeling the chemical structure should be modified in order to gain more inhibitory activity against *M.tuberculosis* growth thereby compensate for the toxicity and more permeable to the resistant strains.

We should shift our focus on, integration of in silico and traditional wet lab drug discovery techniques, applying chemical biology and rational drug design strategies to new biochemical key targets.

References

1. Stephen D Lawn., Alimuddin I Zumla., Tuberculosis. *The Lancet*. 2011, 378: 57-72.
2. World Health Organization (WHO). Global tuberculosis Control. *Tuberculosis*. 2011,
3. Gandhi NR, Nunn P, Dheda K, Schaaf HS, Zignol M, van Soolingen D, Jensen P, Bayona J. Multidrug-resistant and extensively drug-resistant tuberculosis: a threat to global control of tuberculosis. *The Lancet*. 2010, 375:1830-43.
4. Ruth Hershberg., Mikhail Lipatov., Peter M. Small., HadarSheffer., Stefan Niemann., Susanne Homolka., Jared C. Roach., Kristin Kremer., Dmitri A. Petrov., Marcus W. Feldman., Sebastien Gagneux., TB INDIA 2009 RNTCP Status Report. *PLoS Biology*, 2008, 6: 2658-2671.
5. Dye C., Williams B. G., The Population Dynamics and Control of Tuberculosis. *Science*. 2010, 328: 856–861.
6. Neel R Gandhi., Anthony Moll., A Willem Sturm., Robert Pawinski., Thiloshini Govender., Umesh Laloo., Kimberly Zeller., Jason Andrews., Gerald Friedland., Extensively drug-resistant tuberculosis as a cause of death in patients co-infected with tuberculosis and HIV in a rural area of South Africa. *The Lancet*. 2006, 368: 1575 -1580.
7. Hershberg R., Lipatov M., Small PM., Sheffer H., Niemann S et al., High Functional Diversity in Mycobacterium tuberculosis Driven by Genetic Drift and Human Demography. *PLoS Biol*. 2008, 6: 2658 – 2671.
8. Riley R. L., Aerial dissemination of pulmonary tuberculosis. *American review of Tuberculosis*. 1957, 76: 931–941.
9. Scanning electron micrograph of mycobacterium tuberculosis bacteria [figure on internet] Available from: http://explow.com/mycobacterium_tuberculosis_tb
10. Liem Nguyen., Jean Pieters., Mycobacterial Subversion of Chemotherapeutic Reagents and Host Defense Tactics: Challenges in Tuberculosis Drug Development. *Annual Review of Pharmacology and Toxicology*. 2009, 49: 427-453.
11. Barkan D., Hedhli D., Yan HG., Huygen K., Glickman MS., Mycobacterium tuberculosis lacking all mycolic acid cyclopropanation is viable but highly attenuated and hyperinflammatory in mice. *Infection and immunity*. 2012, 80: 1958-1968.

12. Anil Koul., Eric Arnoult., NacerLounis., Jerome Guillemont., KoenAndries., The challenge of new drug discovery for Tuberculosis. *Nature*.2011, 469: 483-490.
13. Esmail H., Barry C.E., Wilkinson RJ., Understanding latent tuberculosis: the key to improved diagnostic and novel treatment strategies. *Drug Discovery Today*. 2012. 17: 514-521.
14. Barry C. E. III et al., The spectrum of latent tuberculosis: rethinking the biology and intervention strategies. *Nature Reviews Microbiology*.2009, 7: 845–855.
15. Global Report on Surveillance and Response, *Multidrug and Extensive Drug Resistant Tuberculosis*, World Health Organization, 2010.
16. Aamir J Khan., Saira Khowaja, Faisal S Khan, Fahad Qazi, Ismat Lotia, Ali Habib, Shama Mohammed, Uzma Khan, Farhana Amanullah, Hamidah Hussain, Mercedes C Becerra, Jacob Creswell, Salmaan Keshavjee., Engaging the private sector to increase tuberculosis case detection: an impact evaluation study *The Lancet Infectious Diseases*. 2012, 12: 608-616.
17. Carole Mitnick., Jaime Bayona., Eda Palacios., Sonya Shin., Jennifer Furin., Felix Alcántara., Epifanio Sánchez., MadelenySarria., Mercedes Becerra., Mary C. Smith Fawzi., SaidiKapiga., Donna Neuberg., James H. Maguire., Jim Yong Kim., and Paul Farmer., Community-Based Therapy for Multidrug-Resistant Tuberculosis in Lima, Peru. *The New England Journal of Medicine*. 2003, 348: 119–128.
18. Ma Z., Lienhardt C., McIlleron H., Nunn A. J. & Wang X., Global tuberculosis drug development pipeline: the need and the reality. *The Lancet*.2010, 375: 2100–2109.
19. World Health Organization. The Global Plan to Stop TB 2011–2015: Transforming the Fight Towards Elimination of Tuberculosis.
20. Gerhard Walzl., Katharina Ronacher., Willem Hanekom., Thomas J. Scriba & Alimuddin Zumla., Immunological biomarkers of tuberculosis. *Nature Reviews Immunology*.2011, 11: 343-354.
21. Clare V. Smith., Vivek Sharma., James C. Sacchettini., TB drug discovery: addressing issues of persistence and resistance Tuberculosis. *Tuberculosis*.2004, 84: 45-55.
22. Ann M Ginsberg & Melvin Spigelman., Challenges in tuberculosis drug research and development. *Nature Medicine*.2007, 13: 290-294.

23. Nguyen L., Pieters J., Mycobacterial subversion of chemotherapeutic reagents and host defense tactics: challenges in tuberculosis drug development. *Annual Review of Pharmacology and Toxicology*.2009, 49: 427-453.
24. Chopra P., Meena L.S. & Singh Y., New drug targets for Mycobacterium tuberculosis. *Indian Journal of Medical Microbiology*. 2003, 117:1-9
25. Casenghi M., Cole ST., Nathan CF., New approaches to filling the gap in tuberculosis drug discovery. *PLoS Medicine* 2007, 4:e293
26. Ying Zhang., L. Mario Amzel., Tuberculosis Drug Targets. *Current Drug Targets*.2002, 3: 131-154.
27. Vohra R., Gupta M., Chaturvedi R., Singh Y., Attack on the scourge of tuberculosis: patented drug targets. *Recent Patents on Anti-infective Drug Discovery*.2006, 1: 95-106.
28. Edward D Chan., Michael D Iseman., Current medical treatment for tuberculosis. *British Medical Journal*. 2002, 325: 30: 1282-1286.
29. Claire Harper., Tuberculosis, a neglected opportunity? *Nature Medicine*.2007, 13: 309-312.
30. Zhang Y., The magic bullets and tuberculosis drug targets. *Annual Review Pharmacology and Toxicology*.2005, 45: 529-564.
31. Hasan S., Daugelat S., Rao PS., Schreiber M. Prioritizing genomic drug targets in pathogens: application to Mycobacterium tuberculosis. *PLoS. Computational Biology*. 2006, 2 :e 61
32. Mdluli K., Spigelman M., Novel targets for tuberculosis drug discovery. *Current Opinion Pharmacology*.2006, 6: 459-467.
33. Duncan K., Identification and validation of novel drug targets in tuberculosis. *Current Pharmaceutical Design*.2004, 10: 3185-3194.
34. Palomino J.C., Ramos D.F., da Silva P.A., New anti-tuberculosis drugs: strategies, sources and new molecules. *Current Medicinal Chemistry*.2009, 16: 1898-1904.
35. Zhang Y., Post-Martens K., Denkin S., New drug candidates and therapeutic targets for tuberculosis therapy. *Drug Discovery Today*.2006, 11: 21-27.
36. Cole S.T., Brosch R., Parkhill J., Garnier T., Churcher C., Harris D., Gordon S.V., Eiglmeier K., Gas S., Barry C.E. 3rd, Tekaiia F., Badcock K., Basham D., Brown D.,

Chillingworth T., Connor R., Davies R., Devlin K., Feltwell T., Gentles S., Hamlin N., Holroyd S., Hornsby T., Jagels K., Krogh A., McLean J., Moule S., Murphy L., Oliver K., Osborne J., Quail MA., Rajandream M.A., Rogers J., Rutter S., Seeger K., Skelton J., Squares R., Squares S., Sulston JE., Taylor K., Whitehead S., Barrell BG. Deciphering the biology of *Mycobacterium tuberculosis* from the complete genome sequence. *Nature*.1998, 393: 537-544.

37. Brennan P.J., Crick D.C., The cell-wall core of *Mycobacterium tuberculosis* in the context of drug discovery. *Current Topics in Medicinal Chemistry*.2007, 7: 475-488.

38. Khasnobis S., Escuyer V.E., Chatterjee D., Emerging therapeutic targets in tuberculosis: post-genomic era. *Expert Opinion on Therapeutic Targets*.2002, 6: 21-40.

39. Sarkar S., Suresh M.R., An overview of tuberculosis chemotherapy - a literature review. *Journal of Pharmacy and Pharmaceutical Sciences*.2011, 14: 148-161.

40. Eoh H., Brennan P.J., Crick D.C., The *Mycobacterium tuberculosis* MEP (2C-methyl-erythritol 4-phosphate) pathway as a new drug target. *Tuberculosis*.2009, 89: 1-11.

41. Mahapatra S., Yagi T., Belisle J.T., Espinosa BJ., Hill PJ., McNeil M.R., Brennan P.J., Crick D.C., Mycobacterial lipid II is composed of a complex mixture of modified muramyl and peptide moieties linked to decaprenyl phosphate. *Journal Bacteriology*.2005, 187: 2747-2757.

42. Anderson R.G., Hussey H., Baddiley J., The mechanism of wall synthesis in bacteria.The organization of enzymes and isoprenoid phosphates in the membrane. *The Biochemical Journal*. 1972, 127: 11-25.

43. Shan Shan, Xuehui Chen., Ting Liu., Hanchao Zhao., Zihe Rao., Zhiyong Lou., Crystal structure of 4-diphosphocytidyl-2-C-methyl-D-erythritol kinase (IspE) from *Mycobacterium tuberculosis*. *The FASEB Journal article*. 2011, 25:1577-1584

44. Ryo Murakami., Yasunori Muramatsu., Emiko Minami., Kayoko Masuda., Yoshiharu Sakaida., Shuichi Endo., Takashi Suzuki., Osamu Ishida., Toshio Takatsu., Shunichi Miyakoshi., Masatoshi Inukai., Fujio Isono., A novel assay of bacterial peptidoglycan synthesis for natural product screening A novel assay of bacterial peptidoglycan synthesis. *The Journal of Antibiotics*.2009, 62: 153-158.

45. Feng Z., Barletta R.G., Roles of *Mycobacterium smegmatis* D-alanine: D-alanine ligase and D-alanine racemase in the mechanisms of action of and resistance to the

peptidoglycan inhibitor D-cycloserine. *Antimicrobial Agents and Chemotherapy*.2003, 47: 283-291.

46. Strych U., Penland R.L., Jimenez M., Krause K.L., Benedik M.J., Characterization of the alanine racemases from two mycobacteria. *FEMS Microbiology Letters*.2001, 196: 93-98.

47. LeMagueres P., Im H., Ebalunode J., Strych U., Benedik MJ., Briggs JM., Kohn H., Krause KL., The 1.9 Å crystal structure of alanine racemase from *Mycobacterium tuberculosis* contains a conserved entryway into the active site. *Biochemistry*.2005, 44: 1471-1481.

48. Sassetti CM., Boyd D.H., Rubin EJ. Genes required for mycobacterial growth defined by high density mutagenesis. *Molecular Microbiology*.2003, 48: 77-84.

50. Huang H., Berg S., Spencer JS., Vereecke D., D'Haese W., Holsters M., McNeil MR., Identification of amino acids and domains required for catalytic activity of DPPR synthase, a cell wall biosynthetic enzyme of *Mycobacterium tuberculosis*. *Microbiology*, 2008, 154:736-743

51. Belanger A.E., Besra G.S., Ford M.E., Mikusova K., Belisle J.T., Brennan P.J., Inamine J.M., The embAB genes of *Mycobacterium avium* encode an arabinosyltransferase involved in the cell wall arabinan biosynthesis that is the target for the antimycobacterial drug ethambutol. *Proceedings of the National Academy of Sciences, USA*.1996, 93: 11919-11924.

52. Escuyer V.E., Lety M.A., Torrelles J.B., Khoo K.H., Tang J.B., Rithner C.D., Frehel C., McNeil M.R., Brennan P.J., Chatterjee D., The role of the embA and embB gene products in the biosynthesis of the terminal hexaarabinofuranosyl motif of *Mycobacterium smegmatis* arabinogalactan. *The Journal of Biological Chemistry*. 2001, 276: 48854-48862.

53. Alderwick L.J., Seidel M., Sahm H., Besra G.S., Eggeling L., Identification of a novel arabinofuranosyltransferase (AftA) involved in cell wall arabinan biosynthesis in *Mycobacterium Tuberculosis*. *The Journal of Biological Chemistry*.2006, 281: 15653-15661.

54. Sassetti C.M., Boyd D.H., Rubin E.J., Genes required for mycobacterial growth defined by high density mutagenesis. *Molecular Microbiology*.2003, 48: 77-84.

55. Huang H., Scherman M.S., D'Haese W., Vereecke D., Holsters M., Crick D.C., McNeil M.R., Identification and active expression of the *Mycobacterium tuberculosis* gene encoding 5-phospho- α -D-ribose-1-diphosphate: decaprenyl-phosphate 5-phosphor ribosyltransferase, the first enzyme committed to decaprenylphosphoryl-D-arabinose synthesis. *The Journal of Biological Chemistry*.2005, 280: 24539-24543.
56. Brennan, P.J., Crick, D.C., The cell-wall core of *Mycobacterium tuberculosis* in the context of drug discovery. *Current Topics in Medicinal Chemistry*.2007, 7: 475-488.
57. Heath R.J., White S.W., Rock CO., Lipid biosynthesis as a target for antibacterial agents. *Progress in Lipid Research*.2001, 40: 467-497.
58. Schroeder E.K., de Souza N., Santos D.S., Blanchard J.S., Basso L.A., Drugs that inhibit mycolic acid biosynthesis in *Mycobacterium tuberculosis*. *Current Pharmaceutical Biotechnology*.2002, 3: 197-225.
59. McKinney J.D., HönerzuBentrop K., Muñoz-Elías EJ., Miczak A., Chen B., Chan, W.T., Swenson D., Sacchettini J.C., Jacobs W.R. Jr., Russell DG., Persistence of *Mycobacterium tuberculosis* in macrophages and mice requires the glyoxylate shunt enzyme isocitratelase. *Nature*.2000, 406: 735-738.
60. Savvi S., Warner D.F., Kana B.D., McKinney J.D., Mizrahi V., Dawes S.S., Functional characterization of a vitamin B₁₂-dependent methylmalonyl pathway in *Mycobacterium tuberculosis*: implications for propionate metabolism during growth on fatty acids. *Journal of Bacteriology*.2008, 190: 3886-3895.
61. Parish T., Stoker N.G., The common aromatic amino acid biosynthesis pathway is essential in *Mycobacterium tuberculosis*. *Microbiology*.2002, 148: 3069-3077.
62. Ducati R.G., Basso L.A., Santos D.S., Mycobacterial shikimate pathway enzymes as targets for drug design. *Current Drug Targets*.2007, 8: 423-435.
63. Magalhães M.L., Pereira C.P., Basso L.A., Santos D.S., Cloning and expression of functional shikimate dehydrogenase (EC 1.1.1.25) from *Mycobacterium tuberculosis* H37Rv. *Protein Expression and Purification*.2002, 26: 59-64.
64. Oliveira J.S., Pinto C.A., Basso L.A., Santos D.S., Cloning and over expression in soluble form of functional shikimate kinase and 5-enolpyruvylshikimate 3-phosphate synthase enzymes from *Mycobacterium tuberculosis*. *Protein Expression and Purification*.2001, 22: 430-435.

65. Pavelka M.S. Jr., Jacobs W.R. Jr., Comparison of the construction of unmarked deletion mutations in *Mycobacterium smegmatis*, *Mycobacterium bovis* bacillus Calmette- Guérin, and *Mycobacterium tuberculosis* H37Rv by allelic exchange. *Journal of Bacteriology*.1999, 181: 4780-4789.
66. Smith D.A., Parish T., Stoker N.G., Bancroft G.J., Characterization of auxotrophic mutants of *Mycobacterium tuberculosis* and their potential as vaccine candidates. *Infection and Immunity*.2001, 69: 1142-1150.
67. Pavelka M.S. Jr., Chen B., Kelley C.L., Collins F.M., Jacobs W.R. Jr., Vaccine efficacy of a lysine auxotroph of *Mycobacterium tuberculosis*. *Infection and Immunity*.2003, 71: 4190-4192.
68. Paiva A.M., Vanderwall D.E., Blanchard J.S., Kozarich, J.W., Williamson J.M., Kelly T.M., Inhibitors of dihydrodipicolinatereductase, a key enzyme of the diaminopimelate pathway of *Mycobacterium tuberculosis*. *Biochimica et BiophysicaActa*. 2001, 1545: 67-77.
69. Gerum A.B., Ulmer J.E., Jacobus D.P., Jensen N.P., Sherman D.R., Sibley C.H., Novel *Saccharomyces cerevisiae* screen identifies WR99210 analogues that inhibit *Mycobacterium tuberculosis* dihydrofolate reductase. *Antimicrobial Agents and Chemotherapy*.2002, 46: 3362-3369.
70. Huovinen P., Sundström L., Swedberg G., Sköld O., Trimethoprim and sulfonamide resistance. *Antimicrobial Agents and Chemotherapy*.1995, 39: 279-289.
71. Bellinzoni M., De Rossi E., Branzoni M., Milano A., Peverali F.A., Rizzi M., Riccardi G., Heterologous expression, purification, and enzymatic activity of *Mycobacterium tuberculosis* NAD(+) synthetase. *Protein Expression and Purification*.2002, 25: 547-557.
72. Boshoff HI., Xu X., Tahlan K., Dowd C.S., Pethe K., Camacho L.R., Park T.H., Yun C.S., Schnappinger D., Ehrt S., Williams K.J., Barry C.E., Biosynthesis and recycling of nicotinamide cofactors in *Mycobacterium tuberculosis*. An essential role for NAD in nonreplicating bacilli. *The Journal of Biological Chemistry*. 2008, 283: 19329-19341.
73. Morgunova E., Meining W., Illarionov B., Haase I., Jin G., Bacher A., Cushman M., Fischer M., Ladenstein R., Crystal structure of lumazine synthase from *Mycobacterium*

tuberculosis as a target for rational drug design: binding mode of a new class of purine triene inhibitors. *Biochemistry*.2005, 44: 2746-2758.

74. Haouz A., Vanheusden V., Munier-Lehmann H., Froeyen M., Herdewijn P., Van Calenbergh S., Delarue M., Enzymatic and structural analysis of inhibitors designed against *Mycobacterium tuberculosis* thymidylate kinase. New insights into the phosphoryl transfer mechanism. *The Journal of Biological Chemistry*.2003, 278: 4963-4971.

75. Vanheusden V., Munier-Lehmann H., Pochet S., Herdewijn P., Van Calenbergh S. Synthesis and evaluation of thymidine-5'-O-monophosphate analogues as inhibitors of *Mycobacterium tuberculosis* thymidylate kinase. *Bioorganic and Medicinal Chemistry Letters*.2002, 12: 2695-2698.

76. Yang F., Curran S.C., Li L.S., Avarbock D., Graf J.D., Chua M.M., Lu G., Salem J., Rubin H., Characterization of two genes encoding the *Mycobacterium tuberculosis* ribonucleotide reductase small subunit. *Journal of Bacteriology*.1997, 179: 6408-6415.

77. Yang F., Lu G., Rubin H., Isolation of ribonucleotide reductase from *Mycobacterium tuberculosis* and cloning, expression, and purification of the large subunit. *Journal of Bacteriology*.1994, 176: 6738-6743.

78. Gong C., Martins A., Bongiorno P., Glickman M., Shuman S., Biochemical and genetic analysis of the four DNA ligases of mycobacteria. *The Journal of Biological Chemistry*.2004, 279: 20594-20606.

79. Srivastava S.K., Tripathi R.P., Ramachandran R., NAD⁺-dependent DNA Ligase (Rv3014c) from *Mycobacterium tuberculosis*. Crystal structure of the adenylation domain and identification of novel inhibitors. *The Journal of Biological Chemistry*.2005, 280: 30273-30281.

80. Meganathan R., Biosynthesis of menaquinone (vitamin K₂) and ubiquinone (coenzyme Q): a perspective on enzymatic mechanisms. *Vitamins & Hormones*.2001, 61: 173-218.

81. Cole S.T., and Alzari P.M., Towards new tuberculosis drugs. *Biochemical Society Transactions*.2007, 35: 1321-1324.

82. McLean K.J., Dunford A.J., Neeli R., Driscoll M.D., Munro A.W., Structure, function and drug targeting in *Mycobacterium tuberculosis* cytochrome P450 systems. *Archives of Biochemistry and Biophysics*.2007, 464: 228-240.
83. Leys D., Mowat C.G., McLean K.J., Richmond A., Chapman S.K., Walkinshaw M.D., Munro A.W., Atomic structure of *Mycobacterium tuberculosis* CYP121 to 1.06 Å⁰ reveals novel features of cytochrome P450. *The Journal of Biological Chemistry*.2003, 278: 5141-5147.
84. Teo JW., Thayalan P., Beer D., Yap A.S., Nanjundappa M., Ngew X., Duraiswamy J., Liung S., Dartois V., Schreiber M., Hasan S., Cynamon M., Ryder N.S., Yang X., Weidmann B., Bracken K., Dick T., Mukherjee K., Peptide deformylase inhibitors as potent antimycobacterial agents. *Antimicrobial Agents and Chemotherapy*.2006, 50: 3665-3673.
85. Khasnobis S., Escuyer V.E., Chatterjee D., Emerging therapeutic targets in tuberculosis: post-genomic era. *Expert Opinion on Therapeutic Targets*.2002, 6: 21-40.
86. Monfeli R.R., Beeson C., Targeting iron acquisition by *Mycobacterium tuberculosis* Infectious Disorders. *Drug Targets*.2007, 7: 213-220.
87. Weinberg E.D., Miklossy J., Iron withholding: a defense against disease., *Journal of Alzheimer's Disease*.2008, 13: 451-463.
88. Ferreras J.A., Ryu J.S., Di Lello F., Tan D.S., Quadri L.E., Small-molecule inhibition of siderophore biosynthesis in *Mycobacterium tuberculosis* and *Yersinia pestis*. *Nature Chemical Biology*.2005, 1: 29-32.
89. Av-Gay Y., Everett M., The eukaryotic-like Ser/Thr protein kinases of *Mycobacterium tuberculosis*. *Trends in Microbiology*.2000, 8: 238-244.
90. Fernandez P., Saint-Joanis B., Barilone N., Jackson M., Gicquel B., Cole ST., Alzari P.M., The Ser/Thr protein kinase PknB is essential for sustaining mycobacterial growth. *Journal of Bacteriology*.2006, 188: 7778-7784.
91. Sareen D., Newton GL., Fahey R.C., Buchmeier N.A., Mycothiol is essential for growth of *Mycobacterium tuberculosis* Erdman. *Journal of Bacteriology*.2003, 185: 6736-6740.

92. Imramovsky A., Polanc S., Vinsova J., kocevar M., Jampilek J., Reckova Z., Kaustova J., A new modification of anti-tubercular active molecules. *Bioorganic & Medicinal Chemistry*.2007, 15: 2551-2559.
93. Navarrete-Vázquez G., Molina-Salinas G.M., Duarte-Fajardo, Z.V., Vargas-Villarreal J., Estrada-Soto S., Gonzalez-Salazar F., Hernandez-Nuñez E., Said-Fernández, S., Synthesis and antimycobacterial activity of 4-(5-substituted-1,3,4-oxadiazol-2-yl) pyridines. *Bioorganic & Medicinal Chemistry*.2007, 15: 5502-5508.
94. Hearn M.J., Cynamon M.H., Chen M.F., Coppins R., Davis J., Joo-On Kang H., Noble A., Tu-Sekine B., Terrot MS., Trombino D., Thai M., Webster ER., Wilson R. Preparation and antitubercular activities in vitro and in vivo of novel Schiff bases of isoniazid. *European Journal of Medicinal Chemistry*.2009, 44: 4169-4178.
95. Delaine T., Bernades-Genisson V., Quemard A., Constant P., Meunier B., Bernadou J., Development of isoniazid-NAD truncated adduct embedding a lipophilic fragment as potential bi-substrate InhA inhibitors and antimycobacterial agents. *European Journal of Medicinal Chemistry*.2010, 45: 4554-4561.
96. Meng Q., Luo H., Lu Y., Li W., Zhang W., Yao Q., Synthesis and evaluation of carbamate prodrugs of SQ109 as anti tuberculosis agents. *Bioorganic & Medicinal Chemistry Letters*.2009, 19: 2808-2810.
97. Zhang X., Hu Y., Chen S., Luo R., Yue J., Zhang Y., Duan W., Wang H., Synthesis and evaluation of (S,S)-N,N'-bis[3-(2,2',6,6'-tetramethylbenzhydryloxy)-2-hydroxypropyl]-ethylenediamine (S2824) analogs with anti-tuberculosis activity. *Bioorganic & Medicinal Chemistry Letters*.2009, 19: 6074-6077.
98. Cunico W., Gomes C.R., Ferreira M.L., Ferreira T.G., Cardinot D., de Souza M.V., Lorencó M.C., Synthesis and anti-mycobacterial activity of novel amino alcohol derivatives. *European Journal of Medicinal Chemistry*.2011, 46: 974-978.
99. Nava-Zuazo C., Estrada-Soto S., Guerrero-Alvarez J., Leon-Rivera I., Molina-Salinas G.M., Said-Fernández S., Chan-Bacab MJ., Cedillo-Rivera R., Moo-Puc R., Mirón-Lopez G., Navarrete-Vázquez G., Design, synthesis and in vitro anti protozoal, antimycobacterial activities of N-{2-[(7-chloroquinolin-4-yl) amino]ethyl} ureas. *Bioorganic & Medicinal Chemistry*.2010, 18: 6398-6403.

100. Imramovsky A., Vinsova J., Ferriz JM., Buchta V., Jampilek J., Salicylanilide esters of N-protected amino acids as novel antimicrobial agents. *Bioorganic & Medicinal Chemistry Letters*.2008, 19: 348-351.
101. Ferriz J.M., Vavrova K., Kunc F., Imramovsky A., Stolarikova J., Vavrikova E., Vinsova J, Salicylanilide carbamates: Anti tubercular agents active against multi drug resistant *Mycobacterium tuberculosis* strains. *Bioorganic & Medicinal Chemistry*.2009, 18: 1054-1061.
102. Petrlikova E., Waisser K., Divisova H., Husakova P., Vrabcova P., Kunes J., Kolar K., Stolarikova J., Highly active antimycobacterial derivatives of benzoxazine. *Bioorganic & Medicinal Chemistry*.2010, 18: 8178-8187.
103. Eswaran S., Adhikari A.V., Chowdhury I.H., Pal N.K., Thomas K., New quinolone derivatives: synthesis and investigation of antibacterial and antituberculosis properties. *European Journal of Medicinal Chemistry*.2010, 45: 3374-3383.
104. Eswaran S., Adhikari A.V., Kumar R., New 1,3-oxazolo[4,5-c] quinoline derivatives: Synthesis and evaluation of antibacterial and antituberculosis properties. *European Journal of Medicinal Chemistry*.2009, 45: 957-966.
105. Goncalves R.S., Kaiser C.R., Lourenco M.C., de Souza M.V., Wardell J.L., Wardell SM., da Silva AD., Synthesis and antitubercular activity of new mefloquine oxazolidine derivatives. *European Journal of Medicinal Chemistry*.2010, 45: 6095-6100.
106. Mao J., Yuan H., Wang Y., Wan B., Pak D., He R., Franzblau S.G., Synthesis and antituberculosis activity of novel mefloquine-isoxazole carboxylic esters as prodrugs. *Bioorganic & Medicinal Chemistry Letters*.2009, 20: 1263-1268.
107. Kini S.G., Bhat A.R., Bryant B., Williamson J., Dayan F.E., Synthesis, antitubercular activity and docking study of novel cyclic azole substituted diphenyl ether derivatives. *European Journal of Medicinal Chemistry*.2008, 44: 492-500.
108. Eswaran S., Adhikari A.V., Pal NK., Chowdhury I.H., Design and synthesis of some new quinoline-3-carbohydrazone derivatives as potential antimycobacterial agents. *Bioorganic & Medicinal Chemistry Letters*.2009, 20: 1040-1044.
109. Yang CL., Tseng CH., Chen YL., Lu CM., Kao CL., Wu MH., Tzeng CC., Identification of benzofuro [2,3-b] quinoline derivatives as a new class of antituberculosis agents. *European Journal of Medicinal Chemistry*.2009, 45: 602-607.

110. Zhang Y., Post-Martens K., Denkin S., New drug candidates and therapeutic targets for tuberculosis therapy. *Drug Discovery Today*.2006, 11: 21-27.
111. Wube A.A., Hufner A., Thomaschitz C., Blunder M., Kollroser M., Bauer R., Bucar F., Design, synthesis and antimycobacterial activities of 1-methyl-2-alkenyl- 4(1H)-quinolones. *Bioorganic & Medicinal Chemistry*.2010, 19: 567-579.
112. De Logu A., Palchykovska L.H., Kostina V.H., Sanna A., Meleddu R., Chisu L., Alexeeva IV., Shved AD., Novel N-aryl- and N-hetryl phenazine-1-carboxamide as potential targets for the treatment of infections sustained by drug-resistant and multidrug-resistant *Mycobacterium tuberculosis*. *International Journal of Antimicrobial Agents*.2008, 33: 223-229.
113. Vicente E., Perez-Silanes S., Lima L.M., Ancizu S., Burguete A., Solano B., Villar R., Aldana I., Monge A., Selective activity against *Mycobacterim tuberculosis* of new quinoxaline 1,4-di-N-oxides. *Bioorganic & Medicinal Chemistry*.2008, 17: 385-389.
114. Sainath S.R., Raghunathan R., Ekambaram R., Raghunathan M., In vitro activities of the newly synthesised ER-2 against clinical isolates of *Mycobacterium tuberculosis* susceptible or resistant to antituberculosis drugs. *International Journal of Antimicrobial Agents*.2009, 34: 451-453.
115. Shiradkar M., Suresh Kumar G.V., Dasari V., Tatikonda S., Akula KC., Shah R., Clubbed triazoles: A novel approach to antitubercular drugs. *European Journal of Medicinal Chemistry*.2006, 42: 807-816.
116. Gill C., Jadhav G., Shaikh M., Kale R., Ghawalkar A., Nagargoje D., Shiradkar M., Clubbed [1,2,3] triazoles by fluorine benzimidazole: A novel approach to H37Rv inhibitors as a potential treatment for tuberculosis. *Bioorganic & Medicinal Chemistry Letters*.2008, 18: 6244-6247.
117. Jadhav G.R., Shaikh M.U., Kale R.P., Shiradkar M.R., Gill C.H., SAR study of clubbed [1,2,4]-triazolyl with fluorobenzimidazoles as antimicrobial and anti tuberculosis agents. *European Journal of Medicinal Chemistry*, 2008, 44 (7), 2930-2935.
118. Klimesova V., Koci J., Waisser K., Kaustova J., Mollmann U., Preparation and invitro evaluation of benzyl sulfanyl benzoxazole derivatives as potential anti tuberculosis agents. *European Journal of Medicinal Chemistry*.2008, 44: 2286-2293.

119. Patel N.B., Khan R.H., Rajani S.D., Pharmacological evaluation and characterizations of newly synthesized 1,2,4-triazoles. *European Journal of Medicinal Chemistry*.2010, 45: 4293-4299.
120. Suresh Kumar G.V., Rajendra Prasad Y., Mallikarjuna B.P., Chandrashekar S.M., Synthesis and pharmacological evaluation of clubbed isopropylthiazole derived triazolothiadiazoles, triazolothiadiazines and mannich bases as potential antimicrobial and antitubercular agents. *European Journal of Medicinal Chemistry*.2010, 45: 5120-5129.
121. Izumizono Y., Arevalo S., Koseki Y., Kuroki M., Aoki S. Identification of novel potential antibiotics for tuberculosis by in silico structure-based drug screening. *European Journal of Medicinal Chemistry*.2011, 46: 1849-1856.
122. Manikannan R., Venkatesan R., Muthusubramanian., Yogeeswari P., Sriram D., Pyrazole derivatives from azines of substituted phenacyl aryl/cyclohexyl sulfides and their antimycobacterial activity. *Bioorganic & Medicinal Chemistry Letters*.2010, 20: 6920-6924.
123. Samadhiya P., Sharma R., Srivastava S.K., Srivastava S.D., Synthesis and biological evaluation of 4-thiazolidinone derivatives as antitubercular and antimicrobial agents. *Arabian Journal of Chemistry*. doi: 10.1016/j.arabjc.2010.11.015, (Dec, 2010), ISSN 1878-5352.
124. Karthikeyan S.V., Bala B.D., Raja V.P., Perumal S., Yogeeswari P., Sriram D. A highly atom economic, chemo-, regio and stereoselective synthesis and evaluation of spiro-pyrrolothiazoles as antitubercular agents. *Bioorganic & Medicinal Chemistry Letters*.2009, 20: 350-353.
125. Turan-Zitouni G., Ozdemir A., Kaplancikli Z.A., Benkli K., Chevallet P., Akalin G., Synthesis and antituberculosis activity of new thiazolyldiazone derivatives. *European Journal of Medicinal Chemistry*.2007, 43: 981-985.
126. Turan-Zitouni G., Kaplancikli Z.A., Ozdemir A., Synthesis and antituberculosis activity of some N-pyridyl-N-thiazolyldiazine derivatives. *European Journal of Medicinal Chemistry*.2010, 45: 2085-2088.
127. Sankar C., Pandiarajan K., Synthesis and anti-tubercular and antimicrobial activities

of some 2r,4c-diaryl-3-azabicyclo[3.3.1]nonan-9-one N-isonicotinylhydrazone derivatives. *European Journal of Medicinal Chemistry*.2010, 45: 5480-5485.

128. Bairwa R., Kakwani M., Tawari N.R., Lalchandani J., Ray M.K., Rajan M.G., Degani M.S., Novel molecular hybrids of cinnamic acids ad guanylhydrazones as potential antitubercular agents. *Bioorganic & Medicinal Chemistry Letters*.2010, 20: 1623-1625.

129. Correia C., Carvalho M.A., Proenca M.F., Synthesis and in vitro activity of 6-amino-2, 9-diarylpurines for *Mycobacterium tuberculosis*. *Tetrahedron*.2009, 65: 6903-6911.

130. Khoje A.D., Kulendrn A., Charnock C., Wan B., Franzblau S., Gundersen L.L., Synthesis of non-purine analogs of 6-aryl-9-benzylpurines, and their antimycobacterial activities. Compounds modified in the imidazole ring. *Bioorganic & Medicinal Chemistry*.2010, 18: 7274-7282.

131. Singh K., Singh K., Wan B., Franzblau S., Chibale K., Balzarini J., Facile transformation of biginelli pyrimidin-2(1H)-ones to pyrimidines. In vitro evaluation as inhibitors of *Mycobacterium tuberculosis* and modulators of cytostatic activity. *European Journal of Medicinal Chemistry*.2011, 46: 2290-2294.

132. Gasse C., Douguet D., Huteau V., Marchal G., Munier-Lehmann H., Pochet S., Substituted benzyl-pyrimidines targeting thymidine monophosphate kinase of *Mycobacterium tuberculosis*: Synthesis and in vitro anti-mycobacterial activity. *Bioorganic & Medicinal Chemistry*.2008, 16: 6075-6085.

133. Odell LR., Nilsson MT., Gising J., Lagerlund O., Muthas D., Nordqvist A., Karlen A., Larhed M., Functionalized 3-amino-imidazol[1,2-a]pyridines: A novel class of drug like *Mycobacterium tuberculosis* glutamine synthase inhibitors. *Bioorganic & Medicinal Chemistry Letters*.2009, 19: 4790-4793.

134. Fassihi A., Azadpour Z., Delbari N., Saghaie L., Memarian H.R., Sabet R., Alborzi A., Miri R., Pourabbas B., Mardaneh J., Mousavi P., Moeinifard B., Sadeghi-aliabdi H. Synthesis and antitubercular activity of novel 4-susbtituted imidazolyl-2.6-dimethyl-N3,N5-bisaryl-1,4-dihydropyridine-3,5-dicaroxamides", *European Journal of Medicinal Chemistry*.2009, 44: 3253-3258.

135. Mantu D., Luca M.C., Moldoveanu C., Zbancioc G., Mangalagiu., Synthesis and

antituberculosis activity of some new pyridazine derivatives. Part II. *European Journal of Medicinal Chemistry*.2010, 45: 5164-5168.

136. Sethuraman Indumathi., Subbu Perumal., Debjani Banerjee., Perumal Yogeewari., Dharmarajan Sriram., (L)-Proline-catalysed facile green protocol for the synthesis and antimycobacterial evaluation of [1,4]-thiazines. *European Journal of Medicinal Chemistry*.2009, 44: 4978–4984.

137. Güzel O., Karali N., Salman A., Synthesis and antituberculosis activity of 5-methyl/trifluoromethoxy-1H-indole-2,3-dione 3-thiosemicarbazone derivatives. *Bioorganic & Medicinal Chemistry*.2008, 16: 8976-8987.

138. Karali N., Gürsoy A., Kandemirli F., Shvets N., Kaynak F.B., Özbey., Kovalishyn V., Dimoglo A., Synthesis and structure-antituberculosis activity relationship of 1H-indole-2,3-dione derivatives. *Bioorganic & Medicinal Chemistry*.2007, 15: 5888-5904.

139. Kamal A., Shett RVCRCN., Azeza, S., Ahmed, SK., Swapna P., Reddy A.M., Khan I.A., Sharma S., Abdullah S.T., Anti-tubercular agents. Part 5: Synthesis and biological evaluation of benzothiadiazine 1,1-dioxide based congeners. *European Journal of Medicinal Chemistry*.2010 45: 4545-4553.

140. Termentzi A., Khouri I., Gaslonde T., Prado S., Saint-Joanis B., Bardou F., Amanatiadou E.P., Vizirianakis I., Kordulakova J., Jackson M., Brisch R., Janin YL., Daffe M., Tillequin F., Michel S., Synthesis, biological activity and evaluation of the mode of action of novel antitubercular benzofurobenzopyrans substituted on A ring. *European Journal of Medicinal Chemistry*.2010, 45: 5833-5847.

141. Santos J.L., Yamasaki P.R., Chin C.M., Takashi C.H., Pavan F.R., Leite CQF., “Synthesis and in vitro anti *Mycobacterium tuberculosis* activity of a series of phthalimide derivatives. *Bioorganic & Medicinal Chemistry*.2009, 17: 3795-3799.

142. Yoya G.K., Bedos-Belval F., Constante P., Duran H., Daffe M., Balatas M., Synthesis and evaluation of a novel series of pseudo-cinnamic derivatives as antituberculosis agents. *Bioorganic & Medicinal Chemistry Letters*.2008, 19: 341- 343.

143. D’Oca., Cda R., Coelho T., Marinho T.G., Hack C.R., Duarte Rda C., da Silva P.A., D’Oca M.G., Synthesis and antituberculosis activity of new fatty acid amides. *Bioorganic & Medicinal Chemistry Letters*.2010, 20: 5255-5257.

144. Stover C.K. et al., A small-molecule nitroimidazopyran drug candidate for the treatment of tuberculosis. *Nature*. xxxx, 405: 962–966.
145. Baker W.R. et al. *Nitroimidazole antibacterial compounds and methods of use thereof* United States patent 5668127, 2009.
146. Baker W.R. et al. *Nitro-[2,1-b]imidazopyran compounds and antibacterial uses thereof* United States patent 6087358, 2009.
147. Barry C.E. et al., Prospects for clinical introduction of nitroimidazole antibiotics for the treatment of tuberculosis. *Current Pharmaceutical Design*.2004, 10: 3239–3262.
148. Lenaerts A.J. et al., Preclinical testing of the nitroimidazopyran PA-824 for activity against *Mycobacterium tuberculosis* in a series of in vitro and in vivo models. *Antimicrobial Agents and Chemotherapy*.2005, 49: 2294–2301.
149. Tyagi S. et al., Bactericidal activity of the nitroimidazopyran PA-824 in a murine model of tuberculosis. *Antimicrobial Agents and Chemotherapy*.2005, 49: 2289–2293.
150. Nuermberger E. et al., Combination chemotherapy with the nitroimidazopyran PA-824 and first-line drugs in a murine model of tuberculosis. *Antimicrobial Agents and Chemotherapy*.2006, 50: 2621–2625.
151. Sasaki H. et al., Synthesis and antituberculosis activity of a novel series of optically active 6-nitro-2,3-dihydroimidazol[2.1-b]oxazoles. *J. Med. Chem.* 2006, 49: 7854–7860.
152. Matsumoto M. et al., OPC-67683, a nitro-dihydro-imidazooxazole derivative with promising action against tuberculosis in vitro and in mice. *PLoS Med.* 2006, 3: 2131-2144.
153. Van Gestel., J.F.E. et al., *Quinoline derivatives and their use as mycobacterial Inhibitors*. International patent WO/2004/011436, 2004.
154. Andries K. et al., A diarylquinoline drug active on the ATP synthase of *Mycobacterium tuberculosis*. *Science*.2005, 307: 223–227.
155. Gaurrand S., Conformational analysis of R207910, a new drug candidate for the treatment of tuberculosis, by a combined NMR and molecular modeling approach. *Chemical Biology and Drug Design*.2006, 68: 77–84.
156. Huitric, E. et al., In vitro antimycobacterial spectrum of a diarylquinoline ATP synthase inhibitor. *Antimicrobial Agents and Chemotherapy*.2007, 51: 4202–4204.

157. Arora S.K. et al., Design, synthesis, modelling and activity of novel antitubercular compounds Abstract, 227th. ACS National Meeting, Anaheim, CA, Division of Medicinal Chemistry (Abstract # 63).
158. Arora, S.K. et al. "Pyrrole derivatives as antimycobacterial compounds", International patent, 2004, WO/2004/026828
159. Matsumoto M. et al., Screening for novel antituberculosis agents that are effective against multidrug resistant tuberculosis. *Current Topics in Medicinal Chemistry*. 2007, 7: 499–507.
160. Rivers E.C., Mancera R.L., New anti-tuberculosis drugs in clinical trials with novel mechanisms of action. *Drug Discovery Today*.2008, 13: 1090-1098.
161. Janin Y.L., Antituberculosis drugs: ten years of research. *Bioorganic and Medicinal Chemistry*.2007, 15: 2479-2513.
162. Shi R., Sugawara I., Development of new anti-tuberculosis drug candidates. *The Tohoku Journal of experimental medicine*.2010, 22: 97-106.
163. De Jong B. C., Israelski D. M., Corbett E. L., Small P. M., Clinical management of tuberculosis in the context of HIV infection. *Annual Review of Medicine*. 2004, 55: 283-301.
164. Alland D., Kalkut G. E., Moss, A. R., Transmission of tuberculosis in New York City. An analysis by DNA fingerprinting and conventional epidemiologic methods. *The New England Journal of Medicine*. 1994, 330: 1710-1716.
165. Whalen C., Horsburgh C. R., Hom D., Accelerated course of human immunodeficiency virus infection after tuberculosis. *American Journal of Respiratory and Critical Care Medicine*.1995, 151: 129-135.
166. Tumul Srivastava, W. Haq and S. B. Katti., Carbodiimide mediated synthesis of 4-thiazolidinones by one-pot three-component condensation. *Tetrahedron*.2002, 58: 7619-7624.
167. National Committee for Clinical Laboratory Standards. Antimycobacterial susceptibility testing for *Mycobacterium tuberculosis*. Proposed standard M24-T.National Committee for Clinical Laboratory Standards, Villanova, Pa., 1995.
168. Toutain P. L., Bousquet-Me'lou., Bioavailability and its assessment. *Journal of Veterinary Pharmacology and Therapeutics*.2004, 27: 455–466.

169. Kota Jagannath., Madhusudana Rao Chaluvadi., Ramesh Mullangi., N.V.S. Rao Mamidi., Nuggehally R. Srinivas., Intravenous pharmacokinetics, oral bioavailability and dose proportionality of ragaglitazar, a novel PPAR-dual activator in rats. *Biopharmaceutics & Drug Disposition*.2004, 25: 323 – 328.
170. Toutain P. L., Bousquet-Me'lou A., Plasma clearance. *Journal of Veterinary Pharmacology and Therapeutics*.2004, 27: 415–425.
171. Toutain P. L., Bousquet-Me'lou A., Volume of distribution. *Journal of Veterinary Pharmacology and Therapeutics*.2004, 27: 441–453.
172. Guidance for industry: Bioanalytical method validation-USA FDA 2001.
Available from:
<http://www.fda.gov/downloads/Drugs/GuidanceComplianceRegulatoryInformation/Guidances/UCM070107.pdf>
173. N-(2-(4-(benzyloxy) phenyl)-4-oxo-1,3-thiazinan-3-yl)isonicotinamide(16): Anal. Calcd for C₂₃H₂₁N₃O₃S: C, 65.85; H, 5.01; N, 10.02; O, 11.44; S, 7.64 Found C, 65.89; H, 4.99.; N, 9.97 1H NMR (300 MHz,CDCl₃) δ ppm; 2.79–2.87 (m, 4H, CH₂CH₂), 5.21 (s,2H,CH₂) 5.60 (s, 1H, CH), 6.8-7.01(m, 4H, Ar-H of Phenyl), 7.41-7.58(m, 5H, Ar-H Of benzyl), 8.1-8.81(m, 4H, Ar-H of pyridyl), 8.4 (s, 1H, NH, D₂O exchangeable) 13C NMR (75MHz, CDCl₃): δ170.1, 163.4, 157.3, 147.9 (2C), 141.1, 138.8, 130.3, 128.2(2C), 127.1(2C), 125.2, 124.1(2C), 120.8(2C), 114.12(2C), 70.1, 62.02, 36.2, 32.1.
174. Food and Drug Administration of the United States (May 2001) Guidance for industry Bioanalytical Method Validation. Available from:<http://www.fda.gov/cder/guidance/index.html>
175. Ph. Hubert., P. Chiap., J. Crommen., B. Boulanger., E. Chapuzet., N. Mercier., S. Bervoas-Martin., P. Chevalier., D. Grandjean., P. Lagorce., M. Lallier., M.C. Laparra., M. Laurentie J.C. Nivet., The SFSTP guide on the validation of chromatographic methods for drug bioanalysis: From the Washington conference to the laboratory. *Analytica Chimica Acta*.1999, 391: 135-148.
176. Bansal S., DeStefano A., Key Elements of Bioanalytical Method Validation for Small Molecules. *American Association of Pharmaceutical Scientists Journal*.2007, 9: E109-E114.

177. Viswanathan C.T., Bansal S., Booth B., DeStefano A.J., Rose M.J., Sailstad J., Shah V.P., Skelly J.P., Swann P.G., Weiner R. Workshop/Conference Report — Quantitative Bioanalytical Methods Validation and Implementation: Best Practices for Chromatographic and Ligand Binding Assays. *American Association of Pharmaceutical Scientists Journal*.2007, 9: E30-E42.
178. Toutain P.L; Bousquet-Melou A., Plasma terminal half-life. *Journal of Veterinary Pharmacology and Therapeutics*.2004, 27: 427-439.
179. Anand B. D., Renu S. D., Ramesh P., In vivo pharmacokinetic and tissue distribution studies in mice of alternative formulations for local and systemic delivery of Paclitaxel: gel, film, prodrug, liposomes and micelles. *Current Drug Delivery*.2005, 2: 35-44.
180. Lanao J.M., Fraile M.A., Drug tissue distribution: study methods and therapeutic implications. *Current Pharmaceutical Design*.2005, 11: 3829-45.
181. Krystyna S., Anna K., tissue distribution and excretion of n-methyl-2-pyrrolidone in male and female rats. *International Journal of Occupational Medicine and Environmental Health*.2006, 19: 142 – 148.
182. Xiaona Li., Qiao Wang., Xiaowei Zhang., Xiaona Sheng., Yanan Zhou., Min Li., Xiujuan Jing., Deqiang Li., Lantong Zhang., HPLC study of pharmacokinetics and tissue distribution of morroniside in rats. *Journal of Pharmaceutical and Biomedical Analysis*.2007, 45: 349-55.
183. Zakia Bibi., Role of cytochrome P₄₅₀ in drug interactions. *Nutrition & Metabolism*.2008, 5: 1-10.
184. Michalets E.L., Update: clinically significant cytochrome P₄₅₀ drug interactions. *Pharmacotherapy*.1998, 18: 84–112.
185. Cupp M.J., Tracy T.S., Cytochrome P₄₅₀: new nomenclature and clinical implications. *American Family Physician*. 1998, 57: 107-116.
186. Lin J.H., Lu A.Y.H., Inhibition and Induction of Cytochrome P₄₅₀ and the Clinical Implications. *Clinical Pharmacokinetics*. 1998, 35: 361–390.
187. Ito K., Iwatsubo T., Kanamitsu S., Ueda K., Suzuki H., Sugiyama Y. Prediction of pharmacokinetic alterations caused by drug–drug interactions: metabolic interaction in the liver. *Pharmacological Reviews*. 1998, 50: 387–412.

188. Therapeutic products programme guidance document: Drug-Drug Interactions: Studies In Vitro and In Vivo. Available from: http://www.hc-sc.gc.ca/dhp-mps/alt_formats/hpfbdgpsa/pdf/prodpharma/drug_medi_int-eng.pdf
189. Rodda B. E., Davis R. L. Determining the probability of an important difference in bioavailability. *Clinical Pharmacology and Therapeutics*.1980, 28: 247–252.
190. Guidance for Industry: Drug *Metabolism/Drug Interaction Studies in the Drug Development Process: Studies In Vitro*. U.S. Food and Drug Administration.1997. [assessed on 2 January 2012]. Available from: <http://www.fda.gov/cder/guidance.htm>.
191. Guengerich F.P., Role of cytochrome P₄₅₀ enzymes. *Advances in Pharmacology*.1997, 4: 37-35.
192. Shu-Feng Zhou., Li-Ping Yang., Zhi-Wei Zhou., Ya-He Liu., Eli Chan., Structure, function, regulation and polymorphism and the clinical significance of human cytochrome P₄₅₀ 1A2. *Drug Metabolism Reviews*.2004, 42: 268–354.
193. Pelkonen O., Turpeinen M., Hakkola J., Honkakoski P., Hukkanen J., Raunio H., Inhibition and induction of human cytochrome P₄₅₀ enzymes: current status. *Archives of Toxicology*.2008, 82: 667–715.
194. Allan E. Rettie., Jeffrey P. Jones., Clinical and Toxicological relevance of CYP2C9: Drug-Drug Interactions and Pharmacogenetics. *Annual Review of Pharmacology and Toxicology*.2005, 45: 477-494.
195. Lorna Goshman., Kristie Roller., Clinically Significant Cytochrome P₄₅₀ Drug Interactions. *Journal of the Pharmacy Society of Wisconsin*.1999, 23 – 37.
196. Paul F. Hollenberg., Characteristics and common properties of Inhibitors, Inducers, and Activators of Cyp enzymes. *Drug metabolism reviews*.2002, 34: 17–35.
197. Christopher G Rowan., Clinical importance of the drug interaction between statins and CYP3A4 inhibitors. University of Pennsylvania. 2010.
198. K. Ito., T. Iwatsubo., S.Kanamitsu., K. Ueda., H. Suzuki., Y. Sugiyama., Prediction of Pharmacokinetic Alterations Caused by Drug-Drug Interactions: Metabolic Interaction in the Liver. *Pharmacological reviews*.1998, 50: 387-411.
199. Hiroshi Marumo., Kumi Satoh., Atsuko Yamamoto., Shigeru Kaneta., Kazuo Ichihara., Simvastatin and Atorvastatin Enhance Hypotensive Effect of Diltiazem in Rats. *Yakugaku Zasshi*.2001, 121: 761-764.

200. [Honig P.K.](#), [Wortham D.C.](#), [Zamani K.](#), [Conner D.P.](#), [Mullin J.C.](#), [Cantilena L.R.](#), Terfenadine-ketoconazole: pharmacokinetic and electrocardiographic consequences. *Journal of American Medical Association*. 1993, 269: 1513–1519.
201. Alcaide B., Almendros P., Luna A., Torres M. R., Proline-Catalyzed Diastereoselective Direct Aldol Reaction Between 4-Oxoazetidines-2-carbaldehydes and Ketones. *Journal of Organic Chemistry*. 2006, 71: 4818–4822.
202. Janey J. M., Hsiao Y., Armstrong III J. D., Proline-Catalyzed, Asymmetric Mannich Reactions in the Synthesis of a DPP-IV Inhibitor. *Journal of Organic Chemistry*. 2006, 71: 390-392.
203. (a) Kotrusz P., Toma S., L-Proline Catalyzed Michael Additions of Thiophenols to α,β -Unsaturated Compounds, Particularly α -Enones, in the Ionic Liquid [bmim] PF₆. *Molecules*. 2006, 11: 197–205
- (b) Chen H., Wang Y., Wei S., Sun J., L-Proline derived triamine as a highly stereo selective organo catalyst for asymmetric Michael addition of cyclohexanone to nitroolefins. *Tetrahedron: Asymmetry*. 2007, 18: 1308-1312.
204. (a) Ramachary D. B., Chowdari N. S., Barbas III C. F., Organocatalytic Asymmetric Domino Knoevenagel/Diels–Alder Reactions: A Bioorganic Approach to the Diastereospecific and Enantioselective Construction of Highly Substituted Spiro[5,5]undecane-1,5,9-triones. *Angewandte Chemie International*. 2003, 115: 4365–4369.
- (b) Kim I., Kim S. G., Choi J., Lee G. H., Facile synthesis of benzo-fused 2,8-dioxabicyclo[3.3.1]nonane derivatives via a domino Knoevenagel condensation/hetero-Diels–Alder reaction sequence. *Tetrahedron*. 2008, 64: 664-671.
205. (a) Yadav J. S., Kumar S. P., Kondaji G., Rao R. S., Nagaiah K., A Novel L-Proline Catalyzed Biginelli Reaction: One-Pot Synthesis of 3,4-Dihydropyrimidin-2(1H)-ones under Solvent-Free Conditions. *Chemistry Letters*. 2004, 33: 1168–1169
- (b) Mabry J., Ganem B., Studies on the Biginelli Reaction: A Mild and Selective Route to 3,4-Dihydropyrimidin-2(1H)-ones via Enamine Intermediates. *Tetrahedron Letters*. 2006, 47: 55–56.
206. Srinivasan M., Perumal S., (L)-Proline-Catalyzed Novel Tandem Reactions of 1-Substituted Piperidin-4-ones with (E)-4-Arylbut-3-en-2-ones: N-Substituent Mediated

Product Selectivity and Synthesis of Novel Nitrogen Heterocycles. *Tetrahedron*. 2007, 63: 2865-2874.

207. Reddy D.B., Reddy M.M., Reddy P.V.R., Phenacylthio/sulfonyl Acetates as Synthons. Part 3. Synthesis and Conformational Aspects of Some 1,4-Thiomorpholines. *Indian Journal of Chemistry*. 1993, 32: 1018-1023.

208. Sriram D., Yogeewari P., Dinakaran M., Thirumurugan R., Antimycobacterial activity of novel 1-(5-cyclobutyl-1,3-oxazol-2-yl)-3-(sub)phenyl/pyridylthiourea endowed with high activity toward multi-drug resistant tuberculosis. *Journal of Antimicrobial Chemotherapy*. 2007, 59: 1194-1196.

209. Parish T., Stoker N.G., [*glnE is an essential gene in Mycobacterium tuberculosis*](#). *Journal of Bacteriology*. 2000, 182: 5715-5720.

210. Herrmann K. M., The Shikimate Pathway: Early Steps in the Biosynthesis of Aromatic Compounds. *Plant Cell*. 1995, 7: 907-919.

211. Walsh C.T., Liu J., Rusnak F., Sakaitani M., Molecular Studies on Enzymes in Chorismate Metabolism and the Enterobactin Biosynthetic Pathway. *Chemistry Reviews*. 1990, 90: 1105-1129.

212. De Man J. C., MPN tables for more than one test *Journal of Applied Microbiology*, 1,(1975), 61-67.

213. Phase, version 3.3, Schrodinger, LLC, New York, NY, 2011.

214. Dixon S. L., Smondyrev A. M., Rao S. N., PHASE, a novel approach to pharmacophore modeling and 3D database searching. *Chemical biology & drug design*. 2006, 67: 370-372.

215. Burns C. J., Bourke D. G., Andrau L., Bu X., Charman S. A., Donohue A. C., Fantino E., Farrugia M., Feutrill J. T., Joffe M., Phenylaminopyrimidines as inhibitors of Janus kinases (JAKs). *Bioorganic and Medicinal Chemistry Letters*. 2009, 19: 5887-5892.

216. LigPrep, version 2.5, Schrodinger, LLC, New York, NY, 2011.

217. Li Y., Wang, Y., Zhang F., Molecular simulation of a series of benzothiazole PI3K α inhibitors: probing the relationship between structural features, anti-tumor potency and selectivity. *Journal of Molecular Modeling*. 2010, 16: 1449-1460.

Appendix

List of Publications

From Thesis work

1. Ramani AV, Monika A, Indira VL, Karyavardhi G, Venkatesh J, Jeankumar VU, Manjashetty TH, Yogeeswari P, Sriram D; Synthesis of highly potent novel anti-tubercular isoniazid analogues with preliminary pharmacokinetic evaluation. *Bioorganic and Medicinal Chemistry Letters*, 2012, 22, 2764-2767.
2. Ramani AV, Madhu B B, Yogeeswari P, Sriram D; quantitative structure-activity relationship studies on substituted 1, 1-dioxo-1, 4,-thiazinane-2-carboxylate anti-tubercular agents. *International Journal of Drug Design and Discovery*, 2012 [In press]
3. Ramani V A, Indira VL, Satya V, Sandeep G, Yogeeswari P, Sriram D; Study of pharmacokinetics and tissue distribution of BITS-17 in rat plasma and tissue homogenate using a validated LC method *Journal of Bioanalysis & Biomedicine (JBABM)* [revision communicated]
4. Ramani V A, Jeankumar VU, Mallika A, Madhu B B, Yogeeswari P, Elena S, Sriram D; Synthesis, *in-vitro* biological activity and quantitative structure–activity relationship of novel substituted 1, 1-dioxo-1, 4,-thiazinane-2-carboxylate as antitubercular agents [Communicated]

List of Posters

1. Siddharth Sai, A.V.Ramani, V.U.Jean Kumar, P.Yoggeswari, D.Sriram, Design, synthesis and invitro evaluation of novel 1,4 thiazine derivatives as potential antitubercular agents , *MedChem-2011 Conference on Antiinfective drug discovery & development*, 28-29th October 2011, Indian institute of technology, Chennai, India.(won the best paper in poster section)

2. A.Monica, A.V.Ramani, V.U.Jean Kumar, H.M.Thimappa, P.Yogeswari, D.Sriram, One pot synthesis of novel substituted 1,3 thiazinyl isonicotinamides, invitro and pharmacokinetic evaluation for the treatment of tuberculosis, 63rd Indian Pharmaceutical Congress 2011, 19-21 December 2011, Bangalore, India (won the second best paper award in poster section)

Biography of Prof. D. Sriram

Prof. D. Sriram is presently working as Associate Chair Professor in the Department of Pharmacy, Birla Institute of Technology & Science- Pilani, Hyderabad Campus. He received his Ph. D. (Medicinal Chemistry) from Institute of Technology, Banaras Hindu University, Varanasi, India in the year 2000. From then he is involved in teaching and research (approx 12 years). He has authored more than 175 publications. He is a life member of Associations of Pharmacy Teachers of India, Association of microbiologists of India and member of Canadian Society of Pharmaceutical Sciences. He is principal investigator for many projects funded by reputed funding agencies like UGC, CSIR, ICMR, CSIR-OSDD, UGC, DBT-VINNOVA [BITS-Karolinska], DBT-COE [BITS-IISc]. His main research areas are Tuberculosis and Cancer drug discovery. He is a Collaborative Research Scientist at. Karolinska Institute, Sweden, Indian Institute of Science, India, N.I.I. New Delhi, India, Indian Institute of Chemical Technology, India, Glaxo Smith Kline, Spain, AstraZeneca, India. He has guided 5 PhD students and guiding 11 of them. He is a chief editor of International Journal of Drug Design and Discovery and expert reviewer of my prestigious journals.

Biography of A.V.Ramani

A.V.Ramani has completed Masters of Pharmacy from College of Pharmaceutical Sciences Manipal. (Mangalore University) Karnataka in 1995. She is presently working as a lecturer in the Department of Pharmacy, Birla Institute of Technology & Science- Pilani, Hyderabad Campus, from 2009. From 2009 she is working for her Ph.D. under the supervision of Prof. D. Sriram. Before joining BITS she worked in various pharmaceutical industries like Dr.Reddy's Laboratories Ltd, Hyderabad; Divis laboratories limited, Hyderabad and Eros Pharma Ltd. Bangalore.